FACULTAD DE CIENCIAS

DEPARTAMENTO DE BIOLOGÍA MOLECULAR

"Papel de la vía endocítica en la infección del Virus de la Peste Porcina Africana"

TESIS DOCTORAL

Miguel Ángel Cuesta Geijo

Madrid, 2013

FACULTAD DE CIENCIAS
DEPARTAMENTO DE BIOLOGÍA MOLECULAR
UNIVERSIDAD AUTÓNOMA DE MADRID

"Papel de la vía endocítica en la infección del Virus de la Peste Porcina Africana"

Memoria presentada para optar al grado de Doctor en Ciencias por:

Miguel Ángel Cuesta Geijo

Directora de Tesis

Covadonga Alonso Martí

Tutor académico

Jose Antonio López Guerrero

El presente trabajo de Tesis ha sido realizado en el Departamento de Biotecnología del Instituto Nacional de Investigaciones agrarias y alimentarias (INIA) financiada por una Beca de Formación de Personal Investigador (FPI) otorgada por el Ministerio de Ciencia e Innovación (MICINN)

INFORME DEL DIRECTOR DE TESIS PARA LA AUTORIZACIÓN DE DEFENSA DE TESIS DOCTORAL

(Doctoral Thesis Supervisor's report to dissertation authorization)

(En el caso de existir más de un director de la tesis doctoral, deberá presentarse un informe de cada uno de los co-directores)

(In case of more than one Thesis Supervisor, a report of each one must be submitted)

D/Dª COVADONGA ALONSO MARTI
(Thesis Supervisor´s name and surname)

Director/a de la tesis doctoral de D/Dª MIGUEL ANGEL CUESTA GEIJO
(PhD Candidate´s name and surname) **informa favorablemente** la solicitud de autorización de defensa de la tesis doctoral con el Título ***(Title of the PhD Dissertation):***"Papel de la vía endocítica en la infección del Virus de la Peste Porcina Africana" presentada por dicho/a doctorando/a.

(favorably reports on the application for dissertation authorization submitted for the PhD Candidate)

Programa de Doctorado *(Doctoral program)*: RD 56/2005
La tesis está sometida a procesos de confidencialidad: SÍ □ NO □x
(Thesis is under confidentiality procedures: Yes / No)
La tesis se presenta como compendio de publicaciones: SÍ □ NO □x
(Thesis is submitted as a compendium of publications: Yes / No)

Resultados y valoración ***(Results and assessment):***

ANTECEDENTES DE LA CUESTIÓN Y OBJETIVOS PROPUESTOS
(Background of the field and main goals)

La introducción está bien presentada y estructurada y demuestra un conocimiento bibliográfico exhaustivo y profundo. Es muy informativo del estado de la cuestión tanto en cuanto aspectos básicos como avances muy recientes en endocitosis y la señalización necesaria para la maduración de la vía endocítica. Además, enmarca lo que dichos avances han supuesto para la comprensión del proceso de entrada de los virus mediante endocitosis en general y se propone abordar de forma concreta el estudio de la entrada del VPPA por esta vía y las dianas moleculares claves para que se lleve a cabo una infección productiva. Identifica de forma muy clara un área desconocida y crucial del ciclo viral y los objetivos, muy actuales y novedosos en cuanto al estado del arte en endocitosis y las infecciones víricas, lo plantean de forma directa y apropiada.

DESARROLLO DEL TRABAJO Y METODOLOGÍA
(Procedure and Development of the general matter and methodology)

El doctorando ha realizado un trabajo brillante, ambicioso y detallado, planteándose continuamente nuevos retos demostrando una gran iniciativa intelectual en el diseño de la investigación. La metodología es apropiada y rigurosa. La memoria está bien redactada y ordenada de forma sistemática y comprensiva. Los resultados son relevantes y novedosos en cuestiones escasamente clarificadas, no solo para VPPA sino para diversos modelos víricos cuya repercusión está siendo valorada de forma creciente en la actualidad.

APORTACIONES DE CARÁCTER GENÉRICO O EXPERIMENTAL
(Contribution to the experimental and general field)

Los resultados de esta tesis doctoral tienen importancia desde el punto de vista del nuevo conocimiento aportado sobre las primeras fases de la infección VPPA y las dianas moleculares tempranas de este virus que son poco conocidas para otras enfermedades víricas. Hoy en día la maduración endosomal parece que puede jugar un papel de mayor relevancia que el simple transporte del virus al interior de la célula, sino que es crucial en la clasificación y destino del material genético del virus, en la respuesta innata al mismo e incluso en el establecimiento del nicho de replicación del virus en la célula infectada. Este conocimiento desde el punto de vista de la ciencia básica, puede ser la base del desarrollo de estrategias antivirales de amplio espectro frente a este y otros modelos víricos.

PUBLICACIONES A QUE HAYA DADO LUGAR
(Publications appeared already)

1.Cuesta-Geijo M.A., I. Galindo, B. Hernáez, J.I. Quetglás, I. Dalmau-Mena and C. Alonso. Endosomal maturation, Rab7 GTPase and Phosphoinositides in African Swine Fever Virus entry. PLoS ONE 2012, 7(11): e48853. PMID:23133661

2. C. Alonso, I. Galindo, M.A. Cuesta-Geijo, M. Cabezas, B. Hernáez, R. Muñoz-Moreno. African Swine Fever Virus-Cell Interactions: From Virus Entry to Cell Survival. Virus Research 2013 173: 42-57. PMID:23262167

3. Hernaez B., M. Cabezas, R. Muñoz-Moreno, I. Galindo, M.A.Cuesta-Geijo and C. Alonso A179L, a new viral Bcl2 homolog targeting Beclin 1 autophagy related protein. Current Molecular Medicine 2013, 13(2): 305-316. PMID: 23228131

4. Galindo I., B. Hernáez, M.A. Cuesta-Geijo, I. Dalmau-Mena and C. Alonso. The ATF6 branch of Unfolded Protein Response and Apoptosis are activated to promote African Swine Fever virus infection. Cell Death and Disease 2012 Jul 5;3:e341. PMID: 22764100

5. Quetglas J.I., Hernaez B., I. Galindo, R. Muñoz-Moreno, M.A.Cuesta-Geijo and C. Alonso Small Rho GTPases and cholesterol biosynthetic pathway intermediates in African swine fever virus infection. Journal of Virology 2012 Feb;86(3):1758-67 PMID: 22114329

6. Cuesta-Geijo, M.A., M. Chiappi, I. Galindo, R. Muñoz-Moreno, F.J. Chichón, J.L. Carrascosa and C. Alonso. Cholesterol homeostasis is an early target of a double stranded DNA virus infection at the endocytic pathway (manuscrito en preparación).

7. Galindo I., N. Familiar, M.A. Cuesta-Geijo, K. Babickova and C. Alonso. African swine fever virus entry in primary macrophages (manuscrito en preparación).

8. Intracellular transport linked to motor protein-binding peptides of viral origin. Dalmau-Mena I., M.A. Cuesta-Geijo, I. Galindo, R. Muñoz-Moreno and C. Alonso. PLoS ONE 2013 (en revisión).

VALORACIÓN GLOBAL
(Final evaluation)

Es un trabajo brillante y novedoso con aportaciones científicas altamente relevantes y la consecución de sus objetivos definiendo dianas moleculares tempranas de la infección por VPPA abre la puerta al desarrollo de nuevos antivirales frente a esta y otras familias de virus que utilizan mecanismos similares de infección.

(Rellenar solo en el caso de que la tesis se presente como compendio de publicaciones):
(To fill in only in case that thesis is submitted as a compendium of publications):

Se autoriza la presentación de la tesis como compendio de publicaciones: SÍ ☐ NO ☒x
(Authorizing the submission of the thesis as a compendium of publications: Yes /No)

<u>Ratificación del informe por la Comisión Académica del programa de doctorado</u> (*)

El Responsable de la Comisión Académica ratifica el informe favorable del director de tesis para la autorización de defensa de la tesisdoctoral presentada por dicho/a doctorando/a.

Madrid, a de de 20

Marque lo que proceda:

□ Programa de doctorado del RD 185/1985 □ Programa de doctorado del RD 778/1998	□ Director del Departamento Correo electrónico: …	Fdo.: ….
	□ Director en funciones Correo electrónico: …	
	□ Subdirector Correo electrónico: …	
□ Programa de doctorado del RD 56/2005 □ Programa de doctorado del RD1393/2007	□ Coordinador del programa Correo electrónico: …	Fdo.: ….
□ Programa de doctorado del RD 99/2011	□ Responsable de la Comisión Académica Correo electrónico: …	Fdo.: ….

Agradecimientos

Hace algo más de cuatro años estaba llamando a la puerta del que después sería mi laboratorio, el laboratorio 2 del Edificio Central del INIA. Recuerdo que se acababan de mudar del edificio Z, y Bruno y Pepe estaban colocando todo en el nuevo labo. "Estaba interesado en hacer la Tesis de Máster en este laboratorio", le comenté a Cova. A los pocos días conocí a una chica que me pareció muy seria, Inma.

Ahora, a punto de leer mi Tesis Doctoral y echando la vista atrás, puedo decir que ha sido una etapa que marcará mi vida, ya que me ha hecho crecer tanto en lo personal como en lo profesional.

Sin embargo no sería justo finalizar este trabajo sin dedicar unas líneas a agradecer el esfuerzo de otras personas que han aportado su experiencia, trabajo, ayuda y apoyo para hacer el camino un poquito más llano hasta esta Tesis.

Agradecer en primer lugar a la Dra. Covadonga Alonso por darme la oportunidad de formar parte de su equipo de trabajo y realizar en él la Tesis de Máster y la Tesis Doctoral. Gracias por acogerme con paciencia, cariño, por depositar tu confianza en mí y por iniciarme en la carrera científica. Te agradezco mucho la gran implicación, esfuerzo y tesón que has puesto en mi trabajo, ofreciéndome una guía científica constante en la línea de investigación en todo momento, principalmente en los que el camino estaba más oculto. Han sido de mucho provecho las largas charlas y discusiones científicas que hemos tenido en relación a este trabajo con el fin de ver la luz. Me he sentido escuchado y valorado, y por supuesto he aprendido mucho en ellas. Por supuesto agradecerte esos momentos de comprensión, apoyo y ayuda en momentos delicados en mi vida, fue muy importante para mí.

Quería tener unas palabras de agradecimiento para Jose Ángel, gracias por compartir tus conocimientos de formas distintas con tus consejos científicos, tu punto de vista, opiniones y claridad de ideas, aunque sea a horas "difíciles".

Agradezco al Dr. Jose Antonio López Guerrero (JAL), por ejercer como mi Tutor académico, estar disponible siempre que lo he necesitado, y poner las cosas tan fáciles. Gracias por brindarme tu ayuda.

Quiero agradecer de manera especial a Inma y Bruno su participación en este trabajo.

Inma, algo más que una compañera de trabajo, gracias por todo. Es la persona a la que le sale todo bien siempre. Gracias por tu ayuda desinteresada todos estos años, y especialmente en estos últimos meses. Gracias por poner a nuestra disposición tu gran experiencia científica, tus ideas y tus consejos, y por supuesto valorar la paciencia con la que lo haces. Siempre estás para ayudar y para resolver cualquiera de nuestros problemillas y problemazos del día a día. Eres verdaderamente importante para todos dentro del labo. Gracias. Y no menos importante, ese fino sentido del humor del que haces gala constantemente…al final, me doy cuenta de que te has ganado el Reiki.

Bruno, gracias por regalarme tu experiencia, tus conocimientos y tus consejos, siempre con una sonrisa, con buen humor, con tus canciones y una disposición excelente. Por ayudarme en mis primeros pasos en la ciencia enseñándome las técnicas de laboratorio y a moverme con soltura. Por tu infinita paciencia, pero fundamentalmente, por enseñarme a pensar y a ser crítico. Nunca olvidaré los buenísimos ratos que hemos pasado en el laboratorio y tu apoyo en momentos duros. Me llevo un amigo.

Muchas gracias a mis compañeras de laboratorio, sabéis que os quiero mucho y que me encantan esos ratos en los que toca despellejar a Miguel Ángel. Gracias a Raquel, a Marta, y a Inma Dalmau, que junto con Inma forman ese clan indestructible que tantos momentos especiales ha brindado, todos ellos apuntados en el cuaderno secreto. Marta, muchas gracias por tu trabajo y entrega para todos en el labo, así da gusto! Agradeceros lo bien que os habéis portado siempre conmigo, toda la ayuda a lo largo de todo este tiempo es digna de mención, especialmente en esta última fase de la Tesis. También quería darle las gracias a Nerea, ya que en estos últimos meses ha sido mis manos en muchas ocasiones. Gracias.
También a toda la gente que ha pasado por el laboratorio todo este tiempo, Bárbara, Berta y Eva.
En resumen, ¡¡¡sois geniales!!! Hacéis que ir a trabajar cada día sea un gustazo!

A mis compañeras del laboratorio de enfrente, Silvia, con las que compartí historias de juergas por Ávila, ¡ojito!, recetas y buenas conversaciones (mucha suerte en tus planes futuros, a la siguiente lo consigues), a Carmen, que me hizo perder el miedo a los geles de acrilamida, esa tarta para el día de mi cumple siempre la recordaré, a Eva, ya sabes, a darlo todo sea la hora que sea, para el recuerdo quedará aquella mañana mítica del oocito en el microscopio. Gracias también por tu ayuda. También a Benoit, que además de buena persona y amigo, es el informático de emergencia. Javi y Susana, a vosotros os deseo mucha suerte con vuestras respectivas familias, que acaban de crecer.

Quería tener unas palabras para la mesa de boda (o a veces no) de la cafetería que aun no he nombrado, María, Estela, Ana y Teresa. Y para el resto de gente del departamento con el que he compartido algunos momentos, Yanín, Maite, Edu, Blanca, Vicky y Paloma. Gracias al grupo de inmunología por sus ayudas constantes con el citómetro, a Conchi, con la que comparto el premio de mejor bailarín de Country, Belén, María, Zoraida y Paloma.
Mención aparte para Marga, gracias por tu humor, por esos ratos inolvidables de verdad (la gente tiembla cuando entras en el labo), por tus preparaciones, por ser tan servicial y dispuesta…y no menos importante, por la miel, el orujo, los torreznos, el orégano, el parking para ir al Calderón…

Algunos experimentos de esta tesis no habrían podido llevarse a cabo sin la ayuda de algunas personas y su buen hacer.

Gracias a Pedro Lastres, responsable del servició de citometría de flujo del Centro de Investigaciones Biológicas (CIB) de Madrid.

Sólo tengo palabras de agradecimiento para el Dr. Jose Carrascosa y su equipo del CNB. Han realizado un trabajo increíblemente dedicado y meticuloso en la microscopía electrónica de transmisión. Agradecer al Dr. Carrascosa su tiempo y su gran experiencia en forma de acertados consejos. También a Javi Chichón y Mari Jose, siempre se aprende de cualquier conversación con vosotros. De manera particular agradecer a Michele Chiappi su grandísima colaboración, su dedicación, su minucioso trabajo y su buen hacer. Gracias por haberte volcado de esta manera en esta colaboración. Ha sido un placer trabajar codo con codo durante este tiempo, he descubierto a un tío genial, muy humana y gran persona. Te deseo mucha suerte en tus proyectos.

Me he sentido muy cómodo con vosotros todo este tiempo.

Quería también recordar a mis amigos de toda la vida, por ser así, por su interés y por su cariño…aunque han empezado a pensar que escribir la Tesis era una excusa para no ir con ellos. A Xavi, Míguel, Pablo, Miguel, Lomba y Carlos (aunque llegó después, se ha hecho un hueco muy importante en mi vida). A todos mis monitores de Satri, que siempre me dan tanta fuerza.

A Lourdes, Víctor y Cris, porque ellos han vivido esta tesis de verdad, con sus momentos buenos y no tan buenos, desde el principio hasta el final. Gracias por vuestro apoyo, por desearme siempre lo mejor de una forma tan sincera, por caminar siempre a mi lado y por ofrecerme vuestra mejor versión.

En último lugar quiero dar gracias a mis padres, junto con Elena, de mi familia solo he sentido apoyo, cariño e interés en que todo llegara a buen puerto.

Al fin y al cabo, esta tesis también ha sido fruto de su esfuerzo.

Resumen

En este trabajo de tesis hemos caracterizado que la infección del virus de la peste porcina africana (VPPA) es dependiente de la vía endocítica. Una vez el VPPA se internaliza en las células, se incorpora inmediatamente a la vía endocítica. Esta vía comprende una serie de vesículas que sufren cambios madurativos altamente regulados por las Rab GTPasas y los fosfoinosítidos (FIs). Estos cambios modifican las características fisiológicas de las vesículas endocíticas a lo largo del proceso de maduración. La infección, comienza con el paso del VPPA por los endosomas tempranos (EE), dada la elevada colocalización entre el virus con estas vesículas desde los primeros minutos de la infección. Posteriormente, el VPPA alcanzaba los endosomas tardíos (LE), donde se producía la desencapsidación de un modo dependiente de pH ácido antes de la primera hora post infección.

La señalización relacionada con la vía endocítica era crucial para el éxito de la infección, en concreto una diana molecular de gran relevancia, la GTPasa Rab7, reguladora de la dinámica del LE. La infectividad del VPPA resultaba severamente afectada cuando se anulaba la función de la GTPasa Rab7. Otra señalización relevante para el LE es dependiente del fosfatidil inositol 3,5 bifosfato. El bloqueo de la síntesis de este FI, especialmente antes de la infección, producía una disminución de la expresión de proteínas virales y de la producción viral.

Una de las etapas cruciales de la infección, correspondió a los cuerpos multivesiculares (MBVs), un estadío madurativo intermedio, previo al LE. Los MBVs se caracterizan por presentar numerosas vesículas intraluminales (ILVs) en su interior. Las ILVs están enriquecidas por un lípido no convencional, el ácido lisobisfosfatídico (LBPA). Al anular su acción mediante un anticuerpo bloqueante, se afectaba la capacidad infectiva del virus. Asimismo, se demostró que la infección por VPPA en sus primeras etapas era altamente dependiente del flujo de colesterol libre desde los endosomas (LE) hacia sus destinos celulares.

Las mencionadas moléculas de señalización de la vía endocítica son dianas moleculares para el virus y las membranas endosomales podrían jugar un papel como plataformas para la formación de la organela de replicación viral (ORV) o factoría vírica. Hasta ahora, se consideraba que las ORVs eran acúmulos de proteínas y DNA viral en los que no podía detectarse ninguna organela a excepción de ribosomas. Sin embargo, hemos descrito por primera vez, que las membranas endosomales se encuentran entremezcladas con los focos de acúmulo de proteínas víricas en las fases iniciales de su formación. Además, la formación de la factoría del VPPA conlleva una redistribución de todos los compartimentos endosomales hacia el área donde se constituye el complejo de ensamblaje del virus, resultando fundamental en las etapas iniciales de la infección por VPPA.

Abstract

In this thesis we have characterized the dependence of the African swine fever virus (ASFV) infection on the endocytic pathway. Once ASFV is internalized into cells, it is immediately incorporated to the endocytic pathway. This pathway comprises a number of vesicles undergoing maturational changes highly regulated by Rab GTPases and phosphoinositides (PIs). These changes modify the physiological characteristics of the endocytic vesicles along the maturation process. Infection begins with the passage of ASFV through early endosomes (EE), given the high colocalization between virus proteins and these vesicles found from the first 30 minutes of infection. Subsequently, according to our results, ASFV reaches the late endosomes (LE) where desencapsidation occurs in an acid pH-dependent manner before the first hour post infection.

The endocytic pathway related signaling is crucial for a successful ASFV infection, specifically a highly relevant molecular target is the GTPase Rab7, regulating dynamics of LE. ASFV infectivity was severely affected when impairing the Rab7 function. Another relevant LE signaling was phosphatidylinositol 3,5 bisphosphate dependent. Blocking the synthesis of this PI, especially starting before infection, caused a severe decrease in viral protein expression and virus production.

A crucial endosomal stage for ASFV infection corresponded to multivesicular bodies (MBV), an intermediate maturation stage prior to LE. MBVs are characterized by numerous intraluminal vesicles (ILVs). ILVs are enriched by an unconventional lipid, the lysobisphosphatidic acid (LBPA) which directly correlates with intracellular cholesterol levels. By withdrawing its action with a blocking antibody, virus infectivity was also affected. Furthermore, it was demonstrated that ASFV infection at its early stages was highly dependent on the flow of free cholesterol from LE to their cell destinations.

The mentioned signaling molecules of the endocytic pathway might are molecular targets for the virus. Also, endosomal membranes might play a role as a scaffold for the formation of viral replication organelle or viral factory. Until now, it was assumed that viral factories were composed by proteins and viral DNA in bulk accumulations, in which no organelle could be detected, exception made for ribosomes. However, we have described for first time that endosomal membranes were found interspersed between early aggregates of viral proteins accumulation at the initial stages of the viral replication site formation, which is microtubule dependent. Furthermore, the formation of ASFV factory entailed redistribution of all endosomal compartments to the area where the assembly complex of the virus is constituted, resulting in a key process for ASFV infection.

Índice

Abreviaturas

A: Adenina

aa(s): Aminoácido(s)

ABCA1: Transportador de colesterol A1 *("ATP-binding cassette transporter A1")*

Ad: Adenovirus

ADN: Acido Desoxirribonucleico

AG: Aparato de Golgi

AP2: Proteína adaptadora 2 *("Adaptator protein 2")*

ARN: Ácido Ribonucleico

ARNm: ARN mensajero

ATCC: Colección americana de cultivos celulares *("American Type and cell culture collection")*

ATP: Adenosín trifosfato

BAR: Dominio Bin-Amphiphysin-Rvs

BA71V: Aislado del VPPA obtenido en Badajoz en 1971 adaptado a células Vero

B54GFP: Virus recombinante obtenido a partir de BA71V que expresa la proteína viral p54 fusionada a la proteína verde fluorescente GFP

BA54ChFP: Virus recombinante obtenido a partir de BA71V que expresa la proteína viral p54 fusionada a la proteína roja fluorescente ChFP

BSA: Albumina de suero bovino *("Bovine serum albumin")*

CD: β-metil ciclodextrina

CLIC: Transportador independiente de clatrina *("Clathrin- independent carrier")*

CORVET complex: Complejo de anclaje vacuolar/endosomal de clase C *("Class C core vacuole/endosome tethering complex")*

DHC: Cadena pesada de la dineína *("Dynein heavy chain")*

Din: Dinasore

DLC8: Cadena ligera de 8 kD de la dinéina citoplásmica *("Dynein light chain")*

DMEM: Medio de Eagle modificado por Dulbecco *("Dulbecco's modified Eagle's médium")*

DN: Dominante negativo

E70: Aislado español del VPPA aislado en 1970 adaptado a linea células estable de mono

ECV: Vesícula endosomal de transporte

EE: Endosoma temprano *("Early endosome/s")*

EEA1: Antígeno 1 de endosoma temprano *("Early endosome antigen 1")*

EFSA: Autoridad de seguridad de alimentación europea *("European Food Safety Authority")*

EGF: Factor de crecimiento epidérmico *("Epidermal growth factor")*

ESCRT: Complejo requerido para el transporte *endosomal ("Endosomal sorting complex required for transport")*

PI: Fosfoinosítidos

FtdIns: Fosfatidilinositol

MGF: Familia multigénica *("Multigene family")*

FACS: Separador celular activado por fluorescencia *("Fluorescence-activated cell sorter")*

FPP: Farnesilpirofosfato

Ftasa: Farnesiltransferasa

FtdIns3P: Fosfatidilinositol 3 fosfato

FtdIns(3,5)P_2: Fosfatidil inositol 3, 5 bifosfato

FYVE (dominio): dominio proteico nombrado a partir de cuatro proteínas en las cuales está presente: Fab1p, YOTB, Vac1 y EEA1

FV: Factoría viral

GEEC: Proteínas ancladas a GPI del endosoma temprano*("GPI-anchored protein enriched early endosomal compartment")*

GFP: Proteína verde fluorescente *("Green fluorescent protein")*

GGPP: Geranilgeranilpirofosfato

GPI: Glicosilfosfatidilinositol *("Glycosylphosphatidylinositol")*

GTPasa: Guanosina trifosfatasa

H: Hora

His: Histidina

HIV: Virus de la inmunodeficiencia humana *("Human immunodeficiency virus")*

HMG-CoA: 3-hidroxi-3-metilglutaril-Coenzima A

HOPS complex: Complejo de fusión homotípica y organización vacuolar *("Homotypic fusion and vacuole protein sorting complex")*

Hpi: Horas post-infección

HSV: Virus del herpes simplex

IAP: Proteínas inhibidoras de apoptosis *("Inhibitors of Apoptosis")*

IFI: Inmunofluorescencia indirecta

IgG: Inmunoglobulina G

ILV: Vesícula intraluminal /es *("Intraluminal vesicle/s")*

KD: Kilodalton

Kpb: Kilopares de bases

LBPA: Ácido lisobisfosfatídico *("Lysobisphospahtidic acid")*

LDL: Lipoproteínas de baja densidad *("Low density lipoproteins")*

LE: Endosoma tardío/s *("Late endosome/s")*

LI: Lisosoma/s

ME: Microscopía/pio electrónica/o

MP: Membrana plasmática

moi: Multiplicidad de infección *("Multiplicity of infection")*

MTOC: Centro organizador de microtúbulos *("Microtubule-organizing center")*

MVB: Cuerpos multivesiculares *("Multivesicular Body/ies")*

MVD: Mevalonato descarboxilasa difosfato

NFAT: Factor nuclear de células T activadas *("Nuclear factor of activated T-cells")*

NK: "*Natural killer"*

nm: nanómetros

OIE: Oficina Internacional de Epizootias

ON: Toda la noche *("Over night")*

ORFs: Marcos de lectura abierta *("Open reading frames")*

ORP1L: Proteína L1 relacionada con la proteína de unión a oxisterol *("Oxysterol-binding protein (OSBP)–related protein 1L (ORP1L"))*

Pb: Pares de bases

PBS: Tampón fosfato salino *("Phosphate buffer saline")*

PH (dominio): Dominio con homología a la Pleckstrina *("Pleckstrin homology")*

PIK: Fosfoinositido quinasas *("Phosphoinosistide kinase")*

PI3K: Fosfatidilinositol 3 quinasa *("Phophatidylinositol 3 Kinase")*

PIKfyve: Fosfatidil inositol 3 fosfatasa 5 kinasa que contiene un dominio FYVE *("FYVE finger-containing phosphoinositide kinase")*

PP: Poliproteína

PP1: Fosfatasa celular 1

PPA: Peste porcina Africana

RE: Retículo endoplásmico

RILP: Proteína lisosomal que interacciona con Rab7 *("Rab7 interacting lisosomal protein")*

Rpm : Revoluciones por minuto

RT: Temperatura ambiente *("Room temperature")*

SBF : Suero bovino fetal

SDS : Dodecil sulfato sódico *("Sodium dodecyl sulfate")*

SDS-PAGE : Electroforesis en geles de poliacrilamida en presencia de SDS *("Sodium dodecyl sulfate polyacrylamide gel electrophoresis")*

SNAREs: Receptor SNAP *("Soluble NSF attachment protein receptor")*

SFV: Virus del bosque de Semliki *("Semliki Forest Virus")*

SV40: Virus del simio 40 *("Simian virus 40")*

T: Timina 6I

TEMED : N, N, N´N´-tetrametilendiamino.

TGN: Red trans del Golgi *("Trans Golgi network")*

TNF : Factor de necrosis tumoral ("*Tumor necrosis factor")*

TNFR : Receptor para TNF *("TNF receptor")*

Trp : Triptófano

TRPML1: Miembro 1 de los canales de cationes de la subfamilia de la Mucolipina *("Transient receptor potential cation channel, mucolipin subfamily, member 1")*

UFP : Unidad formadora de placa

UV : Ultravioleta

VAP-A: Proteína A de membrana (del RE) asociada a proteínas de membrana de las vesículas *("Vesicle- associated membrane- protein A (VAMP)- associated protein A (VAP-A)")*

V-ATPasa: ATPasa vacuolar *("vacuolar ATPase")*

VPPA: Virus de la peste porcina africana

VSV: Virus de la estomatitis vesicular *("Vesicular stomatitis virus")*

WB: "*Western Blot*"

WT: Fenotipo salvaje *("Wild type")*

Se ha optado por mantener diversas palabras en inglés, debido a que éstas no presentan una traducción directa al castellano, y una traducción forzada podría dar lugar a errores de interpretación. Para reflejar este hecho, aquellas palabras mantenidas en inglés se reflejan con letra cursiva y entre comillas.

"Blebbing"

"Budding"

"Switch"

"Knock out"

"Scavenger"

"Sorting"

Introducción

1. LA PESTE PORCINA AFRICANA

1.1 Breve descripción y situación actual

La Peste Porcina Africana **(PPA)** es una enfermedad altamente contagiosa que afecta a la mayoría de miembros de la familia *Suidae.* Presenta un cuadro prácticamente asintomático en sus hospedadores naturales, que son los cerdos salvajes africanos. Estos animales pueden sufrir infecciones persistentes, convirtiéndose en portadores del virus. El agente etiológico de la enfermedad es el Virus de la Peste Porcina Africana **(VPPA)**. El VPPA puede replicar su genoma y transmitirse a través de garrapatas que actúan como reservorios en el ciclo selvático del virus (Plowright et al., 1969; Thomson, 1985; Thomson et al., 1980), por ello VPPA se considera el único virus **ADN** que puede ser clasificado como un Arbovirus (ARBO, artrópodo transmitido) (Kleiboeker, 2002; Kleiboeker and Scoles, 2001). El virus replica en células del sistema fagocítico mononuclear, fundamentalmente monocitos y macrófagos (Carrasco et al., 1996a; Carrasco et al., 1996b; Fernandez et al., 1992; Perez et al., 1994; Ramiro-Ibanez et al., 1995). La PPA cursa como una fiebre hemorrágica aguda en el cerdo doméstico con una mortalidad del 100% en 7-10 días (Gomez-Villamandos et al., 2003) aunque también puede cursar de forma subaguda (Ramiro-Ibanez et al., 1997).

La PPA está incluida en la Lista A de la Oficina Internacional de Epizootias (OIE), que comprende las 15 enfermedades zoosanitarias producidas por aquellos patógenos transmisibles con una devastadora capacidad de propagación más allá de las fronteras nacionales (Kleiboeker, 2002).

La PPA fue descrita por primera vez por Montgomery (Montgomery, 1921) en el este de África, concretamente en Kenia. Actualmente, la PPA es enzótica en la mayoría de los países del África subsahariana (Lubisi et al., 2005; Lubisi et al., 2009; Roger et al., 2001) y en la Isla de Cerdeña, Italia (Giammarioli et al., 2011). Se extendió desde el continente africano a Europa en 1957. El primer caso de PPA en España tuvo lugar en el año 1960 (Polo-Jover and Sánchez-Botija, 1961) en Badajoz debido a la importación de una piara procedente de Portugal y con origen inicial en las antiguas colonias portuguesas de Mozambique. Gracias a las medidas de control puestas en marcha desde 1985 (Real Decreto 425/1985), se consideró erradicada la enfermedad en España en 1994 (BOE 213/ 1995).

A partir de un brote en el año 2007 en la región del Cáucaso (Georgia, Armenia y Azerbaiyán), la enfermedad se ha ido extendiendo en diversos países europeos, Rusia, Ucrania, Bielorrusia, etc. entre cerdos domésticos y jabalíes (Gabriel et al., 2011). La amenaza de la propagación de la PPA en el territorio de otros países de Europa del Este y

en Asia, por ejemplo, Kazajstán, y desde allí a países del sudeste asiático y China, constituye una grave amenaza para la industria mundial del ganado porcino con importantes consecuencias socioeconómicas. En estas circunstancias, sería prioritario disponer de una vacuna eficaz frente a la infección, actualmente inexistente.

2. EL VIRUS DE LA PESTE PORCINA AFRICANA

El VPPA forma parte de la superfamilia de virus núcleo-citoplásmicos DNA de gran tamaño junto a *Iridoviridae* y *Poxviridae* y es el único miembro de la familia *Asfaviridae* (International Committee on Taxonomy of Viruses. A.M.Q. King, 2011) y es el agente causante de esta enfermedad.

2.1 Morfología y estructura del virión

Las partículas virales del VPPA poseen una estructura compleja, similar a la familia *Iridoviridae.* Está constituido por aproximadamente 54 proteínas, entre las cuales se incluyen diversas enzimas necesarias para la transcripción de los genes tempranos del virus, como la ARN polimerasa o enzimas de modificación del ARNm (Kuznar et al., 1980; Salas et al., 1981). Presenta simetría icosaédrica, conteniendo varias capas concéntricas, cuyo diámetro total se aproxima a los 200 nm (Carrascosa et al., 1984; Carrascosa et al., 1986). Estas son desde la más interna a la más externa: nucleoide, core viral, membrana interna, cápsida y envuelta externa (Figura 1).

El nucleoide de 80 nm, de material proteico electrón-denso, contiene el genoma viral (Andres et al., 1997), nucleoproteínas, (Andres et al., 2002b; Borca et al., 1996; Munoz et al., 1993) y la maquinaria transcripcional para la síntesis y modificación de los ARNs tempranos. Está rodeado por una *matriz protéica* o core viral que procede en su mayoría del procesamiento de poliproteínas pp220 y pp60 (Andres et al., 2002b; Andres et al., 1997) originando las seis principales proteínas del core viral: proteínas p150, p37, p34 and p14, derivadas de la poliproteína pp220 y las proteínas p35 and p15, productos de la poli proteína pp62 (Andres et al., 2002a; Andres et al., 1997; Simon-Mateo et al., 1997; Simon-Mateo et al., 1993).

La cápside viral está mayoritariamente compuesta por la proteína p72 (Andres et al., 1997; Cobbold and Wileman, 1998; Garcia-Escudero et al., 1998), organizada en unos 2000 capsómeros de apariencia hexagonal, de longitud de 13 nm y anchura de 5-6 nm y que presentan un poro central. La distancia entre capsómeros es de 7,4 nm (Carrascosa et al., 1984). Otro componente de la cápside es la proteína pE120R, involucrada en el transporte de partículas virales maduras para la salida por gemación desde la célula, con la participación de la quinesina como motor para el transporte anterógrado del virus

(Andres et al., 2001). Los vértices de la cápside están constituidos por la proteína pB438L (Epifano et al., 2006). Por último, los viriones que salen de la célula por gemación adquieren una envuelta externa que rodea la cápside y que puede englobar a más de un virión (Carrascosa et al., 1984). Dicha membrana es dispensable para la infección (Andres et al., 2001; Breese and Hess, 1966).

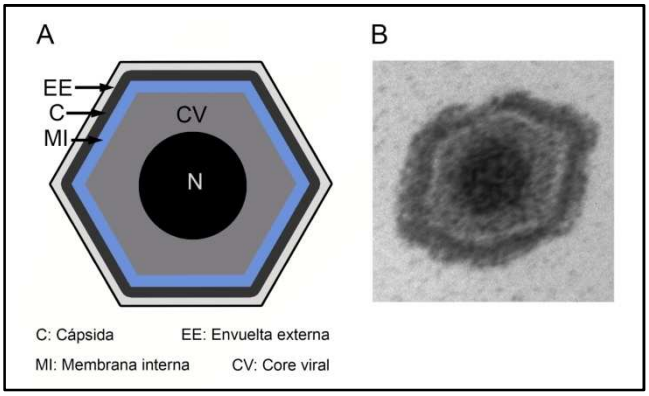

Figura 1. Estructura del virión de VPPA. (A) Representación esquemática de la estructura del virión de VPPA, donde se pueden apreciar las capas de la partícula viral. Las principales proteínas estructurales del virión a las que se harán referencia en esta tesis son p72 y pE120R en la cápside, la p54 localizada en la membrana interna y la p30, situada externamente en el virión. (B) Imagen de microscopía electrónica del VPPA.

2.2 Genómica funcional del VPPA

La estructura del genoma del VPPA es similar a la de los Poxvirus, consta de una molécula de ADN lineal bicatenario con los extremos unidos covalentemente entre sí en forma de horquilla (Gonzalez et al., 1986). La longitud del genoma varía entre los diferentes aislados virales, siendo esta entre 170 y 193 kilopares de bases (kpb) (Chapman et al., 2008; de Villiers et al., 2010; Yanez et al., 1995).

El gran tamaño de su genoma permite al virus codificar, entre 151 y 167 marcos de lectura abierta (ORFs, del inglés "*open reading frames*"), las cuales se encuentran separadas entre sí por menos de 200 pares de bases (pb) y son transcritas desde ambas hebras de ADN. Las grandes diferencias en la longitud del genoma y número de genes de unos aislados a otros, son en gran parte debido a la ganancia o pérdida de ORFs de las familias multigénicas codificadas por el virus (MGF en inglés "*multigene family*").

Actualmente se conoce la secuencia completa de 12 aislados de campo de diferentes procedencias geográficas y de un aislado adaptado a cultivo celular procedente de un aislado de campo español, denominado BA71V (Enjuanes et al., 1976; Gonzalez et al., 1986; Yanez et al., 1995), la más reciente, es la del aislado Georgia (Chapman et al., 2011).

El análisis de la secuencia del genoma de BA71V permitió clasificar algunos de sus genes más representativos de acuerdo a su función asignada. La nomenclatura empleada para designar los genes se basa en la fragmentación de la enzima de restricción EcoR I desde el extremo 5', según el número de aminoácidos codificados y la dirección en la que el gen es

transcrito (L hacia la izquierda y R hacia la derecha) (Rodriguez et al., 1992). Aquellos genes caracterizados en el aislado de Malawi, se nombran de acuerdo a otra nomenclatura.

Localizada en el extremo 5´ en cada gen hay una secuencia corta que contiene el promotor que es reconocido por el complejo de la ARN polimerasa viral. Las secuencias de promotores son generalmente cortas y ricas en A + T y son reconocidas por factores de transcripción codificados por el virus, específicos para las diferentes etapas de expresión génica del virus: genes tempranos (inmediatamente tempranos y tempranos), intermedios y tardíos.

2.2.1 Expresión génica del VPPA

La expresión génica del VPPA parece seguir un mecanismo en cascada, similar al descrito para los poxvirus (Moss, 2001). Los genes inmediatamente tempranos y tempranos se expresan antes del inicio de la replicación del ADN (genes pre-replicativos), debido a la acción de enzimas implicadas en la transcripción, empaquetadas en el core viral. Estos genes codifican enzimas implicadas en el metabolismo de nucleótidos y en la replicación del ADN, así como la expresión de factores de transcripción necesarios para la expresión de los genes tardíos (Almazan et al., 1992; Almazan et al., 1993; Kuznar et al., 1980; Rodriguez et al., 1996; Salas et al., 1981)..

La replicación del ADN viral, mediante un mecanismo de autoiniciación (Baroudy et al., 1982), emplea la ADN polimerasa del propio virión (Martins et al., 1994; Moreno et al., 1978) y tiene lugar en dos fases: una pequeña fase inicial que tiene lugar en el núcleo (Garcia-Beato et al., 1992; Rojo et al., 1999; Tabares and Sanchez Botija, 1979), y una segunda y mayoritaria fase de replicación (con un pico máximo a las 8 hpi) que tiene lugar en áreas citoplásmicas perinucleares de la célula huésped, denominadas factorías víricas.

Las enzimas requeridas para la replicación son expresadas también inmediatamente después de la penetración del core viral, parcialmente desencapsidado en el citoplasma, como se ha mencionado anteriormente (Salas et al., 1983).

Tras el inicio de la replicación del ADN en el citoplasma, aproximadamente 6 h después de la infección, comienzan a transcribirse los genes intermedios y tardíos (genes post-replicativos) (Rodriguez et al., 1996; Salas et al., 1986). Estos genes codifican las proteínas estructurales del virión y enzimas como polimerasas y factores de transcripción tempranos, que serán empaquetados en los nuevos viriones (Kuznar et al., 1980; Pena et al., 1993; Salas et al., 1988). Se conoce muy poco acerca de los mecanismos reguladores específicos que controlan la expresión de los genes del VPPA en esta secuencia temporal.

2.2.2 Productos génicos

El genoma del VPPA contiene una serie de genes que codifican numerosas proteínas de rango de huésped, genes de virulencia y reguladoras de diferentes funciones celulares. Un ejemplo es el gen *DP71L* en el aislado BA71V (Yanez et al., 1995) y *23-NL* en el aislado Malawi (Zsak et al., 1996) que inhibe el cese global de la síntesis de proteínas inducido por la fosforilación de de eIF-2α por PKR u otras quinasas como PERK (Rivera et al., 2007; Zhang et al., 2010). También las *MGF 360 y 530* (Zsak et al., 2001b) determinan el tropismo, virulencia y en la supresión de la respuesta a interferón (Afonso et al., 2004; Zsak et al., 2001a). El VPPA codifica para proteínas implicadas en la evasión del sistema inmune, como el *EP402R o CD2v*, un gen homólogo al *CD2* celular (Borca et al., 1998; Borca et al., 1994) y el *A238L*, homólogo viral de las proteínas celulares IκB, que actúa bloqueando la activación de la transcripción de genes inmunomoduladores (Granja et al., 2008; Miskin et al., 1998). El virus regula la respuesta apoptótica de la célula infectada mediante el homólogo viral a la proteína anti-apoptótica celular Bcl-2, codificado por el gen *A179L*, actúa evitando la muerte celular programada de la célula antes de completarse la replicación del genoma viral (Brun et al., 1996; Hernaez et al., 2004a). Recientemente se ha descrito un papel dual para *A179L* que inhibe la autofagia mediante la interacción con Beclin 1 (Hernaez et al., 2013). El producto del gen *A224L*, homólogo a las proteínas celulares inhibidoras de apoptosis (IAP) inhibe la activación de la caspasa 3 (Nogal et al., 2001).

2.3 Ciclo infectivo

El ciclo infectivo del VPPA comienza con la adsorción y la entrada en la célula. Tiene una duración de 18 a 24 horas (Costa, 1990), desarrollándose principalmente en macrófagos en el tejido linfático y en monocitos, megacariocitos y leucocitos polimorfonucleares presentes en sangre y médula ósea (Plowright et al., 1968; Ramiro-Ibanez et al., 1996; Ramiro-Ibanez et al., 1997). El virus fue adaptado a crecer en la línea celular Vero, obteniendo así el aislado no virulento BA71V (Enjuanes et al., 1976), que se ha convertido en el mejor caracterizado a nivel molecular y ha permitido grandes avances en el estudio del ciclo infectivo del VPPA.

2.3.1 Unión y entrada del VPPA en la célula

El VPPA se internaliza en la célula diana por endocitosis mediada por receptor dependiente de temperatura y pH ácido, (Alcami et al., 1989a; Valdeira and Geraldes, 1985), sin que se conozca la naturaleza de la/s proteína/s celular/es implicada/s. Hasta el

momento se han identificado las proteínas del virión p12 y p54 involucradas en el reconocimiento de la célula diana y la proteína p30 como implicada en la internalización del virus (Angulo et al., 1992; Angulo et al., 1993; Gomez-Puertas et al., 1998). Esta fase inicial del ciclo parece requerir complejas interacciones entre estas 3 proteínas virales, sin descartar la mediación de co-receptores celulares.

En efecto, se ha podido demostrar la neutralización del virus *in vitro*, mediante anticuerpos específicos frente a p54 y p30 (Gomez-Puertas et al., 1996), obtenidos en animales infectados con virus atenuados. Sin embargo, no han tenido éxito ensayos de neutralización del virus con diferentes anticuerpos dirigidos frente a diversos epítopos presentes en p12.

La célula diana del virus es el macrófago porcino y es muy restrictivo en su tropismo celular. La infección productiva del VPPA en macrófagos está ligada a la expresión del receptor "*scavenger*" CD163 (Sanchez-Torres et al., 2003), de modo que anticuerpos frente a dicho receptor inhiben la adsorción del virus en macrófagos. Asimismo, *in vivo*, tanto en sangre periférica como en órganos linfoides, el virus infecta de forma preferente la subpoblación de macrófagos que expresan este marcador de maduración celular. Es muy limitado el número de líneas celulares que infecta en cultivo y son escasas aquellas en las que VPPA puede completar su ciclo replicativo, encontrando restricciones para la infección productiva a diferentes niveles (Carrascosa et al., 1999). La línea celular Vero es la más utilizada para numerosos estudios en VPPA, ya que es permisiva para los virus adaptados a cultivo.

La entrada del virus en la célula infectada se ha caracterizado como un proceso dependiente de dinamina y mediado por clatrina (Hernaez and Alonso, 2010). El análisis bioquímico y molecular de la entrada del VPPA utilizando el inhibidor específico de la dinamina, dinasore (Din) y el mutante dominante negativo (DN) de dinamina 2 revelaron que la endocitosis del virus es dependiente de la GTPasa dinamina (Hernaez and Alonso, 2010). Además, la utilización del inhibidor clorpromacina y el "*knock out"* del adaptador de la clatrina Epsina 15 por expresión de un DN, afectan profundamente a la infectividad viral y consecuentemente la producción de virus. A tiempos tempranos de la infección, los viriones colocalizan con las cadenas pesadas de clatrina (Hernaez and Alonso, 2010), observaciones apoyadas por las imágenes de microscopía electrónica de partículas virales adsorbidas frecuentemente en fosetas que recuerdan a invaginaciones recubiertas de clatrina (Alcami et al., 1989a).

Se han señalado otras vías posibles de entrada para el virus como macropinocitosis (Sanchez et al., 2012) o fagocitosis (Basta et al., 2010), aunque debido a su función en la

incorporación de nutrientes en la mayoría de células de mamíferos, serían poco compatibles con el estricto rango de células susceptibles al virus. Es desconocido si estas rutas de entrada son eficientes para una infección productiva y si podrían constituir rutas alternativas o cooperativas de entrada (Alonso et al., 2013).

Además, la entrada de VPPA requiere colesterol, ya que es sensible a la eliminación del colesterol en la membrana por β-metil-ciclodextrina (Bernardes et al., 1998; Hernaez and Alonso, 2010). Además de dinamina, clatrina y sus adaptadores, también en fases tempranas de la infección, son necesarias la actividad de la enzima PI3K, la activación de la GTPasa Rac1 y la integridad de la ruta de biosíntesis del colesterol (Quetglas et al., 2012). Algunos de los requerimientos del VPPA a nivel de su entrada están resumidos en el Video 1, uno de cuyos fotogramas se muestra en la Figura 2.

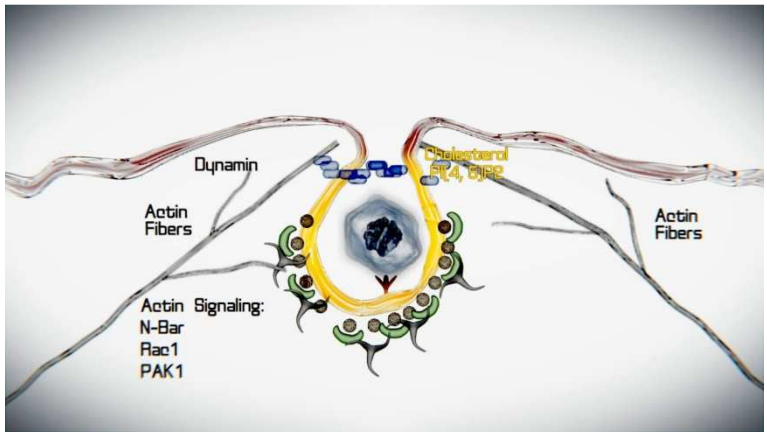

Figura 2. Fotograma del video 1 con el esquema de la entrada del VPPA en células vero. Se muestran las moléculas implicadas en la entrada del VPPA en las células mediante endocitosis mediada por clatrina, además de las fibras de actina, próximas a la membrana plasmática.

Una vez que el virus ingresa en la célula, la mayor parte de las rutas de entrada confluyen en la vía endocítica. Con los datos actuales, habría que averiguar si en dicha ruta se encuentra la mayor restricción del virus para desarrollar una infección productiva, cuyo estudio es el objetivo de este trabajo de tesis.

2.3.2 Morfogénesis y etapas finales

Las fases finales del ciclo infectivo comprenden el ensamblaje y la liberación de los viriones maduros (Smith and Enquist, 2002). La primera indicación morfológica de ensamblaje de los viriones formados *de novo,* es la acumulación dentro de la factoría vírica (FV) de membranas virales, que generalmente aparecen como pequeñas estructuras curvas y abiertas, y son los precursores de la membrana viral interna, procedentes de las cisternas del RE, ausentes en la factoría, pero no en la periferia de esta (Andres et al., 1998).

La factoría vírica del VPPA se reconoce como un acúmulo ADN y proteínas víricas en la zona perinuclear que hasta el momento ha sido descrito como carente de organelas

excepto ribosomas. Su formación comienza a partir de múltiples acúmulos de pequeño tamaño o factorías tempranas que son móviles alrededor del núcleo y que posteriormente confluyen en una sola ubicación coincidente con el MTOC (Hernaez et al., 2006).

Estas áreas perinucleares se caracterizan por la presencia de partículas virales totalmente ensambladas, observándose también una serie ordenada de partículas virales intermedias cuya cápside presenta, desde un único lado, hasta los seis que forman el hexágono definitivo. El ensamblaje de las partículas virales generadas durante el ciclo infectivo, conlleva también la inclusión del ADN viral sintetizado, junto con las enzimas que incorpora el virión, en el interior de cápsidas de nueva síntesis (Nunes et al., 1975). El proceso de incorporación del genoma viral no siempre se completa, ya que es muy frecuente observar partículas virales vacías en la membrana plasmática para ser liberadas por gemación a las células vecinas.

Parte de las partículas víricas infecciosas recién constituidas es transportada hacia la membrana citoplasmática por un mecanismo mediado por microtúbulos (Andres et al., 2001). Finalmente, estos viriones son expulsados de la célula por gemación precedida de la evaginación de la membrana citoplasmática (Breese and Hess, 1966), dando lugar a viriones extracelulares, que se rodean de una envuelta lipídica laxa y frágil. Este proceso no es muy eficiente, ya que la fracción de virus extracelular es relativamente baja con respecto a la fracción de virus intracelular. Sin embargo, se piensa que el efecto citopático producido en las células infectadas por el VPPA, puede representar finalmente un segundo mecanismo de liberación masiva de las partículas víricas producidas. La apoptosis tardía descrita en las células infectadas (Hernaez et al., 2004b; Hernaez et al., 2006; Ramiro-Ibanez et al., 1996; Ramiro-Ibanez et al., 1997), finalizaría con la generación de cuerpos apoptóticos cargados de viriones maduros. En la fase final del proceso de apoptosis, se produce un burbujeo o "*blebbing"* de la MP, cuya inhibición disminuye en gran medida la liberación de virus al medio extracelular (Galindo et al., 2012). Los cuerpos apoptóticos pueden ser consumidos por células fagocíticas, lo que significa la difusión de los viriones a nuevas células pasando inadvertido para el sistema inmune (Teodoro and Branton, 1997).

3. ENDOCITOSIS

3.1 Endocitosis y explotación de las vías endocíticas por los virus

Existen multitud de rutas a través de las cuales las células incorporan material desde el exterior (Dharmawardhane et al., 2000; Kirkham and Parton, 2005; Mayor and Pagano, 2007; McMahon and Boucrot, 2011; Rothberg et al., 1992; Schmid and McMahon, 2007; Sorkin, 2004). La explotación de la vía endocítica celular conlleva una serie de ventajas

relevantes para los virus. Una de la más importantes es la posibilidad de atravesar fácilmente el citoplasma, rebosante de múltiples estructuras celulares, evitando así la red de actina cortical (Sodeik, 2000). Otra de la ventajas de los virus al ser endocitados es el evitar dejar "pruebas" en la membrana plasmática de la célula detectables por las defensas celulares (Marsh and Helenius, 2006). Además, algunas de las características propias de las vesículas endocíticas, al sufrir procesos madurativos como la acidificación del pH, se convierten en sensores que estos patógenos son capaces de identificar como el lugar preciso para comenzar procesos de desencapsidación y penetración en el citoplasma (Marsh and Helenius, 1989). Teniendo en cuenta las ventajas que confiere, no es de extrañar que multitud de virus animales exploten esta vía de entrada (Greber, 2002; Marsh and Helenius, 1989; Marsh and Helenius, 2006; Smith and Helenius, 2004).

Normalmente, la entrada de los virus en la célula comienza con la unión de proteínas de anclaje y la asociación con uno o más receptores. Los virus utilizan las moléculas presentes en sus envueltas externas para imitar la estructura de ligandos celulares y unirse a receptores celulares de distinta naturaleza, como por ejemplo moléculas de adhesión celular, componentes de la matriz extracelular y azúcares. Sin embargo estos receptores son desconocidos en el caso del VPPA. Se han descrito casos de agrupamiento de receptores en microdominios de la MP tras ser activados por la unión de partículas virales (Coyne and Bergelson, 2006). Estas interacciones con receptores son generalmente débiles, pero el contacto con múltiples receptores hace que la interacción sea de gran avidez y que la unión a la célula huésped sea prácticamente irreversible. Después se desencadena la activación de mecanismos de señalización celular, en los que suelen participar multitud de quinasas (Pelkmans et al., 2005) y que finalmente desembocan en la internalización de la partícula viral (Marsh and Helenius, 2006; Mercer et al., 2010).

Tras el paso a través de la MP y la liberación al lumen de endosomas, caveosomas o RE, se producen cambios conformacionales en el virión que promoverán su penetración en el citoplasma con el fin de liberar el material genético, la cápside viral o la partícula viral intacta (Mercer et al., 2010), o bien directamente por penetración al citoplasma tras fusionarse con la MP dependiendo del modelo vírico estudiado.

Así, los virus envueltos pueden internalizarse en la célula a través de la vía endocítica mediante vesículas recubiertas de clatrina como el virus de bosque de Semliki (Helenius et al., 1980), el virus de la estomatitis vesicular (VSV, del inglés *"vesicular stomatitis virus"*) (Cureton et al., 2009; Johannsdottir et al., 2009), el virus de la Influenza A (Lakadamyali et al., 2004), o el VPPA (Hernaez and Alonso, 2010) acomodándose estas a la forma del virión (Mercer et al., 2010). También, la ruta de las caveolas ha sido reportada para la entrada de otros virus, como el coronavirus humano 229E (Kawase et al., 2009; Nomura et al., 2004),

el virus del simio 40 (SV40, del inglés "*simian virus 40*") (Anderson et al., 1996). Ambas rutas necesitan de la GTPasa dinamina para la fisión de la vesícula y su desprendimiento de la MP. Finalmente se produce un cambio en la partícula vírica en las diferentes vesículas que es dependiente de pH ácido, propio de este tipo de compartimentos endocíticos.

Como se ha mencionado, algunos virus pueden fusionar directamente con la MP liberando la cápside al citosol directamente. El virus de la inmunodeficiencia humana (HIV, de inglés, *"human inmunodeficiency virus"*) es un ejemplo de virus que utiliza este mecanismo (Thorley et al., 2010), aunque también se puede internalizar por la vía endocítica (Daecke et al., 2005; Miyauchi et al., 2009). El virus vaccinia, o el HSV tipo I también son capaces de entrar en la célula huésped por fusión directa con la MP, pero también pueden utilizar la vía endocítica (Nicola et al., 2003; Townsley et al., 2006). Los virus no envueltos penetrarán a través de perturbaciones en la MP formando un poro en la membrana plasmática (Tsai, 2007), así como utilizando una variedad de mecanismos que finalmente conducen a penetrar en organelas internas. Estas incluyen membranas endosomales como Adenovirus (Wickham et al., 1993), el aparato de Golgi (AG) explotado por el virus del Papiloma (Day et al., 2003), o el RE, utilizado por el SV40 (Pelkmans et al., 2001; Schelhaas et al., 2007). En la Tabla nº1 se resumen las características de las vías de entrada para diversas familias de virus.

3.2 Mecanismos de endocitosis

Las vías endocíticas mejor caracterizadas son aquellas dependientes de la dinamina, como la endocitosis dependiente de clatrina y otras vías de endocitosis, entre las que destaca la ruta de las caveolas/balsas de lípidos o "*lipid rafts".* Además se han descrito, rutas independientes de la dinamina como la macropinocitosis, fagocitosis, etc. (Doherty and McMahon, 2009; Marsh and Helenius, 2006; Mercer et al., 2010). Estudios recientes acerca de diferentes vías de entrada utilizadas por los virus, han demostrado que estas funcionan como una compleja red de rutas interconectadas (Vazquez-Calvo et al., 2012), permitiendo así caracterizar tanto nuevas rutas de endocitosis, como nuevas conexiones entre las organelas de diferentes rutas (Pelkmans and Helenius, 2003). Otros mecanismos menos estudiados son la endocitosis mediada por flotilina/Arf6 (Donaldson, 2003; Glebov et al., 2006; Kalia et al., 2006; Langhorst et al., 2008), por Interleuquina 2 (Lamaze et al., 2001), o por otros transportadores independientes de clatrina (CLIC del inglés *"Clathrin-independent carrier"*/o por unión a GPI (Glicosilfosfatidilinositol) (GEEC, del inglés "*GPI-anchored protein enriched early endosomal compartment")* (Kirkham and Parton, 2005;

Mayor and Pagano, 2007). La endocitosis mediada por clatrina es el mecanismo más conocido a nivel molecular. Además de su relevancia en los procesos fisiológicos de la célula (internalización de receptores, etc.), es utilizado por diversos virus envueltos como vía de entrada en las células mamíferas, por ejemplo el VSV (Sun et al., 2005), el virus del bosque de Semliki (Helenius et al., 1980) y el virus del Nilo Occidental (Chu and Ng, 2004). Influenza y HIV-1 también pueden usar esta vía como alternativa (Daecke et al., 2005; Sieczkarski and Whittaker, 2002). Las vesículas recubiertas de clatrina son constituidas tras un proceso en cinco etapas a juzgar por los estudios de ultraestructura y biología celular. Estos son, iniciación, selección de carga, ensamblaje del recubrimiento, escisión de la MP y desensamblaje del revestimiento. Tras la selección de carga e iniciación de la invaginación, los trieskeliones de clatrina (unidad de ensamblaje), polimerizan en hexágonos y pentágonos recubriendo la vesícula en formación a través de adaptadores, por ejemplo Proteína adaptadora 2 (AP2), proteínas de dominio BAR (Doherty and McMahon, 2009; Merrifield, 2012; Merrifield et al., 2002; Taylor et al., 2011; Traub, 2009) y otras proteínas accesorias, como AP180 y Epsinas (Epsina15, Ede1 en levaduras). Una vez la vesícula recubierta de clatrina se escinde al citosol gracias a la colaboración de la GTPasa dinamina, proceso en el cuál puede cooperar la actina en caso necesario (Cureton et al., 2009; Cureton et al., 2010; Moreno-Ruiz et al., 2009; Pizarro-Cerda et al., 2010; Veiga and Cossart, 2005), la vesícula pierde su revestimiento y las moléculas implicadas se reciclan de nuevo hacia la MP (McMahon and Boucrot, 2011; Merrifield, 2012; Merrifield et al., 2002; Merrifield et al., 2005). Ejemplos característicos de proteínas internalizadas mediante endocitosis mediada por clatrina son, el factor de crecimiento epidérmico (EGF, del inglés "*epidermal growth factor*") o la transferrina. Este mecanismo de endocitosis es altamente eficiente y rápido, ya que desde el reclutamiento de las moléculas necesarias hasta la escisión de las vesículas recubiertas de clatrina transcurren 30-100 segundos (Taylor et al., 2012; Taylor et al., 2011). Una vez que la vesícula revestida de clatrina es internalizada y pierde su revestimiento, fusiona con los endosomas tempranos (EE, del inglés "*early endosomes*"). Estas vesículas son actualmente reconocidas como la principal estación de clasificación de la vía endosomal (Huotari and Helenius, 2011).

Aun utilizando diferentes vías de entrada, diversos patógenos confluyen en la vía endocítica, siendo el control y la utilización de este sistema celular un objetivo común a diversas familias de virus como patógenos intracelulares estrictos, en su proceso de infección. Por ello nuestro estudio, se ha centrado en la función de la vía endocítica y su señalización en la infección por el VPPA.

Tabla nº1. Ejemplos de rutas de internalización y organelas de desencapsidación de distintas familias de virus.

Vía preferente de entrada	**Familia (ADN/ARN)**	**Replicación nuc/cito**	**Ejemplo de virus envuelto (S/N)**	**Dependencia pH ácido (S/N) y "uncoating"**	**Receptor**	**Referencias**
Clatrina	Rabdovirus (ssARN-)	Citop	V. estomatitis Vesicular (S)	(S) <6,4 EE/MVB	¿?	(Le Blanc et al., 2005) (Mire et al., 2010) (Matlin et al., 1982)
Clatrina	Alfavirus (ssARN+)	Citop	V. Bosque de Semliki (S)	(S) EE	¿Gags?	(Sieczkarski and Whittaker, 2003) (Marsh et al., 1983)
Clatrina	Alfavirus (ssARN+)	Citop	V. Sindbis (S)	(S) <6,2 ¿LE?	¿Gags?	(Smit et al., 1999) (DeTulleo and Kirchhausen, 1998)
Clatrina/ Nueva vía	Flavivirus (ssARN+)	Citop	V. del Dengue (S)	(S) LE	GAGs, DC-SIGN	(van der Schaar et al., 2008) (Acosta et al., 2009)
Clatrina	Flavivirus (ssARN+)	Citop	V. de Hepatitis C (S)	(S) EE	GAGs, LDLR, SRB1, CD81	(Meertens et al., 2006) (Helle and Dubuisson, 2008)
Clatrina	Adenovirus (dsADN)	Nuc	Adenovirus tipo 2 y 5 (N)	(S) <6 EE	CAR, αV integrins	(Gastaldelli et al., 2008) (Medina-Kauwe, 2003) (Miyazawa et al., 2001)
Clatrina	Picornavirus (ssARN+) Aphtho	Citop	V. de la fiebre Aftosa (N)	(S) EE ¿ER?	αV integrins	(Johns et al., 2009) (O'Donnell et al., 2005)
Clatrina	Picornavirus (ssARN+)	Citop	Rinovirus humano tipo 2 (N)	(S) < 5,6 MVB/LE	Receptor LDL	(Brabec-Zaruba et al., 2009) (Snyers et al., 2003)
Clatrina	Reovirus (dsARN)	Citop	Reovirus (S)	(S) EE	JAM1	(Ehrlich et al., 2004) (Forzan et al., 2007)
Clatrina	Parvovirus (ssADN)	Nuc	Parvovirus canino (N)	(S) LE	Receptor de transferrina	(Cotmore and Tattersall, 2007) (Suikkanen et al., 2003)
Clatrina	Retrovirus (ssARN)	Nuc	Leucosis aviar (S)	(S) ¿LE?	Receptor de transferrina	(Diaz-Griffero et al., 2005) (Diaz-Griffero et al., 2002) (Mothes et al., 2000)
Clatrina/nueva vía	Mixovirus (ssARN-)	Nuc	Influenza A (S)	(S) < 5,6 LE	Sialoglico-proteínas	(Sieczkarski and Whittaker, 2003) (Rust et al., 2004) (Chen and Zhuang, 2008) (Matlin et al., 1981)

Tabla nº 1. Continuación.

Vía preferente de entrada	Familia (DNA/RNA)	Replicación nuc/cito	Ejemplo de virus envuelto (S/N)	Dependencia pH ácido (S/N)	Receptor	Referencia
Macro/ Fusión MP	Poxvirus (dsADN)	Citop	Virus Vaccinia	(S/N) < 5,0) Macropinosoma Fusión MP	¿Gags?	(Locker et al., 2000) (Mercer and Helenius, 2008) (Townsley et al., 2006)
Macro	Adenovirus (dsADN)	Nuc	Adenovirus tipo 3 (N)	(S) (< 6) Macropinosoma ¿EE por endocitosis?	CD46, αV integrins	(Amstutz et al., 2008) (Sirena et al., 2004)
Macro/CAV?	Picornavirus (ssARN+)	Citop	Ecovirus tipo 1 (N)	(S) Macropinosoma Caveolas?	α2β1 integrins	(Liberali et al., 2008) (Karjalainen et al., 2008)
Macro	Picornavirus (ssARN+)	Citop	Virus Coxackie B (S)	(S/N)	CAR	
Macro/ Fusión MP	Virus del Herpes (dsADN)	Nuc	Virus del Herpes Simple 1 (S)	(S) (< 6) Fusión MP/EE	¿Gags?	(Nicola et al., 2003) (Nicola et al., 2005) (Butcher et al., 1990)
Macro	Virus del Herpes (dsADN)	Nuc	Virus del Herpes humano 8/(VSKH)	(S) LE	¿Gags?	(Liu et al., 2002)
Macro/ Fusión MP	Retrovirus (ssARN+)	Nuc	Virus VIH 1 (S)	(S) Fusión MP/endosomas	CD4, CCR5, CXCR4,CCR2	(Marechal et al., 2001) (Liu et al., 2002) (Nguyen et al., 2006) (Fontenot et al., 2007) (Kubo et al., 2012)
CAV1/LR	V. Polyoma (dsADN)	Nuc	Virus del simio 40 (N)	(S) RE	GM1	(Engel et al., 2011) (Pelkmans et al., 2001) (Anderson et al., 1996)
CAV1/LR	V.Papiloma (dsADN)	Nuc	Virus del papiloma humano 31 (N)	(S) RE/EE	¿Gags?	(Smith et al., 2007) (Sapp and Bienkowska-Haba, 2009)

Nuc: nuclear, Citop: citoplásmica, N: No, S: Si, Clatrina: Endocitosis mediada por clatrina, Macro: Macropinocitosis, CAV: caveolas, MP: Membrana plasmática, CAV1: caveolina 1, LR: *"Lipid Rafts"* o balsas lipídicas

3.3 La vía endocítica, compartimentos, maduración y características

De modo esquemático, la vía endocítica está constituida por un sistema de degradación, en el que se transportarán fluidos, componentes de la MP y otras moléculas cuyo destino final es la eliminación. Aunque este sistema no es unidireccional. Existe un circuito de reciclaje para los componentes que han de ser devueltos a la MP y para diversos ligandos y receptores.

Podemos distinguir diferentes compartimentos a la largo de la vía endocítica que son el resultado de los cambios producidos por la maduración de los endosomas (Figura 3). Así morfológica y fisiológicamente podemos diferenciar los EE (del inglés "*early Endosomes"*), que reciben la carga endocitada desde la MP, los cuerpos multivesiculares (MVB, "*multivesicular bodies*"), endosomas tardíos (LE, "*late endosomes*") y lisosomas (LI).

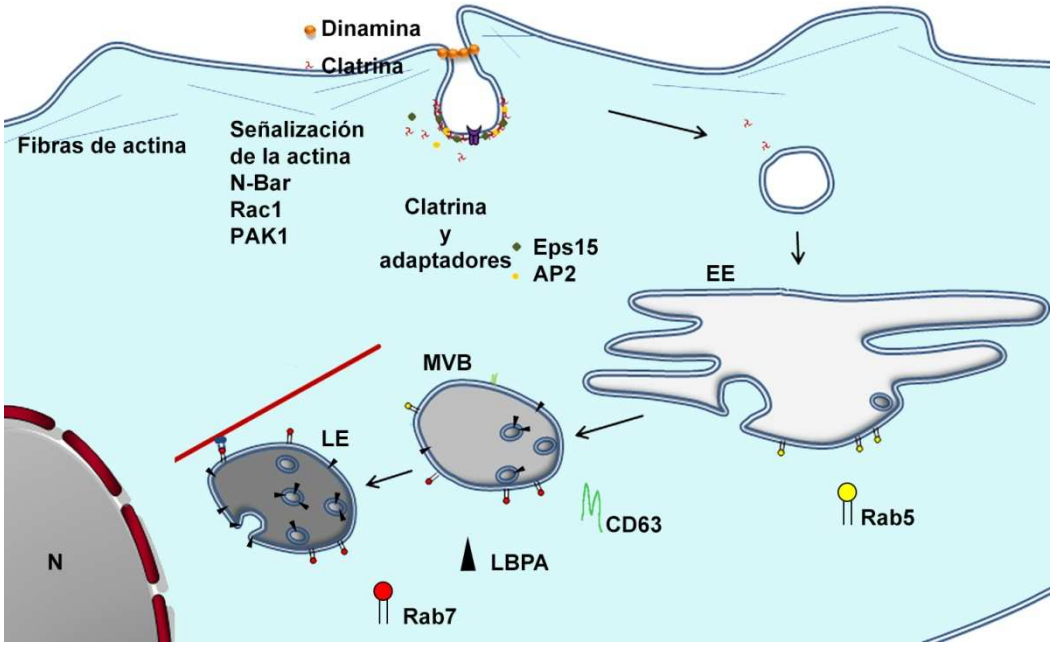

Figura 3. Red endosomal: En el esquema se muestran las principales proteínas implicadas en la señalización de la actina, que colabora con la clatrina para generar y constreñir las vesículas recubiertas de clatrina. Estas a su vez, se reciclan a la membrana plasmática cuando la vesícula recién formada circula por el citoplasma. Las principales vesículas reflejadas son los endosomas tempranos (EE), cuerpos multivesiculares (MVB) y endosomas tardíos (LE). El dominio vacuolar de las organelas anteriores contienen vesículas intraluminales (ILV), más numerosas en los LE. Los endosomas contienen componentes específicos, así Rab5 es propia de EE, mientras que CD63, LBPA y Rab7 son característicos de vesículas más maduras de la vía.

3.3.1 Endosomas tempranos

Los EEs reciben la carga endocitada no solo desde la endocitosis mediada por clatrina, sino también de otras vías, incluyendo vías dependientes de caveolas, GEEC y ARF6 (Doherty and McMahon, 2009; Mayor and Pagano, 2007). Los EEs constituyen el primer compartimento que recibe la carga que llega desde la MP, por ejemplo son

compartimentos dinámicos con una elevada capacidad de fusión entre ellos (homotípica) y con un pH luminal alcalino entre 6,8 y 6,1 (Gruenberg et al., 1989). El virus del bosque de Semliki es capaz de fusionar su envuelta a el pH propio de lo EEs (Sieczkarski and Whittaker, 2003) haciendo innecesario el paso por los LEs. El VSV muestra un amplio rango de pH para hacerlo, lo que le convierte en independiente de los LEs (Gruenberg, 2009; Le Blanc et al., 2005; Sieczkarski and Whittaker, 2003). Sin embargo, numerosos virus requieren del pH ácido del LE para completar su mecanismo de entrada.

El EE es un orgánulo de elevada complejidad y organización que consiste en una región o dominio de cisternas y estructuras tubulares laterales de unos 60 nm de diámetro, desde los que se generan los endosomas de reciclaje, que devolverán el material endocitado a la MP. Estas cisternas parten de un dominio de estructura vesicular central de aproximadamente 300-400 nm de diámetro (Gruenberg, 2001). En este dominio vesicular se generan las vesículas intraluminales (ILVs, del inglés, "*intraluminal vesicles*") por invaginaciones de la membrana limitantes del EE, partir de la acción del ESCRT o complejo de clasificación endosomal requerido para el transporte (ESCRT, del inglés "*endosomal sorting complex required for transport*"). Las formación de las ILVs será de gran importancia funcional, y son representativas de la maduración del orgánulo que progresa en la vía degradativa.

Las Rab GTPasas son una familia de pequeñas GTPasas monoméricas que funcionan como interruptores moleculares en el tráfico de vesículas, alternando dos estados conformacionales, unido a GDP "apagado", o unido a GTP "activado (Jordens et al., 2005; Stenmark, 2009). Por interacción con uno o más de sus efectores, las proteínas Rab crean subdominios altamente específicos, otorgando junto con los fosfoinosítidos o FIs**,** lo que se conoce como "identidad" a la membrana endosomal. Rab5 se sitúa en la membrana de los EE regulando la maduración de estas vesículas, junto con sus efectores. Uno de ellos, el antígeno 1 del EE (EEA1**,** del inglés "*Early Endosome Antigen 1"*) participa en procesos de fusión homotípica en el EE. De modo general, el paso o maduración de los EE a los LE viene marcado por el cambio en las Rab GTPasas presentes en las membranas de ambas vesículas, siendo Rab5 propia de EE y Rab7 propia de LE (Zerial and McBride, 2001).

3.3.2 Maduración endosomal

La formación de un nuevo LE a partir de un EE, es precedido por la generación de un dominio de Rab7 en el EE (Rink et al, 2005; Vonderheit and Helenius, 2005). A partir de este, se generará la formación de un endosoma híbrido con Rab5 y Rab7 en su membrana. La regulación de procesos madurativos subyacentes pasan la estricta regulación de la presencia en las membranas endosomales de estas Rab GTPasas y de su capacidad para

intercambiarse en la transición desde EE a LE, que viene marcado por la pérdida de Rab5, y la adquisición de Rab7 en la membrana (Cabrera and Ungermann, 2010; Poteryaev et al., 2010; Rink et al., 2005).

El modo en que los dominios del EE se pierden durante la formación del LE está por dilucidar, aunque existen dos posibles hipótesis. Los EE que contienen en su membrana Rab5-GTP, después de reclutar Rab7, es convertido a Rab5-GDP y así se disocia de la membrana endosomal junto con sus efectores (Rink et al, 2005). La otra opción es la aportada por dos autores relevantes en el campo de la endocitosis como son Jean Gruenberg y Harald Stenmark. Estos recogen la generación de MVBs/ECV (del inglés "*endosomal carrier vesicle*"), como un orgánulo intermediario entre EE y LE (Gruenberg and Stenmark, 2004).

Los MVBs se constituyen a partir del dominio vesicular de EEs (Gruenberg and Stenmark, 2004), conteniendo de este modo las moléculas internalizadas por endocitosis. También reciben cargas desde la red del trans-Golgi (TGN), por ejemplo los precursores de enzimas lisosomales (Raiborg et al., 2003). Son orgánulos que consisten en una membrana limitante que encierra en el lumen gran cantidad de ILVs de 40-90 nm (Katzmann et al., 2002). La presencia de ILVs en el lumen es característica de MVB/LE y dan al orgánulo su característica morfología multivesicular. Estas comienzan a generarse en los EEs en un proceso regulado por el ESCRT y que tiene lugar en la cara citosólica de los EEs, en "placas" características que contienen clatrina y componentes del ESCRT. Esta maquinaria es responsable de la clasificación de proteínas de membrana y receptores ubiquitinados dentro de las ILVs, desde los EEs y MVBs hacia los LEs/LIs (Raiborg et al., 2002; Raiborg and Stenmark, 2009; Sachse et al., 2002). En gran parte de tipos celulares estos MVBs maduran "hacia", o fusionan con LEs, los cuales fusionan en último término con LIs (Raiborg et al., 2003), participando en este proceso el fosfatidil inositol 3,5 bifosfato (FtdIns(3,5)P_2). Los FIs son profundamente relevantes en la coordinación de la maduración de las vesículas, completando una importante transformación y maduración, la cual provee a los patógenos aprovechan esta ruta, de las características fisiológicas necesarias para completar las etapas iniciales de sus ciclos infectivos (Huotari and Helenius, 2011). (La función de los FIs se tratará con mayor detalle más adelante).

3.3.3 Endosomas tardíos

Los LE presentan un pH luminal en un rango desde 6,0 a 4,8, más ácido que el de los EEs. Esta acidificación se debe fundamentalmente a la acción de las ATPasas vacuolares (V-ATPasas), que bombean protones hacia el lumen del endosoma (Marshansky and Futai, 2008), aunque la acidificación también está afectada por la Na^+/K^+ ATPasa y los canales

por los que penetran iones como el Cl^-, o salen cationes como Ca^{2+}, Na^+ y K^+ (Huynh and Grinstein, 2007; Marshansky and Futai, 2008).

Como mencionamos anteriormente, el pH del LE es crucial para diversas infecciones víricas. Bunyavirus y el virus del Dengue necesitan alcanzar los LEs, para conseguir una infección productiva (Lozach et al., 2010; Sieczkarski and Whittaker, 2003; van der Schaar et al., 2008). El virus del HSV tipo 1, requiere pH ácido solo en función del tipo celular al que infecta (Nicola et al., 2005; Nicola et al., 2003). Al igual que la generación de las ILVs, la acidificación del pH es un indicador de la maduración endosomal. Los LEs son generados a partir del dominio vesicular del EEs. Las ILVs, y otras grandes partículas como virus, también están presentes en el lumen de los LEs y son en estos mucho más numerosas que en los EEs. La membrana de los LE puede contener colesterol, esfingolípidos, V-ATPasas, clatrina y componentes del ESCRT, todas ellas moléculas importantes para el correcto funcionamiento del orgánulo (Mukherjee and Maxfield, 2004).

Hoy en día se ha avanzado en gran medida en el conocimiento de la vía endocítica siendo considerada un órgano de clasificación activa de proteínas, lípidos, receptores, etc. a sus destinos celulares o para su reciclaje o degradación. Existe una población de ILVs diferente a la generada a partir del ESCRT descrita más arriba, que es propia de los LEs y rica en ácido lisobisfosfatídico (LBPA, del inglés "*Lysobisphosphatidic acid*"). El LBPA es un isómero estructural del fosfatidil glicerol, abundante principalmente en las ILVs del MVBs/LEs (Kobayashi et al., 2002; Kobayashi et al., 1998a), que tiene un papel en el control de las invaginaciones de la membrana endosomal y por tanto en la biogénesis del LE. El pH ácido induce al LBPA a deformar la membrana, lo que conduce a una invaginación, así se genera una población de ILVs a partir de la acción del LBPA, ricas en este fosfolípido. La función del LBPA está bajo el control de la proteína citosólica Alix, que se une a las membranas endosomales a través del LBPA (Bissig et al., 2013; Dikic, 2004; Matsuo et al., 2004). Por tanto, LBPA no solo es un marcador endosomal, sino que también tiene un papel importante en la regulación de la dinámica y función de las membranas internas del MVB y los LE.

3.3.4 Flujo de colesterol a través de la vía endocítica

El colesterol se encuentra principalmente en ILVs ricas en LBPA (Mobius et al., 2003), así la cantidad de LBPA también está relacionada con el nivel total de colesterol en las células, posiblemente por el papel del LBPA en su función de generar ILVs y por tanto en el control y capacidad de almacenaje endosomal de colesterol (Chevallier et al., 2008).

Las ILVs contienen mayores cantidades de colesterol, esfingolípidos, fosfatidilinositol 3 fosfato (FtdIns3P) y LBPA que la membrana del endosoma, y en función del momento de la

generación de estas ILVs su contenido será diferente. Así, el colesterol y el FtdIns3P es más abundante en ILVs más tempranas, mientras que LBPA y ceramidas están en altas cantidades en ILVs presentes en LEs (Mobius et al., 2003).

Los niveles celulares de colesterol están regulados a tres niveles: en la biosíntesis *de novo* de colesterol, a nivel de la incorporación de colesterol extracelular en forma de lipoproteínas de baja densidad (LDLs, del inglés "*low density lipoproteins"*) mediante endocitosis (Goldstein and Brown, 1984). Estas son las dos vías de incremento del colesterol celular (Ikonen, 2008). La regulación del nivel de colesterol celular se completa con la salida de colesterol de la célula mediante el transportador ABCA1 en la periferia celular (Cannon et al., 2006; Schmitt and Tampe, 2002) que regula la homeostasis de colesterol y fosfolípidos.

En condiciones fisiológicas normales el colesterol, en forma de LDLs, se internaliza por endocitosis y llega hasta los compartimentos endosomales tardíos, donde se hidroliza, generándose colesterol libre que se acumula en las ILVs de estos compartimentos, posteriormente se transporta al citosol por la acción de dos genes NPC1 and NPC2, cuyas formas mutadas causan la enfermedad de Niemann Pick, en la cual colesterol y esfingolípidos se acumulan en MVB/LEs (Karten et al., 2009; Sturley et al., 2004), causando una alteración del tráfico madurativo en la vía endolisosomal (Lebrand et al., 2002; Sobo et al., 2007; Vitner et al., 2010b).

Existen evidencias de que las ILVs ricas en LBPA pueden fusionar con la membrana limitante del LE, a este proceso, controlado por la proteína citosólica Alix, se le conoce como "*backfusion*" (Abrami et al., 2004; Kobayashi et al., 2002; Le Blanc et al., 2005). Puesto que el colesterol es distribuido a diversos destinos celulares desde las ILVs de los LEs, es altamente probable que este proceso involucre "*backfusion*" (Abrami et al., 2004; Le Blanc et al., 2005). Este es el fenómeno propuesto para el reciclaje de MHC II en células dendríticas, para los receptores de manosa 6 fosfato y las tetraspaninas, todos ellos se encuentran en las ILVs (Kleijmeer et al., 2001; Kobayashi et al., 2002; Kobayashi et al., 1998b; Trombetta and Mellman, 2005). La "*backfusion*" también ha sido sugerida como mecanismo de liberación de tóxicos y la cápsida de algunos virus envueltos como el VSV al citosol (van der Goot and Gruenberg, 2006).

Por otro lado, el colesterol sintetizado *de novo*, debe ser transportados desde el RE a otros orgánulos, como endosomas, LI, AG, mitocondrias y la MP (Holthuis and Levine, 2005). La proteína VAP-A del RE, y la proteína ORP1L en el LE, son dos proteínas importantes implicadas en estos procesos (Raychaudhuri and Prinz, 2010; Rocha et al., 2009). Se ha demostrado que los virus pueden afectar los niveles de colesterol celular durante la infección, como en el caso del virus de Hepatitis C (Syed et al., 2010). Además, cuando el

colesterol se reduce en las células huésped, la producción viral se ve afectada (Desplanques et al., 2010; Medigeshi et al., 2008). Las enzimas involucradas en los pasos intermedios de la biosíntesis de colesterol tales como 3-hidroxi-3- metilglutaril coenzima A reductasa (HMG-CoA) y mevalonato descarboxilasa difosfato (MVD) son importantes en la replicación viral (Mackenzie et al., 2007; Rothwell et al., 2009; Sidorkiewicz et al., 2009). Las estatinas, un tipo muy conocido de inhibidores utilizados para disminuir los niveles de colesterol en el tratamiento de enfermedades cardiovasculares mediante la inhibición de la HMG-CoA reductasa, también son eficaces contra el HIV (Oh and Hegele, 2007), el virus de Influenza (Fedson, 2006; Kruger et al., 2006) y el virus de Hepatitis C (Bader et al., 2008). Además, la vía del colesterol también es importante en la infección del virus del Nilo Occidental y el virus del Dengue (Lee et al., 2008; Mackenzie et al., 2007; Rothwell et al., 2009).

Del mismo modo que se ha visto su relevancia en diversas infecciones víricas, analizaremos la necesidad de la homeostasis del flujo del colesterol y el efecto de su acumulación en los LEs en la infección del VPPA.

3.4 Otras moléculas de señalización necesarias para la maduración de la vía endocítica. Los fosfoinosítidos

Los FIs derivan de la fosforilación reversible en 3 de los 5 grupos hidroxilo del anillo de inositol del FtdIns. Su generación local en las membranas está fuertemente regulada por la acción de fosfatasas y fosfoinositido quinasas (PIK) que provocan rápidas interconversiones entre ellos, alcanzando un gran control en la compartimentalización en la vía endocítica. La acción reguladora de los FIs se basa principalmente en dichas interconversiones, ya que permitirán la unión a la membrana del orgánulo a aquellas proteínas que presenten un dominio de unión a ese FI en particular, como por ejemplo proteínas con dominio PH (dominio con homología a la pleckstrina, del inglés *"Pleckstrin homology"*), o dominio FYVE (Fab1p, YOTB, Vac1 y EEA1)(Lemmon, 2008; Vicinanza et al., 2008).

En el caso que nos ocupa, los FIs más relevantes son FtdIns3P y FtdIns $(3,5)P_2$, dos lípidos que contribuyen a la identidad en las membranas de EE y LE (Figura 4). El FtdIns3P se encuentra principalmente en la cara citosólica de las membranas de EE, generados principalmente por la Fosfatidil inositol 3 kinasa (PI3K), la cual es reclutada por Rab5 GTP a través de la interacción directa con p150 (Behnia and Munro, 2005; Christoforidis et al., 1999; Zerial and McBride, 2001). FtdIns$(3,5)P_2$ es importante en pasos posteriores en la vía degradativa. Es generado por la fosfatidil inositol 3 fosfato 5 kinasa**,** PIKfyve. Su actividad está regulada por su activador ArPIKfyve y por la FtdIns$(3,5)P_2$ fosfatasa

(Shisheva, 2008), con la que forma un complejo estable fundamental para el funcionamiento de ambas actividades, quinasa y fosfatasa (Ikonomov et al., 2009; Sbrissa et al., 2008). El bloqueo de la síntesis de FtdIns(3,5)P_2 dirige la generación de un fenotipo altamente vacuolado (Ikonomov et al., 2001; Jefferies et al., 2008; Nicot et al., 2006; Rusten et al., 2006).

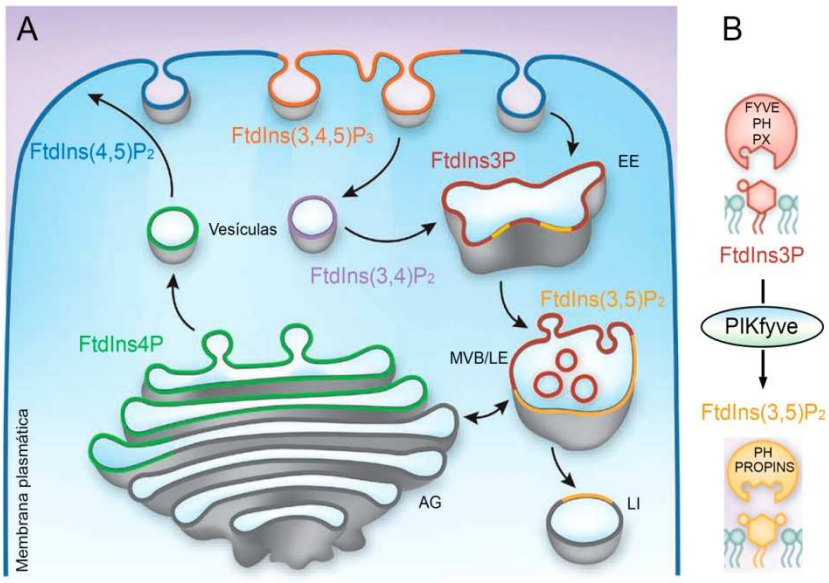

Figura adaptada y modificada de (Kutateladze, 2010).

Figura 4. Localización subcelular de PIs. (A) Los PIs se concentran en las diferentes organelas celulares. Por simplificar, se muestran los PIs predominantes en cada organela. (B) La conversión de FtdIns3P a FtdIns(3,5)P_2 es catalizada por la enzima PIKfyve. Se muestran los dominios proteicos que interaccionan con ambos PIs (FYVE, PH, PX y PROPIN).

En resumen, el programa madurativo de los endosomas conlleva diversos cambios en la señalización relacionada con esta vía, a saber, 1) el cambio de Rabs **o Rab "*switch*"**: Rab5 se cambia por Rab7 2) **La formación de ILVs**, 3) **La acidificación luminal** y el cambio de la composición iónica del lumen del endosoma: aumento de Cl^- y cambio en la concentración de Ca^{2+}, Na^+, K^+. 4) **La conversión de FtdIns3P a FtdIns(3,5)P_2,** 5) el cambio en **su tamaño y morfología**: Las extensiones tubulares presentes en EEs se pierden y el endosoma adquiere una forma y redonda u ovalada y aumenta de tamaño. 6) **la ganancia de hidrolasas y proteínas de membrana lisosomales**, 7) **El cambio en la especificidad de fusión**. El LE adquiere los complejos de anclaje para fusionar entre sí, con los LIs, o con autofagosomas. 8) La conversión del complejo **Corvet** a complejo **HOPS** en las membranas. Los complejos HOPS/Corvet están involucrados en varios procesos, incluyendo anclaje de membrana, el cambio de Rab5/Rab7 y también median el ensamblaje de las **SNAREs** y por tanto los eventos de fusión y finalmente, 9) **el cambio en la motilidad citoplasmática a posiciones cercanas al MTOC**: El LE se asocia con un conjunto de motores microtubulares que les permiten desplazarse hacia la región perinuclear. El transporte de los endosomas mediante microtúbulos, está directamente

ligado a su maduración, a la expresión de Rab7 en LE y a la unión de esta proteína a RILP ("*Rab Interacting Lysosomal Protein"*) y a OSBP1 ("*oxysterol binding protein*" 1) y mediante estas, al complejo motor microtubular.

En conjunto y aisladamente, todos los factores implicados la maduración de la vía endocítica son potenciales dianas de control y regulación por parte de los virus que penetran a través de esta vía, cuyo estudio constituye el objetivo de esta tesis.

Objetivos

1. Estudiar los compartimentos endosomales que atraviesa el VPPA en su paso por la vía endocítica.
2. Analizar las condiciones de dependencia de la vía endocítica y del pH ácido del endosoma en la infección productiva por VPPA.
3. Estudiar la relevancia de las Rab GTPasas, el ácido lisobisfosfatídico y las vesículas intraluminales de los endosomas tardíos como posibles dianas del virus.
4. Investigar la importancia del flujo de salida de colesterol de los endosomas para la infección.
5. Investigar el papel de otras moléculas de señalización de la vía endocítica como los fosfoinosítidos en la infección.
6. Analizar el papel de las membranas endosomales en los estadíos tempranos de formación de la factoría vírica.

Materiales y métodos

1. CULTIVOS CELULARES

Para la realización del presente trabajo se han empleado las siguientes líneas celulares:

Vero (ATCC CCL81), fibroblastos derivados de riñón de mono verde africano *Cercopithecus aethiops. Se utilizaron* para realizar infecciones con VPPA.

COS 7 (ATCC CRL-1651), fibroblastos derivados de riñón de mono verde africano *Cercopithecus aethiops*. La línea fue derivada de la línea celular CV-1 (ATCC ® CCL-70) mediante transformación con un mutante de origen defectivo de SV40 que codifica para el antígeno T wild type. Se utilizaron para realizar expresiones transitorias.

Ambas líneas se cultivaron en medio de Eagle modificado por Dulbecco (DMEM; Biowhittaker) suplementado con L-glutamina 2mM (Gibco BRL), penicilina 100 UI/ml (Gibco BRL), estreptomicina 100 µg/ml (Gibco BRL) aminoácidos no esenciales (Gibco BRL) y suero bovino fetal inactivado por calor al 5% en el caso de células Vero y al 10% para las células COS (v/v, Biowhittaker), Las células crecieron en condiciones controladas de temperatura (37ºC) y CO_2 (5%), subcultivandose cada 2 días empleando tripsina/EDTA (0.25% y 0.025% p/v respectivamente; Gibco BRL) para desprenderlas de los frascos de cultivo.

2. VIRUS E INFECCIONES VIRALES

2.1 Virus empleados

Se emplearon los aislados Ba71V (Enjuanes, et al.,1976) de VPPA adaptados a la línea celular Vero. Infecta eficazmente células COS (Carrascosa et al., 1999).

Virus BA71-54GFP (B54GFP), generado a partir del aislado BA71V. Expresa la proteína estructural p54 en fusión a GFP en el locus del gen Timidina Kinasa (K196R). El locus original de p54 está delecionado para evitar la competición entre ambas proteínas a la hora de incorporarse a la partícula viral.

Virus B54ChFP, expresa la proteína viral p54 fusionada a la proteína fluorescente mCherry y bajo el control del promotor de la proteína p54. Fué construido siguiendo el procedimiento descrito en Hernaez et al. 2006.

Ambos virus recombinantes muestran la proteína p54 fluorescente, localizada en la factoría viral.

2.2 Obtención de inóculos y purificación del VPPA

Para obtener inóculos procedentes de diferentes aislados del VPPA, se infectaron monocapas confluentes de células Vero con el aislado correspondiente a una multiplicidad de infección de 0.1 ufp/célula, dejando transcurrir la infección a 37ºC y 5% CO_2 hasta observar un efecto citopático generalizado (4 a 5 días). Entonces, se recogieron las células y el medio y se sonicaron al 50% de la potencia con un sonicador de sonda (Sonoplus, Bandelin) 3 veces durante 10 segundos. A continuación se centrifugaron a baja velocidad

10 minutos a 4º C para eliminar restos celulares. Posteriormente se centrifugaron los sobrenadantes a 27000 x g durante 4 horas a 4°C. Finalmente el sedimento obtenido fue resuspendido en 4 ml de medio con 10% SBF y almacenado a –80°C hasta su uso.

Cuando interesó semipurificar el inóculo de VPPA obtenido, éste se centrifugó a través de un colchón de sacarosa al 40 % en PBS a 40000 x g durante 20 minutos a 4°C.

En todos los casos se titularon los inóculos virales por plaqueo en agarosa de diluciones decimales seriadas del inóculo obtenido.

2.3 Infecciones con VPPA

Se realizaron siempre sobre células Vero o COS sembradas la noche anterior y a diferentes multiplicidades de infección, según el experimento. Las células a infectar se sembraron a dos densidades diferentes: $9x10^4$ y $6x10^4$ cel/cm^2, dependiendo de los requerimientos del experimento. El inóculo vírico se añadió siempre sobre el mínimo volumen necesario para cubrir el tapiz celular. Se dejó transcurrir un periodo de adsorción de 90 minutos a 37°C, tras el cual se retiró el inóculo y se añadió medio fresco. Cuando se requirió sincronización de la infección, el periodo de adsorción se realizó a 4°C, permitiendo la adsorción del virus a la célula, pero impidiendo la internalización en ésta.

La multiplicidad de infección (moi, del inglés "*multiplicity of infection"*) utilizada dependió del objetivo de cada experimento, detallándose en paticular para cada caso.

Cuando las infecciones se realizaron en presencia de alguna droga, las células se pretrataron un tiempo antes de infectar, normalmente 1 hora. Si el experimento requería sincronización, se pasaban después a 4°C. El inhibidor normalmente estuvo presente durante todo el experimento o se añadió a distintos tiempos en el curso del experimento.

En todos los casos, tras la adsorción, se lavaron las células con medio fresco para eliminar los viriones que no se habían adsorbido a las células.

La adsorción y sincronización por espinoculación (Carter et al., 2005) (previamente también fue utilizada (O'Doherty et al., 2000)) se realizó en experimentos de microscopía electrónica. Las células previamente enfriadas a 4° se infectaron a moi de 100 ufp/célula. La adsorción viral se realizaba durante 60minutos en centrífuga refrigerada a 1500 rpm.

2.4 Titulación de inóculos de VPPA

Las titulaciones se realizaron por plaqueo en agarosa sobre monocapas de células Vero al 90% de confluencia, infectadas con diluciones decimales seriadas del inóculo viral, permitiendo una adsorción en medio con SBF 2.5%, a 37°C y durante 90 minutos. A continuación se retiró el inóculo viral y se añadió una mezcla de medio completo 2X más agarosa de bajo punto de fusión (Gibco) al 2 % atemperada a 37°C. Las placas producidas por BA71V se tiñeron y contabilizaron con cristal violeta 1% (p/v) a los 10-15 días.

2.5 Transfecciones e infecciones de células COS

Utilizamos los siguientes vectores para realizar transfecciones transitorias:

Rab7 Wild-type humano fusionado a GFP y un mutante dominante negativo (Rab7 T22N), el cual debería tener una afinidad reducida por la unión a GTP, y por tanto mantenerse inactivo (Vitelli et al., 1997). El mutante Rab7T22N se generó por sustitución de Asparagina por Treonina en la región GKT/S (Feng et al., 1995)

Las construcciones se clonaron fusionando la proteína GFP en el extremo N-terminal del vector pGreenLantern (Gibco-BRL, Grand Island NY, USA) cedidos gentilmente por el Dr. Craig Roy, Universidad de Yale, USA).

Se transfectaron las células empleando Fugene (Roche), diluido en DMEM en ausencia de antibióticos y SBF. Tras añadir el ADN (1 μg / 10^6 células), en una relación de volúmenes 3:1 de Fugene: ADN, se añadió esta mezcla de transfección a una monocapa de células al 80 % de confluencia. El medio se sustituyó por medio fresco al 10% a las 6 horas.

Se dejó progresar la transfección durante 24 horas, tras las cuales, se trataron las células con tripsina durante 1 minuto, retirándose cuidadosamente. Las células despegadas fueron resuspendidas en DMEM 5% con 100mg/ml de gentamicina.

Un total de $1,2X10^8$ células por cada vector transfectado fueron analizadas y separadas en un citómetro de flujo, unido a un sorter modelo FACS Vantage, Becton Dickinson, mediante un laser de argón a 488nm.

Las células que expresaban GFP fueron contadas y posteriormente sembradas en placas durante 12 horas. Al día siguiente, las células se infectaron con VPPA a una moi de 1 y fueron analizadas por inmunofluorescencia.

3. REACTIVOS

3.1 Inhibidores

Bafilomicina A1 (Sigma Aldrich): Inhibidor lisosomotrópico derivado de *Streptomyces griseus* que bloquea la función de la ATPasa vacuolar impidiendo la acidificación de los endosomas (Valdeira et al., 1998; Yoshimori et al., 1991) .

NH_4Cl (Sigma Aldrich): Base suave que neutraliza el pH ácido de vesículas endocíticas (Ohkuma and Poole, 1978; Valdeira et al., 1998).

Dinasore (Merck): Inhibidor específico de la GTPasa dinamina, bloqueando los procesos dependientes de ella, de modo que la formación de las vesículas recubiertas queda eficazmente bloqueada (Macia et al., 2006).

YM201636 (Symansis, Cell Signalling Science): Potente y específico inhibidor de la fosfatidil inositol fosfato kinasa de mamíferos, PIKfyve, bloqueando la síntesis de FtdIns(3,5)P2. Desencadena una serie de alteraciones en la vía degradativa (Jefferies et al., 2008).

U18666A: (Sigma Aldrich) Esteroide anfipático muy utilizado para bloquear el tráfico intracelular de colesterol e imitar el fenotipo de Niemann-Pick tipo C, una enfermedad hereditaria de almacenamiento lisosomal. Bloquea la salida de colesterol libre desde el LE (Liscum and Faust 1989).

3.2 Antibióticos

Ampicilina (Roche), Kanamicina (Roche), Gentamicina (Gibco), y Penicilina/Estreptomicina (Gibco).

3.3 Colorantes

Cristal violeta (Sigma Aldrich): colorante que tiñe las células, se utilizó para revelar placas de lisis. Rojo Ponceau (Sigma Aldrich): que tiñe de manera reversible las proteínas sobre una membrana de nitrocelulosa.

3.4 Electroforesis

Acrilamida:bisacrilamida al 40% (BioRad). Agarosa convencional (Conda). Agarosa de bajo punto de fusión (Gibco). Marcadores de peso molecular para geles de proteínas: Precision Plus Protein WesternC (BioRad), revelado con "Precision Protein StrepTactin-HRP Conjugate" (Bio-Rad). TEMED: N,N,N´,N´-tetrametilendiamiino (Sigma Aldrich), β-mercaptoetanol (Sigma Aldrich), PFA: Persulfato amónico, Laemmli (Bio Rad).

3.5 Otros reactivos

Lysotracker Red DND-99 (Molecular Probes): Tinte fluorescente para marcar organelas ácidas (Bucci et al., 2000).

Complejo filipina (Sigma Aldrich): Químico fluorescente de alta afinidad por la unión a colesterol. Se utiliza para teñir colesterol intracelular (Kruth et al., 1986).

3.6Anticuerpos y cromógenos (Tabla nº 2)

Anticuerpos primarios	Isotipo	Uso/Dilución	Procedencia
Anti-p72 (Clon 1BC11) (R)	IgG1	IFI /1:1000	Ingenasa
Anti-p72 (Clon 18BG3) (R)	IgG2a	WB / 1:	Ingenasa
Anti-p30 (R)	IgG	WB /1:500 IFI / 1:100	Dr. Escribano (INIA,Madrid)
Anti-p150 (Clon 17AH2) (R)	IgG2a	IFI/sin diluir	Ingenasa
Antisuero-pE120R (policlonal) (C)	IgG	IFI/ 1:500	Inmunización con proteína

			recombinante
Anti-EEA1 (Clon14/EEA1) (R)	IgG1	IFI / 1:50	BD biosciences
Anti-CD63 (Clon H5C6) (R)	IgG1	IFI / 1:200	Developmental studies H.B.
Anti-Rab7 (Clon D95F2) (C)	IgG	IFI / 1:200	Cell Signalling
Anti-Lamp1 (policlonal) (C)	IgG	IFI / 1:50	Abcam
Anti-LBPA (Clon 6C4) (R)	IgG1k	IFI / 1:50	Dr. Gruenberg (U. Ginebra)
Anti-tubulina	IgG1	WB /1: 2000	Sigma

Anticuerpos secundarios	**Uso/Dilución**	**Procedencia**
Anti-IgG de ratón -Alexa Fluor ™ 488	IFI /1:300	Molecular Probes
Anti-IgG de ratón -Alexa Fluor ™ 594	IFI /1:200	Molecular Probes
Anti IgG de conejo-Alexa Fluor ™ 488	IFI /1:200	Molecular Probes
Anti IgG de conejo-Alexa Fluor ™ 594	IFI /1:500	Molecular Probes
Anti IgG de ratón-HRP	WB / 1:5000	Amersham
Anti IgG de conejo -HRP	WB / 1:5000	Amersham

(*): (C) = anticuerpo generado en conejo; (R) = anticuerpo generado en ratón

Cromógenos	**Uso/Dilución**	**Procedencia**
LysoTracker Red DND-99™	75 nM	Molecular Probes
To-pro3	IFI /1:1000	Invitrogen
Filipina	50 µg/ml	Sigma

4. MÉTODOS DE INMUNODETECCIÓN DE PROTEÍNAS

4.1Western Blot (WB)

Las células infectadas se lavaron en PBS y se recogieron a distintos tiempos, en función del experimento, en buffer Laemmli (Bio Rad). Los lisados se sonicaron e incubaron a 100ºC durante 5 min. Las proteínas fueron separadas por electroforesis en geles de poliacrilamida desnaturalizantes (SDS-PAGE) en concentraciones del 10 %. Una vez separadas se transfirieron a una membrana de nitrocelulosa con un poro de 0.45 µm (Bio-Rad) por transferencia húmeda a 100 V constantes durante 1 hora. Para la inmunodetección de las proteínas sobre dicha membrana se adaptó el protocolo de Bakkali (Bakkali et al., 1994) a las recomendaciones de la casas comerciales suministradoras de los anticuerpos empleados (Tabla nº2). Para detectar las proteínas virales p30 y p72 y α-tubulina (proteína usada como control de carga), las membranas se incubaron con el anticuerpo correspondiente (Tabla nº2). Como anticuerpos secundarios se utilizó peroxidasa de rábano (HRP) acoplada a los anticuerpos secundarios, diluida 1:5000 (GE Healthcare). Para revelar el marcador de proteínas "Precision Plus Protein WesternC" (Bio-Rad) se utilizó el "Precision Protein StrepTactin-HRP Conjugate" (Bio-Rad).

Para el revelado de las proteínas, se empleó "ECL detection kit" (Amersham), siguiendo las recomendaciones de la casa comercial. La expresión de las proteínas se analizó utilizando el software "Immun-Star WesternC Kit" (Bio-Rad) en el "Molecular Imager Chemidoc XRSplus Imaging System". Las bandas fueron cuantificadas por densitometría y los datos se normalizaron utilizando el software "Image lab" (Bio-Rad).

4.2 Inmunofluorescencia indirecta (IFI)

Para tal efecto, las células se sembraron a una densidad variable ($3x10^4$ células/cm^2 para ensayos con infecciones y $5x10^4$ células/cm^2 para ensayos con transfección), sobre cubreobjetos redondos de 13 mm de diámetro. Una vez transcurrido el tiempo de infección o transfección deseado, las células se fijaron utilizando formaldehido o paraformaldehido al 4% durante 15 minutos. Tras la fijación, la fluorescencia de los grupos aldehídos se apagaron por incubación con NH_4Cl 50 mM en PBS 10 minutos y las células se permeabilizaron utilizando tritón X-100 al 0,1% o 0,3%, o bien saponina al 0,5% durante 10 minutos. Posteriormente se realizó una incubación con albumina de suero bovina (BSA, del inglés *"bovine serum albumin"*) al 2% (Sigma Aldrich) en PBS durante 45 minutos a temperatura ambiente (RT, del inglés "*room temperature"*) para bloquear las uniones inespecíficas.

Las células se incubaron con la correspondiente dilución del anticuerpo primario (Tabla nº 2) 1h a 37°C en cámara húmeda o durante toda la noche (ON, del inglés *"over night"*) a 4°.

Los anticuerpos secundarios normalmente se incubaron durante 45 minutos a RT. Para marcar el ADN se utilizó To-pro3 (Invitrogen) diluido 1:1000, durante 5 minutos a RT y en oscuridad. Finalmente se montaron sobre los porta objetos utilizando el medio de montaje Prolong (Invitrogen).

Se lavaron las células siempre con PBS después de cada paso.

5. MICROSCOPÍA

5.1 Microscopía de fluorescencia convencional

De manera rutinaria, se empleó un fotomicroscopio dotado de cámara digital (Leica) y de los filtros necesarios para detectar la emisión de fluorescencia de los fluoróforos y cromógenos utilizados y descritos en esta tesis.

5.2 Microscopía confocal: se empleó un microscopio Leica TCS SPE, utilizando habitualmente un objetivo de inmersión en aceite 63X. El análisis de las imágenes se realizó con el software Leica Application Suite advanced fluorescence software (LAS AF). Se llevaron a cabo contajes de eventos de colocalización y de células, reconstrucciones en 3D, proyecciones laterales y diversos montajes de imágenes según cada experimento en particular. Los eventos de colocalización entre proteínas virales y endosomas fueron relativizados al número total de viriones asociado a la célula, y expresados como porcentaje.

Todas las imágenes fueron adquiridas a una resolución de 512 x 512 pixeles, salvo en los casos en los que era necesario utilizar zoom para tener mayor detalle, en este caso se adquirieron a una resolución de 1024 x 1024 pixeles. Las imágenes obtenidas se procesaron con el programa Adobe Photoshop CS6 (Adobe Systems Inc.).

5.3 Microscopía electrónica de transmisión

Las monocapas de células Vero se sembraron al 90 % de confluencia sobre cubres de vidrio previamente esterilizados y se infectaron a una moi de 100 ufp/célula. Se permitió la adsorción del virus a 4° durante 1 hora por la técnica de espinoculación a 1200 rpm. Posteriormente se fijaron químicamente las células con una solución de 2,5% Glutaraldehido / 2% paraformaldehido en PBS durante 1 h a RT y se realizó un tratamiento con OsO_4 al 1% durante 45 min. Después se lavó con H_2O milliQ para retirar los excesos, y Acetato de Uranilo al 1% durante 45 min para aportar contraste y estabilidad a las muestras. Tras esta incubación se hizo una nueva serie de lavados para eliminar los excesos.

Finalmente las muestras se embebieron en la resina EPON y se realizaron cortes de 70nm de grosor en la muestra.

Las muestras fueron deshidratadas para sustituir el agua de las células por moléculas de solvente miscible con los componentes de la resina epoxídica de inclusión. En este caso se realizó en concentraciones crecientes de etanol seccosolv en H_2O milliQ (50 %, 75%, 95%, 100%) durante 15 minutos por cada incubación a temperatura ambiente. Finalmente la muestra se dejó infiltrando una primera vez en resina EML-812 (Taab Laboratories) diluida en etanol seccosolv 1:1 P/V durante una hora a RT y, sucesivamente durante los siguientes dos días se hicieron cambios de resina 100% cada 12 horas hasta polimerizar en cápsulas (Ted Pella Inc.) en un incubador a 60°C durante dos días.

Una vez descapsulada la muestra, se realizaron cortes seriados de 70 nm de grosor, se tiñeron con acetato de uranilo saturado durante 20 min y finalmente se hicieron lavados seriados de 5 min en H_2O milliQ. Las muestras así preparadas se visualizaron en el microscopio electrónico de transmisión (Jeol JEM 1011 de 100kV y filamento de tungsteno) asociado a una cámara Gatan ES1000W.

El programa informático utilizado fue "Digital Micrograph".

6. TRANSFECCIÓN DE CÉLULAS DE ORIGEN MAMÍFERO

Se transfectaron células COS empleando Fugene HD (Roche), diluido en DMEM en ausencia de antibióticos y SBF. Tras añadir el ADN, en una relación de volúmenes 3:1 de Fugene:ADN, se añadió esta mezcla de transfección a una monocapa de células al 80 % de confluencia. El medio se sustituyó por medio fresco a las 6 horas. Las células transfectadas se seleccionaron y separaron mediante "sorter" en el citometro de flujo.

7. CITOMETRÍA DE FLUJO

Las células sembradas en placa fueron levantadas tras un tratamiento con tripsina y lavadas con PBS y buffer de FACS (del inglés, *"fluorescence-activated cell sorter"*) (PBS, 0,01% de azida sódica, y 0,1% de BSA), las células se fijaron y se permeabilizaron con Perm2 (BD science) durante 10 min a temperatura ambiente. La detección de las células infectadas se realizó por incubación con anticuerpo monoclonal anti-p30 (diluido 1:100 en buffer de FACS) durante 30 min a 4 ° C, seguido de incubación con un anticuerpo anti-mouse conjugado a ficoeritrina (PE) (Dako) (diluido 1:50 en buffer de FACS) durante 30 min a 4 ° C. Después de un extenso lavado, se analizaron 10000 células por experimento en un citómetro de flujo FACS Calibur (BD Science). Las tasas de infección obtenidas fueron relativizados a los datos obtenidos en las células control.

8. ENSAYOS CON LYSOTRACKER

Se realizó un marcaje de los compartimentos endosomales ácidos incubando las células con Lyso Tracker Red DND-99 (Molecular Probes) 75 nM durante 30 min a 37°. A continuación, las células Vero se fijaron para IFI, y así junto con un marcaje específico de las membranas endosomales, determinar las organela ácidas.

Para analizar el efecto de la Baf en la tinción de Lyso Tracker, las células pre tratadas con Lyso Tracker fueron incubadas con Baf 200 nM y fotografiadas *in vivo* a distintos tiempos después de la adición de Baf (1, 5, 10, 15 minutos), también se llevaron a cabo ensayos de IFI en células fijadas. La intensidad de fluorescencia se midió con el software LAS AF en unidades arbitrarias en tres puntos máximos de fluorescencia (tres ROIs similares, m 30x30) por imagen, sustrayendo el fondo. Se analizaron 32 imágenes por muestra.

9. ANÁLISIS DE CITOTOXICIDAD Y USO DE REACTIVOS

La viabilidad celular en presencia de los diferentes reactivos usados en este trabajo se determinó con el kit comercial "Cell titter 96 Aqueous Non-Radioactive Cell Proliferation Assay" (Promega) siguiendo las instrucciones de la casa comercial. Se seleccionaron aquellas concentraciones de uso cuya toxicidad no excedió del 20%. Todos los reactivos fueron diluidos en DMSO para generar *"stocks"* y posteriormente en DMEM 2% a la concentración óptima para la realización del experimento. Ver figura del anexo.

10. INHIBICIÓN DE LA ACIDIFICACIÓN ENDOSOMAL Y ENDOCITOSIS POR DINAMINA

El stock de Baf (Sigma) se disolvió en DMSO a una concentración de 100uM se almacenó a -20°C. Se utilizó a una concentración de 200nM, diluida en DMEM 2% (Stuart and Brown, 2006; Umata et al., 1990). La solución stock de NH_4Cl (Sigma Aldrich) se preparó en PBS 1M y la dilución utilizada fue de 10mM diluida en DMEM 2%. La solución stock de Din (Merck) se preparó a 10mM en DMSO y se utilizó a 80 μM diluida en DMEM 2%. Las células se sembraron al 70% de confluencia, y al día siguiente el medio de cultivo se reemplazó por medio a 4°C durante 15 min. Se infectaron las células a moi de 1ufp/célula, añadiendo el virus sobre el medio frío realizándose la adsorción durante 90 min a 4°C. Tras un lavado en frío, las células pasaron rápidamente a un incubador a 37°. En función de los diferentes tiempos post infección analizados, el medio de cultivo fue reemplazado por medio a 37°C con Baf o NH_4Cl. Las células se recogieron a un tiempo de 8hpi para su análisis por WB.

Para los experimentos de tratamiento con pH ácido, las células fueron pre tratadas con Baf 200 nM yDin 80 μM o DMSO como control. Después, las células se enfriaron rápidamente a 4°C antes de añadir el virus, dejando un periodo de adsorción de 90 min en presencia de

ambos inhibidores, las células se lavaron y se les aplicó un pulso durante 1 h con DMEM a pH 5,4 o 7,4 en ausencia de inhibidores. Posteriormente se dejó proseguir la incubación durante 6 horas a pH 7,4 y 37° con DMEM en presencia de los inhibidores para que su efecto no disminuya.

Para los ensayos de IFI de retención de partículas virales en los LEs, las células se pre trataron durante 1 hora con Baf o un volumen equivalente de DMSO como control. Después se enfriaron a 4°C durante 15-20 min para sincronizar la infección, a moi de 10 ufp/célula. La adsorción progreso durante 90 min a 4°C. Después del correspondiente lavado en frío, el medio de cultivo fue reemplazado por medio fresco atemperado con o sin Baf o un volumen equivalente de DMSO. La infección progresó durante 3 horas, después de las cuales se procesaron las muestras para IFI.

11. INHIBICIÓN DE LA CONVERSIÓN DE FOSFOINOSÍTIDOS

YM201636 (Symansis, Cell Signalling Science) es un inhibidor específico de la actividad de PIKfyve, la cual inhibe la síntesis de FtdIns(3,5)P2 a partir de FtdIns3P. La solución stock se preparó diluida en DMSO a una concentración de 0,8mM y se almacenó a -20°C. Se determinó una concentración de uso de 1 μM como la menor concentración no citotóxica que inducía vacuolación citoplásmica tras 30 min de incubación. Las células se trataron con YM201636 durante 2 horas antes de la infección o a los tiempos indicados, y fue mantenida durante todo el experimento, o a los tiempos post infección indicados en cada caso particular.

12. TRATAMIENTOS CON LBPA Y U18666A (U)

12.1 Tratamiento con LBPA

Antes de la infección, las células Vero fueron pre incubadas con el anticuerpo monoclonal anti LBPA (6C4) a una concentración de 50 μg/ml, (gentilmente cedido por el Dr. Jean Gruenberg, Dpt. De Bioquímica, Universidad de Ginebra) a 37°C durante 24 horas. Este anticuerpo es internalizado en fase fluida mediante endocitosis y acumulado en los LEs. Posteriormente las células fueron procesadas para IFI utilizando un anticuerpo secundario anti ratón A488 y así poder confirmar la correcta internalización del anticuerpo. Para analizar el efecto del anticuerpo en la infección viral, se infectaron, a moi de 1 ufp/célula, células tratadas previamente o no con el anticuerpo. Las células se procesaron para analizar por IFI la expresión de la proteína viral p30 a 8 hpi, la infectividad a partir de células que muestran factoría viral y la producción viral a 24 hpi mediante titulación.

12.2 Tratamiento con U

U es un esteroide anfipático ampliamente utilizado como químico para bloquear el tráfico intracelular de colesterol, imitando así el fenotipo ocasionado por la enfermedad de Niemann Pick tipo C, un desorden lisosomal de carácter hereditario. U bloquea la salida de colesterol libre desde los LEs. La propiedad anfipática del compuesto se piensa que es el mecanismo de acción causante de la acumulación del colesterol en LEs y LIs. U también inhibe la biosíntesis del colesterol por inhibición de la enzima oxidoescualeno ciclasa y desmosterol reductasa (Liscum and Faust, 1989).

Tras confirmar que el bloqueo de la función del LBPA era determinante para la infección del VPPA, realizamos experimentos para analizar el impacto en la infección de la acumulación de colesterol en los LEs, donde el LBPA participa activamente.

Las células Vero fueron incubadas en presencia de U a distintas concentraciones (1, 5, y 10 μM), durante 16 h, para después infectar a moi de 1ufp/célula.

El impacto de la droga U sobre el colesterol fue determinado por visualización en el microscopio usando el químico Filipina.

La filipina (Sigma) es un químico fluorescente que presenta alta afinidad en su unión al colesterol intracelular, por lo que es ampliamente utilizado para su detección (Kruth et al., 1986). Tras la fijación, las células se incubaron durante 1 hora con filipina (50 μg/ml), y se procesaron para analizarlas por IFI, y visualizada bajo una excitación de 390 a 415 nm, la señal de emisión se sitúa entre los 450 y 470 nm.

13. ANÁLISIS DE DATOS

Los valores mostrados en los gráficos corresponden a la media de los datos obtenidos +/- la desviación estándar. El análisis de la varianza de los datos se llevó a cabo con el paquete estadístico GraphPad INSTAT. La corrección de Bonferroni se aplicó para comparaciones múltiples. Las diferencias se consideraron estadísticamente significativas cuando el *p* valor fue menor de 0,05 (*), si el *p* valor era menor de 0,01 se indica como (**), y si era menor de 0,001 se indica de este modo (***).

Resultados

1. PAPEL DE LOS COMPARTIMENTOS ENDOCÍTICOS EN LA INFECCIÓN DEL VPPA

1.1 Relevancia de los compartimentos endosomales en la infección del VPPA

Los trabajos iniciales sobre la entrada del VPPA y otros más recientes de nuestro grupo, han definido como la vía principal de entrada del VPPA en las células la endocitosis mediada por clatrina (Alcami et al., 1989a; Hernaez and Alonso, 2010; Valdeira and Geraldes, 1985). Sin embargo existe cierta controversia ya que otros autores han señalado un posible mecanismo de entrada por macropinocitosis (Sanchez et al., 2012) e incluso, se ha señalado la posibilidad de una cooperación entre ambas vías de entrada (Alonso et al., 2013).

Con el fin de profundizar en el conocimiento del mecanismo de entrada del virus e identificar posibles dianas terapéuticas en las primeras etapas de la infección de VPPA, llevamos a cabo un estudio del progreso del virus a través de la vía endocítica y su relevancia en la infección. En este sentido, el primer objetivo, consistió en identificar las vesículas endocíticas que pudieran estar involucradas en los pasos inmediatamente posteriores a la entrada en la célula diana, hasta el momento de la llegada del virión a la zona perinuclear en el MTOC. En el área perinuclear es donde se formará el sitio de replicación del virus, también llamado factoría viral u organela de replicación, donde tendrá lugar el ensamblaje de los nuevos viriones.

Para ello estudiamos la localización del virus mediante microscopía confocal en los primeros minutos de la infección. Se procedió a la observación de los viriones en la superficie de células Vero durante un período de adsorción a la membrana de 90 min a 4°C, mediante la detección de la proteína mayoritaria de la cápside p72. Se realizaron infecciones en células Vero con el aislado BA71V adaptado a cultivo celular. Como control, se estudiaron las preparaciones empleando proyecciones laterales para poder determinar la localización de los viriones en la superficie con exactitud, ya que la superposición de imágenes en este caso podría dar lugar a imágenes equívocas. Un ejemplo de este análisis puede observarse en la Figura 5. Los viriones localizados claramente en la membrana celular aparecen marcados como puntos a, b, y c (Figura 5 A). La proyección lateral (Figura 5 B) permite distinguir claramente como los puntos d, e y f se encuentran en un plano superior, en la MP, lo que evita un error frecuente en la identificación de los viriones que están internalizados y próximos al núcleo.

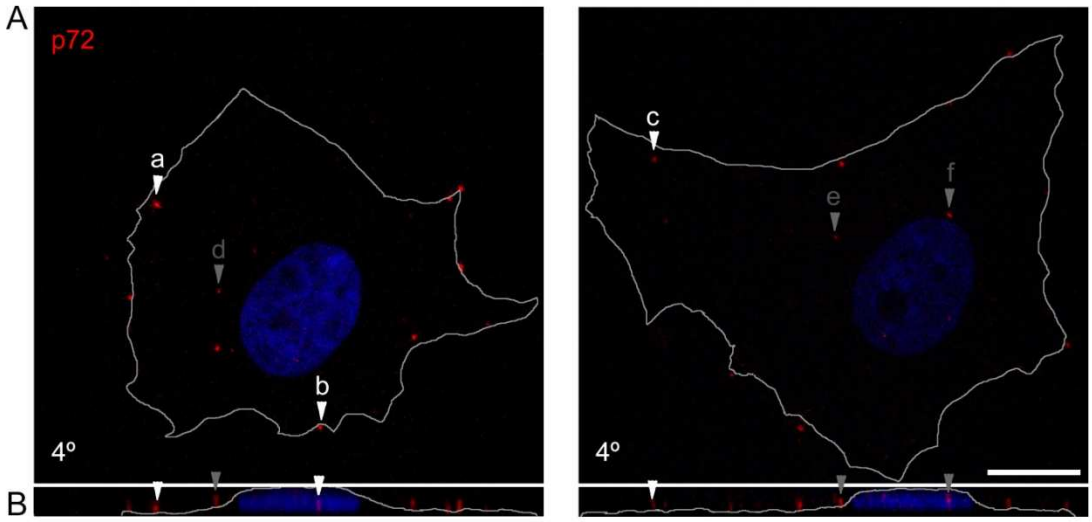

Figura 5. Localización del VPPA en la fase de adsorción a la célula diana. Imágenes representativas de microscopía confocal que muestran viriones inmuno-marcados para detectar la proteína de la cápside p72 (rojo). Tras la infección a una moi de 5 ufp/célula se realizó la adsorción viral a 4°C durante 90 min. Después se procesaron las células para IFI. (A) La figura muestra viriones adsorbidos en la MP identificados como a, b, c. Los viriones próximos a núcleo, están identificados como d, e, f. Sin embargo en las proyecciones laterales (B) se observa cómo estos están localizados en una posición superior respecto a los que se localizan próximos a la MP, lo que indica que también están fuera de la célula, a pesar de que parece que están en el interior, próximos al núcleo. Barra 10 µm.

Seguidamente, para determinar la incorporación del VPPA a la vía endocítica, utilizamos anticuerpos frente a dos proteínas de la cápside del virus, p72 y pE120R por un lado, y marcadores de distintas vesículas endosomales por otro, para analizar la colocalización entre ellos utilizando microscopía confocal (Figura 6).

Se infectaron células Vero con el aislado BA71V de VPPA a alta moi (10 ufp/célula) con el fin de observar mayor número de eventos de colocalización en la misma célula. La realización de un período de adsorción viral, durante 90' a 4°C, permite que los viriones queden adsorbidos a la membrana plasmática y de este modo se favorece la internalización simultánea de todos ellos al reemplazar el medio de infección a 4 °C por medio atemperado. Después, las muestras infectadas de forma sincronizada fueron fijadas a distintos tiempos post-infección.

Para detectar los distintos compartimentos endosomales, se utilizaron diversos marcadores de los estadíos de maduración característicos de estas vesículas. Así, para el marcaje de endosomas tempranos ("*early endosomes*" o EE), cuerpos multivesiculares ("*multivesicular bodies*" o MVB), endosomas tardíos ("*late endosomes*" o LE), y lisosomas (LI) se usaron anticuerpos frente a EEA1 ("*early endosomal antigen*" 1/antígeno 1 de endosoma temprano, un efector de Rab5), CD63 para MVB, Rab7 para detectar LE, y

Lamp1 ("*lysosomal-associated membrane protein" 1/Proteína 1 asociada a la membrana del lisosoma),* respectivamente (Figuras 6 A-D).

Se observó que la colocalización entre las cápsides virales y los EEs aumentaba entre 1 y 30 minutos post-infección, para descender posteriormente (Figura 6 E). A diferencia de lo que ocurría con el marcador de EE, la colocalización entre la cápside viral y los compartimentos endocíticos tardíos (anticuerpos frente a Rab7, CD63 y Lamp1) era escasa a los tiempos analizados 1, 15, 30, 60 minutos post infección (mpi) (Figura 6 E). Esto planteaba diversas hipótesis alternativas; bien que el proceso de penetración al citosol fuera tan rápido desde el LE que no pudiera detectarse en su interior, o bien que el virus desencapsidara liberándose al citosol desde los EEs. Finalmente, la ausencia de marcaje de la cápside viral podría ser debida a que en dichos compartimentos la cápside hubiera comenzado a degradarse y por tanto no fuera posible observarla en los endosomas tardíos o LE.

Para comprobar esta hipótesis, analizamos la colocalización entre la proteína del core viral, p150, situada en una posición más interna en el virión, y Rab7, un marcador característico de LE. En efecto, pudimos comprobar que la colocalización entre p150 y las vesículas positivas para Rab7 era superior al 60% a 45 mpi y por lo tanto, los cores virales ya desprovistos de cápside podían ser detectados en compartimentos tardíos (Figuras 6 F, G). En detalle la colocalización entre Rab7 y los cores virales era evidente (Figuras G1-G4) y en cambio, la colocalización con Lamp1 entre 30 y 60 mpi se reducía al 15% (Figura 6 H). Estas observaciones parecen indicar que la desencapsidación y penetración del core viral en el citoplasma son procesos que en efecto ocurren rápidamente, entre 45-60 mpi, pero la salida de los viriones desencapsidados se realizaría desde los LE, ya que disminuía el porcentaje de cores virales colocalizando con vesículas positivas para Lamp1. Por lo tanto, los viriones internalizados en los primeros minutos de la infección colocalizaron con los endosomas tempranos marcados con anticuerpos frente a la proteína de la cápside. En estadíos madurativos del endosoma más avanzados solo se pudieron observar los cores virales, indicando que la desencapsidación del virus podría ocurrir en el interior de los LE.

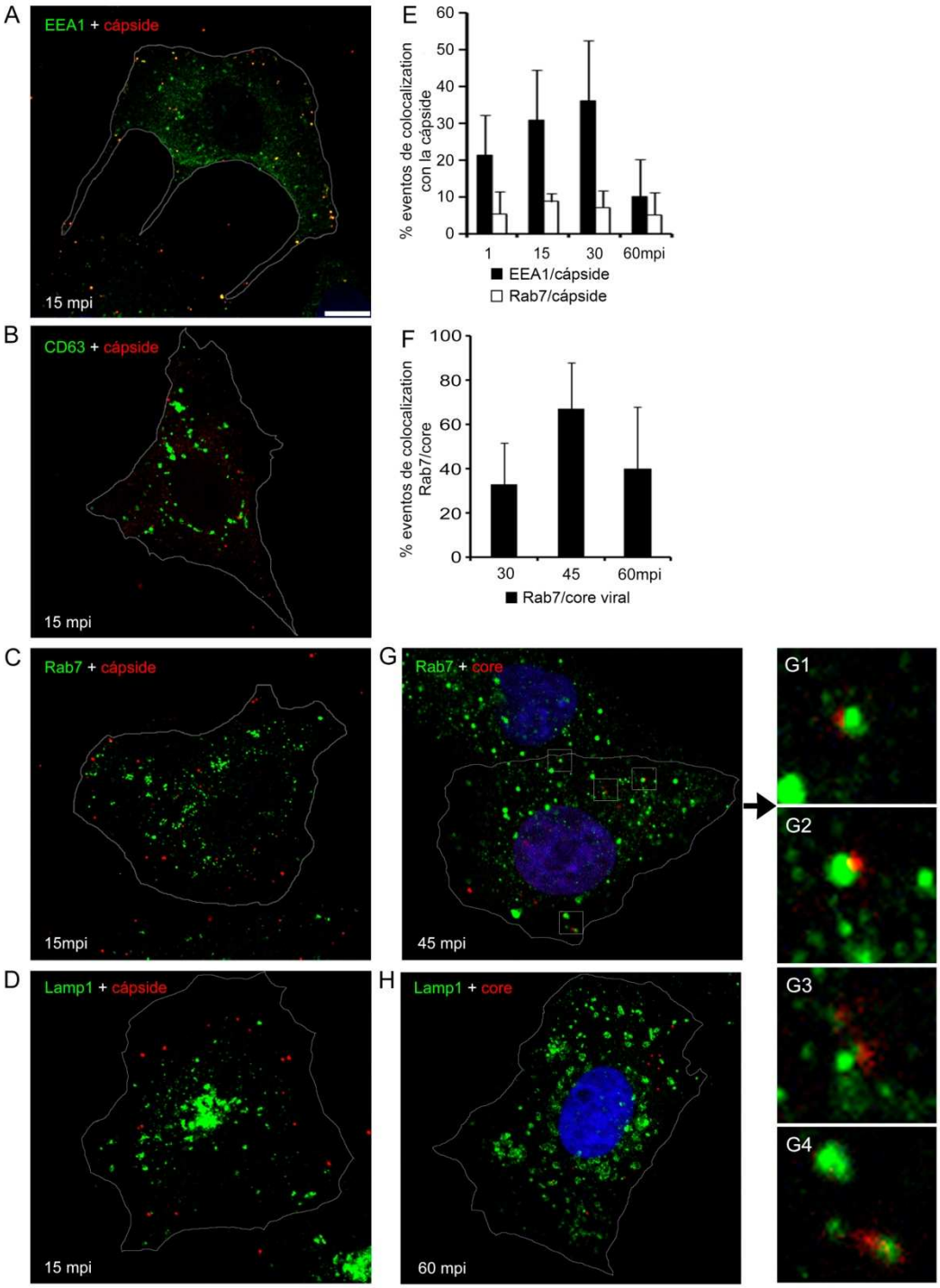

Figura 6. Colocalización viral con endosomas en etapas tempranas de la infección. Imágenes representativas de microscopía confocal de células Vero infectadas con VPPA, donde se muestra la colocalización entre la cápside viral, marcada por las proteínas p72 y pE120R (rojo), y los distintos compartimentos endosomales (verde), EEs marcados con EEA1 (A), MVBs marcados en CD63 (B), LEs marcados en Rab7 (C) y LIs marcados en Lamp1 (D) a los 15 mpi. Barras de escala, 10 μm. Las células se infectaron a una moi de 10 ufp/célula y tras la adsorción, la infección se dejó progresar los minutos indicados. (E) Los porcentajes de eventos de colocalización de la proteína de la cápside p72 con el marcador de EE o LE se expresaron como valor medio, relativizados al total de partículas virales por célula individual. El contaje se

realizó en 10 células por tiempo en duplicados. (F) Porcentajes de colocalización de la proteína del core viral p150 con el marcador de LE realizados de forma similar. (G) Imagen de microscopía confocal representativa de la colocalización de los cores virales con endosomas positivos para Rab7. Los núcleos se tiñeron con TOPRO3. (G1-4) Detalle de la colocalización entre cores virales y LEs de las áreas enmarcadas en (G). (H) Colocalización de la proteína del core viral p150 con el marcador lisosomal Lamp1.

1.2 La entrada del VPPA depende del pH ácido intraluminal y de la endocitosis

Los resultados anteriores indican que el VPPA durante su entrada, alcanzaría los compartimentos tardíos endocíticos, caracterizados por presentar pH ácido en el lumen. En la vía endocítica, el EE, como primera estación de carga y reparto presenta un pH luminal cercano a 6,5. A medida que se produce el progreso madurativo de las vesículas hacia MVB y LE, se alcanza un pH próximo a 5,5. Finalmente cuando estos llegan a los LI y se fusionan entre sí constituyendo endolisosomas, el pH se acidifica hasta 4,5-5, propio de los LI.

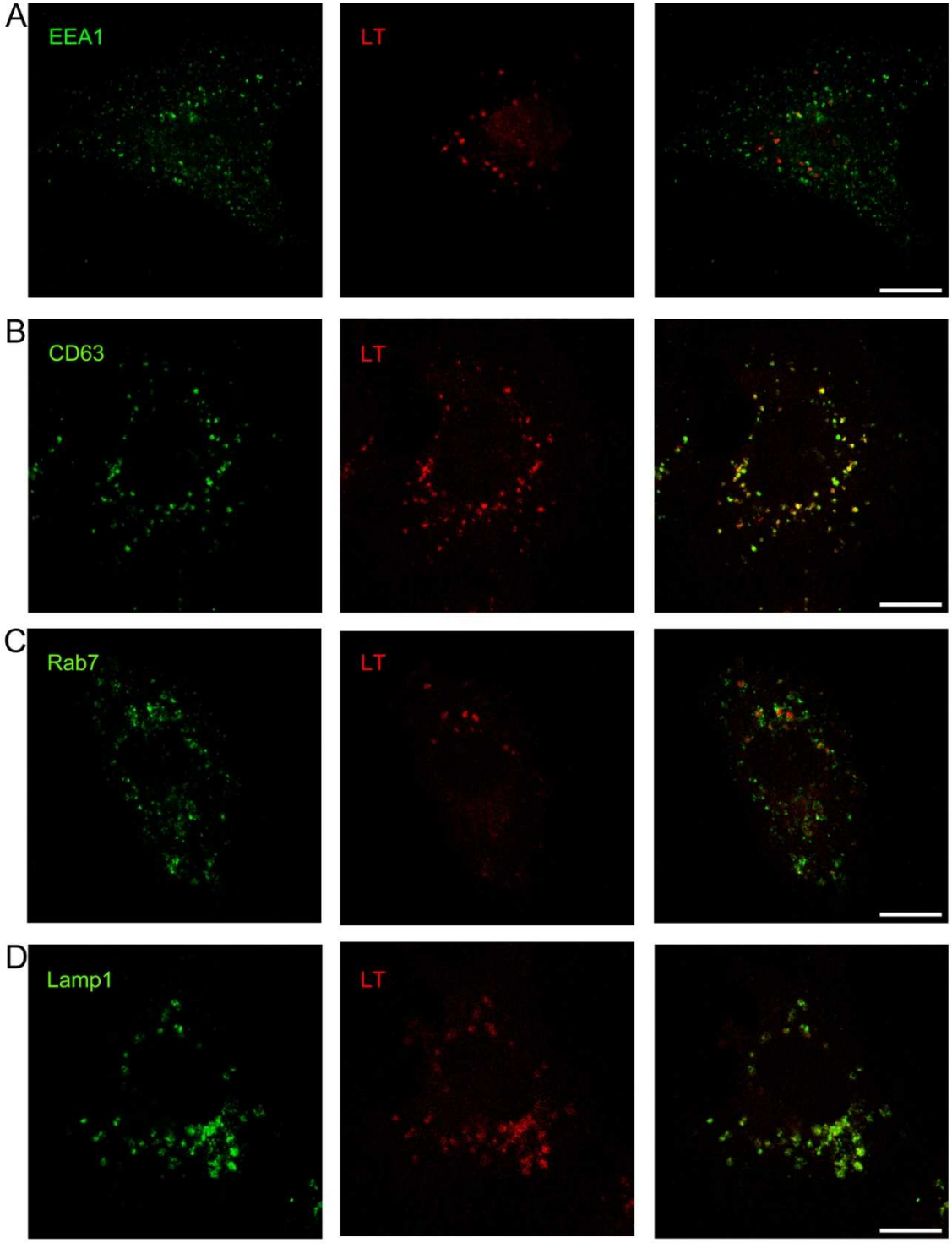

Figura 7. Tinción con Lysotracker de compartimentos endosomales ácidos. Microfotografías representativas de microscopía confocal que muestran la colocalización entre compartimentos ácidos, marcados con Lysotracker, sensible a pH (rojo) y membranas de los diferentes compartimentos endosomales (verde); (A) EEs marcados con EEA1 con los que apenas existe colocalización, y el resto de vesículas donde sí se aprecia colocalización, (B) MVBs marcados en CD63, LEs marcados en Rab7 (C) y LIs marcados en Lamp1 (D). Barra 10 μm.

Existen numerosos inhibidores de la disminución de pH endosomal, la cloroquina, las bases suaves como el cloruro de amonio (NH_4Cl) y la Bafilomicina A1 (Baf) entre otros. Para corroborar la acción de este inhibidor, realizamos un ensayo en células Vero con una tinción sensible a pH, Lysotracker, para demostrar cuáles son los compartimentos ácidos en dicha línea celular. En este ensayo, el Lysotracker marcaba intensamente los endosomas ácidos LE, MVB y LI (Figuras 7 B-D), sin embargo, como era esperable, no encontramos tinción con Lysotracker en vesículas positivas para marcadores de EE (Figura 7 A). La acidificación de los compartimentos tardíos endosomales es dependiente de la ATPasa vacuolar (vATPasa), cuya actividad es inhibida por la Baf, causando una rápida alcalinización de estas organelas, como se muestra en la Figura 8 A, donde se observó la rápida alcalinización del compartimento, con reducción de la fluorescencia de Lysotracker, demostrando que la acidificación endosomal se bloquea eficazmente en presencia de Baf.

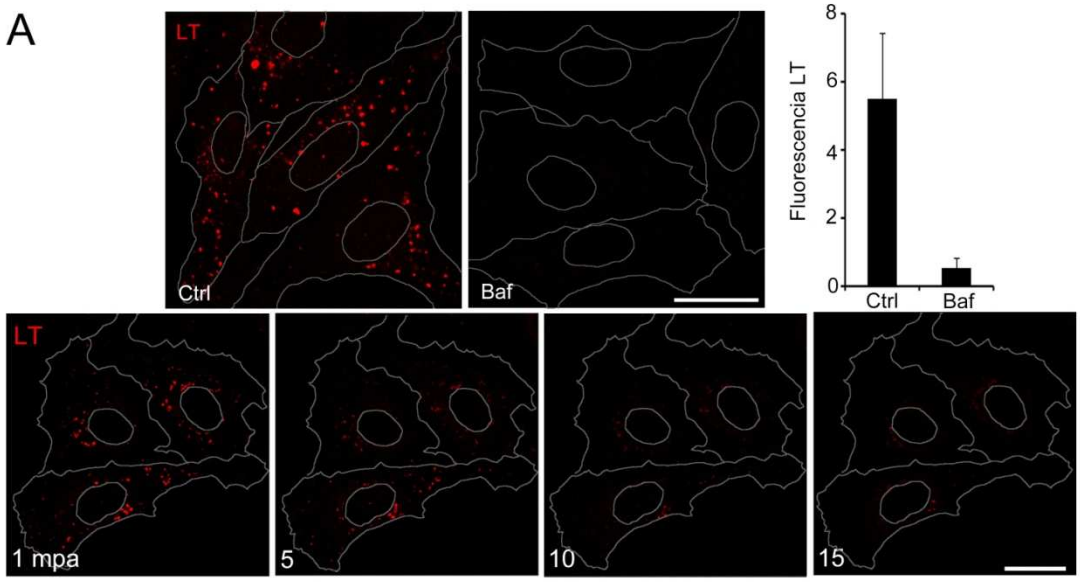

Figura 8: Alcalinización de los endosomas en presencia del inhibidor de la ATPasa vacuolar Baf. Inhibición de la acidificación intraluminal de los endosomas por Baf mostrada con el cromógeno sensible a pH ácido Lysotracker, en rojo. Barra 25 µm, mpa: minutos post-adición de Baf.

Para determinar de forma más completa si el papel de la acidificación era directamente dependiente de la acidificación en el lumen de las vesículas endosomales, se comprobó si la inhibición de la infección con Baf podía ser restaurada con un pulso de medio ácido. Resultaba importante, no solo evaluar que los viriones entraban en las células sino que su entrada por esta vía daba lugar a una infección productiva. Por ello dirigimos nuestra atención hacia una fase posterior al paso de los viriones por la vía endocítica, y

determinamos su efecto en un marcador de infección, en este caso la expresión de la proteínas virales tempranas, como la proteína vírica p30 y procedimos con el ensayo.

Se trataron previamente las células con Baf y se sincronizó la infección al permitir la adsorción viral durante 90' a 4°C, para después sustituir por medio atemperado a 37°C. Posteriormente se aplicó un pulso de 1 hora a un pH ácido (5,4). Después la infección se dejó proseguir hasta 6 hpi a pH 7,4 en presencia del inhibidor y se procesaron la células para analizar la expresión de p30 por WB y por citometría de flujo (Figura 9 A, C). En la Figura 9 F se muestran los perfiles de FACS representativos.

Las células tratadas previamente con Baf y mantenidas en medio a pH fisiológico, mostraban una expresión reducida de p30 respecto a su control. La inhibición de la infección producida por la Baf no era recuperable con al aplicar un pulso de una hora de duración a pH ácido obteniéndose similares resultados. La infección no se recuperaba, por lo que el efecto de la Baf no podía ser revertido en medio ácido, haciéndose necesaria la acidificación intraluminal de las vesículas.

Para determinar si la endocitosis es un requerimiento de la infección, examinamos el efecto de la inhibición de la GTPasa dinamina en la expresión de la proteína viral temprana p30. La dinamina es necesaria para en la escisión de la MP de vesículas endocíticas hacia el citoplasma en los procesos de endocitosis mediados por receptor, clatrina y caveolas principalmente. Se realizó la adsorción del virus durante 90' a 4°C en presencia del inhibidor de dinamina Dinasore (Din) y después el medio fue reemplazado por medio atemperado a 37°C con Din a pH 5,4 y 7,4 o con DMSO. Posteriormente, se permitió el progreso de la infección durante 6 horas, las células se recogieron para analizar la expresión de p30 por WB y la infectividad en porcentaje de células infectadas mediante citometría de flujo. A pH fisiológico la expresión de proteína viral decrecía alrededor de un 60 % en células tratadas con Din, respecto al control con DMSO (Figura 9 B, D). En la Figura 9 E se muestran los perfiles de FACS representativos.

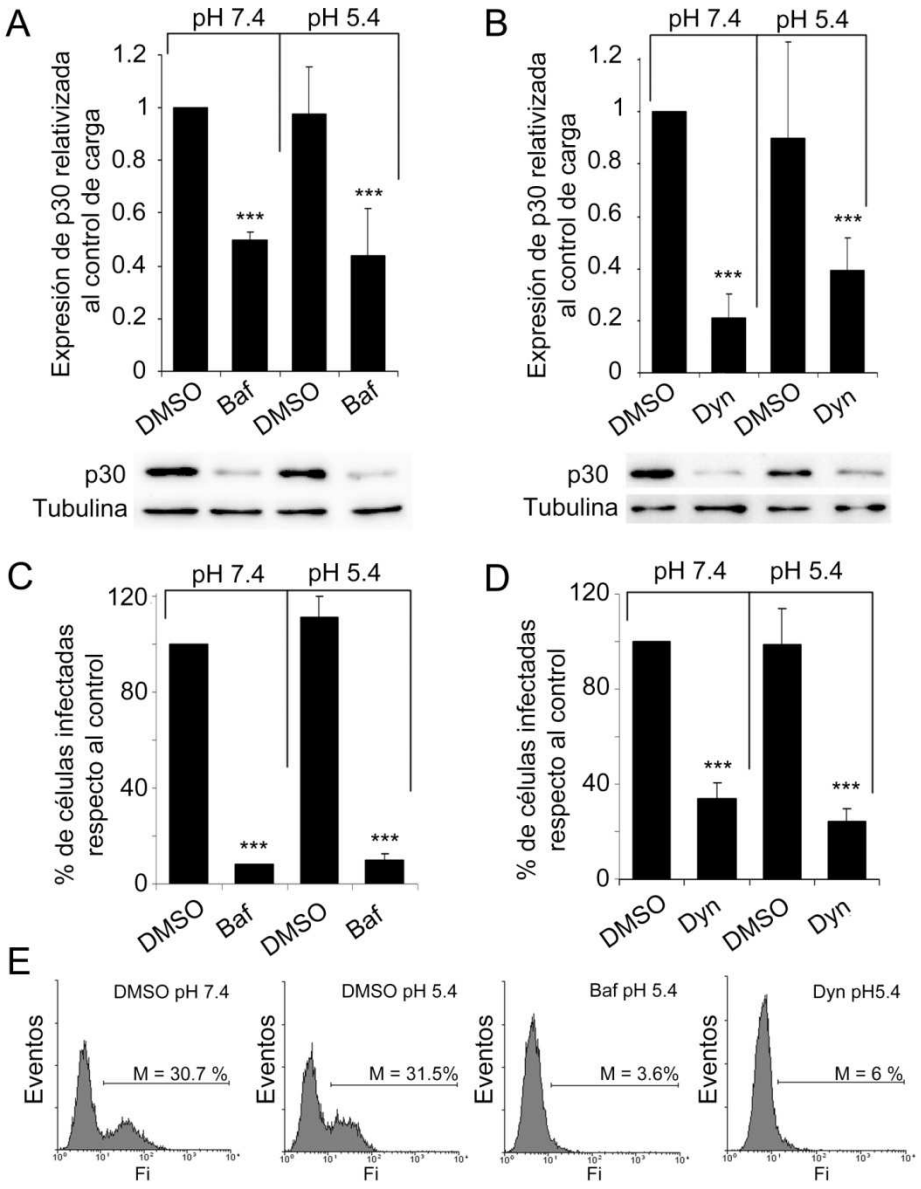

Figura 9. El pH ácido intraluminal y la endocitosis son necesarios para la infectividad de VPPA. (A-D) La inhibición de la acidificación intraluminal de los endosomas con Baf y la inhibición de la endocitosis con Din afectaba a la infectividad del virus medida por expresión de la proteína temprana p30. La inhibición causada por la Baf y Din no se recuperaba con el tratamiento con medio ácido. (A) Expresión de la proteína viral temprana p30 en las células pre-tratadas con 200 nM Baf o DMSO pulsadas 1 h con pH 5,4 post-adsorción o mantenidas a pH 7,4 durante 6 h. La baja expresión de la proteína viral p30 por WB en células pre-tratadas con Baf no se recuperaba con medio a pH ácido. (B) La expresión de la proteína p30 se cuantificó por WB tras 6 hpi en células pre tratadas con Din 80 µM o DMSO y un pulso posterior con medio a pH 5,4 o 7,4 durante 1 h tras la adsorción. (C) Citometría de flujo de células Vero tratadas previamente con Baf o DMSO e infectadas, tras la adsorción se aplicó un pulso a pH 5,4 o 7,4 durante 1 h. Las células infectadas fueron detectadas por FACS y los datos se normalizaron a los obtenidos en células tratadas con DMSO. (D) Citometría de flujo de células Vero tratadas previamente con Din e infectadas en medio a pH 7,4 o a pH 5,4 1 h. Los asteriscos denotan diferencias significativas (***= P<0.001). (E) Perfiles de FACS representativos obtenidos durante el análisis.

Estos experimentos demuestran que el pH ácido intraluminal en los endosomas es necesario para la infección. En células tratadas con medio ácido no se recuperó la infección, registrándose una reducción en torno al 80 % respecto a los valores obtenidos a pH fisiológico. Estos resultados son coincidentes con otros estudios que descartan la entrada por fusión de las membranas del virus con la membrana plasmática al mismo tiempo que confirman como vía mayoritaria la endocitosis mediada por dinamina. En conjunto, con los resultados obtenidos con Din y Baf podemos concluir que tanto la endocitosis como la acidificación endosomal son requeridos para la infección productiva del VPPA. Es decir, que la restricción de la infección productiva por VPPA a nivel de su entrada, está fundamentalmente condicionada por su paso por la vía endocítica, sea cual sea el mecanismo por el cual el virus logre atravesar la MP. Por esta acción, como se señalará posteriormente en discusión, estos compuestos han sido propuestos para su uso como antivirales.

1.3 Perfil temporal de la dependencia de pH ácido en la infección del VPPA

Tras comprobar que el pH ácido endosomal era necesario para la infectividad del VPPA y la expresión de sus proteínas tempranas (p30), se procedió a analizar el perfil temporal de la dependencia del pH a lo largo de la infección. Tras sincronizar las infecciones, el medio fue reemplazado por medio fresco atemperado con NH_4Cl 10 mM o Baf 200 nM a los tiempos correspondientes, como se aclara en el esquema (Figura 10 A). La infección se dejó progresar durante 8 hpi en todos los casos y las células fueron procesadas para analizar la expresión de p30 por WB (Figura 10 B). De esta forma, encontramos que el pH ácido era relevante para la infección durante la primera hora post-infección (45-60 mpi) y no a partir de este tiempo, ya que cuando el inhibidor se añadía a tiempos posteriores, la expresión de p30 se recuperaba hasta alcanzar niveles similares a los controles. Este tiempo es coincidente con la localización del virus en los LE como mostramos en la Figura 6 F, G.

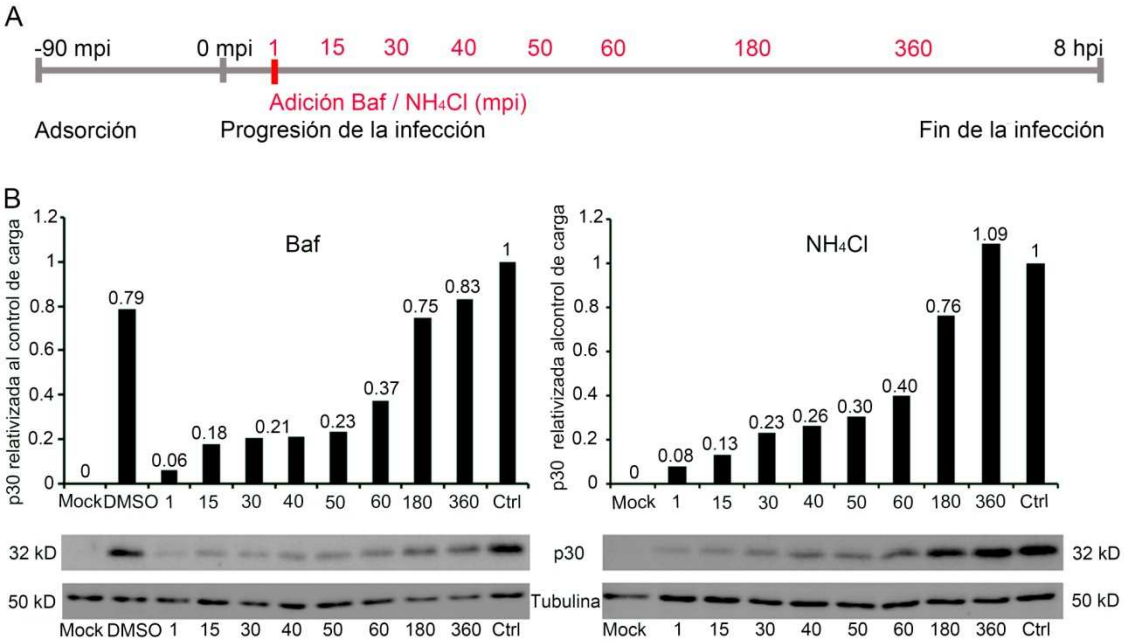

Figura 10. El pH ácido del LE es requerido en las etapas tempranas de la infección de VPPA, en la primera hora post-infección. (A) Esquema representativo de la realización del experimento. (B) Expresión de la proteína viral temprana p30 determinada por WB a 6 hpi utilizando anticuerpos específicos. El requerimiento de pH ácido resultó evidente en la primera hora post-infección pero no posteriormente.

Estos resultados indican que el pH ácido, es un factor determinante para el éxito de la infección, en la primera hora post-infección, momento en el que probablemente se produce la desencapsidación viral, como sugería la colocalización con las proteínas de la cápside y del core, pero no a tiempos posteriores. Estos hallazgos sugerían un papel crucial de los compartimentos tardíos endosomales ácidos en el proceso de desencapsidación y posterior penetración en el citoplasma desde el LE alrededor de los 45-60 mpi.

1.4 La desencapsidación del VPPA ocurre en los endosomas tardíos

La siguiente cuestión era determinar la función exacta de la acidificación endosomal en la entrada del virus. La primera posibilidad era que el pH ácido del endosoma fuera un requisito para la degradación de la cápside dentro de un proceso secuencial de pérdida de las envueltas que rodean al ácido nucleico para su protección en el medio externo, evitando así una exposición prematura del ADN viral y su eventual degradación. Esta pérdida secuencial de envueltas (o "*uncoating*"), es necesaria para la infección productiva e incluye la desencapsidación, que resulta en la liberación los cores del virus por degradación de las proteínas de la cápside. Si el pH ácido fuera necesario para la

desaparición de la cápside, el bloqueo en el avance de la infección por inhibir la acidificación debería resultar en una retención demostrable de partículas virales sin desencapsidar en los LEs. En ese caso se observaría un aumento en la colocalización entre la proteína mayoritaria de la cápside, p72, y vesículas positivas para Rab7, al bloquear el paso anterior a la salida del virión desde los LEs en condiciones de inhibición de acidificación.

Para comprobarlo se trataron las células con Baf 200 nM durante 1 h, tras la cual fueron infectadas a alta moi (10 ufp/célula), sincronizando la infección como se ha descrito anteriormente. La infección progresó durante 3 hpi y se procesaron las células para su análisis por microscopía confocal comparando las células tratadas con inhibidor con los controles con DMSO. Como era esperado se observó un aumento en la colocalización entre la proteína mayoritaria de la cápside p72 y vesículas positivas para Rab7 en células tratadas con Baf (Figura 11 A-D), en contraposición a las células control que mostraban una colocalización escasa, similar a la que encontrábamos de partida (Figura 6 C, E).

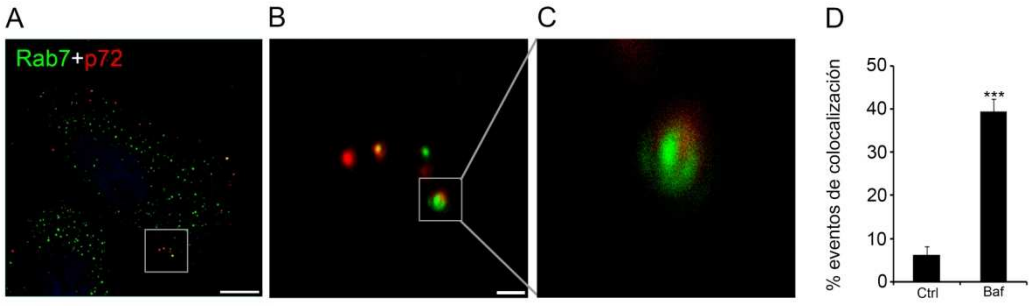

Figura 11. Imágenes de microscopía confocal representativas de células tratadas con Baf y fijadas a 3 hpi. (A) En ellas se observa la proteína viral p72 por inmuno-marcaje (rojo) y los LE marcados con Rab7 (verde); Barra 10 µm. (B-C) Detalle de la colocalización entre la cápside viral y LE en células tratadas previamente con Baf; B y C corresponden a las áreas recuadradas en la imagen previa a mayor aumento; barra 1 µm. (D) Cuantificación de los eventos de colocalización relativizados a los viriones totales asociados a cada célula individual, realizado en 130 viriones y expresados como la media y desviaciones estándar de dos experimentos independientes. La colocalización aumenta de forma significativa en presencia de Baf. Los asteriscos denotan diferencias estadísticamente significativas (*** $P<0.001$).

El incremento en la colocalización de cápsides virales y Rab7 en células tratadas con el agente inhibidor de la acidificación endosomal, señala que la desencapsidación se produce en los compartimentos positivos para Rab7.

Estas observaciones experimentales son otra demostración de que el VPPA utiliza la vía endosomal para la infección y que un incremento de pH en vesículas ácidas puede causar un bloqueo en la progresión de la infección, a juzgar por la retención de partículas virales encapsidadas observadas en células tratadas con Baf. Estos resultados indican que la

desencapsidación es un evento clave para la progresión de la infección y en condiciones basales ocurre en el interior del LE.

Como demostración última del proceso de entrada del VPPA, abordamos estudios ultraestructurales en colaboración con el laboratorio de José Carrascosa del Centro Nacional de Biotecnología, de la Universidad Autónoma de Madrid. Basados en la información obtenida de los tiempos de paso del virus por los diferentes componentes de la vía endosomal, se obtuvieron preparaciones de células Vero infectadas con el aislado BA71V para observar al microscopio electrónico.

A los 15 mpi se observaba el virus en zonas del citoplasma cercanas a la membrana plasmática. El VPPA se reconocía con facilidad con su cápside completa y su característica estructura icosaédrica rodeando el core con un llamativo nucleoide denso a los electrones. Se realizaron preparaciones a los tiempos en que se produce la desencapsidación del virus, 30 y 45 mpi. A estos tiempos se observaban viriones en el interior de endosomas, en zonas más interiores de la célula cuya morfología era compatible con cuerpos multivesiculares (MVBs; Fig. 12 A). Estos mostraban múltiples pequeñas vesículas en su interior compatibles con vesículas intraluminales (ILVs). Estos acúmulos de ILVs se observaban frecuentemente próximos al virus. No se encontraron imágenes de viriones íntegros en el interior de estos endosomas. De forma característica, los viriones identificados en el interior de los MVBs, habían perdido la cápside total o parcialmente (Fig.12 A) y con ello su simetría icosaédrica, redondeándose. Asimismo, el core aparecía menos denso a los electrones o fragmentado, una vez liberado de la cápside.

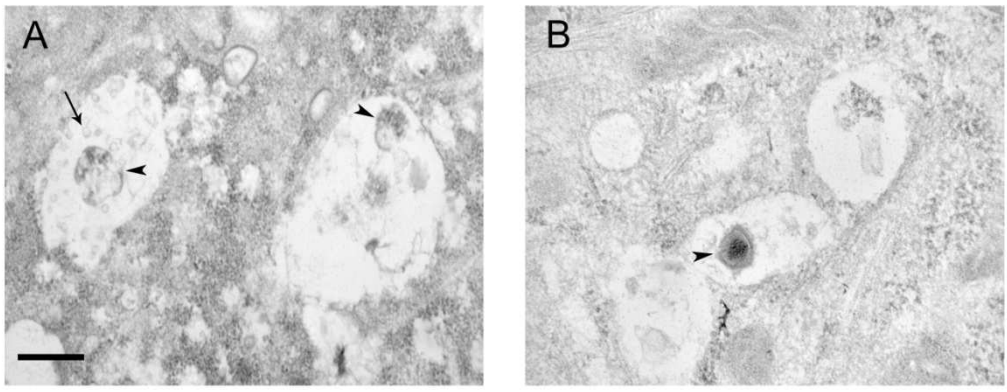

Figura 12. Imágenes representativas del estudio ultraestructural del paso del virus por la vía endocítica. (A) Endosomas rellenos de vesículas intraluminales (ILVs; flechas). En su interior no se observaron viriones íntegros de simetría icosaédrica, en cambio si se observan viriones redondeados en proceso de desencapsidación (puntas de flecha). (B) En presencia de Baf si era posible reconocer viriones íntegros encapsidados, señalados por puntas de flecha, retenidos en el interior de endosomas. Barra 500 nm.

Además, se realizaron preparaciones en condiciones de inhibición de la acidificación de los endosomas con Baf de forma similar a las analizadas por microscopía confocal a los mismos tiempos. No se encontraron imágenes de viriones desencapsidados en MVB. Al contrario, se encontraron viriones con su cápside completa en el interior de endosomas (Figura 12 B), incluso en posiciones muy internas, cercanas a la membrana nuclear correspondientes a viriones intactos, retenidos en el interior de los endosomas cuya maduración se había detenido, impidiendo la progresión de la infección.

2. MOLÉCULAS DE SEÑALIZACIÓN DE LA VÍA ENDOCÍTICA EN LA INFECCIÓN POR VPPA

2.1 Relevancia de la actividad de la GTPasa Rab7

La vía endocítica es un proceso celular altamente regulado, una vez comprobado el requerimiento la vía endocítica para la infección, analizamos las moléculas de señalización implicadas en la integridad de esta vía. Teniendo en cuenta los resultados anteriores, que señalaban la importancia de los endosomas tardíos, la GTPasa Rab7, que contribuye a la maduración de este compartimento endosomal, deberían tener un papel crucial en la infección. La relevancia de la GTPasa Rab7 en infectividad y expresión de proteínas virales de VPPA fue comprobada mediante la expresión transitoria del mutante dominante negativo de Rab7 (GFP-Rab7 DN), T22N y comparada con la expresión transitoria del fenotipo salvaje (GFP-Rab7 WT, del inglés, "*wild type"*) en células COS, 24 h después de la transfección. Esta línea celular fue seleccionada porque siendo susceptible a la infección por el VPPA (Carrascosa et al., 1999), presenta una mayor eficiencia de transfección que las células Vero.

Los transfectantes transitorios que expresaban GFP fueron seleccionados ó "sorteados" mediante un citometría de flujo. Las células transfectadas seleccionadas se sembraron nuevamente en placas e infectadas 24 h a baja moi. A este tiempo se puede observar claramente la factoría viral formada, próxima al MTOC, en la que se acumulan las proteínas virales de nueva síntesis y el ADN viral.

La Figura 13 A, muestra el porcentaje de células transfectadas seleccionadas por "*sorting*". El análisis posterior reveló que el número de células infectadas detectadas con un anticuerpo monoclonal frente a p72 mediante IFI, decrecía desde un 43,5% en células que expresaban Rab7 WT hasta 1,65% para células transfectadas con el plásmido Rab7 DN de un total de 400 células infectadas por experimento (Figura 13 B panel izquierdo y derecho, respectivamente). Este ensayo demuestra que la expresión transitoria de Rab7 DN redujo la infectividad, lo que indica que la GTPasa Rab7 y su función en la maduración del

endosoma, son necesarias para una infección productiva por VPPA, lo cual es acorde con el importante papel que juegan los LE en la desencapsidación del virus.

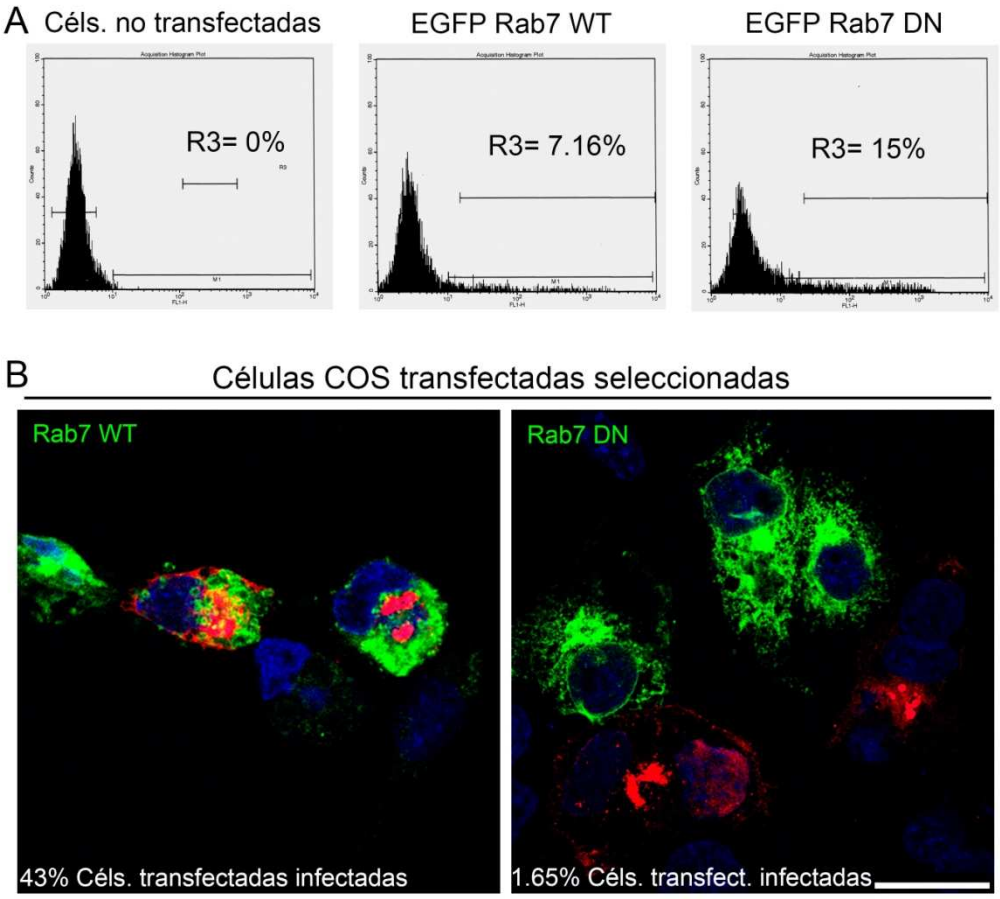

Figura 13. Relevancia de la actividad de la GTPasa Rab7 en la infección de VPPA. (A) Perfiles de FACS representativos obtenidos durante el análisis de las células COS 7 transfectadas con el fenotipo salvaje de la proteína Rab7 fusionada a GFP (GFP-Rab7 WT) y el mutante dominante negativo (GFP-Rab7 DN, T22N) . R3 representa los transfectantes que expresan GFP y que fueron seleccionados por "*sorting*". (B) Imágenes de microscopía confocal representativas de células transfectadas seleccionadas y posteriormente infectadas e inmuno-marcadas para la proteína viral p72 (rojo). Los porcentajes de células infectadas en los transfectantes transitorios descendían desde el 43,5% en células que expresaban Rab7 WT hasta el 1,65% en células que expresaban Rab7 DN. Barra 25 µm.

2.2 Papel del ácido lisobisfosfatídico (LBPA) en la infección de VPPA

En los estudios ultra estructurales observamos los viriones desencapsidados en el interior de endosomas con características de cuerpos multivesiculares. Estos endosomas tardíos se caracterizan por la presencia de numerosas vesículas en su interior, llamadas vesículas intraluminales o ILVs. Como se ha menciaonado en la introducción, el LBPA es un isómero estructural del fosfatidil glicerol, abundante principalmente en las membranas internas del MVB/LE (Kobayashi et al., 2002; Kobayashi et al., 1998a). Existen evidencias de que

LBPA no solo es un marcador endosomal, sino que también tiene un papel importante en la regulación de la dinámica y función de las membranas internas del MVB. El LBPA es un lípido importante para la generación de las ILVs en los MVB/LE y este proceso está fuertemente controlado por la proteína citosólica Alix (Matsuo et al., 2004). De modo que alterar la interacción entre LBPA y Alix supone alterar la maduración de MBV y LE, ya que la generación de ILVs es fundamental para el programa madurativo de los endosomas.

En primer lugar, se analizó la localización del LBPA en los LE mediante IFI, ya que es un lípido mayoritario en las ILVs y colocaliza con Rab7 (Figura 14 A). Para ello, en este caso, utilizamos un anticuerpo frente a LBPA como marcador endosomal, sin función bloqueante, y procedimos a comprobar la correcta internalización del citado anticuerpo en las células sin infectar, tras 24 h mediante endocitosis como se ilustra en la Figura 14 B.

Con el fin de analizar el significado funcional de Alix en el LE en el contexto de la infección, se procedió a bloquear la unión entre Alix y LBPA incubando las células Vero previamente a la infección con el anticuerpo bloqueante 6C4 frente a LBPA, cedido por el Dr. Jean Gruenberg (Pattanakitsakul et al., 2010).

Las células tratadas tras 24 h de incubación en presencia del anticuerpo y controles sin tratar, se infectaron con un VPPA recombinante fluorescente (B54GFP; moi de 1 ufp/célula). Este virus recombinante expresa GFP como proteína de fusión de la proteína p54 y se puede observar su acumulación de forma característica a nivel de la factoría viral en las células infectadas. Los cultivos de células tratadas con el anticuerpo bloqueante mostraban una reducción del número de células infectadas de un 50% respecto al control (Figura 14 C, D). De igual modo, la adición del anticuerpo frente a LBPA producía una disminución en la expresión de la proteína viral temprana p30 a 6 hpi con respecto a los controles mediante la técnica de WB (Figura 14 E, F).

Además examinamos la producción viral en las células con la función de LBPA alterada. La producción de virus intracelular decrecía un 50% respecto a las células control (Figura 14 G). Por lo tanto, se demostró que el tratamiento con el anticuerpo frente a LBPA afectaba significativamente a la infectividad y producción viral. De tal modo que podemos afirmar que el LBPA es una diana molecular cuya función es importante para a la infección del VPPA desde las etapas tempranas del ciclo infectivo.

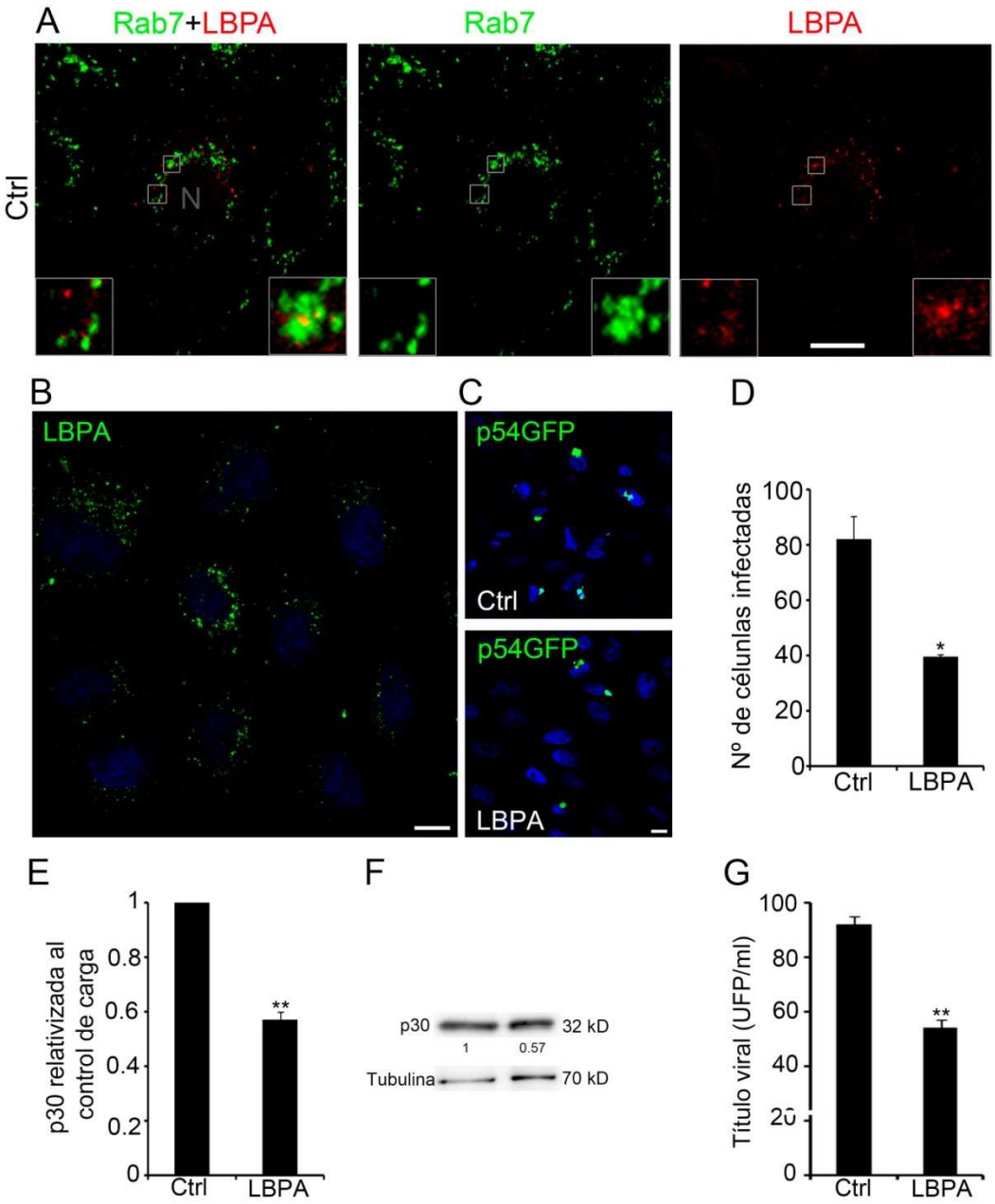

Figura 14. Relevancia del LBPA en la infección de VPPA. (A) Imagen representativa de microscopía confocal que muestra la colocalización entre membranas inmuno-marcadas para Rab7 y LBPA. Barra 10 µm. (B) Imagen de microscopía confocal representativa que muestra la internalización del anticuerpo bloqueante anti-LBPA en células Vero (verde); Barra 10 µm. (C) Imagen de microscopía confocal representativa de células Vero infectadas con el virus recombinante B54GFP pre-tratadas con el anticuerpo anti LBPA o sin tratar. Barras 10 µm. (D) Cuantificación de la infectividad en células control o en células pre-tratadas con anti-LBPA. Los datos están expresados como medias y desviaciones estándar de los porcentajes de dos experimentos independientes. Los asteriscos denotan diferencias estadísticamente significativas (*=P<0.05). (E, F) Expresión de la proteína p30 en células incubadas previamente con anti-LBPA y células control, en valores obtenidos a partir de la densitometría de las bandas del WB adyacente. (G) Cuantificación de la producción viral en células tratadas con el anticuerpo bloqueante anti-LBPA y células control. Los datos están expresados como medias y

desviaciones estándar de dos experimentos independientes. Los asteriscos denotan diferencias estadísticamente significativas (** P< 0.01).

2.3 Relevancia del flujo de colesterol desde los endosomas tardíos en la infección del VPPA

Los lípidos tienen un papel importante en la infección del VPPA, en concreto, el contenido en colesterol de la membrana plasmática (Hernaez and Alonso, 2010), la totalidad de la ruta de biosíntesis del colesterol y las proteínas preniladas de forma más específica (Quetglas et al., 2012), tienen un papel fundamental en distintas fases de la infección. Los niveles de colesterol están regulados en la célula a tres niveles: en la biosíntesis *de novo* de colesterol, a nivel de la incorporación de colesterol extracelular en forma de LDLs mediante endocitosis dependiente de clatrina y a nivel del flujo de salida de colesterol de la célula (Canon et al, 2006).

La acumulación de colesterol en los LE supone una profunda alteración en su función, y afecta profundamente a la infección de ciertos virus que se internalizan en las células mediante endocitosis, como el virus de influenza y el VSV. En el caso del virus del Dengue, se ha comprobado que al inhibir el flujo de salida de colesterol de los endosomas, los virus quedan retenidos en los compartimentos tardíos endosomales (Lakadamyali et al., 2004; Liscum and Faust, 1989; Poh et al., 2011).

Para analizar el impacto en la infección del VPPA de la interrupción de la salida del colesterol desde las ILVs del MBV/LE, se procedió al bloqueo del flujo de colesterol con el fármaco U18666A (U) (Liscum and Faust, 1989), ya que actúa en el equilibrio del colesterol celular a través de dos mecanismos: 1) mediante el bloqueo del transporte de colesterol endocitado en forma de LDL (lipoproteína de baja densidad), lo que resulta en una acumulación de colesterol en los MVB/LE y, 2) mediante la supresión los pasos intermedios de síntesis *de novo* de esterol a través de óxidoescualeno ciclasa(Sexton et al., 1983). Este fármaco, interrumpe el tráfico normal de la vía endocítica, produce acúmulo de endosomas cargados de colesterol en la zona perinuclear, fenotipo similar al que aparece en la enfermedad de Niemann Pick. Para realizar estos ensayos se procedió en primer lugar a comprobar la distribución de MVB/LE en células tratadas con concentraciones no citotóxicas (10 μM) del fármaco U durante 16 h. En la Figura 15 se observa la localización hacia el núcleo de los LE inmuno-marcados con anticuerpos frente a CD63, LBPA y Rab7 en células tratadas con U, ya que estas vesículas almacenan el colesterol libre. En las células sin tratamiento, en cambio se observa la distribución citoplásmica habitual de las vesículas endosomales de forma dispersa.

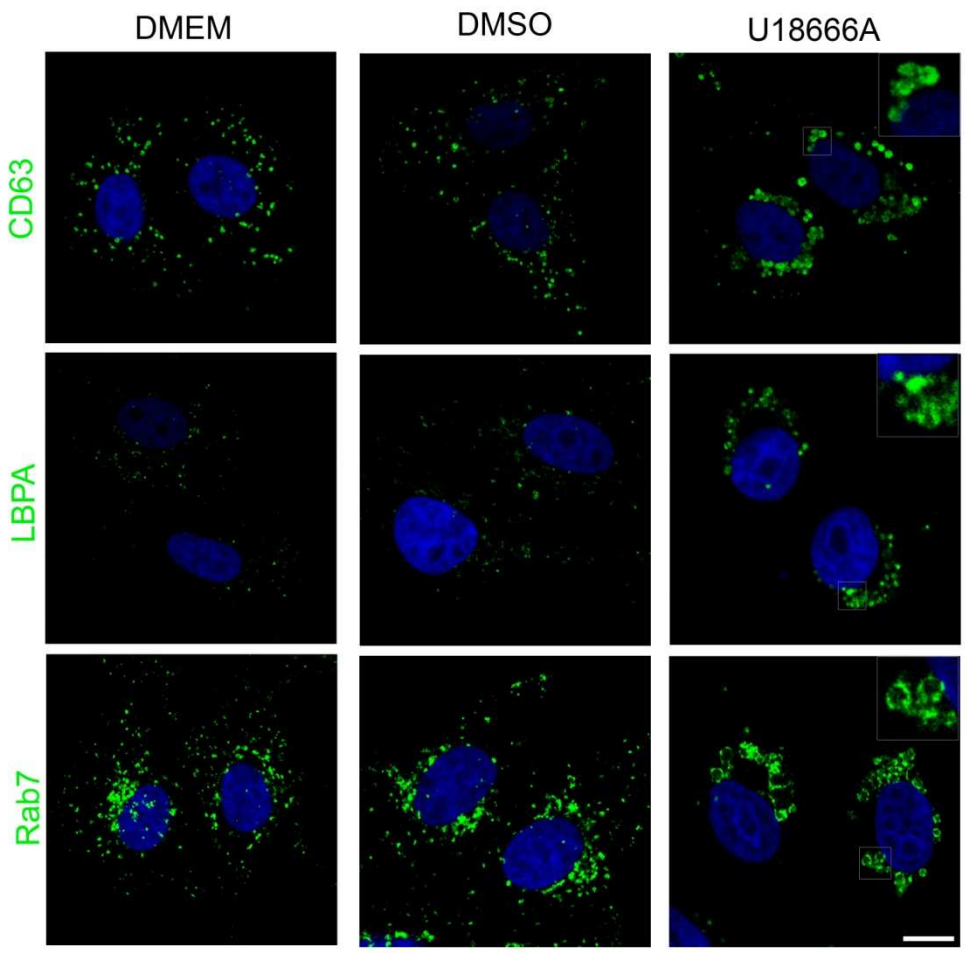

Figura 15. Redistribución de compartimentos tardíos endosomales y colesterol tras el tratamiento con U18666A. Imágenes representativas de microscopía confocal en las que se muestra la localización de vesículas inmuno-marcadas (verde) para CD63, Rab7 y LBPA en condiciones de control (DMEM o DMSO) o tratadas con U18666A. Barra 10 μm.

Se realizaron dobles marcajes de los marcadores endosomales tardíos y colesterol, (Figura 16) marcado con Filipina, un reactivo fluorescente ampliamente utilizado para detectar el colesterol celular, ya que presenta alta afinidad de unión a este compuesto (Sobo et al., 2007). Se observó acumulación de colesterol en el interior de los compartimentos tardíos, inmuno-marcados con CD63 y LBPA, alrededor del núcleo en las células tratadas con U. En cambio, el colesterol se distribuía de manera homogénea y difusa en el citoplasma y la membrana plasmática de células control.

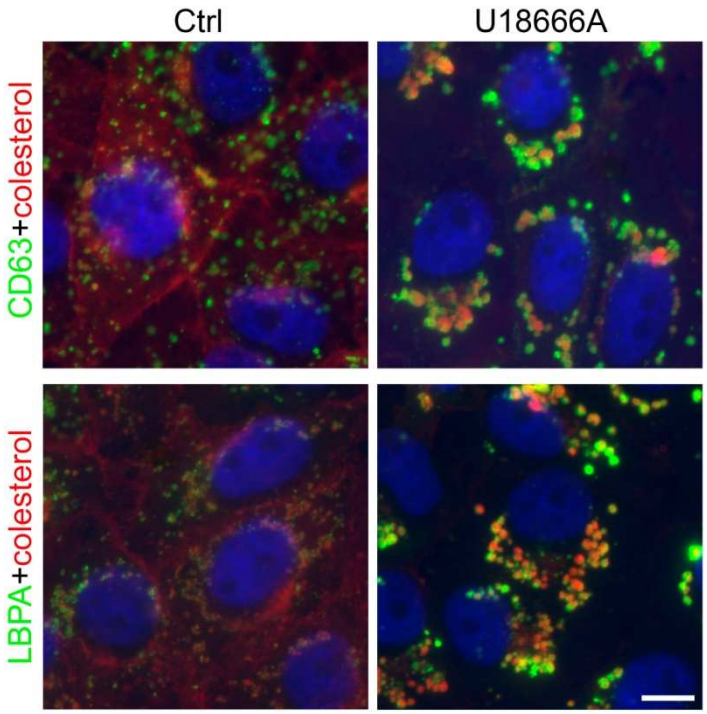

Figura 16. Redistribución del colesterol celular en células tratadas con U. Imágenes representativas de microscopía de fluorescencia en las que se muestra la redistribución de las membranas endosomales inmuno-marcadas con CD63 y LBPA por un lado (verde) y por otro el colesterol celular, teñido con Filipina (rojo) en células pre-tratadas con droga U y células control (DMSO). Barra 10 µm.

La diferencia entre la distribución de colesterol entre células control y tratadas con U en un campo microscópico más amplio se muestra en la Figura 17 A. Tras confirmar el efecto de U en la localización de las vesículas y el colesterol celular, se procedió a comprobar su impacto en el contexto de la infección. Se trataron las células con U durante 16 h previas a la infección, para permitir la acumulación de colesterol en LE/LI. Posteriormente, se realizaron infecciones con el aislado BA71V a una moi de 1 ufp/célula, y se midió la infectividad mediante la expresión de la proteína temprana p30 por citometría de flujo en células tratadas y control. La infectividad decrecía de una manera dosis dependiente hasta un 80% en las células tratadas respecto al control tomado como el 100% (Figuras 17 B, C). También se analizó la síntesis de proteínas tempranas (p30) mediante WB, en condiciones similares a las anteriores, decreciendo igualmente la expresión proteica hasta la mitad en las tratadas, respecto al control (Figuras 17 D, E).

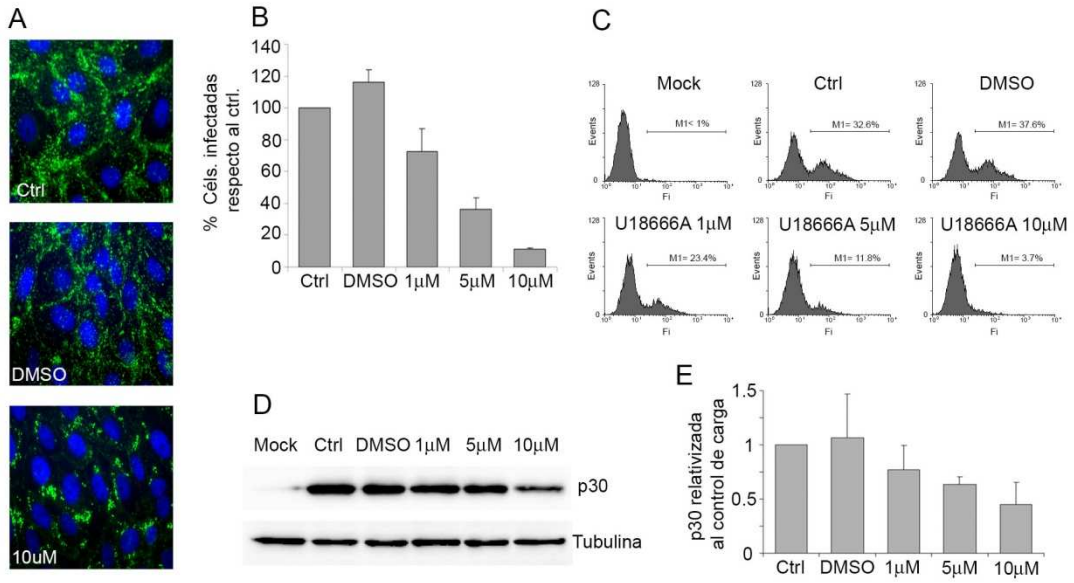

Figura 17. Efecto del bloqueo del flujo de colesterol de los LE. (A) Imágenes representativas de la localización del colesterol en células tratadas con la droga U y control. El colesterol (verde) se visualiza por la alta avidez de la Filipina para unirse al colesterol. (B, C) Gráfico que muestra el impacto dosis dependiente del fármaco U y en células control en la infección viral a una moi de 1 ufp/célula durante 6 hpi en forma de porcentaje y desviación estándar. A la derecha se muestran perfiles de FACS representativos de cada condición. (D, E) Expresión de la proteína viral p30 mediante WB en células tratadas con U a concentraciones crecientes y en células control. Gráfico de la densitometría del WB, con los datos relativizados respecto al control de carga y a los controles sin tratar.

Asimismo, pudimos demostrar la retención del virus en LE en condiciones de inhibición de la salida de colesterol desde el endosoma con el agente U utilizando microscopía electrónica, en experimentos similares a los anteriormente descritos, tratando previamente con U 5 y 10 µM e infectando posteriormente con BA71V (moi 1 ufp/célula) para fijar a 45 mpi.. En las células incubadas previamente con U 10 µM, se produjo una detención del tráfico de endosomas, que se observaban en agregados en la zona perinuclear, dilatados por el acúmulo de colesterol en su interior y fusionados entre sí. Estos contenían frecuentemente estructuras concéntricas similares a hojas de cebolla por acúmulo de esfingolípidos, cómo los descritos en la enfermedad de Niemann Pick (Taksir et al., 2012) (Figura 18 A). A esta dosis inhibitoria del agente U (10 µM), se pudieron detectar viriones íntegros sin desencapsidar retenidos en los LE cargados de lípidos (Figura 19 A), y localizados en zonas cercanas al núcleo (Fig. 18 B).A dosis menores de U (5 µM), se podían observar viriones retenidos en estadíos morfológicos ciertamente alterados (Figura 19 A-D).

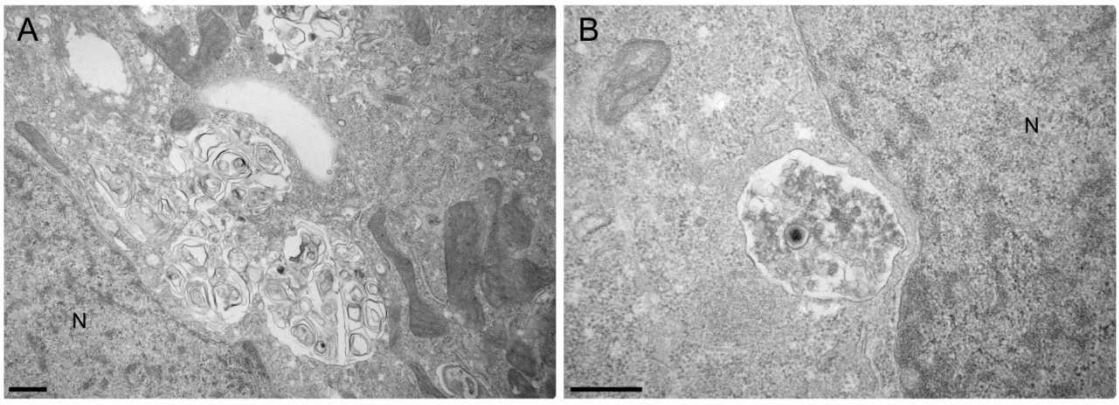

Figura 18. **Ultraestructura de células Vero tratadas con U 10 µM e infectadas con VPPA.** (A) Acúmulo perinuclear de endosomas cargados de lípidos o fenotipo similar a la enfermedad de Niemann Pick. Barra 200 nm. (B) Retención de virión sin desencapsidar en compartimentos endosomales cargados de colesterol por efecto del agente U (10 µM). El tráfico de endosomas está alterado y se acumulan en la zona perinuclear. N: núcleo celular. Barra 500 nm.

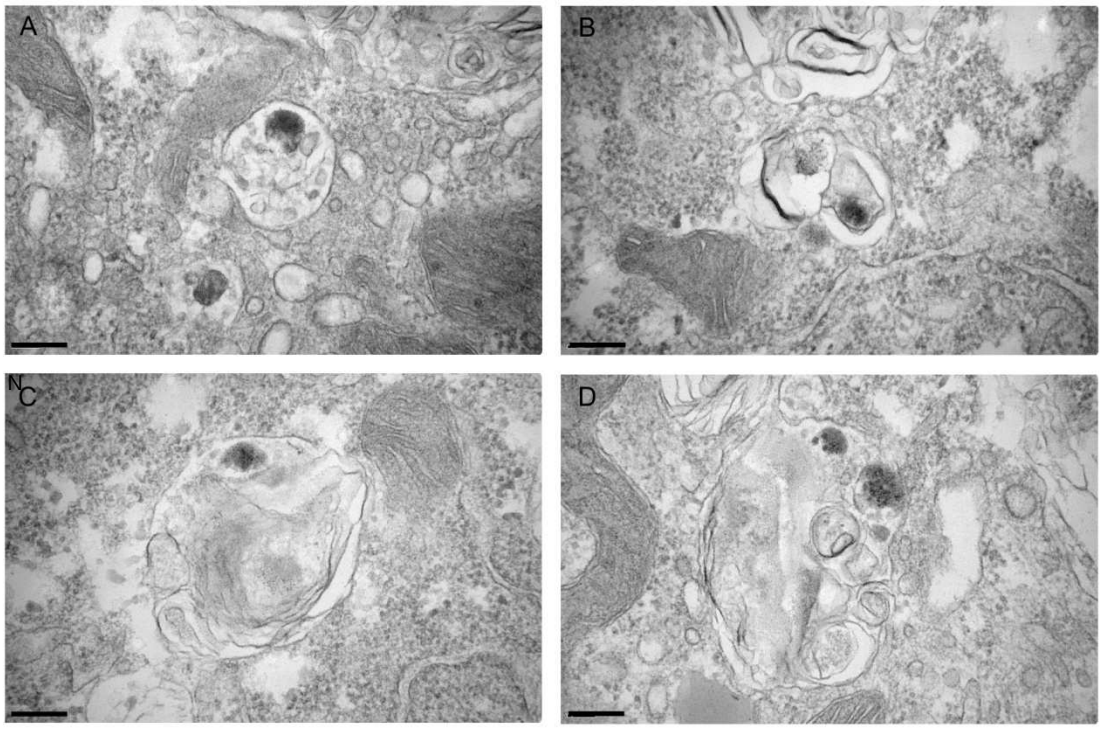

Figura 19. Ultraestructura de células Vero tratadas con U 5 µM e infectadas con VPPA. (A-D) A dosis menores del agente U (5 µM) se pudieron observar en el interior de los agregados de endosomas cargados de lípidos, viriones de aspecto morfológico alterado. Barra 200 nm.

Estos resultados nos permitieron concluir que la acumulación de colesterol en los LE, lugar donde se encuentra mayoritariamente el LBPA, es un factor que afecta severamente a la infección del VPPA en sus etapas tempranas cuando se bloquea el transporte de colesterol en los endosomas.

En resumen, las moléculas de señalización de la vía endocítica son dianas celulares relevantes para la infección de VPPA, y su importancia reside en su papel en la maduración de los endosomas, especialmente en el LE, como es el caso de la Rab7 GTPasa. También la función del LBPA en el mantenimiento de la homeostasis intraluminal del LE es importante en la infección viral. El flujo de colesterol de los LE, apunta un papel fundamental en la infección. Todas ellas constituyen potenciales dianas terapéuticas para el diseño futuro de estrategias de intervención frente al virus.

2.4 Fosfoinosítidos. Estudio del papel de FtdIns(3,5)P_2 y la interconversión mediada por PIKfyve en la infección

La maduración endosomal requiere la conversión de Rab5 a Rab7 generándose un endosoma híbrido con las dos poblaciones de GTPasas. Rab7 recluta sus proteínas efectoras de forma progresiva que participarán en el progreso madurativo. Sin embargo, la conversión de las GTPasas dependerá en gran medida de la conversión de fosfoinosítidos en la membrana endosomal (FIs), manteniendo estrictamente regulada la población de estos en cada etapa de la vía endocítica.

Los FIs son lípidos requeridos para la maduración de los endosomas, participando en ella de forma organizada junto con las Rab GTPasas. Por este motivo, analizamos la función de uno de los FIs relevantes y característicos de la regulación de la vía endocítica, el FtdIns(3,5)P_2. El FtdIns(3,5)P_2 es esencial en la dinámica de LE/LI, compartimentos con marcaje positivo para la GTPasa Rab7 (de Lartigue et al., 2009; Huotari and Helenius, 2011).

YM201636 es un potente inhibidor de la fosfatidil inositol 5 quinasa de la clase 3, también llamada PIKfyve, de mamíferos (Jefferies et al., 2008), esta sintetiza FtdIns(3,5)P_2 a partir de FtdIns3P principalmente). Por lo que la acción de esta enzima resulta fundamental para el mantenimiento de la homeostasis de la vía endocítica.

Por ello quisimos analizar el efecto de provocar un desequilibrio en la conversión de estos FIs utilizando el inhibidor de esta quinasa en la infección por VPPA. La concentración de trabajo fue determinada en 1 μM a partir de un ensayo de citotoxicidad. Dicha concentración no resultaba tóxica, y su efecto era patente, ya que producía un característico fenotipo vacuolar por la fusión de los endosomas cuya maduración se interrumpe en el citoplasma celular**.** Dicho fenotipo aparece debido a la alteración en el equilibrio hacia la acumulación de FtdIns3P en detrimento de su conversión hacia FtdIns(3,5)P_2 que causa una alteración en el Ca^{2+} y en las dinámicas de fusión y bloqueo de la maduración endosomal en la fusión de LE y LI, que causa la vacuolación citoplásmica característica. Estudiamos si la inhibición de la actividad de PIKfyve afectaba al ciclo

infectivo del virus en función del tiempo en el que se aplicaba dicha inhibición. Así, las células se trataron previamente con YM201636 1 µM dos horas antes de infectar, también se trataron con dicho inhibidor en el momento de la infección, y dos horas después de la infección. Las células fueron infectadas a una moi de 1 ufp/célula durante 24 h.

La inhibición de la actividad de PIKfyve desembocaba en una reducción de la producción viral significativa hasta del 90% en las células tratadas dos horas antes de la infección y menores si el inhibidor se añadía posteriormente, siempre en comparación con el control con DMSO (Figura 20 A).

Con el fin de determinar su efecto sobre la infectividad viral, el inhibidor fue añadido cada hora, comenzando desde 1 h antes de la infección que es el tiempo necesario para observar fenotipo vacuolar por la acción de este inhibidor (Jefferies et al., 2008) y hasta 5 hpi. Se contabilizaron células positivas para la proteína viral temprana p30 a las 6 hpi, una hora más tarde. El ensayo mediante IFI reveló una reducción de un número medio de 60 células infectadas por campo de gran aumento en células control a menos de 20, como media de un contaje de 20 campos al azar en la detección de p30 en células tratadas con el inhibidor desde 1 h antes de la infección hasta 4 hpi, pero no a tiempos posteriores. La figura 20 B recoge un gráfico representativo de dicho contaje.

Algo reseñable es que de las células tratadas con el inhibidor YM201636, las escasas células en las que la replicación viral progresaba y llegaba a observarse la factoría viral tras 16 hpi, el patrón vacuolar no se apreciaba. Es decir, el 100% de las células en las que se observaba factoría viral no mostraban patrón vacuolar a diferencia de lo observado en las células vecinas no infectadas (Figura 20 C). Este efecto no ha sido nunca reportado, sin embargo podría indicar que el virus ejerce un cierto control sobre la dinámica de membranas en la vía endocítica como se discutirá en el siguiente apartado.

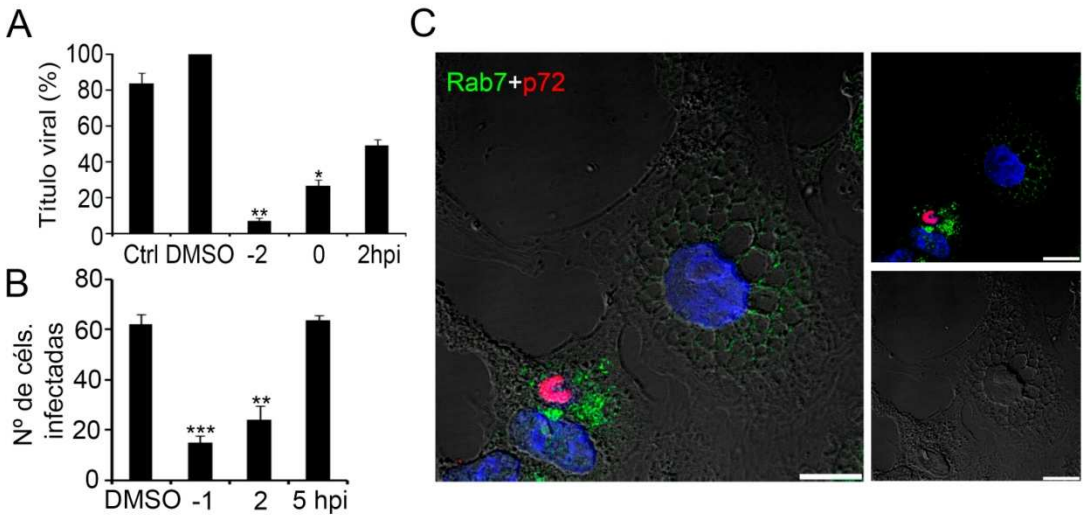

Figura 20. Papel de PIKfyve en la infección de VPPA. (A) Cuantificación de la producción de virus en células tratadas o no con YM201636 1mM, inhibidor de PIKfyve, o DMSO. Los datos están expresados como media y

desviación estándar de tres experimentos independientes. Los asteriscos denotan diferencias estadísticamente significativas (**= P<0.01; *= P<0.05). (B) Número de células infectadas en células tratadas con YM201636 o volumen equivalente de DMSO a distintos tiempos. Los datos son expresados como número de células infectadas a 6 hpi (moi de 1ufp/célula) obtenidos de 20 campos al azar, son media y desviación estándar de dos experimentos independientes. Los asteriscos denotan diferencias estadísticamente significativas (***= P<0.001; **= P<0.01). (C) Imágenes de microscopía confocal representativas de células infectadas y no infectadas, tratadas con YM201636, inmuno-marcadas para detectar Rab7 (verde) y la proteína viral p72 (rojo). El característico fenotipo vacuolar debido a la alteración de la dinámica de fusión endosomal era muy evidente. Las células infectadas se reconocen en la imagen por mostrar la factoría viral en rojo y carecer de vacuolización citoplásmica. Barra 10 μm.

3. FORMACIÓN DEL ORGÁNULO DE REPLICACIÓN O FACTORÍA VÍRICA

3.1 Reclutamiento de membranas endosomales hacia la FV

La replicación, morfogénesis y ensamblaje del VPPA tiene lugar en el citoplasma, en zonas perinucleares especializadas conocidas como factoría viral. Dichos lugares de ensamblaje localizan próximos al MTOC y al AG. Una vez establecidas, las factorías víricas están constituidas por acúmulos de ADN y proteínas víricas que llegan a alcanzar gran tamaño, hasta 8 micras de diámetro (Alonso et al, 2013). Nos propusimos averiguar si las membranas endosomales podrían tener un papel en la formación del sitio de replicación viral. Con la excepción de ribosomas, las FVs no presentan organelas en su interior cuando se analizan mediante ME (Quetglas et al., 2012). Además, reclutan mitocondrias y a su alrededor se reorganizan los filamentos intermedios formando una jaula de vimentina (Andres et al., 1998; Heath et al., 2001; Nunes et al., 1975; Rojo et al., 1998). También, el citoesqueleto de microtúbulos es necesario para la constitución de la FV (de Matos and Carvalho, 1993; Heath et al., 2001), aunque en las últimas etapas del ciclo viral, se produce finalmente una desorganización del citoesqueleto. Sin embargo, el proceso de formación del orgánulo de replicación del virus o factoría vírica es aún desconocido.

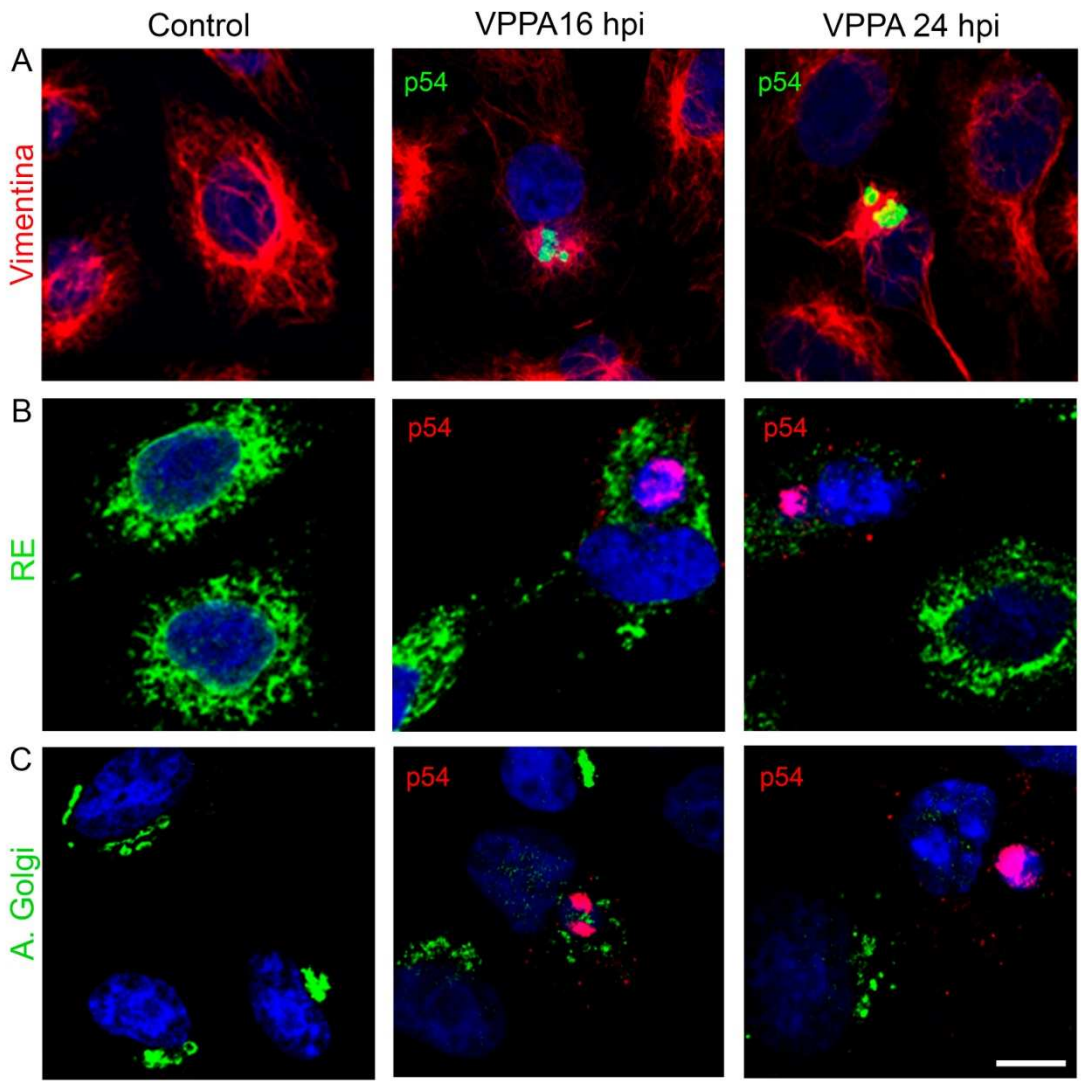

Figura 21. Cambios en algunos orgánulos celulares y del citoesqueleto en células infectadas con VPPA. Imágenes representativas de microscopía confocal de diferentes inmuno-marcajes de distintas estructuras celulares, (A) filamentos de vimentina, (B) retículo endoplásmico y (C) aparato de Golgi en células sin infectar (control) o células infectadas con VPPA, en las que se visualiza la proteína viral p54 localizada en la factoría vírica, a diferentes tiempos post infección. Barra 10 µm.

En la Figura 21 se muestran algunos de los procesos que ocurren durante la constitución de la FV, como son la reorganización del citoesqueleto de vimentina (Stefanovic et al., 2005) (Figura 21 A), la localización del RE alrededor de la FV (Rojo et al., 1998) (Figura 21 B) y la progresiva desorganización del AG a medida que progresa la infección (Netherton et al., 2006) (Figura 21 C).

Respecto al origen de las membranas de las que se acompaña la generación de la factoría se ha postulado que pueden proceder del RE. Así, se observa como el RE se sitúa rodeando a la FV en los momentos iniciales, para luego desorganizarse de forma similar al aparato de Golgi a 24 hpi. También, las membranas procedentes del RE parecen ser los

precursores de la membrana interna lipídica del virión de VPPA (Alejo et al., 1999; Andres et al., 1998; Hawes et al., 2008; Rodriguez et al., 2004; Rouiller et al., 1998).

Es conocido que diversos patógenos intracelulares se sirven de membranas para constituir su nicho de replicación con diversos objetivos. Así tenemos bacterias intracelulares (Garcia-del Portillo and Finlay, 1995; Meresse et al., 1999; Steele-Mortimer et al., 1999) o virus, por ejemplo el virus de la Hepatitis C (Romero-Brey et al., 2012) y otros virus ARN (Novoa et al., 2005) y también virus ADN como el citomegalovirus humano (Alwine, 2012; Das et al., 2007) o el virus vaccinia (Chen et al., 2009), todos ellos necesitan de membranas celulares de diversos orígenes para formar su sitio de replicación.

Tras haber analizado la implicación de las distintas poblaciones de endosomas en la entrada del virus, prestamos atención a estos compartimentos en etapas algo posteriores de la infección viral, en concreto en la constitución de la factoría vírica. De este modo, intentamos averiguar el posible papel de los endosomas como sistema de aporte de membranas para la formación del lugar de replicación del virus y así investigar un proceso tan determinante como es la constitución del nicho de replicación y ensamblaje.

Así pues, comparamos la distribución de membranas en células infectadas con la factoría constituida a 16 hpi con células control, utilizando distintos marcadores endosomales. Se usaron anticuerpos frente a EEA1, CD63, Rab7 y Lamp1 frente a EE, MVB, LE y LI respectivamente. Las células control mostraban la característica distribución de los endosomas dispersos en el citoplasma. La figura 22 ilustra una marcada diferencia en la distribución y localización de las vesículas endosomales en células infectadas, identificadas por la presencia de la factoría viral. En ellas se observa un marcado reclutamiento de las membranas inmuno-marcadas con los diferentes anticuerpos a la zona de la factoría vírica.

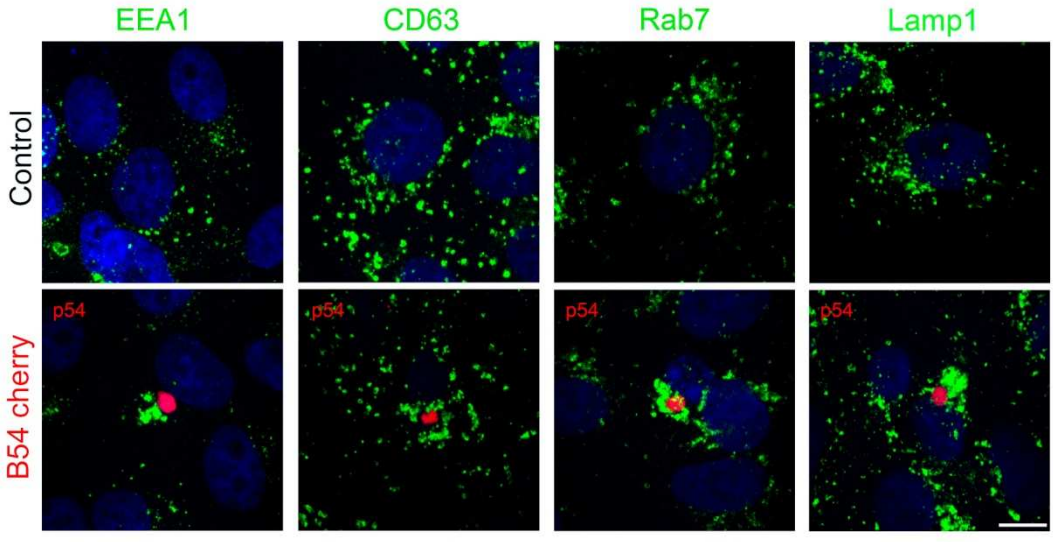

Figura 22. Redistribución de membranas endosomales alrededor de la factoría viral. Imágenes de microscopía confocal representativas que muestran células infectadas con el virus recombinante B54CherryFP a una moi de 1 ufp/célula a 16 hpi. Se realizaron IFIs con distintos marcadores de vesículas endocíticas. Los EEs marcados con EEA1, MVBs con CD63, LEs con Rab7 y LIs marcados con Lamp1 (verde). Observamos un marcado reclutamiento en torno a la factoría viral (rojo) de membranas positivas para todos los marcadores utilizados. Barra 10 μm.

El siguiente paso fue analizar dos características del reclutamiento observado. Por un lado la frecuencia con la que ocurría este evento en las células infectadas, y por otro el área que ocupaban estos acúmulos en comparación con las factorías virales. Se realizaron infecciones en células Vero manteniendo las condiciones del experimento anterior y observamos reclutamiento de membranas positivas para EEA1, CD63, Rab7 y LI en el 85%-95% de los casos como se observa en la Figura 23 A, B. El área ocupada por estos acúmulos no resultó ser muy variable cuando la FV viral ya está bien constituida (16 y 24 hpi), un promedio de 18 μm^2, medido con el marcador que mostró el valor de acumulación más elevado, Rab7. El área ocupada por la FV era de 13 μm^2 de tamaño promedio a las 16 hpi (Figura 23 C, D).

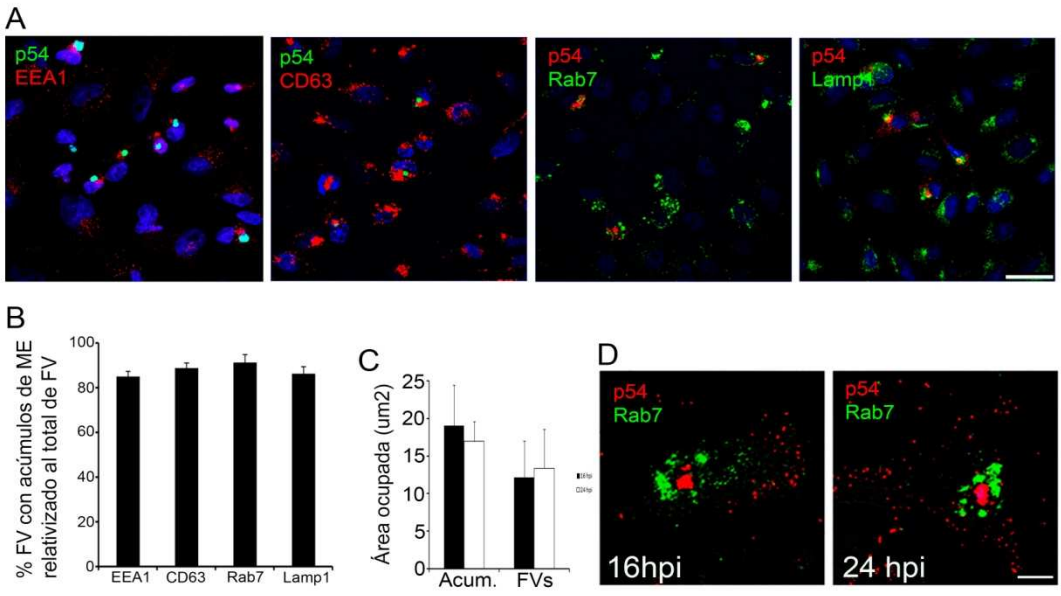

Figura 23. El reclutamiento de endosomas a la factoría es un proceso generalizado en las células infectadas. (A) Imágenes representativas de microscopía confocal que muestran el inmuno-marcaje de las diferentes vesículas endocíticas de forma similar a la figura anterior en el color señalado para cada marcador, en células Vero infectadas con el virus recombinante B54ChFP a 16 hpi, moi de 1 ufp/célula. La presencia de acúmulos en células infectadas se contabilizó sobre un total de 50 FVs por compartimento endocítico y por triplicado. (B) Los resultados se muestran en el gráfico, como media y desviación estándar de los porcentajes de FV con reclutamiento de membranas inmuno-marcadas respecto a FV contabilizadas totales. (C) Valores de área media y desviación estándar ocupados por la FV y los acúmulos membranosos a 16 y 24 hpi en células

Vero infectadas con el virus recombinante B54ChFP (moi1 ufp/célula). Los contajes se realizaron en mas de 10 células para cada condición y por duplicado sobre membranas positivas para el inmuno-marcaje de Rab7 (verde), en (D) se muestran imágenes representativas de microscopía confocal de los datos mostrados en (C).

Estos resultados señalan que la presencia de membranas endosomales alrededor de a la FV puede ser relevante para la constitución de la FV, ya que se trata de un hecho muy generalizado en las células infectadas con VPPA.

Con el fin de obtener más información acerca del reclutamiento de membranas, patente en casi la totalidad de las FVs, analizamos la progresión de la formación de estos acúmulos a diferentes tiempos post-infección. Encontramos una acumulación progresiva de membranas endocíticas alrededor de la factoría con todos los marcadores utilizados, desde 10 hpi a 24 hpi (Figura 24 A-D). A mayor aumento se podía observar que estos marcadores aparecían entremezclados entre los focos iniciales de acúmulo de proteínas víricas sintetizadas *de novo* (Figura 24 a-d).

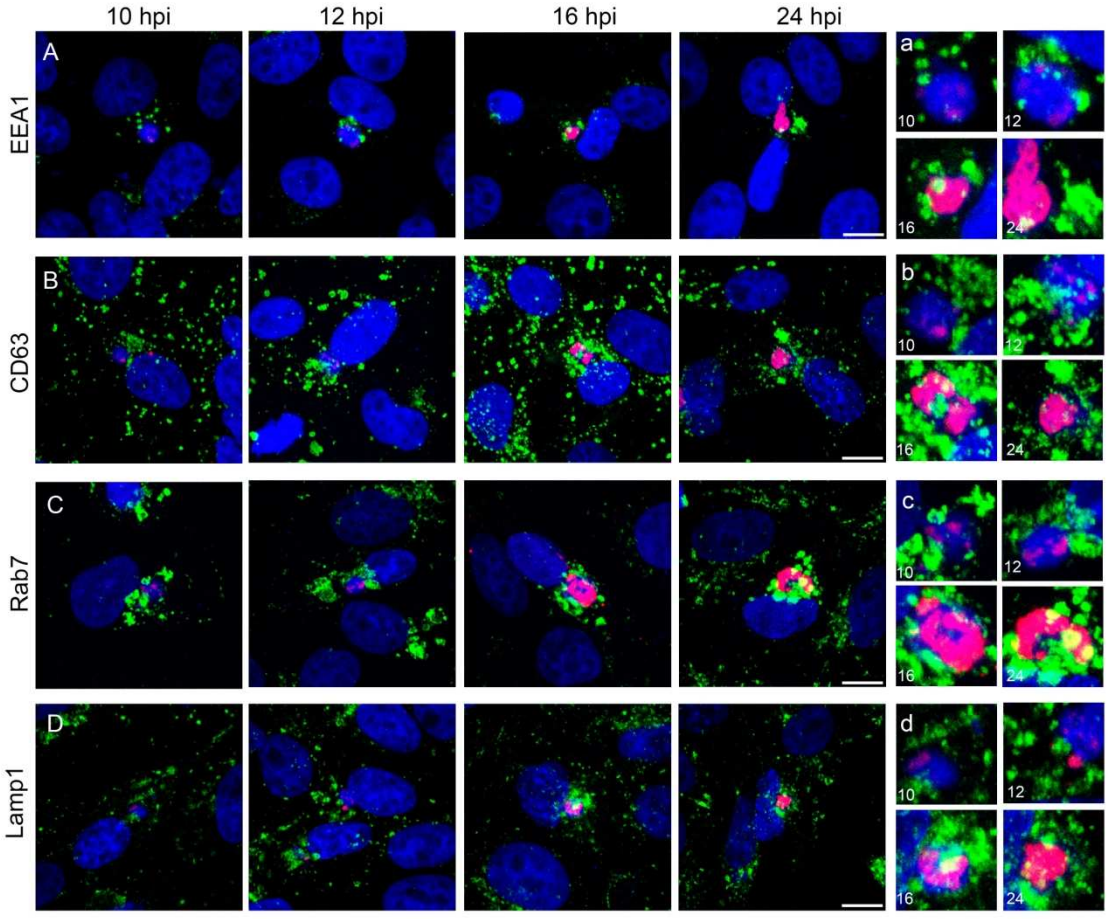

Figura 24. Acumulación de membranas endosomales en células infectadas. Imágenes microscopía confocal representativas que muestra células Vero infectadas utilizando una, con el virus recombinante BA54ChFP a diferentes tiempos post-infección (10-24 hpi; moi de 1 ufp/célula). Se realizaron IFIs con distintos marcadores de vesículas endocíticas (verde), EEs marcados con EEA1 (A), MVBs con CD63 (B), LEs

con Rab7 (C) y LIs marcados con Lamp1 (D). Los recuadros (a-d) muestran a mayores aumentos los marcajes de a) EEs, b) MVBs, c) LEs y d) LIs y son un detalle de las factorías por cada tiempo analizado. Barra 10 µm.

Los acúmulos de endosomas se situaban alrededor de la factoría y en contacto con ella, siendo algo característico en casi el total de las células infectadas que presentaban factoría viral. En la Figura 25 A se muestra una imagen de proyección máxima desde el plano superior, donde se aprecian las interacciones de las membranas con la FV, recogido también en la proyección lateral en la figura 25 B. Cuando descomponemos la imagen en los planos de los que está constituida, se observa la interacción de las membranas con surcos o entrantes de la FV (Figura 25 a-f). Asimismo las membranas endosomales aparecen entre los focos iniciales de acúmulo de proteínas víricas presumiblemente cohesionándolas para formar posteriormente una estructura única compacta o FV (Figura 25 g-k).

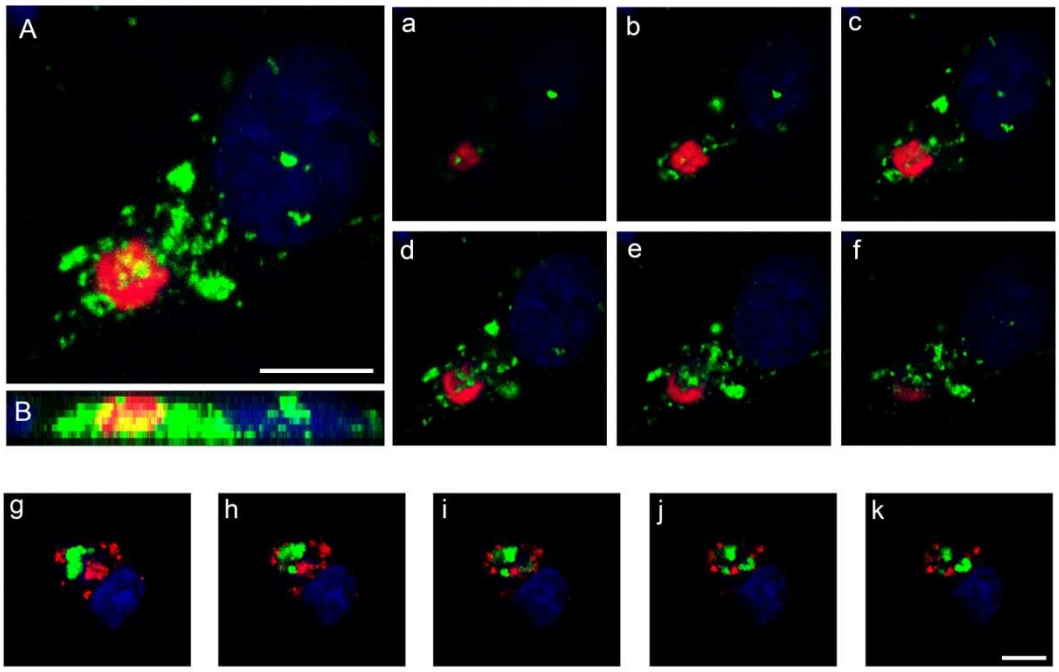

Figura 25. Interacción de las membranas endosomales con la factoría viral. Imágenes representativas de microscopía confocal en la que se observa el reclutamiento de membranas endosomales (verde) alrededor y en contacto con la factoría viral (rojo). (A) Máxima proyección de una célula infectada con el virus recombinante B54ChFP a moi de 1 ufp/célula durante 16 hpi. (B) Proyección lateral de la misma célula infectada. (a-f) Selección de imágenes que muestran la sucesión desde el plano superior al inferior de la imagen de microscopía confocal. Nótese en el plano "d" la inserción de membranas en el surco de la factoría viral. Barra 10 µm. (g-k) Células Vero infectadas con B54GFP. Selección de imágenes por planos en que se observa la situaciónde las membranas endosomales entre focos iniciales de acúmulo de proteínas individuales antes de formar una única estructura compacta.

De tal modo, se pudo constatar por primera vez que el VPPA induce una intensa reorganización de la vía endocítica en la célula infectada que pueden tener un papel fundamental como aporte de membranas para la formación de la organela de replicación del virus dando cohesión a la factoría viral en formación. Este hecho no había sido reportado previamente.

3.2 Dependencia del citoesqueleto de microtúbulos en la redistribución de endosomas hacia la FV

El citoesqueleto de microtúbulos es necesario para la formación del orgánulo de replicación del virus, por lo tanto realizamos experimentos con agentes despolimerizantes de microtúbulos como Nocodazol, para comprobar su efecto en los momentos previos a la formación de este orgánulo. Se infectaron células Vero con el virus BA71V (moi 1 ufp/célula), y se trataron con 10 μM Nocodazol 1 h previa a la infección (-1 hpi), simultáneamente con la infección (0 hpi) y a 2 y 4 hpi como se refleja en el esquema (Figura 26 A).El análisis por FACS reveló que la síntesis de la proteína tardía p54 se veía profundamente afectada a cualquiera de los tiempos analizados (Figura 27 B, C).

A través de IFI, pudimos observar que en las células control, tratadas con DMSO, la FV presenta un aspecto compacto y está rodeada de acúmulos de membranas inmuno-marcadas con Rab7 como es característico. En las células tratadas desde horas más tempranas, o bien se inhibía completamente la formación de la factoría (Figura 26 C), o bien, en escasas células se podían observabar acúmulos de proteína vírica dispersos, sin llegar a cohesionar en una FV definida (Figura 26 D a, b, c, d).

El tráfico de endosomas en la célula es dependiente de microtúbulos y por lo tanto, la adición de Nocodazol además de inhibir la formación de la FV, también inhibía el reclutamiento de endosomas a la FV, mostrándose estos dispersos o junto a los pequeños acúmulos de proteína vírica dispersos (Figura 26 D b, c, d).

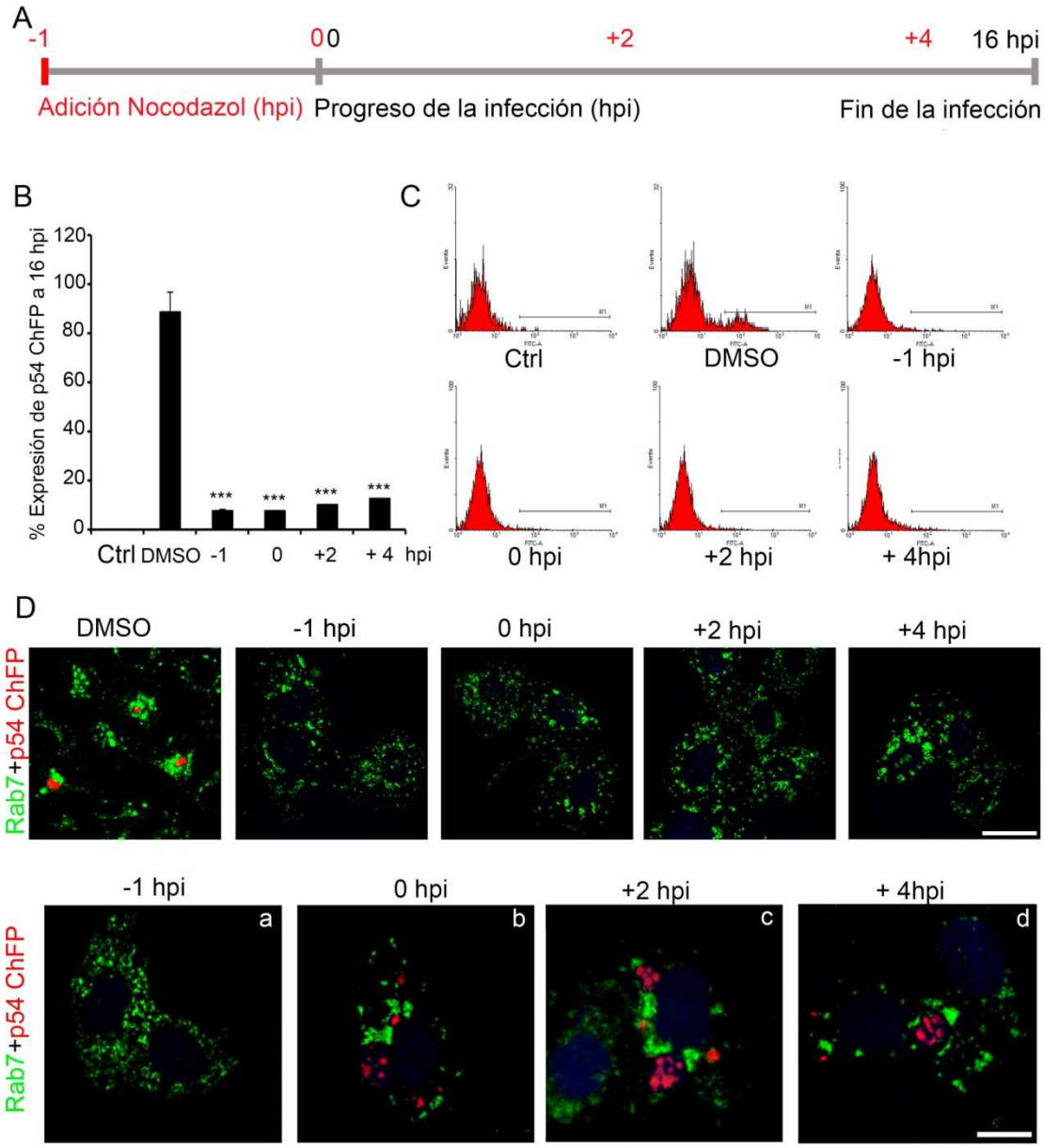

Figura 26. Efecto del Nocodazol en la formación de la FV. (A) Esquema que resume el desarrollo del experimento. (B y C) El gráfico y los perfiles de FACS muestran la expresión de p54 en condiciones control y de adición de Ncodazol a distintis tiempos, tras 16 hpi. (***= P<0.001). (D) Imágenes de microscopía confocal representativas de las observaciones anteriores. Barra 25 µm (D a, b, c, d) muestra los escasos eventos observados en la constitución de la FV según los tiempos de aplicación del tratamiento con Nocodazol. La FV fue detectada por la expresión de la proteína viral p54 (rojo) fusionada a ChFP, y el reclutamiento de membranas a su alrededor (inmuno-marcadas con un anticuerpo frente a Rab7 (en verde) tras 16 hpi en células tratadas con Nocodazol a diferentes tiempos post infección. Barra 10 µm.

En el esquema representado en la figura 27 A se muestra el desarrollo del abordaje experimental siguiente; een células infectadas con el virus BA71V y detectadas con una proteína temprana p30 a 6 hpi (tinción citoplásmica difusa), se observaba reclutamiento

de endosomas en las células tratadas con DMSO o ausencia del mismo cuando habían sido tratadas con Nocodazol, agente despolimerizante de microtúbulos (Figura 27 B).

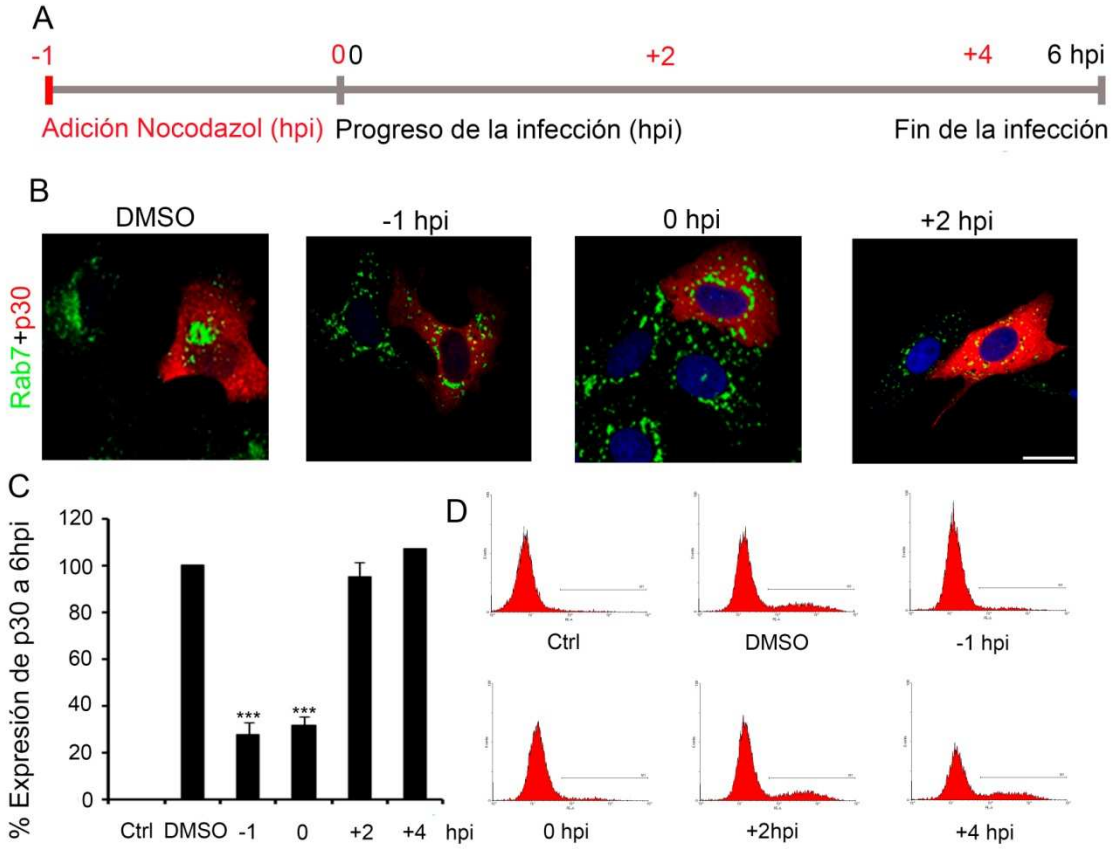

Figura 27. Efecto del Nocodazol en el reclutamiento de membranas endosomales. (A) Esquema-resumen del desarrollo del experimento. (B) Imágenes representativas obtenidas a partir de microscopía confocal. En ellas se observa como la adición de Nocodazol a distintos tiempos post infección afecta al reclutamiento de membranas inmuno marcadas con un anticuerpo frente a Rab7 (verde) que en presencia de Nocodazol se mantienen dispersas por el citoplasma incluso en células infectadas detectadas por la expresión de proteína viral temprana p30 (rojo). Las figuras (C y D) muestran como la expresión de p30 se reduce al añadir Nocodazol antes de la infección pero no si se añade a tiempos posteriores. (***= P<0.001). Barra 25 µm.

La expresión de la proteína viral temprana p30 se recuperaba hasta niveles del control al añadir Nocodazol a partir de las 2 hpi (Figura 27 C y D), cuando el virus ya ha desencapsidado. Sin embargo el reclutamiento de los endosomas ya no se produce, tal y como se muestra en la figura 27 B, cuando se añade Nocodazol tras 2 h de infección. El Nocodazol es un agente depolimerizante de microtúbulos de acción reversible, por lo que se procedió a analizar si se recuperaba el tráfico de endosomas tras el lavado del medio que contenía este agente (Figura 28) (Video).

Conjuntamente, estos experimentos refuerzan la noción de la relevancia de las membranas endosomales en la formación del orgánulo de replicación compacto que es característico de la infección y el papel de los microtúbulos en este proceso.

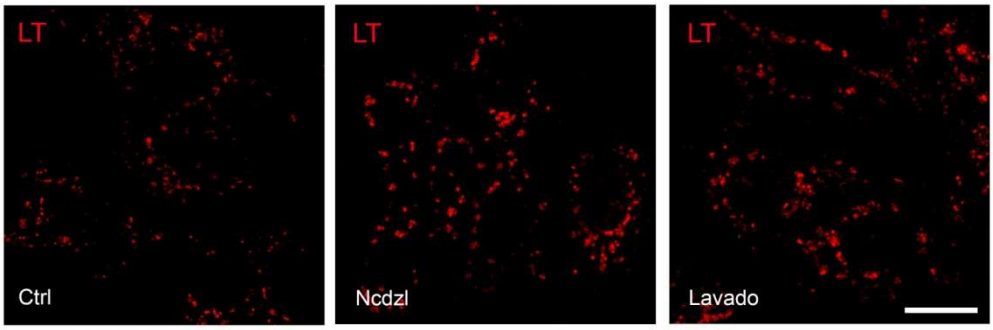

Figura 28. Efecto del Nocodazol (Ncdzl) en el tráfico de vesículas ácidas. Las vesículas ácidas se identificaron utilizando Lysotracker (LT) (rojo). En condiciones control se observa un movimiento fluido de endosomas a través del citoplasma. Tras 1 h de tratamiento con Ncdzl, la despolimerización de microtúbulos produce una retención total de endosomas en forma de pequeños agregados. Tras el lavado de Ncdzl y sustitución por DMEM, el movimiento de vesículas individuales se recupera progresivamente. En la figura, aún quedan patentes pequeñas agrupaciones de vesículas ácidas. Barra 25 µm.

La formación del orgánulo de replicación vírica compacto depende del reclutamiento de endosomas a la zona perinuclear donde se inicia el acúmulo de DNA y proteínas virales en focos independientes y que su confluencia en una factoría vírica única depende directamente del transporte de los endosomas mediante los microtúbulos a la zona de la factoría vírica en formación.

Como mencionamos en la introducción, el transporte de los endosomas mediante microtúbulos, está directamente ligado a su maduración, a la expresión de Rab7 en LE y a la unión de esta proteína a RILP ("*Rab Interacting Lysosomal Protein"*) y OSBP1 ("*oxysterol binding protein*" 1) y mediante estas, al complejo motor microtubular. Por este motivo, no es de extrañar que la función los microtúbulos y del complejo motor microtubular ligado a dineína sería fundamental para el reclutamiento de endosomas y por ende, de membranas endosomales para la formación de la FV.

En resumen, hemos demostrado que la entrada del VPPA era altamente dependiente de la integridad de la vía endocítica, siendo la acidificación endosomal especialmente crítica para la desencapsidación del virus. Pero también lo fueron el proceso de maduración endosomal y la señalización, relacionadas con los cuerpos multivesiculares y los endosomas tardíos, especialmente Rab7, el ácido lisobisfosfatídico, el flujo de salida de colesterol del endosoma y también los fosfoinosítidos y sus enzimas convertidoras. FInalmente, el aporte de membranas endosomales y el tráfico de los endosomas mediado

por microtúbulos demostraron ser muy relevantes para la correcta formación del nicho de replicación viral en el proceso de infección.

Discusión

1. COMPARTIMENTOS ENDOSOMALES IMPLICADOS EN LAS PRIMERAS ETAPAS DE LA INFECCIÓN

Numerosos patógenos y en especial los virus, necesitan valerse de la maquinaria celular, estando diseñados para llevar a cabo casi la totalidad de sus procesos, desde su mera supervivencia hasta la replicación de su genoma y la evasión del sistema inmune mediante manipulación de la célula infectada (Gruenberg and van der Goot, 2006). A partir de su entrada en la célula huésped, los virus se sirven de la maquinaria celular endocítica, destinada a la entrada de nutrientes, a la regulación negativa de receptores y otros procesos de señalización.

Otras ventajas que ofrece el aprovechamiento de la vía endocítica para alcanzar el lugar de replicación para los virus, consiste en atravesar con facilidad la intrincada red de actina cortical y el denso citosol repleto de orgánulos y transportarse hasta el lugar óptimo de penetración. De este modo, además de aprovechar las características fisiológicas del compartimento en el que viajan, evaden el sistema inmune (Marsh and Helenius, 1989; Marsh and Helenius, 2006). Es habitual, a tenor de las ventajas que aporta, que numerosos patógenos se aprovechen de la vía endocítica.

Los trabajos pioneros acerca de la entrada del VPPA en la célula huésped señalaron la endocitosis mediada por receptor como la vía mayoritaria de entrada en la célula huésped (Alcami et al., 1989a; Alcami et al., 1989b; Alcami et al., 1990; Valdeira and Geraldes, 1985). Trabajos mas recientes, demostraron que la entrada del VPPA en las células era dependiente de clatrina, epsina15 y de la actividad de la GTPasa dinamina. Además, la presencia de colesterol en membranas celulares, pero no la organización de las balsas lipídicas/caveolas eran necesarios para una infección productiva de VPPA. Por el contrario, inhibidores de los canales de Na^+/K^+ y de la polimerización de la actina no afectaron significativamente la infectividad, sugiriendo que la macropinocitosis no constituye una vía de entrada mayoritaria. A tenor de estos resultados, se concluyó que la vía principal de entrada del VPPA para desencadenar una infección productiva es dependiente de clatrina y dinamina, sin excluir otros mecanismos de entrada alternativos o cooperativos que han sido descritos (Hernaez and Alonso, 2010).

Según observaciones de ME (Alcami et al., 1989a) el virus puede aparecer en hendiduras o vesículas recubiertas de clatrina y los viriones adsorbidos en la superficie de la célula colocalizan con esta molécula con microscopía confocal (Hernaez and Alonso, 2010). Con estos datos que señalaban la endocitosis como la vía preferente de entrada, los siguientes pasos se dirigieron a determinar los compartimentos endocíticos involucrados en las primeras etapas de la infección de VPPA.

En el presente trabajo de tesis se han obtenido resultados que evidencian el paso del VPPA a través de la vía endocítica y el papel fundamental que esta vía representa en el desarrollo de una infección productiva. En concreto, el virus pasa a través de los EE y los LE y en este compartimento tardío, el virus desencapsida como primer paso en su proceso de desenvolvimiento o "*uncoating"*.

La utilización de anticuerpos frente a cada uno de los compartimentos de la vía endocítica (EE, MVB, LE o LI) y marcaje del virus con anticuerpos frente a las proteínas de la cápsida viral p72 o E120R, han permitido demostrar que las cápsides virales colocalizaban en un alto porcentaje con EE y de manera creciente desde los primeros minutos hasta los 30 mpi. Sin embargo, a partir de ese tiempo, la colocalización con EE decrecía. La colocalización de la proteína de la cápside con marcadores de compartimentos tardíos MVB, LE y LI, era escasa a cualquiera de los tiempos seleccionados a lo largo de la primera hora post-infección.

Diferentes familias de virus difieren de sus requerimientos endosomales para llevar a cabo una infección productiva, ya que cada virus necesita diferentes condiciones propias de las distintas poblaciones de endosomas para penetrar en el citosol. Uno de los más conocidos es el virus del bosque de Semliki (SFV), que sufre una fusión entre las membranas del virus y la membrana del endosoma a pH de aproximadamente 6,2 que son las condiciones fisiológicas del EE (Marsh and Helenius, 1989; White et al., 1980; White et al., 1981). Dicha fusión es provocada por la glicoproteína viral E1, conduciendo a la liberación de la cápsida al citosol (Marsh and Helenius, 2006). Posteriormente, las proteínas virales, además de los virus que no llegaron a fusionarse con éxito, se transportan hacia LE y LI para ser degradados (Vonderheit and Helenius, 2005).

El SFV, sin embargo causa la formación de vacuolas citopáticas que contienen pequeñas invaginaciones, las cuales derivan de LE. Se cree que representan lugares de síntesis de ARN (Froshauer et al., 1988). Otros virus cuyo genoma es ARN+ también modifican las membranas intracelulares para crear un nicho de replicación apropiado para su genoma (Miller and Krijnse-Locker, 2008). Aunque no se conoce con exactitud como ocurre la fusión en el EE, sin embargo, la liberación de la cápsida está acoplada a las invaginaciones de las membranas del LE y a la replicación del ARN, pudiendo ser procesos no continuos (Gruenberg, 2009).

Basados en nuestros hallazgos, postulamos que la desencapsidación de VPPA podría ocurrir en endosomas con un pH más ácido que los EE de forma rápida en el tiempo y consecuentemente la colocalización entre viriones y LE sería difícil de observar. Esta hipótesis es consistente con observaciones previas de ME de cores virales en el citoplasma de células infectadas 60 mpi después de la adsorción viral, es decir, partículas virales sin

cápsida, aunque el proceso de la desencapsidación en si no fue posible de demostrar en aquellos primeros estudios (Alcami et al., 1989a).

Para confirmar o descartar dicha hipótesis analizamos la localización del core viral con endosomas en los primeros pasos del virus tras la entrada, utilizando anticuerpos frente a la proteína del core viral p150, basándonos en la franja temporal del experimento anterior. De este modo resultó posible observar colocalización entre los cores virales y los LEs, siendo máxima esta localización en LE a los 45 mpi, mientras que la proteína de la cápside apenas era detectable en estos compartimentos.

Estos resultados sugerían que la desencapsidación del VPPA ocurre probablemente en compartimentos endosomales tardíos, de manera que este virus podría requerir algunas de las características fisiológicas propias de estas organelas, como puede ser el pH ácido.

2. PAPEL DE LA ACIDIFICACIÓN ENDOSOMAL

Para confirmar este hecho, demostramos que la acidificación endosomal es determinante para una infección productiva. Para ello se utilizó un inhibidor de la ATPasa vacuolar, necesaria para la acidificación de estas organelas la Bafilomicina (Baf) (Toei et al., 2010),, que causa una rápida alcalinización de los LEs.

Nuestros resultados mostraron que el pH endosomal era un requerimiento del VPPA para que la infección progresara, como demuestra el hecho de que el tratamiento con medio a pH ácido no restauró el efecto causado por la Baf sobre el pH endosomal, ya que inhibe específicamente la acidificación intraluminal del endosoma. Estos datos excluyen que el tratamiento con medio ácido pueda inducir fusión de membranas y conducir a una infección productiva por dicho mecanismo.

Más aun, el requerimiento de endocitosis se reforzaba por el hecho de que el tratamiento con medio a pH ácido no se tradujo en una infección productiva en tras la adsorción del virus sobre células tratadas con Dinasore (Din), inhibidor de la GTPasa dinamina. De este modo, se hubiera facilitado la entrada del virus en la célula huésped por una vía alternativa que no fuera dinamina-dependiente.

Estos datos coinciden con los de otros grupos que han publicado que la fusión con la MP inducida artificialmente por el descenso de pH del medio, no conseguía una infección productiva en células tratadas con otras drogas lisosomotrópicas (Valdeira et al., 1998; Valdeira and Geraldes, 1985). Hallazgos similares han sido descritos para el virus de la estomatitis vesicular (VSV), un caso clásico de internalización dependiente de clatrina. Al inducir la fusion con la MP, desciende su infectividad al menos un orden de magnitud respecto a la infección perpetrada a través de endosomas (Le Blanc et al., 2005).

Los requerimientos de pH ácido por parte del VPPA eran necesarios para la infectividad viral antes de la primera hora post-infección y no después de este tiempo, hecho que concuerda con la observación de cores virales en el citosol en imágenes obtenidas por microscopía electrónica ya comentadas mas arriba.

En estos experimentos era posible en cambio obtener marcaje positivo mediante inmunofluorescencia para la cápside viral en el interior de LEs en condiciones intraluminales alcalinas. Las partículas virales encapsidadas quedaban retenidas en MVB/LE según demostraron los estudios ultraestructurales y no encontrábamos degradación de la cápsida bajo la inhibición del pH ácido endosomal. Esto significa que el VPPA no podía desencapsidar y liberar el core viral al citosol en dichas condiciones y por consiguiente el ciclo infectivo se detenía en dichas condiciones. Así se confirmó el requerimiento de pH ácido, propio de LE para la desencapsidación viral y salida desde el endosoma, que tendría lugar durante la primera hora post infección para el VPPA. Dicha observación es consistente con la accesibilidad del ADN viral a nucleasas y la temporalización de síntesis de ARN temprano y síntesis de proteínas tempranas reportados previamente (Alcami et al., 1989a).

Observamos que la desencapsidación de VPPA podía detenerse en LE positivos para Rab7 en células tratadas con Baf, bloqueando de este modo la progresión de la infección viral. Tras alcanzar los LE y desencapsidar, podría tener lugar finalmente la salida del core viral hacia el citosol para comenzar su replicación en el área perinuclear. De manera característica, era posible observar viriones icosaédricos con la cápside intacta en la zona perinuclear, solo en condiciones de inhibición de la acidificación con Baf. En cambio en los controles, en el interior de MVBs solo se observaban viriones en distintas fases de dergadación con pérdida de la cápsida y perdiendocon ello su simetría característica.

Existe una estrecha relación entre maduración endosomal y su localización subcelular. Uno de los pasos requeridos para dicha maduración incluye la progresión del endosoma hacia el area perinuclear (Rink et al., 2005), la cual es alcanzada a través de microtúbulos (Gruenberg, 2009; Huotari and Helenius, 2011). Como han mostrado trabajos anteriores, el tráfico endosomal del VPPA y el éxito de la infección se basan en el transporte funcional a través de la red microtubular (Alonso et al., 2001). Además, la activación de Rac1, la cual provoca estabilización de microtúbulos es crucial para la infección en etapas tempranas de la infección (Quetglas et al., 2012).

De forma similar, un reciente artículo acerca del virus de simio 40 (SV40) mostraba que la elevación del pH vacuolar utilizando inhibidores de la acidificación como Baf y NH_4Cl también era determinante en la infección (Engel et al., 2011). El tráfico intracelular de SV40 incluye el paso por EE, maduración en endosomas híbridos, LEs y finalmente

endolisosomas. Los agentes que elevaban el pH de organelas endocíticas inhibían la infección y la fracción de virus internalizado (reducida al 20%) y los viriones no se transportaba más allá de EE en presencia de Baf y posteriormente a LE, en células tratadas con monensina en el caso del SV40.

El pH ácido, propio de los LE, es un requerimiento común a diversas familias de virus de los cúales comentaremos algunos de los ejemplos mas conocidos como el virus de influenza A (Engel et al., 2011) y bunyavirus (Lozach et al., 2010). La mayoría de serotipos de adenovirus (Ad) penetran en células a partir de endocitosis mediada por clatrina y posteriormente, el pH endosomal tiene un papel fundamental al inducir cambios conformacionales en la particula viral. Mas aun, se ha demostrado, que dichos cambios conformacionales aumentan su capacidad de unión al motor microtubular dineína, y esta puede ser una de las razones de la importancia que tiene la exposición del adenovirus a pH ácido para el éxito de la infección. (Scherer and Vallee, 2011).

Otro ejemplo de la relevancia del pH endosomal en las infecciones víricas es el caso de rinovirus. Rinovirus entra en las células por vías dependientes o no de endocitosis mediada por clatrina o por macropinocitosis. Sin embargo, hay coincidencia en la necesidad de exponerse al bajo pH de los LE, donde los viriones sufren cambios conformacionales liberandose así el ARN viral, a través de uno de los ejes de la cápsida icosaédrica (Fuchs and Blaas, 2010).

También el virus del Dengue utiliza la membrana de los LE para la fusion producida por un bajo pH, el cual determinará el tiempo y el lugar de la liberación del genoma viral al citosol (Zaitseva et al., 2010).

El caso de VSV es especial, ya que la fusión con la membrana tiene lugar por el cambio conformacional de la glicoproteína G mediado por pH ácido y, a diferencia de lo descrito para SFV, ocurre en un paso posterior al EE (Le Blanc et al., 2005; Luyet et al., 2008). Sin embargo, la fusión en VSV ocurre en vesículas intermedias entre EE y LE y no en los propios LE como sucede en el caso del virus de Influenza (Le Blanc et al., 2005; Luyet et al., 2008).

Estos modelos víricos, tienen en común el requerimiento de pH ácido y de la utilización de la vía endocítica para el éxito de la infección, que hasta ahora no estaban bien definidos para el VPPA.

3. IMPACTO DEL MUTANTE NEGATIVO DE LA GTPasa RAB7 EN LA INFECCIÓN DEL VPPA

Los resultados anteriores señalan un papel fundamental para los LE en la desencapsidación viral y en el progreso de la infección. Seguidamente, se analizó la

relevancia de la GTPasa Rab7, necesaria en la maduración de los endosomas tardíos para apoyar estos resultados. Analizamos el impacto en la infección de la expresión del mutante negativo de Rab7, GTPasa implicada en la coordinación y regulación de procesos que involucran fundamentalmente a los LE. La expression transitoria del mutante negativo de Rab7 afectaba severamente a la infección de VPPA. Este efecto se ha observado también en otros virus envueltos como Influenza (Sieczkarski and Whittaker, 2003). Tras la infección de células seleccionadas por la expresión transitoria de Rab7 DN, la infectividad del VPPA caía dramaticamente comparado con las células con las que expresaban Rab7 salvaje o WT. De este modo se confirmaba que el VPPA se clasificaría en adelante en la categoría de virus que penetran a nivel de endosomas tardíos, también llamados *"late penetrating viruses"* (Lozach et al., 2010).

4. EFECTO DE LA INHIBICIÓN DE PIKfyve EN LA INFECCIÓN DEL VPPA

Según el resultado anterior, en el que la función de la GTPasa Rab7 era fundamental en la infección, se abordó el análisis del FtdIns(3,5)P_2, un fosfoinosítido (FI) que junto a Rab7 gobierna la homeostasis de compartimentos tardíos de la vía endocítica, ya que está implicado en procesos fundamentales que regulan su funcionamiento.

Como se ha descrito en la introducción, existen toda una serie de cambios madurativos en las vesículas endocíticas, que guían el paso de EE a LE. Uno de los cambios más importantes en esta transformación es la conversión del FtdIns3P, implicado en procesos relacionados con el EE, a FtdIns(3,5)P_2, cuya función se desempeña en los compartimentos tardíos.

Esta conversión, donde Rab7GTP se activaría y se uniría a la membrana endosomal, ejerce un fuerte control sobre la regulación de este proceso madurativo, es decir, en la retroalimentación o "*feedback*" positivo para la síntesis de FtdIns3P mediante la enzima PI3K, de manera que la presencia de Rab7 GTP inclina la balanza hacia la síntesis de FtdIns(3,5)P_2 como se explicará a continuación. Esto ocurre, debido a que PI3K, interactúa tanto con Rab5 como con Rab7, sin embargo lo hace en diferentes estados de activación. PI3K es reclutada a la membrana endosomal por Rab5 en su forma activa (unida a GTP) (Christoforidis et al., 1999), mientras que la interacción con Rab7 es con su forma inactiva, unida a GDP (Stein et al., 2003). Esto permite una alta regulación del proceso y la activación de Rab7 reduce a su vez la interacción de la PI3K en las membranas endosomales, ejerciéndose de este modo un control en la síntesis de FtdIns3P y a su vez, aumentando la población de FtdIns(3,5)P_2, necesario en funciones madurativas del endosoma.

La conversión de Fis está fuertemente vinculada con los pasos de maduración de los endosomas. Componentes de la maquinaria del ESCRT, responsable de la generación de ILVs, son reclutados tanto por FtdIns3P y FtdIns(3,5)P_2 (Katzmann et al., 2002; Katzmann et al., 2003; Teo et al., 2006; Whitley et al., 2003). Así, la formación de las ILVs y la organización de la carga será un proceso coordinado con el resto del programa madurativo.

FtdIns(3,5)P_2 es generado por PIKfyve, cuya localización en la membrana de está vinculada a la presencia de FtdIns3P, ya que se une a través de su dominio FYVE a la membrana endosomal, por lo que la generación de FtdIns(3,5)P_2 está vinculada a las membranas ricas en FtdIns3P que lo utiliza como sustrato.

El bloqueo de la síntesis de FtdIns(3,5)P_2, por ejemplo mediante la inhibición de la enzima convertidora PIKfyve, dirige la generación de un fenotipo altamente vacuolado (Ikonomov et al., 2001; Jefferies et al., 2008; Nicot et al., 2006; Rusten et al., 2006). PIKfyve parece estar vinculado a la regulación de canales iónicos (Shisheva, 2008) de Ca^{2+} en el LE. Se ha demostrado recientemente que los canales permeables al Ca^{2+}, TRPML1, son directamente activados por la presencia de FtdIns(3,5)P_2 capacitando el flujo de Ca^{2+} (Dong et al., 2010). El Ca^{2+} es un importante regulador de los eventos de fusión homo y heterotípica entre LE, LI y vacuolas, y también en la reformación de lisosomas desde los endolisosomas (Luzio et al., 2007). La generación localizada de FtdIns(3,5)P_2 en membranas endosomales permite así el control de la actividad de canales iónicos de Ca^{2+} en ciertas regiones y puede permitir la regulación de la fusion/fisión del LE de un modo espaciotemporal. Así es posible que el fenotipo altamente vacuolado de las células con la actividad PIKfyve bloqueada, sea el resultado del desequilibrio osmótico provocado por la deficiente regulación de los canales iónicos endosomales (Shisheva, 2008).

Parece más que justificado, dado el fuerte control de síntesis de FtdIns(3,5)P_2 y su acción sobre la vía degradativa, el análisis del papel de FtdIns(3,5)P_2 en el contexto de la infección y por ello ha sido objeto de análisis en esta tesis doctoral.

Debido a que una gran parte de las vías de transporte degradativas parecen estar reguladas por FtdIns(3,5)P_2, utilizamos un fármaco bloqueante de la síntesis de FtdIns(3,5)P_2 altamente específico y recientemente descrito, YM201636, inhibidor selectivo de PIKfyve (Jefferies et al., 2008). Como hemos explicado anteriormente afectará la vía degradativa y se producirá un desequilibrio en la dinámica de fusión de endosomas (Johnson et al., 2006), produciendo una severa vacuolación del citoplasma (Griffiths et al., 1990; Johnson et al., 2006; Lin et al., 2004; Rohn et al., 2000).

Como se esperaba, el bloqueo de la acción de PIKfyve tuvo un impacto negativo en la infección de VPPA, de modo que la infectividad y la producción viral decrecían cuando el

inhibidor se añadía antes de la infección, y después de dos horas, aunque su impacto no era tan severo, si bien es cierto que no alcanzaba los niveles de las células control.

Estos resultados apoyan los requerimientos de pH ácido por parte del virus durante las etapas tempranas de la infección ya que el flujo de cationes como el Ca^{2+} y otros iones, afectan a la acidificación endosomal (Huotari and Helenius, 2011; Marshansky and Futai, 2008), mediante la actividad de dichos canales permitiendo la regulación del tráfico de membranas en una forma espaciotemporal (Dong et al., 2010; Shisheva, 2008).

En conclusión, la severa alteración en la maduración de los LE causada por la inhibición de PIKfyve afecta profundamente la infección de VPPA, como ocurre con otros patógenos dependientes de los compartimentos endosomales tardíos como es el caso de Salmonella (Kerr et al., 2010).

Curiosamente, en las escasas células infectadas que aparecían en el contexto de la inhibición de PIKfyve con factoría viral reconocible (16 hpi), no se observaba citoplasma vacuolado, a diferencia del 100% de las células no infectadas. Este hecho podría indicar que el virus, podría ejercer algun control que involucre a PIKfyve, si no fuera así, sería posible observar células vacuoladas a pesar de desarrollarse la infección. Es difícil determinar el punto clave de control que ejerce el virus ya que la actividad de PIKfyve y por tanto la síntesis de FtdIns(3,5)P_2 actúan sobre un amplio espectro de procesos célulares, centrados en el óptimo mantenimiento de organelas ácidas del sistema endolisosomal (Bonangelino et al., 1997; Bonangelino et al., 2002), como hemos visto, fundamentales para la infección viral y que serán objeto de futuros estudios. A modo de resumen estas funciones en la ruta degradativa endocítica serían (Dove et al., 2009), 1) el control en el tamaño y forma de endosomas y lisosomas (Bryant et al., 1998; Dove et al., 2004; Rudge et al., 2004), 2) la acidificación de organelas (Odorizzi et al., 1998; Rusten et al., 2006), 3) la recuperación de proteínas desde los lisosomas/vacuolas al endosoma (Dove et al., 1997; Dove et al., 1999; Sbrissa and Shisheva, 2005), 4) la clasificación de proteínas dependiente de ubiquitina en MVB (Michell et al., 2006) y finalmente 5) la regulación de canales iónicos (Shen et al., 2011).

5. PAPEL FUNCIONAL DEL LBPA EN LA INFECCIÓN DEL VPPA

En nuestro estudio de la fase de entrada de VPPA y en el momento de la desencapsidación quedó de manifiesto el papel crucial de la maduración del LE. El ácido lisobisfosfatídico (LBPA) es un fosfolípido que se encuentra mayoritariamente en las ILVs del LE (Kobayashi et al., 2002) y ha sido ampliamente considerado no solo como un marcador de LE (Kobayashi et al., 1998b), sino también como un lípido regulador de la dinámica de membranas de esta organela, coordinado por la proteína citosólica Alix (Bissig et al., 2013; Kobayashi et al., 2002; Kobayashi et al., 1998a; Kobayashi et al., 1998b; Odorizzi, 2006). El

papel de Alix resulta fundamental en la dinámica de las ILVs y puede cumplir una función reguladora, ya que se ha comprobado que el la mutación de Alix *in vivo* reduce el número de MVB/LE que contienen ILVs en aproximadamente un 50% (Matsuo et al., 2004).

Para abordar el papel del LBPA en la infección del VPPA, utilizamos el anticuerpo monoclonal 6C4 frente a LBPA. Dicho anticuerpo, bloquea la interacción entre LBPA y Alix, lo que es lo mismo que impedir la unión de Alix al LE (Matsuo et al., 2004; Pattanakitsakul et al., 2010). Trabajos anteriores demostraron que la dinámica de MVB está influenciada por el contenido de LBPA en la membrana endosomal ya que la endocitosis por fase fluida del anticuerpo monoclonal 6C4 frente a LBPA produce desorganización de membranas endosomales luminales (Kobayashi et al., 1998).

Nuestros resultados indicaron que el tratamiento con el anticuerpo anti-LBPA endocitado, previo a la infección del VPPA producía una reducción del 50% del número de células infectadas, la síntesis de proteínas y la producción vírica, respecto a las células sin tratar lo que indica un papel para el LBPA en la infección desde las etapas más tempranas.

Alix y LBPA desempeñan un papel crucial en la penetración desde el LE de algunos patógenos en el citoplasma, incluyendo, VSV (Le Blanc et al., 2005; Luyet et al., 2008), el virus de Lassa, el virus de la coriomeningitis linfocitaria, Arenavirus (Pasqual et al., 2011), el virus del Dengue (Pattanakitsakul et al., 2010) y la toxina del ántrax (Abrami et al., 2004).

Según nuestros resultados, Alix también podría tener un papel relevante en la fase temprana de la de la infección por VPPA, cuando el virus alcanza los MVB/LE. Es posible que de forma similar a los patógenos citados anteriomente, LBPA y Alix participen en la salida o "*budding"* del virus desde el LE al citosol, o dado que ambos son necesarios para la generación de ILVs en el LE, estas podrían estar implicadas en algún punto del paso del virus por este compartimento.

6. LA INTERRUPCIÓN DEL FLUJO DE COLESTEROL AFECTA A LA INFECCIÓN DEL VPPA

El colesterol es un componente esencial para diversas estructuras y procesos celulares (Cannon et al., 2006) por lo que el nivel de colesterol celular está regulado a diferentes niveles, como ya se ha descrito en la introducción.

La eliminación de colesterol y el tratamiento con colesterol oxidasa, bloquean la replicación del VPPA en células Vero. El colesterol es necesario en los procesos de fusión con el endosoma, mientras que no afecta a la capacidad de unión o la internalización de los viriones (Bernardes et al., 1998). Asimismo, la eliminación del colesterol de la membrana plasmática mediante β-metil- ciclodextrina (CD), conduce a un fuerte descenso en el

número de células infectadas de forma dosis dependiente, junto a una disminución de la expresión de la proteína viral p30 y de la producción total de virus (Hernaez and Alonso, 2010).

Otro enfoque diferente del papel del colesterol en la infección del VPPA se obtuvo al bloquear su biosíntesis, como elemento importante de la prenilación de las GTPasas de la familia Rho, entre las que se encuentran las Rab GTPasas (Quetglas et al., 2012). Estas GTPasas requieren prenilación post-traduccional para ser funcionalmente activas (McTaggart, 2006; Van Aelst and D'Souza-Schorey, 1997) ya que para su localización, inserción en las membranas y las interacciones con otras proteínas necesitan incorporaciones en su extremo carboxilo de farnesil o geranilgeranil pirofosfato (Van Aelst and D'Souza-Schorey, 1997). Estos grupos prenilos derivan del ácido mevalónico, el cual también es el compuesto inicial donde comienza la ruta de biosíntesis de colesterol. Las estatinas se han utilizado ampliamente para inhibir la prenilación de las Ras GTPasas, particularmente de la subfamilia Rho GTPasas (Glenn et al., 1992; Guijarro et al., 1998; Liao and Laufs, 2005).

En el presente trabajo de tesis, aportamos al estudio de una molécula de demostrada relevancia en la infección por VPPA, el análisis del flujo de colesterol en la vía endocítica.

El colesterol libre, en su tráfico intracelular se acumula en las ILVs ricas en LBPA de los LEs (Chevallier et al., 2008). El nivel de colesterol celular está estrictamente regulado y aumenta por endocitosis de colesterol en forma de LDL y por su síntesis *de novo* (Ikonen, 2008; Ioannou, 2001). En condiciones fisiológicas, el colesterol circula a los compartimientos endosomales, donde las LDL sufren hidrólisis, transformándose en colesterol libre, que se acumula en las ILVs, para su posterior transporte al citosol. El colesterol generado en la síntesis *de novo*, es otra fuente de colesterol célular, y es transportado desde el RE a otros orgánulos, como endosomas, lisosomas, AG, mitocondrias, y MP (Holthuis and Levine, 2005). La proteína VAP-A del RE y la proteína ORP1L en las vesículas, son dos proteínas importantes implicadas en este transporte (Raychaudhuri and Prinz, 2010; Rocha et al., 2009).

La cantidad de LBPA se correlaciona de forma directa con el nivel total de colesterol en las células posiblemente debido al papel del LBPA en el control del almacenamiento endosomal del colesterol (Chevallier et al., 2008) y tanto la excesiva acumulación de colesterol, como de esfingolípidos, causan graves alteraciones de la vía endocítica (Lebrand et al., 2002; Sobo et al., 2007; Vitner et al., 2010a; Vitner et al., 2010b). Estas alteraciones se traducen en una redistribución de los MVB/LE en la zona perinuclear. Esto ocurre en la enfermedad de Niemann Pick tipo C o tras el tratamiento de las células con el fármaco U18666A (U) (Liscum and Faust, 1989) en las que se favorece el transporte

retrógrado mediante motores microtubulares de los MVB/LE y por ello se acumulan alrededor del núcleo, por acción de la dineina (Rocha et al., 2009).

El agente U afecta al equilibrio del colesterol en la célula por dos mecanismos: a) bloqueando el transporte del colesterol endocitado en la forma de LDL, resultando en la acumulación de colesterol en MVB/LE, imitando el fenotipo causado por la enfermedad de Niemann Pick tipo C (Kobayashi et al., 1999; Koh and Cheung, 2006; Liscum and Faust, 1989), y b) por supresión de de síntesis de colesterol *de novo* bloqueando pasos intermedios de síntesis de esteroles dependientes de la oxidoescualeno ciclasa y desmosterol reductasa (Sexton et al., 1983).

En nuestro diseño experimental, comprobamos la acción correcta de la droga U, al observar acumulación de vesículas alrededor del núcleo, mediante inmuno-marcaje de membranas endosomales de compartimentos tardíos y filipina, para detectar el colesterol, contenido en el interior de los compartimentos endocíticos tardíos. Tras el tratamiento con la droga U observamos una reducción dosis dependiente de la infectividad hasta el 80%. Asímismo, la síntesis de la proteína temprana p30 también se redujo en torno a un 50%.

El colapso sufrido por los MVB/LE a causa de la acumulación de colesterol podría provocar que los viriones quedasen atrapados en el MVB/LE sin posibilidad de alcanzar la membrana limitante del endosoma, previniendo una fusión de membranas eficiente que bloquearía la salida del core viral al citoplasma y la progresión de la infección. En efecto, mediante microscopía electrónica se pudo comprobar que numerosos viriones quedaban retenidos en los endosomas cargados de lípidos.

Al igual que en VPPA, para diversas familias virales, la modulación de la homeostasis del colesterol intracelular, especialmente en el compartimiento endosomal, tiene efectos dramáticos en la primeras etapas de la infección. Es el caso del virus del ébola (Carette et al., 2011), el virus de la polio (Danthi and Chow, 2004), el VSV (Gruenberg, 2009; Kobayashi et al., 1999), el virus del dengue (Poh et al., 2012) o el virus de influenza (Lakadamyali et al., 2004). Por lo tanto, las alteraciones en la homeostasis del colesterol intracelular puede ser un blanco potencial para la interrupción de la progresión de los viriones en el sistema endocítico y podría convertirse en una nueva diana para combatir las infecciones virales.

En cuanto al colesterol, la relación funcional directa entre la proteína citosólica Alix y el contenido de LBPA endosomal también están estrechamente relacionados, ya que el mutante de Alix produce un descenso de LBPA endosomal (Cabezas et al., 2005; Matsuo et al., 2004), lo que en último termino se traducirá en una disminución en el número de ILVs y por tanto de capacidad de almacenaje de colesterol en los LE (Matsuo et al., 2004).

provocando la liberación de colesterol desde los MVB/LE, quizá mediante la acción de las proteínas NPC1 y NPC2, así como ABCA1 (Neufeld et al., 2004). Finalmente, el colesterol se transportará rápidamente a la superficie de la célula (Chen et al., 2001; Hao et al., 2002; Lusa et al., 2001; Maxfield and Tabas, 2005).

Como señalan los resultados, la disminución en la capacidad de acumulación de colesterol de los endosomas parece clave en la infección del VPPA. Esto podría estar relacionado con la capacidad de movimiento de los MVB/LE carentes de colesterol, ya que la maduración endosomal está íntimamente relacionado con su transporte hacia el MTOC (Huotari and Helenius, 2011).

La típica localización preferentemente perinuclear de los LEs viene dado por el saldo neto de movimientos hacia los extremos opuestos de los microtúbulos. Rab7 en el LE (Zerial and McBride, 2001) y su proteína efectora RILP (del inglés "*Rab7- interacting lysosomal protein"*) se unen a la subunidad p150glued del complejo de la proteína dinactina (Johansson et al., 2007; Jordens et al., 2001). La proteína p150glued puede unirse a la cadena pesada de la dineína a través de la cadena intermedia de la dineína (DIC, del inglés "*dynein intermediate chain*"). En la membrana del LE existe un sensor para el colesterol, el ORP1L. Cuando los niveles de colesterol en la membrana del LE son escasos, la conformación de ORP1L induce la formación de zonas de contacto entre los LE y el RE. En estos lugares, la proteína del RE, VAP (también conocida como VAMP, del inglés "*vesicle-associated membrane protein"*) puede interactuar con el complejo Rab7-RILP para disociar p150glued y la proteína motora asociada. Así impide el transporte retrógrado endosomal hacia el MTOC, por lo que mantienen una localización periférica en la célula (Rocha et al., 2009). De acuerdo con los datos de Huotari y Helenius (Huotari and Helenius, 2011), de este modo quedaría bloqueado el transporte del endosoma y su maduración, y consecuentemente podría bloquear la acidificación del pH luminal, necesario para la desencapsidación viral.

En el caso contrario, la alteración en el transporte del colesterol desde el LE al citosol como el que produce el fármaco U, resulta en su acumulación en el LE y MVB en la zona del MTOC (Maxfield and Tabas, 2005; Subramanian and Balch, 2008), como hemos mostrado en las imágenes de miscroscopía confocal de LE cargados de colesterol (marcado con Filipina). En este caso se producía una inhibición de la infección y se observaban viriones retenidos en endosomas cargados de lípidos al ME.

En resumen, el VPPA muestra una gran dependencia por las membranas endosomales. Tras su internalización en la célula huésped se inicia el paso del virus por la vía endocítica, atravesando el citoplasma celular en el interior de vesículas endosomales como son el EE,

MVB y LE, objeto de estudio en esta tesis doctoral. Finalmente, el virus debe conseguir abandonar este compartimento antes de producirse la degradación de su contenido al fusionar con el LI.

En conjunto, hemos analizado la interacción del VPPA con diferentes organelas celulares relevantes en las fases tempranas de la infección, relacionados con la vía endocítica y sus moléculas de señalización, como son la GTPasa Rab7, PtdIns(3,5)P_2, y el LBPA. Estas constituyen potenciales dianas moleculares para el desarrollo de estrategias antivirales frente al VPPA. En la figura 29 se muestra el modelo propuesto en función de los resultados obtenidos en este trabajo de tesis, para el paso del VPPA a través de la vía endocítica en las primeras etapas de la infección viral, previas a la constitución del complejo de ensamblaje.

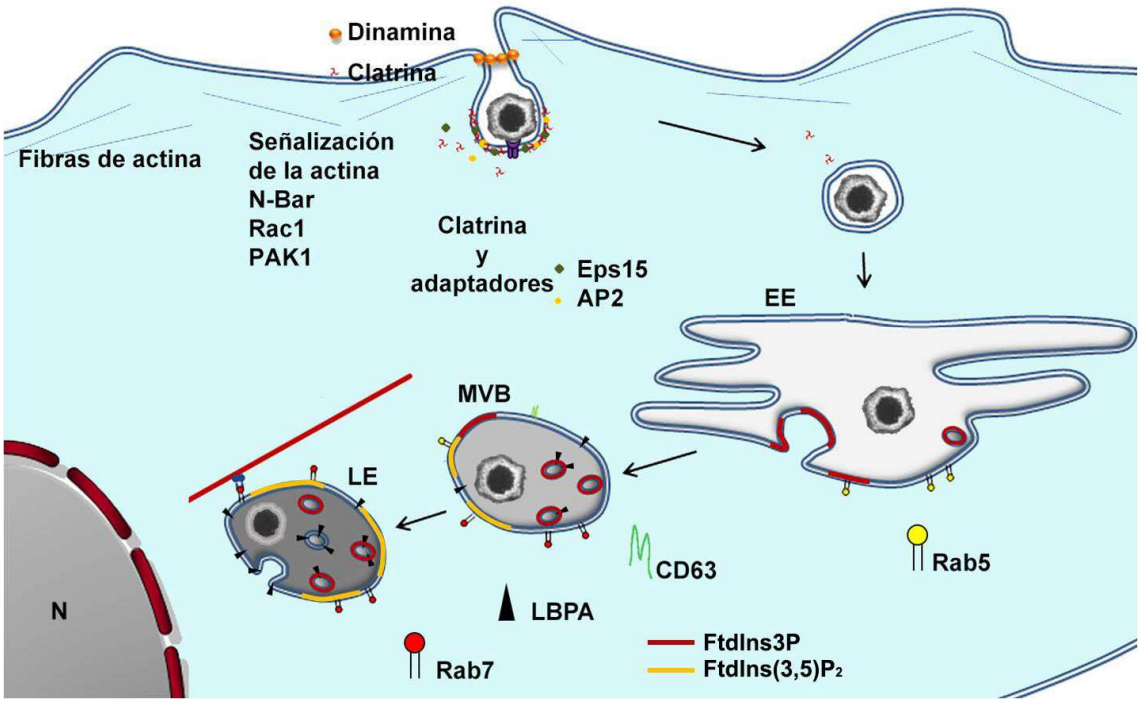

Figura 29. Modelo del progreso de la infección del VPPA a través de la vía endocítica. La dinamina y actina inducen la constricción del cuello de la vesícula recubierta de clatrina para producir su escisión definitiva hacia el citosol. El VPPA alcanza de este modo el endosoma temprano (EE). La maduración del EE hacia cuerpo multivesicular (MVB) y endosoma tardío (LE) requiere la acidificación del pH, interconversión de FtdIns3P a FtdIns(3,5)P_2, mediada por PIKfyve, y, la activación de la GTPasa Rab7 El LBPA también tiene un papel relevante en la infección. El pH ácido propio de los LE es necesario para la desencapsidación viral, que tendrá lugar alrededor de los 45 mpi.

7. REDISTRIBUCIÓN DE MEMBRANAS ENDOSOMALES EN LA CONSTITUCIÓN DE LA FACTORÍA VIRAL

El VPPA induce la formación del sitio de replicación o factoría viral en la región perinuclear, en el que se producirá una gran acumulación de componentes virales y donde

la morfogénesis de los nuevos viriones tiene lugar de forma similar a como se produce en varios virus envueltos (Novoa et al., 2005).

La FV del VPPA se reconoce como un acúmulo de DNA y proteínas víricas en la zona perinuclear que hasta ahora había sido descrito como carente de organelas, excepto ribosomas en su interior (Rojo et al., 1998). Su origen se atribuye al retículo endoplásmico pero el proceso de su formación es aún desconocido. Las mitocondrias se organizan alrededor de las FVs y tanto el RE y como el complejo de Golgi se desorganizan con el progreso de la infección (Netherton et al., 2006).

El VPPA también induce profundos cambios en el citoesqueleto. Los filamentos intermedios acaban formando una robusta jaula de vimentina alrededor de las FVs (Stefanovic et al., 2005). Los microtúbulos se despolimerizan y el citoesqueleto de actina se va desorganizando progresivamente en la célula infectada.

Otros factores propios de la célula huésped necesarios para la formación de la FV son proteínas preniladas, especialmente Rho GTPasas. La inhibición de las Rho GTPasas provoca una alteración de la maduración de los viriones que se acumulan en factorías anormalmente grandes . Inhibidores de la biosíntesis de colesterol como las estatinas, también alteran su formación (Quetglas et al., 2012).

La dependencia del VPPA por los compartimentos endosomales nos hizo investigar si los endosomas estaban implicados en estas etapas posteriores del ciclo infectivo. Así, se demostramos que en etapas avanzadas de la infección, existía una redistribución patente de las organelas endosomales en consonancia con el avance de la infección viral. De modo que cuando comienza a constituirse la factoría vírica (Hernaez et al., 2006), se apreciaba una redistribución de los endosomas hacia el centrosoma, para situarse las membranas endosomales entremezcladas con los focos iniciales de acúmulo de proteínas víricas en la factoría en formación.

Las imágenes de microscopía confocal nos permitieron observar la fuerte remodelación inducida por la infección del VPPA en las membranas del aparato degradativo celular. Una característica común a todas las vesículas endosomales estudiadas es que parecen interactuar de algún modo con la factoría, ya que suelen tener contacto con la factoría viral en formación.

Este fuerte reclutamiento hacia el complejo de ensamblaje viral de material membranoso contrasta con el fenotipo disperso de aspecto vesicular de estas organelas en células que no han sido infectadas. Las membranas positivas para EEA1 hay que señalar que suelen acumularse de manera más discreta que el resto de marcadores y suelen posicionarse en un único punto próximo a la factoría, sin rodearla. El resto de membranas endosomales (marcadas con Rab7, CD63 y Lamp1), mostraron un patrón de distribución más o menos

similar, constituyéndose en acúmulos que rodeaban y entremezclaban con la FV. Su patrón difiere de la redistribución que se produce en membranas del RE, las cuales se sitúan en estadíos muy iniciales en forma de aro más o menos contínuo alrededor del complejo de ensamblaje. Una remodelación similar en el sistema endomembranoso celular ocurre en el citomegalovirus humano (Alwine, 2012; Das et al., 2007).

Es posible que este aporte de membranas facilite el ensamblaje final de la FV y colabore con la formación del nicho de replicación del virus. Puesto que este reclutamiento es patente en casi la totalidad de las células infectadas consideramos que debe tratarse de un hecho definitivamente crucial en este momento del ciclo infectivo del VPPA y para la consecución final de la replicación.

La dependencia del citoesqueleto microtubular en la formación de acumulos de membranas alrededor de la FV quedó patente al observar que la despolimerización de los microtúbulos con Nocodazol conducía a la dispersión de pequeños acúmulos de membranas de LE en el citoplasma de células infectada. Esta misma respuesta al Nocodazol ocurre con los focos iniciales de proteína viral inmuno-marcados para la proteína viral p72 que deberían originar la FV próxima al MTOC y que aparece dispersa en el citoplasma tras el tratamiento con Nocodazol, como ha sido descrito previamente (Alonso et al., 2001). La ausencia de reclutamiento de endosomas en presencia de Nocodazol es coincidente con la presencia de focos independientes de acumulación de proteína que no llegan a cohesionar lo que podría sugerir que las membranas endosomales tienen un papel aglutinador en la formación de la FV.

El hecho de que en células infectadas, la expresión de la proteína temprana p30 se recupere en células tratadas con Nocodazol tras 2 hpi, pero no la acumulación de vesícula positivas para Rab7 en el MTOC, indica que el reclutamiento de membranas endosomales a la FV es un proceso posterior a la desencapsidación viral y aparentemente independiente del transporte del VPPA en el LE hacia el MTOC.

En efecto, numerosos patógenos utilizan membranas de diversos orígenes o incluso reclutan autofagosomas para formar su nicho de replicación. Son numerosas las publicaciones que basan el concepto de identidad de las organelas, derivado de sus proteínas de membrana, composición, función y localización (Behnia and Munro, 2005; Christoforidis et al., 1999; Del Conte-Zerial et al., 2008; Pfeffer and Aivazian, 2004; Zerial and McBride, 2001). Sin embargo, se ha demostrado que los patógenos pueden alterar dicha identidad. Por ejemplo, el citomegalovirus humano puede inducir cambios en la identidad de las organelas endocíticas, como cambios en su localización, formas y tamaños que difieren claramente del fenotipo de las células no infectadas y que probablemente afecte a su función. Este cambio se traduce en acumulaciones masivas alrededor del

complejo de replicación. Incluso proteínas que mostraban una fuerte localización en una determinada organela, esta distribución característica de amrcadores, se ve reducida en las células infectadas (Das and Pellett, 2011; Das et al., 2007), con lo que el concepto de pérdida de identidad es gravemente acusado. Los virus RNA también remodelan membranas intracelulares de la vía secretora para generarar lugares especializados para la replicación del RNA (Altan-Bonnet and Balla, 2012; Hsu et al., 2010). Incluso, otros patógenos intracelulares como Legionella, o Salmonella, pueden pasar desapercibidas al sistma inmune incluidas en organelas del sistema y generar a partir de ellas un nicho replicativo que soportará la replicación y el desarrollo bacteriano (Kagan and Roy, 2002; Kerr et al., 2010; Knodler and Steele-Mortimer, 2003).

Sin embargo, a pesar del patente reclutamiento de membranas de organelas que existe hacia el lugar donde se constituirá la factoría viral en VPPA, se desconoce el mecanismo exacto por el que se produce.

En resumen, el reclutamiento de endosomas a la FV es necesario para la formación del nicho de replicación del VPPA y es directamente dependiente de los microtúbulos implicados en el transporte de endosomas. Este reclutamiento, constituye el aporte de membranas necesario para la correcta formación del orgánulo de replicación.

Conclusiones

1. La entrada del VPPA es dependiente de la vía endocítica y su función es de mayor relevancia que un simple mecanismo de transporte al interior celular, sino que demostró ser crucial en la clasificación y destino del virus.

2. Desde la membrana plasmática, el VPPA atraviesa el endosoma temprano en los primeros 30 minutos de la infección.

3. La acidificación endosomal es determinante para una infección productiva por VPPA durante la primera hora post infección pero no a tiempos posteriores.

4. La inhibición de la infección con inhibidores de la ATPasa vacuolar no puede restaurarse con un pulso de pH ácido.

5. La desencapsidación del virus se produce en compartimentos ácidos endosomales y el VPPA se clasifica como un virus que penetra en el citosol a partir de compartimentos endosomales tardíos.

6. La señalización molecular requerida para la maduración del endosoma tardío, la GTPasa Rab7 y la interconversión de fosfoinosítidos, es necesaria para una infección productiva y constituyen dianas moleculares para la inhibición de la infección.

7. Los endosomas tardíos, los cuerpos multivesiculares tienen un papel relevante en la infección, en concreto el ácido lisobisfosfatídico de estas vesículas que se relaciona con el nivel de colesterol total celular.

8. El bloqueo del flujo de salida de colesterol en la vía endocítica y la alteración del tráfico endosomal que produce, bloquean la progresión de la infección.

9. El bloqueo del flujo de colesterol produce un fenotipo similar al de la enfermedad de Niemann Pick, quedando los viriones retenidos en vesículas cargadas de colesterol y esfingolípidos.

10. El VPPA produce una redistribución de toda la vía endocítica reclutando membranas endosomales a los nichos iniciales de replicación viral siendo determinante para la formación de las factorías víricas.

Bibliografía

Abrami, L., Lindsay, M., Parton, R.G., Leppla, S.H. and van der Goot, F.G. (2004) Membrane insertion of anthrax protective antigen and cytoplasmic delivery of lethal factor occur at different stages of the endocytic pathway. J Cell Biol 166(5), 645-51.

Acosta, E.G., Castilla, V. and Damonte, E.B. (2009) Alternative infectious entry pathways for dengue virus serotypes into mammalian cells. Cell Microbiol 11(10), 1533-49.

Afonso, C.L., Piccone, M.E., Zaffuto, K.M., Neilan, J., Kutish, G.F., Lu, Z., Balinsky, C.A., Gibb, T.R., Bean, T.J., Zsak, L. and Rock, D.L. (2004) African swine fever virus multigene family 360 and 530 genes affect host interferon response. J Virol 78(4), 1858-64.

Alcami, A., Carrascosa, A.L. and Vinuela, E. (1989a) The entry of African swine fever virus into Vero cells. Virology 171(1), 68-75.

Alcami, A., Carrascosa, A.L. and Vinuela, E. (1989b) Saturable binding sites mediate the entry of African swine fever virus into Vero cells. Virology 168(2), 393-8.

Alcami, A., Carrascosa, A.L. and Vinuela, E. (1990) Interaction of African swine fever virus with macrophages. Virus Res 17(2), 93-104.

Alejo, A., Andres, G., Vinuela, E. and Salas, M.L. (1999) The African swine fever virus prenyltransferase is an integral membrane trans-geranylgeranyl-diphosphate synthase. J Biol Chem 274(25), 18033-9.

Almazan, F., Rodriguez, J.M., Andres, G., Perez, R., Vinuela, E. and Rodriguez, J.F. (1992) Transcriptional analysis of multigene family 110 of African swine fever virus. J Virol 66(11), 6655-67.

Almazan, F., Rodriguez, J.M., Angulo, A., Vinuela, E. and Rodriguez, J.F. (1993) Transcriptional mapping of a late gene coding for the p12 attachment protein of African swine fever virus. J Virol 67(1), 553-6.

Alonso, C., Galindo, I., Cuesta-Geijo, M.A., Cabezas, M., Hernaez, B. and Munoz-Moreno, R. (2013) African swine fever virus-cell interactions: from virus entry to cell survival. Virus Res 173(1), 42-57.

Alonso, C., Miskin, J., Hernaez, B., Fernandez-Zapatero, P., Soto, L., Canto, C., Rodriguez-Crespo, I., Dixon, L. and Escribano, J.M. (2001) African swine fever virus protein p54 interacts with the microtubular motor complex through direct binding to light-chain dynein. J Virol 75(20), 9819-27.

Altan-Bonnet, N. and Balla, T. (2012) Phosphatidylinositol 4-kinases: hostages harnessed to build panviral replication platforms. Trends Biochem Sci 37(7), 293-302.

Alwine, J.C. (2012) The human cytomegalovirus assembly compartment: a masterpiece of viral manipulation of cellular processes that facilitates assembly and egress. PLoS Pathog 8(9), e1002878.

Amstutz, B., Gastaldelli, M., Kalin, S., Imelli, N., Boucke, K., Wandeler, E., Mercer, J., Hemmi, S. and Greber, U.F. (2008) Subversion of CtBP1-controlled macropinocytosis by human adenovirus serotype 3. Embo J 27(7), 956-69.

Anderson, H.A., Chen, Y. and Norkin, L.C. (1996) Bound simian virus 40 translocates to caveolin-enriched membrane domains, and its entry is inhibited by drugs that selectively disrupt caveolae. Mol Biol Cell 7(11), 1825-34.

Andres, G., Alejo, A., Salas, J. and Salas, M.L. (2002a) African swine fever virus polyproteins pp220 and pp62 assemble into the core shell. J Virol 76(24), 12473-82.

Andres, G., Garcia-Escudero, R., Salas, M.L. and Rodriguez, J.M. (2002b) Repression of African swine fever virus polyprotein pp220-encoding gene leads to the assembly of icosahedral core-less particles. J Virol 76(6), 2654-66.

Andres, G., Garcia-Escudero, R., Simon-Mateo, C. and Vinuela, E. (1998) African swine fever virus is enveloped by a two-membraned collapsed cisterna derived from the endoplasmic reticulum. J Virol 72(11), 8988-9001.

Andres, G., Garcia-Escudero, R., Vinuela, E., Salas, M.L. and Rodriguez, J.M. (2001) African swine fever virus structural protein pE120R is essential for virus transport from assembly sites to plasma membrane but not for infectivity. J Virol 75(15), 6758-68.

Andres, G., Simon-Mateo, C. and Vinuela, E. (1997) Assembly of African swine fever virus: role of polyprotein pp220. J Virol 71(3), 2331-41.

Angulo, A., Vinuela, E. and Alcami, A. (1992) Comparison of the sequence of the gene encoding African swine fever virus attachment protein p12 from field virus isolates and viruses passaged in tissue culture. J Virol 66(6), 3869-72.

Angulo, A., Vinuela, E. and Alcami, A. (1993) Inhibition of African swine fever virus binding and infectivity by purified recombinant virus attachment protein p12. J Virol 67(9), 5463-71.

Bader, T., Fazili, J., Madhoun, M., Aston, C., Hughes, D., Rizvi, S., Seres, K. and Hasan, M. (2008) Fluvastatin inhibits hepatitis C replication in humans. Am J Gastroenterol 103(6), 1383-9.

Bakkali, L., Guillou, R., Gonzague, M. and Cruciere, C. (1994) A rapid and sensitive chemiluminescence dot-immunobinding assay for screening hybridoma supernatants. J Immunol Methods 170(2), 177-84.

Baroudy, B.M., Venkatesan, S. and Moss, B. (1982) Incompletely base-paired flip-flop terminal loops link the two DNA strands of the vaccinia virus genome into one uninterrupted polynucleotide chain. Cell 28(2), 315-24.

Basta, S., Gerber, H., Schaub, A., Summerfield, A. and McCullough, K.C. (2010) Cellular processes essential for African swine fever virus to infect and replicate in primary macrophages. Vet Microbiol 140(1-2), 9-17.

Behnia, R. and Munro, S. (2005) Organelle identity and the signposts for membrane traffic. Nature 438(7068), 597-604.

Bernardes, C., Antonio, A., Pedroso de Lima, M.C. and Valdeira, M.L. (1998) Cholesterol affects African swine fever virus infection. Biochim Biophys Acta 1393(1), 19-25.

Bissig, C., Lenoir, M., Velluz, M.C., Kufareva, I., Abagyan, R., Overduin, M. and Gruenberg, J. (2013) Viral Infection Controlled by a Calcium-Dependent Lipid-Binding Module in ALIX. Dev Cell.

Bonangelino, C.J., Catlett, N.L. and Weisman, L.S. (1997) Vac7p, a novel vacuolar protein, is required for normal vacuole inheritance and morphology. Mol Cell Biol 17(12), 6847-58.

Bonangelino, C.J., Nau, J.J., Duex, J.E., Brinkman, M., Wurmser, A.E., Gary, J.D., Emr, S.D. and Weisman, L.S. (2002) Osmotic stress-induced increase of phosphatidylinositol 3,5-bisphosphate requires Vac14p, an activator of the lipid kinase Fab1p. J Cell Biol 156(6), 1015-28.

Borca, M.V., Carrillo, C., Zsak, L., Laegreid, W.W., Kutish, G.F., Neilan, J.G., Burrage, T.G. and Rock, D.L. (1998) Deletion of a CD2-like gene, 8-DR, from African swine fever virus affects viral infection in domestic swine. J Virol 72(4), 2881-9.

Borca, M.V., Irusta, P., Carrillo, C., Afonso, C.L., Burrage, T. and Rock, D.L. (1994) African swine fever virus structural protein p72 contains a conformational neutralizing epitope. Virology 201(2), 413-8.

Borca, M.V., Irusta, P.M., Kutish, G.F., Carillo, C., Afonso, C.L., Burrage, A.T., Neilan, J.G. and Rock, D.L. (1996) A structural DNA binding protein of African swine fever virus with similarity to bacterial histone-like proteins. Arch Virol 141(2), 301-13.

Brabec-Zaruba, M., Pfanzagl, B., Blaas, D. and Fuchs, R. (2009) Site of human rhinovirus RNA uncoating revealed by fluorescent in situ hybridization. J Virol 83(8), 3770-7.

Breese, S.S., Jr. and Hess, W.R. (1966) Electron microscopy of African swine fever virus hemadsorption. J Bacteriol 92(1), 272-4.

Brun, A., Rivas, C., Esteban, M., Escribano, J.M. and Alonso, C. (1996) African swine fever virus gene A179L, a viral homologue of bcl-2, protects cells from programmed cell death. Virology 225(1), 227-30.

Bryant, N.J., Piper, R.C., Weisman, L.S. and Stevens, T.H. (1998) Retrograde traffic out of the yeast vacuole to the TGN occurs via the prevacuolar/endosomal compartment. J Cell Biol 142(3), 651-63.

Bucci, C., Thomsen, P., Nicoziani, P., McCarthy, J. and van Deurs, B. (2000) Rab7: a key to lysosome biogenesis. Mol Biol Cell 11(2), 467-80.

Butcher, M., Raviprakash, K. and Ghosh, H.P. (1990) Acid pH-induced fusion of cells by herpes simplex virus glycoproteins gB an gD. J Biol Chem 265(10), 5862-8.
Cabezas, A., Bache, K.G., Brech, A. and Stenmark, H. (2005) Alix regulates cortical actin and the spatial distribution of endosomes. J Cell Sci 118(Pt 12), 2625-35.
Cabrera, M. and Ungermann, C. (2010) Guiding endosomal maturation. Cell 141(3), 404-6.
Cannon, B., Lewis, A., Metze, J., Thiagarajan, V., Vaughn, M.W., Somerharju, P., Virtanen, J., Huang, J. and Cheng, K.H. (2006) Cholesterol supports headgroup superlattice domain formation in fluid phospholipid/cholesterol bilayers. J Phys Chem B 110(12), 6339-50.
Carette, J.E., Raaben, M., Wong, A.C., Herbert, A.S., Obernosterer, G., Mulherkar, N., Kuehne, A.I., Kranzusch, P.J., Griffin, A.M., Ruthel, G., Dal Cin, P., Dye, J.M., Whelan, S.P., Chandran, K. and Brummelkamp, T.R. (2011) Ebola virus entry requires the cholesterol transporter Niemann-Pick C1. Nature 477(7364), 340-3.
Carrasco, L., de Lara, F.C., Martin de las Mulas, J., Gomez-Villamandos, J.C., Hervas, J., Wilkinson, P.J. and Sierra, M.A. (1996a) Virus association with lymphocytes in acute African swine fever. Vet Res 27(3), 305-12.
Carrasco, L., Gomez-Villamandos, J.C., Bautista, M.J., Martin de las Mulas, J., Villeda, C.J., Wilkinson, P.J. and Sierra, M.A. (1996b) In vivo replication of African swine fever virus (Malawi '83) in neutrophils. Vet Res 27(1), 55-62.
Carrascosa, A.L., Bustos, M.J., Galindo, I. and Vinuela, E. (1999) Virus-specific cell receptors are necessary, but not sufficient, to confer cell susceptibility to African swine fever virus. Arch Virol 144(7), 1309-21.
Carrascosa, J.L., Carazo, J.M., Carrascosa, A.L., Garcia, N., Santisteban, A. and Vinuela, E. (1984) General morphology and capsid fine structure of African swine fever virus particles. Virology 132(1), 160-72.
Carrascosa, J.L., Gonzalez, P., Carrascosa, A.L., Garcia-Barreno, B., Enjuanes, L. and Vinuela, E. (1986) Localization of structural proteins in African swine fever virus particles by immunoelectron microscopy. J Virol 58(2), 377-84.
Carter, G.C., Law, M., Hollinshead, M. and Smith, G.L. (2005) Entry of the vaccinia virus intracellular mature virion and its interactions with glycosaminoglycans. J Gen Virol 86(Pt 5), 1279-90.
Cobbold, C. and Wileman, T. (1998) The major structural protein of African swine fever virus, p73, is packaged into large structures, indicative of viral capsid or matrix precursors, on the endoplasmic reticulum. J Virol 72(6), 5215-23.
Costa, J.V. (1990) African swine fever. In: G. Darai (Ed), Molecular biology of Iridoviruses., pp. 247-270, Boston.
Cotmore, S.F. and Tattersall, P. (2007) Parvoviral host range and cell entry mechanisms. Adv Virus Res 70, 183-232.
Coyne, C.B. and Bergelson, J.M. (2006) Virus-induced Abl and Fyn kinase signals permit coxsackievirus entry through epithelial tight junctions. Cell 124(1), 119-31.
Cureton, D.K., Massol, R.H., Saffarian, S., Kirchhausen, T.L. and Whelan, S.P. (2009) Vesicular stomatitis virus enters cells through vesicles incompletely coated with clathrin that depend upon actin for internalization. PLoS Pathog 5(4), e1000394.
Cureton, D.K., Massol, R.H., Whelan, S.P. and Kirchhausen, T. (2010) The length of vesicular stomatitis virus particles dictates a need for actin assembly during clathrin-dependent endocytosis. PLoS Pathog 6(9), e1001127.
Chapman, D.A., Darby, A.C., Da Silva, M., Upton, C., Radford, A.D. and Dixon, L.K. (2011) Genomic analysis of highly virulent Georgia 2007/1 isolate of African swine fever virus. Emerg Infect Dis 17(4), 599-605.
Chapman, D.A., Tcherepanov, V., Upton, C. and Dixon, L.K. (2008) Comparison of the genome sequences of non-pathogenic and pathogenic African swine fever virus isolates. J Gen Virol 89(Pt 2), 397-408.

Chen, C. and Zhuang, X. (2008) Epsin 1 is a cargo-specific adaptor for the clathrin-mediated endocytosis of the influenza virus. Proc Natl Acad Sci U S A 105(33), 11790-5.
Chen, W., Sun, Y., Welch, C., Gorelik, A., Leventhal, A.R., Tabas, I. and Tall, A.R. (2001) Preferential ATP-binding cassette transporter A1-mediated cholesterol efflux from late endosomes/lysosomes. J Biol Chem 276(47), 43564-9.
Chen, Y., Honeychurch, K.M., Yang, G., Byrd, C.M., Harver, C., Hruby, D.E. and Jordan, R. (2009) Vaccinia virus p37 interacts with host proteins associated with LE-derived transport vesicle biogenesis. Virol J 6, 44.
Chevallier, J., Chamoun, Z., Jiang, G., Prestwich, G., Sakai, N., Matile, S., Parton, R.G. and Gruenberg, J. (2008) Lysobisphosphatidic acid controls endosomal cholesterol levels. J Biol Chem 283(41), 27871-80.
Christoforidis, S., Miaczynska, M., Ashman, K., Wilm, M., Zhao, L., Yip, S.C., Waterfield, M.D., Backer, J.M. and Zerial, M. (1999) Phosphatidylinositol-3-OH kinases are Rab5 effectors. Nat Cell Biol 1(4), 249-52.
Chu, J.J. and Ng, M.L. (2004) Infectious entry of West Nile virus occurs through a clathrin-mediated endocytic pathway. J Virol 78(19), 10543-55.
Daecke, J., Fackler, O.T., Dittmar, M.T. and Krausslich, H.G. (2005) Involvement of clathrin-mediated endocytosis in human immunodeficiency virus type 1 entry. J Virol 79(3), 1581-94.
Danthi, P. and Chow, M. (2004) Cholesterol removal by methyl-beta-cyclodextrin inhibits poliovirus entry. J Virol 78(1), 33-41.
Das, S. and Pellett, P.E. (2011) Spatial relationships between markers for secretory and endosomal machinery in human cytomegalovirus-infected cells versus those in uninfected cells. J Virol 85(12), 5864-79.
Das, S., Vasanji, A. and Pellett, P.E. (2007) Three-dimensional structure of the human cytomegalovirus cytoplasmic virion assembly complex includes a reoriented secretory apparatus. J Virol 81(21), 11861-9.
Day, P.M., Lowy, D.R. and Schiller, J.T. (2003) Papillomaviruses infect cells via a clathrin-dependent pathway. Virology 307(1), 1-11.
de Lartigue, J., Polson, H., Feldman, M., Shokat, K., Tooze, S.A., Urbe, S. and Clague, M.J. (2009) PIKfyve regulation of endosome-linked pathways. Traffic 10(7), 883-93.
de Matos, A.P. and Carvalho, Z.G. (1993) African swine fever virus interaction with microtubules. Biol Cell 78(3), 229-34.
de Villiers, E.P., Gallardo, C., Arias, M., da Silva, M., Upton, C., Martin, R. and Bishop, R.P. (2010) Phylogenomic analysis of 11 complete African swine fever virus genome sequences. Virology 400(1), 128-36.
Del Conte-Zerial, P., Brusch, L., Rink, J.C., Collinet, C., Kalaidzidis, Y., Zerial, M. and Deutsch, A. (2008) Membrane identity and GTPase cascades regulated by toggle and cut-out switches. Mol Syst Biol 4, 206.
Desplanques, A.S., Pontes, M., De Corte, N., Verheyen, N., Nauwynck, H.J., Vercauteren, D. and Favoreel, H.W. (2010) Cholesterol depletion affects infectivity and stability of pseudorabies virus. Virus Res 152(1-2), 180-3.
DeTulleo, L. and Kirchhausen, T. (1998) The clathrin endocytic pathway in viral infection. Embo J 17(16), 4585-93.
Dharmawardhane, S., Schurmann, A., Sells, M.A., Chernoff, J., Schmid, S.L. and Bokoch, G.M. (2000) Regulation of macropinocytosis by p21-activated kinase-1. Mol Biol Cell 11(10), 3341-52.
Diaz-Griffero, F., Hoschander, S.A. and Brojatsch, J. (2002) Endocytosis is a critical step in entry of subgroup B avian leukosis viruses. J Virol 76(24), 12866-76.
Diaz-Griffero, F., Jackson, A.P. and Brojatsch, J. (2005) Cellular uptake of avian leukosis virus subgroup B is mediated by clathrin. Virology 337(1), 45-54.
Dikic, I. (2004) ALIX-ing phospholipids with endosome biogenesis. Bioessays 26(6), 604-7.

Doherty, G.J. and McMahon, H.T. (2009) Mechanisms of endocytosis. Annu Rev Biochem 78, 857-902.
Donaldson, J.G. (2003) Multiple roles for Arf6: sorting, structuring, and signaling at the plasma membrane. J Biol Chem 278(43), 41573-6.
Dong, X.P., Shen, D., Wang, X., Dawson, T., Li, X., Zhang, Q., Cheng, X., Zhang, Y., Weisman, L.S., Delling, M. and Xu, H. (2010) PI(3,5)P(2) controls membrane trafficking by direct activation of mucolipin Ca(2+) release channels in the endolysosome. Nat Commun 1, 38.
Dove, S.K., Cooke, F.T., Douglas, M.R., Sayers, L.G., Parker, P.J. and Michell, R.H. (1997) Osmotic stress activates phosphatidylinositol-3,5-bisphosphate synthesis. Nature 390(6656), 187-92.
Dove, S.K., Dong, K., Kobayashi, T., Williams, F.K. and Michell, R.H. (2009) Phosphatidylinositol 3,5-bisphosphate and Fab1p/PIKfyve underPPIn endo-lysosome function. Biochem J 419(1), 1-13.
Dove, S.K., McEwen, R.K., Cooke, F.T., Parker, P.J. and Michell, R.H. (1999) Phosphatidylinositol 3,5-bisphosphate: a novel lipid that links stress responses to membrane trafficking events. Biochem Soc Trans 27(4), 674-7.
Dove, S.K., Piper, R.C., McEwen, R.K., Yu, J.W., King, M.C., Hughes, D.C., Thuring, J., Holmes, A.B., Cooke, F.T., Michell, R.H., Parker, P.J. and Lemmon, M.A. (2004) Svp1p defines a family of phosphatidylinositol 3,5-bisphosphate effectors. Embo J 23(9), 1922-33.
Ehrlich, M., Boll, W., Van Oijen, A., Hariharan, R., Chandran, K., Nibert, M.L. and Kirchhausen, T. (2004) Endocytosis by random initiation and stabilization of clathrin-coated pits. Cell 118(5), 591-605.
Engel, S., Heger, T., Mancini, R., Herzog, F., Kartenbeck, J., Hayer, A. and Helenius, A. (2011) Role of endosomes in simian virus 40 entry and infection. J Virol 85(9), 4198-211.
Enjuanes, L., Carrascosa, A.L. and Vinuela, E. (1976) Isolation and properties of the DNA of African swine fever (ASF) virus. J Gen Virol 32(3), 479-92.
Epifano, C., Krijnse-Locker, J., Salas, M.L., Rodriguez, J.M. and Salas, J. (2006) The African swine fever virus nonstructural protein pB602L is required for formation of the icosahedral capsid of the virus particle. J Virol 80(24), 12260-70.
Fedson, D.S. (2006) Pandemic influenza: a potential role for statins in treatment and prophylaxis. Clin Infect Dis 43(2), 199-205.
Feng, Y., Press, B. and Wandinger-Ness, A. (1995) Rab 7: an important regulator of late endocytic membrane traffic. J Cell Biol 131(6 Pt 1), 1435-52.
Fernandez, A., Perez, J., Carrasco, L., Bautista, M.J., Sanchez-Vizcaino, J.M. and Sierra, M.A. (1992) Distribution of ASFV antigens in pig tissues experimentally infected with two different Spanish virus isolates. Zentralbl Veterinarmed B 39(6), 393-402.
Fontenot, D.R., den Hollander, P., Vela, E.M., Newman, R., Sastry, J.K. and Kumar, R. (2007) Dynein light chain 1 peptide inhibits human immunodeficiency virus infection in eukaryotic cells. Biochem Biophys Res Commun 363(4), 901-7.
Forzan, M., Marsh, M. and Roy, P. (2007) Bluetongue virus entry into cells. J Virol 81(9), 4819-27.
Froshauer, S., Kartenbeck, J. and Helenius, A. (1988) Alphavirus RNA replicase is located on the cytoplasmic surface of endosomes and lysosomes. J Cell Biol 107(6 Pt 1), 2075-86.
Fuchs, R. and Blaas, D. (2010) Uncoating of human rhinoviruses. Rev Med Virol 20(5), 281-97.
Gabriel, C., Blome, S., Malogolovkin, A., Parilov, S., Kolbasov, D., Teifke, J.P. and Beer, M. (2011) Characterization of African swine fever virus Caucasus isolate in European wild boars. Emerg Infect Dis 17(12), 2342-5.
Galindo, I., Hernaez, B., Munoz-Moreno, R., Cuesta-Geijo, M.A., Dalmau-Mena, I. and Alonso, C. (2012) The ATF6 branch of unfolded protein response and apoptosis are activated to promote African swine fever virus infection. Cell Death Dis 3, e341.

Garcia-Beato, R., Salas, M.L., Vinuela, E. and Salas, J. (1992) Role of the host cell nucleus in the replication of African swine fever virus DNA. Virology 188(2), 637-49.
Garcia-del Portillo, F. and Finlay, B.B. (1995) Targeting of Salmonella typhimurium to vesicles containing lysosomal membrane glycoproteins bypasses compartments with mannose 6-phosphate receptors. J Cell Biol 129(1), 81-97.
Garcia-Escudero, R., Andres, G., Almazan, F. and Vinuela, E. (1998) Inducible gene expression from African swine fever virus recombinants: analysis of the major capsid protein p72. J Virol 72(4), 3185-95.
Gastaldelli, M., Imelli, N., Boucke, K., Amstutz, B., Meier, O. and Greber, U.F. (2008) Infectious adenovirus type 2 transport through early but not late endosomes. Traffic 9(12), 2265-78.
Giammarioli, M., Gallardo, C., Oggiano, A., Iscaro, C., Nieto, R., Pellegrini, C., Dei Giudici, S., Arias, M. and De Mia, G.M. (2011) Genetic characterisation of African swine fever viruses from recent and historical outbreaks in Sardinia (1978-2009). Virus Genes 42(3), 377-87.
Glebov, O.O., Bright, N.A. and Nichols, B.J. (2006) Flotillin-1 defines a clathrin-independent endocytic pathway in mammalian cells. Nat Cell Biol 8(1), 46-54.
Glenn, J.S., Watson, J.A., Havel, C.M. and White, J.M. (1992) Identification of a prenylation site in delta virus large antigen. Science 256(5061), 1331-3.
Goldstein, J.L. and Brown, M.S. (1984) Progress in understanding the LDL receptor and HMG-CoA reductase, two membrane proteins that regulate the plasma cholesterol. J Lipid Res 25(13), 1450-61.
Gomez-Puertas, P., Rodriguez, F., Oviedo, J.M., Brun, A., Alonso, C. and Escribano, J.M. (1998) The African swine fever virus proteins p54 and p30 are involved in two distinct steps of virus attachment and both contribute to the antibody-mediated protective immune response. Virology 243(2), 461-71.
Gomez-Puertas, P., Rodriguez, F., Oviedo, J.M., Ramiro-Ibanez, F., Ruiz-Gonzalvo, F., Alonso, C. and Escribano, J.M. (1996) Neutralizing antibodies to different proteins of African swine fever virus inhibit both virus attachment and internalization. J Virol 70(8), 5689-94.
Gomez-Villamandos, J.C., Carrasco, L., Bautista, M.J., Sierra, M.A., Quezada, M., Hervas, J., Chacon Mde, L., Ruiz-Villamor, E., Salguero, F.J., Sonchez-Cordon, P.J., Romanini, S., Nunez, A., Mekonen, T., Mendez, A. and Jover, A. (2003) African swine fever and classical swine fever: a review of the pathogenesis. Dtsch Tierarztl Wochenschr 110(4), 165-9.
Gonzalez, A., Talavera, A., Almendral, J.M. and Vinuela, E. (1986) Hairpin loop structure of African swine fever virus DNA. Nucleic Acids Res 14(17), 6835-44.
Granja, A.G., Perkins, N.D. and Revilla, Y. (2008) A238L inhibits NF-ATc2, NF-kappa B, and c-Jun activation through a novel mechanism involving protein kinase C-theta-mediated up-regulation of the amino-terminal transactivation domain of p300. J Immunol 180(4), 2429-42.
Greber, U.F. (2002) Signalling in viral entry. Cell Mol Life Sci 59(4), 608-26.
Griffiths, G., Matteoni, R., Back, R. and Hoflack, B. (1990) Characterization of the cation-independent mannose 6-phosphate receptor-enriched prelysosomal compartment in NRK cells. J Cell Sci 95 (Pt 3), 441-61.
Gruenberg, J. (2001) The endocytic pathway: a mosaic of domains. Nat Rev Mol Cell Biol 2(10), 721-30.
Gruenberg, J. (2009) Viruses and endosome membrane dynamics. Curr Opin Cell Biol 21(4), 582-8.
Gruenberg, J., Griffiths, G. and Howell, K.E. (1989) Characterization of the early endosome and putative endocytic carrier vesicles in vivo and with an assay of vesicle fusion in vitro. J Cell Biol 108(4), 1301-16.
Gruenberg, J. and Stenmark, H. (2004) The biogenesis of multivesicular endosomes. Nat Rev Mol Cell Biol 5(4), 317-23.

Gruenberg, J. and van der Goot, F.G. (2006) Mechanisms of pathogen entry through the endosomal compartments. Nat Rev Mol Cell Biol 7(7), 495-504.

Guijarro, C., Blanco-Colio, L.M., Ortego, M., Alonso, C., Ortiz, A., Plaza, J.J., Diaz, C., Hernandez, G. and Egido, J. (1998) 3-Hydroxy-3-methylglutaryl coenzyme a reductase and isoprenylation inhibitors induce apoptosis of vascular smooth muscle cells in culture. Circ Res 83(5), 490-500.

Hao, M., Lin, S.X., Karylowski, O.J., Wustner, D., McGraw, T.E. and Maxfield, F.R. (2002) Vesicular and non-vesicular sterol transport in living cells. The endocytic recycling compartment is a major sterol storage organelle. J Biol Chem 277(1), 609-17.

Hawes, P.C., Netherton, C.L., Wileman, T.E. and Monaghan, P. (2008) The envelope of intracellular African swine fever virus is composed of a single lipid bilayer. J Virol 82(16), 7905-12.

Heath, C.M., Windsor, M. and Wileman, T. (2001) Aggresomes resemble sites specialized for virus assembly. J Cell Biol 153(3), 449-55.

Helenius, A., Kartenbeck, J., Simons, K. and Fries, E. (1980) On the entry of Semliki forest virus into BHK-21 cells. J Cell Biol 84(2), 404-20.

Helle, F. and Dubuisson, J. (2008) Hepatitis C virus entry into host cells. Cell Mol Life Sci 65(1), 100-12.

Hernaez, B. and Alonso, C. (2010) Dynamin- and clathrin-dependent endocytosis in African swine fever virus entry. J Virol 84(4), 2100-9.

Hernaez, B., Cabezas, M., Munoz-Moreno, R., Galindo, I., Cuesta-Geijo, M.A. and Alonso, C. (2013) A179L, a New Viral Bcl2 Homolog Targeting Beclin 1 Autophagy Related Protein. Curr Mol Med 13(2), 305-16.

Hernaez, B., Diaz-Gil, G., Garcia-Gallo, M., Ignacio Quetglas, J., Rodriguez-Crespo, I., Dixon, L., Escribano, J.M. and Alonso, C. (2004a) The African swine fever virus dynein-binding protein p54 induces infected cell apoptosis. FEBS Lett 569(1-3), 224-8.

Hernaez, B., Escribano, J.M. and Alonso, C. (2004b) Switching on and off the cell death cascade: African swine fever virus apoptosis regulation. In: C. Alonso (Ed), Viruses and apoptosis, pp. 57-70. Springer, Berlin.

Hernaez, B., Escribano, J.M. and Alonso, C. (2006) Visualization of the African swine fever virus infection in living cells by incorporation into the virus particle of green fluorescent protein-p54 membrane protein chimera. Virology 350(1), 1-14.

Holthuis, J.C. and Levine, T.P. (2005) Lipid traffic: floppy drives and a superhighway. Nat Rev Mol Cell Biol 6(3), 209-20.

Hsu, N.Y., Ilnytska, O., Belov, G., Santiana, M., Chen, Y.H., Takvorian, P.M., Pau, C., van der Schaar, H., Kaushik-Basu, N., Balla, T., Cameron, C.E., Ehrenfeld, E., van Kuppeveld, F.J. and Altan-Bonnet, N. (2010) Viral reorganization of the secretory pathway generates distinct organelles for RNA replication. Cell 141(5), 799-811.

Huotari, J. and Helenius, A. (2011) Endosome maturation. Embo J 30(17), 3481-500.

Ikonen, E. (2008) Cellular cholesterol trafficking and compartmentalization. Nat Rev Mol Cell Biol 9(2), 125-38.

Ikonomov, O.C., Sbrissa, D., Fenner, H. and Shisheva, A. (2009) PIKfyve-ArPIKfyve-Sac3 core complex: contact sites and their consequence for Sac3 phosphatase activity and endocytic membrane homeostasis. J Biol Chem 284(51), 35794-806.

Ikonomov, O.C., Sbrissa, D. and Shisheva, A. (2001) Mammalian cell morphology and endocytic membrane homeostasis require enzymatically active phosphoinositide 5-kinase PIKfyve. J Biol Chem 276(28), 26141-7.

International Committee on Taxonomy of Viruses. A.M.Q. King, M.J.A., E.B. Carstens and E.J. Lefkowitz (2011) Virus taxonomy : classification and nomenclature of viruses : ninth report of the International Committee on Taxonomy of Viruses, 1327 p. pp. Academic Press, London ; Waltham, MA.

Ioannou, Y.A. (2001) Multidrug permeases and subcellular cholesterol transport. Nat Rev Mol Cell Biol 2(9), 657-68.

Jefferies, H.B., Cooke, F.T., Jat, P., Boucheron, C., Koizumi, T., Hayakawa, M., Kaizawa, H., Ohishi, T., Workman, P., Waterfield, M.D. and Parker, P.J. (2008) A selective PIKfyve inhibitor blocks PtdIns(3,5)P(2) production and disrupts endomembrane transport and retroviral budding. EMBO Rep 9(2), 164-70.

Johannsdottir, H.K., Mancini, R., Kartenbeck, J., Amato, L. and Helenius, A. (2009) Host cell factors and functions involved in vesicular stomatitis virus entry. J Virol 83(1), 440-53.

Johansson, M., Rocha, N., Zwart, W., Jordens, I., Janssen, L., Kuijl, C., Olkkonen, V.M. and Neefjes, J. (2007) Activation of endosomal dynein motors by stepwise assembly of Rab7-RILP-p150Glued, ORP1L, and the receptor betalll spectrin. J Cell Biol 176(4), 459-71.

Johns, H.L., Berryman, S., Monaghan, P., Belsham, G.J. and Jackson, T. (2009) A dominant-negative mutant of rab5 inhibits infection of cells by foot-and-mouth disease virus: implications for virus entry. J Virol 83(12), 6247-56.

Johnson, E.E., Overmeyer, J.H., Gunning, W.T. and Maltese, W.A. (2006) Gene silencing reveals a specific function of hVps34 phosphatidylinositol 3-kinase in late versus early endosomes. J Cell Sci 119(Pt 7), 1219-32.

Jordens, I., Fernandez-Borja, M., Marsman, M., Dusseljee, S., Janssen, L., Calafat, J., Janssen, H., Wubbolts, R. and Neefjes, J. (2001) The Rab7 effector protein RILP controls lysosomal transport by inducing the recruitment of dynein-dynactin motors. Curr Biol 11(21), 1680-5.

Jordens, I., Marsman, M., Kuijl, C. and Neefjes, J. (2005) Rab proteins, connecting transport and vesicle fusion. Traffic 6(12), 1070-7.

Kagan, J.C. and Roy, C.R. (2002) Legionella phagosomes intercept vesicular traffic from endoplasmic reticulum exit sites. Nat Cell Biol 4(12), 945-54.

Kalia, M., Kumari, S., Chadda, R., Hill, M.M., Parton, R.G. and Mayor, S. (2006) Arf6-independent GPI-anchored protein-enriched early endosomal compartments fuse with sorting endosomes via a Rab5/phosphatidylinositol-3'-kinase-dependent machinery. Mol Biol Cell 17(8), 3689-704.

Karjalainen, M., Kakkonen, E., Upla, P., Paloranta, H., Kankaanpaa, P., Liberali, P., Renkema, G.H., Hyypia, T., Heino, J. and Marjomaki, V. (2008) A Raft-derived, Pak1-regulated entry participates in alpha2beta1 integrin-dependent sorting to caveosomes. Mol Biol Cell 19(7), 2857-69.

Karten, B., Peake, K.B. and Vance, J.E. (2009) Mechanisms and consequences of impaired lipid trafficking in Niemann-Pick type C1-deficient mammalian cells. Biochim Biophys Acta 1791(7), 659-70.

Katzmann, D.J., Odorizzi, G. and Emr, S.D. (2002) Receptor downregulation and multivesicular-body sorting. Nat Rev Mol Cell Biol 3(12), 893-905.

Katzmann, D.J., Stefan, C.J., Babst, M. and Emr, S.D. (2003) Vps27 recruits ESCRT machinery to endosomes during MVB sorting. J Cell Biol 162(3), 413-23.

Kawase, M., Shirato, K., Matsuyama, S. and Taguchi, F. (2009) Protease-mediated entry via the endosome of human coronavirus 229E. J Virol 83(2), 712-21.

Kerr, M.C., Wang, J.T., Castro, N.A., Hamilton, N.A., Town, L., Brown, D.L., Meunier, F.A., Brown, N.F., Stow, J.L. and Teasdale, R.D. (2010) Inhibition of the PtdIns(5) kinase PIKfyve disrupts intracellular replication of Salmonella. Embo J 29(8), 1331-47.

Kirkham, M. and Parton, R.G. (2005) Clathrin-independent endocytosis: new insights into caveolae and non-caveolar lipid raft carriers. Biochim Biophys Acta 1746(3), 349-63.

Kleiboeker, S.B. (2002) Swine fever: classical swine fever and African swine fever. Vet Clin North Am Food Anim Pract 18(3), 431-51.

Kleiboeker, S.B. and Scoles, G.A. (2001) Pathogenesis of African swine fever virus in Ornithodoros ticks. Anim Health Res Rev 2(2), 121-8.

Kleijmeer, M., Ramm, G., Schuurhuis, D., Griffith, J., Rescigno, M., Ricciardi-Castagnoli, P., Rudensky, A.Y., Ossendorp, F., Melief, C.J., Stoorvogel, W. and Geuze, H.J. (2001)

Reorganization of multivesicular bodies regulates MHC class II antigen presentation by dendritic cells. J Cell Biol 155(1), 53-63.
Knodler, L.A. and Steele-Mortimer, O. (2003) Taking possession: biogenesis of the Salmonella-containing vacuole. Traffic 4(9), 587-99.
Kobayashi, T., Beuchat, M.H., Chevallier, J., Makino, A., Mayran, N., Escola, J.M., Lebrand, C., Cosson, P. and Gruenberg, J. (2002) Separation and characterization of late endosomal membrane domains. J Biol Chem 277(35), 32157-64.
Kobayashi, T., Beuchat, M.H., Lindsay, M., Frias, S., Palmiter, R.D., Sakuraba, H., Parton, R.G. and Gruenberg, J. (1999) Late endosomal membranes rich in lysobisphosphatidic acid regulate cholesterol transport. Nat Cell Biol 1(2), 113-8.
Kobayashi, T., Gu, F. and Gruenberg, J. (1998a) Lipids, lipid domains and lipid-protein interactions in endocytic membrane traffic. Semin Cell Dev Biol 9(5), 517-26.
Kobayashi, T., Stang, E., Fang, K.S., de Moerloose, P., Parton, R.G. and Gruenberg, J. (1998b) A lipid associated with the antiphospholipid syndrome regulates endosome structure and function. Nature 392(6672), 193-7.
Koh, C.H. and Cheung, N.S. (2006) Cellular mechanism of U18666A-mediated apoptosis in cultured murine cortical neurons: bridging Niemann-Pick disease type C and Alzheimer's disease. Cell Signal 18(11), 1844-53.
Kruger, P., Fitzsimmons, K., Cook, D., Jones, M. and Nimmo, G. (2006) Statin therapy is associated with fewer deaths in patients with bacteraemia. Intensive Care Med 32(1), 75-9.
Kruth, H.S., Comly, M.E., Butler, J.D., Vanier, M.T., Fink, J.K., Wenger, D.A., Patel, S. and Pentchev, P.G. (1986) Type C Niemann-Pick disease. Abnormal metabolism of low density lipoprotein in homozygous and heterozygous fibroblasts. J Biol Chem 261(35), 16769-74.
Kubo, Y., Hayashi, H., Matsuyama, T., Sato, H. and Yamamoto, N. (2012) Retrovirus entry by endocytosis and cathepsin proteases. Adv Virol 2012, 640894.
Kutateladze, T.G. (2010) Translation of the phosphoinositide code by PI effectors. Nat Chem Biol 6(7), 507-13.
Kuznar, J., Salas, M.L. and Vinuela, E. (1980) DNA-dependent RNA polymerase in African swine fever virus. Virology 101(1), 169-75.
Lakadamyali, M., Rust, M.J. and Zhuang, X. (2004) Endocytosis of influenza viruses. Microbes Infect 6(10), 929-36.
Lamaze, C., Dujeancourt, A., Baba, T., Lo, C.G., Benmerah, A. and Dautry-Varsat, A. (2001) Interleukin 2 receptors and detergent-resistant membrane domains define a clathrin-independent endocytic pathway. Mol Cell 7(3), 661-71.
Langhorst, M.F., Reuter, A., Jaeger, F.A., Wippich, F.M., Luxenhofer, G., Plattner, H. and Stuermer, C.A. (2008) Trafficking of the microdomain scaffolding protein reggie-1/flotillin-2. Eur J Cell Biol 87(4), 211-26.
Le Blanc, I., Luyet, P.P., Pons, V., Ferguson, C., Emans, N., Petiot, A., Mayran, N., Demaurex, N., Faure, J., Sadoul, R., Parton, R.G. and Gruenberg, J. (2005) Endosome-to-cytosol transport of viral nucleocapsids. Nat Cell Biol 7(7), 653-64.
Lebrand, C., Corti, M., Goodson, H., Cosson, P., Cavalli, V., Mayran, N., Faure, J. and Gruenberg, J. (2002) Late endosome motility depends on lipids via the small GTPase Rab7. Embo J 21(6), 1289-300.
Lee, C.J., Lin, H.R., Liao, C.L. and Lin, Y.L. (2008) Cholesterol effectively blocks entry of flavivirus. J Virol 82(13), 6470-80.
Lemmon, M.A. (2008) Membrane recognition by phospholipid-binding domains. Nat Rev Mol Cell Biol 9(2), 99-111.
Liao, J.K. and Laufs, U. (2005) Pleiotropic effects of statins. Annu Rev Pharmacol Toxicol 45, 89-118.
Liberali, P., Kakkonen, E., Turacchio, G., Valente, C., Spaar, A., Perinetti, G., Bockmann, R.A., Corda, D., Colanzi, A., Marjomaki, V. and Luini, A. (2008) The closure of Pak1-

dependent macropinosomes requires the phosphorylation of CtBP1/BARS. Embo J 27(7), 970-81.
Lin, S.X., Mallet, W.G., Huang, A.Y. and Maxfield, F.R. (2004) Endocytosed cation-independent mannose 6-phosphate receptor traffics via the endocytic recycling compartment en route to the trans-Golgi network and a subpopulation of late endosomes. Mol Biol Cell 15(2), 721-33.
Liscum, L. and Faust, J.R. (1989) The intracellular transport of low density lipoprotein-derived cholesterol is inhibited in Chinese hamster ovary cells cultured with 3-beta-[2-(diethylamino)ethoxy]androst-5-en-17-one. J Biol Chem 264(20), 11796-806.
Liu, N.Q., Lossinsky, A.S., Popik, W., Li, X., Gujuluva, C., Kriederman, B., Roberts, J., Pushkarsky, T., Bukrinsky, M., Witte, M., Weinand, M. and Fiala, M. (2002) Human immunodeficiency virus type 1 enters brain microvascular endothelia by macropinocytosis dependent on lipid rafts and the mitogen-activated protein kinase signaling pathway. J Virol 76(13), 6689-700.
Locker, J.K., Kuehn, A., Schleich, S., Rutter, G., Hohenberg, H., Wepf, R. and Griffiths, G. (2000) Entry of the two infectious forms of vaccinia virus at the plasma membane is signaling-dependent for the IMV but not the EEV. Mol Biol Cell 11(7), 2497-511.
Lozach, P.Y., Mancini, R., Bitto, D., Meier, R., Oestereich, L., Overby, A.K., Pettersson, R.F. and Helenius, A. (2010) Entry of bunyaviruses into mammalian cells. Cell Host Microbe 7(6), 488-99.
Lubisi, B.A., Bastos, A.D., Dwarka, R.M. and Vosloo, W. (2005) Molecular epidemiology of African swine fever in East Africa. Arch Virol 150(12), 2439-52.
Lubisi, B.A., Dwarka, R.M., Meenowa, D. and Jaumally, R. (2009) An investigation into the first outbreak of African swine fever in the Republic of Mauritius. Transbound Emerg Dis 56(5), 178-88.
Lusa, S., Blom, T.S., Eskelinen, E.L., Kuismanen, E., Mansson, J.E., Simons, K. and Ikonen, E. (2001) Depletion of rafts in late endocytic membranes is controlled by NPC1-dependent recycling of cholesterol to the plasma membrane. J Cell Sci 114(Pt 10), 1893-900.
Luyet, P.P., Falguieres, T., Pons, V., Pattnaik, A.K. and Gruenberg, J. (2008) The ESCRT-I subunit TSG101 controls endosome-to-cytosol release of viral RNA. Traffic 9(12), 2279-90.
Luzio, J.P., Bright, N.A. and Pryor, P.R. (2007) The role of calcium and other ions in sorting and delivery in the late endocytic pathway. Biochem Soc Trans 35(Pt 5), 1088-91.
Macia, E., Ehrlich, M., Massol, R., Boucrot, E., Brunner, C. and Kirchhausen, T. (2006) Dynasore, a cell-permeable inhibitor of dynamin. Dev Cell 10(6), 839-50.
Mackenzie, J.M., Khromykh, A.A. and Parton, R.G. (2007) Cholesterol manipulation by West Nile virus perturbs the cellular immune response. Cell Host Microbe 2(4), 229-39.
Marechal, V., Prevost, M.C., Petit, C., Perret, E., Heard, J.M. and Schwartz, O. (2001) Human immunodeficiency virus type 1 entry into macrophages mediated by macropinocytosis. J Virol 75(22), 11166-77.
Marsh, M., Bolzau, E. and Helenius, A. (1983) Penetration of Semliki Forest virus from acidic prelysosomal vacuoles. Cell 32(3), 931-40.
Marsh, M. and Helenius, A. (1989) Virus entry into animal cells. Adv Virus Res 36, 107-51.
Marsh, M. and Helenius, A. (2006) Virus entry: open sesame. Cell 124(4), 729-40.
Marshansky, V. and Futai, M. (2008) The V-type H+-ATPase in vesicular trafficking: targeting, regulation and function. Curr Opin Cell Biol 20(4), 415-26.
Martins, A., Ribeiro, G., Marques, M.I. and Costa, J.V. (1994) Genetic identification and nucleotide sequence of the DNA polymerase gene of African swine fever virus. Nucleic Acids Res 22(2), 208-13.
Matlin, K.S., Reggio, H., Helenius, A. and Simons, K. (1981) Infectious entry pathway of influenza virus in a canine kidney cell line. J Cell Biol 91(3 Pt 1), 601-13.

Matlin, K.S., Reggio, H., Helenius, A. and Simons, K. (1982) Pathway of vesicular stomatitis virus entry leading to infection. J Mol Biol 156(3), 609-31.
Matsuo, H., Chevallier, J., Mayran, N., Le Blanc, I., Ferguson, C., Faure, J., Blanc, N.S., Matile, S., Dubochet, J., Sadoul, R., Parton, R.G., Vilbois, F. and Gruenberg, J. (2004) Role of LBPA and Alix in multivesicular liposome formation and endosome organization. Science 303(5657), 531-4.
Maxfield, F.R. and Tabas, I. (2005) Role of cholesterol and lipid organization in disease. Nature 438(7068), 612-21.
Mayor, S. and Pagano, R.E. (2007) Pathways of clathrin-independent endocytosis. Nat Rev Mol Cell Biol 8(8), 603-12.
McMahon, H.T. and Boucrot, E. (2011) Molecular mechanism and physiological functions of clathrin-mediated endocytosis. Nat Rev Mol Cell Biol 12(8), 517-33.
McTaggart, S.J. (2006) Isoprenylated proteins. Cell Mol Life Sci 63(3), 255-67.
Medigeshi, G.R., Hirsch, A.J., Streblow, D.N., Nikolich-Zugich, J. and Nelson, J.A. (2008) West Nile virus entry requires cholesterol-rich membrane microdomains and is independent of alphavbeta3 integrin. J Virol 82(11), 5212-9.
Medina-Kauwe, L.K. (2003) Endocytosis of adenovirus and adenovirus capsid proteins. Adv Drug Deliv Rev 55(11), 1485-96.
Meertens, L., Bertaux, C. and Dragic, T. (2006) Hepatitis C virus entry requires a critical postinternalization step and delivery to early endosomes via clathrin-coated vesicles. J Virol 80(23), 11571-8.
Mercer, J. and Helenius, A. (2008) Vaccinia virus uses macropinocytosis and apoptotic mimicry to enter host cells. Science 320(5875), 531-5.
Mercer, J., Schelhaas, M. and Helenius, A. (2010) Virus entry by endocytosis. Annu Rev Biochem 79, 803-33.
Meresse, S., Steele-Mortimer, O., Finlay, B.B. and Gorvel, J.P. (1999) The rab7 GTPase controls the maturation of Salmonella typhimurium-containing vacuoles in HeLa cells. Embo J 18(16), 4394-403.
Merrifield, C.J. (2012) Fishing for clathrin-coated pit nucleators. Nat Cell Biol 14(5), 452-4.
Merrifield, C.J., Feldman, M.E., Wan, L. and Almers, W. (2002) Imaging actin and dynamin recruitment during invagination of single clathrin-coated pits. Nat Cell Biol 4(9), 691-8.
Merrifield, C.J., Perrais, D. and Zenisek, D. (2005) Coupling between clathrin-coated-pit invagination, cortactin recruitment, and membrane scission observed in live cells. Cell 121(4), 593-606.
Michell, R.H., Heath, V.L., Lemmon, M.A. and Dove, S.K. (2006) Phosphatidylinositol 3,5-bisphosphate: metabolism and cellular functions. Trends Biochem Sci 31(1), 52-63.
Miller, S. and Krijnse-Locker, J. (2008) Modification of intracellular membrane structures for virus replication. Nat Rev Microbiol 6(5), 363-74.
Mire, C.E., White, J.M. and Whitt, M.A. (2010) A spatio-temporal analysis of matrix protein and nucleocapsid trafficking during vesicular stomatitis virus uncoating. PLoS Pathog 6(7), e1000994.
Miskin, J.E., Abrams, C.C., Goatley, L.C. and Dixon, L.K. (1998) A viral mechanism for inhibition of the cellular phosphatase calcineurin. Science 281(5376), 562-5.
Miyauchi, K., Kim, Y., Latinovic, O., Morozov, V. and Melikyan, G.B. (2009) HIV enters cells via endocytosis and dynamin-dependent fusion with endosomes. Cell 137(3), 433-44.
Miyazawa, N., Crystal, R.G. and Leopold, P.L. (2001) Adenovirus serotype 7 retention in a late endosomal compartment prior to cytosol escape is modulated by fiber protein. J Virol 75(3), 1387-400.
Mobius, W., van Donselaar, E., Ohno-Iwashita, Y., Shimada, Y., Heijnen, H.F., Slot, J.W. and Geuze, H.J. (2003) Recycling compartments and the internal vesicles of

multivesicular bodies harbor most of the cholesterol found in the endocytic pathway. Traffic 4(4), 222-31.
Montgomery, R.E. (1921) On a form of a swine fever occurring in British East African (Kenya Colony). J. Comp. Path. Therap 34, 159-191 y 243-262.
Moreno-Ruiz, E., Galan-Diez, M., Zhu, W., Fernandez-Ruiz, E., d'Enfert, C., Filler, S.G., Cossart, P. and Veiga, E. (2009) Candida albicans internalization by host cells is mediated by a clathrin-dependent mechanism. Cell Microbiol 11(8), 1179-89.
Moreno, M.A., Carrascosa, A.L., Ortin, J. and Vinuela, E. (1978) Inhibition of African swine fever (ASF virus replication by phosphonoacetic acid. J Gen Virol 39(2), 253-8.
Moss, B. (2001) Poxviridae: the viruses and their replication. In: K.D. Fields BN, Howley PM, Chanock RM, Hirsch MS, Melnick JL, Monath TP, Roizman B. (Ed), Fields Virology., 4th ed., pp. 2849–2883. Lippincott-Raven Press, Philadelphia.
Mothes, W., Boerger, A.L., Narayan, S., Cunningham, J.M. and Young, J.A. (2000) Retroviral entry mediated by receptor priming and low pH triggering of an envelope glycoprotein. Cell 103(4), 679-89.
Mukherjee, S. and Maxfield, F.R. (2004) Membrane domains. Annu Rev Cell Dev Biol 20, 839-66.
Munoz, M., Freije, J.M., Salas, M.L., Vinuela, E. and Lopez-Otin, C. (1993) Structure and expression in E. coli of the gene coding for protein p10 of African swine fever virus. Arch Virol 130(1-2), 93-107.
Netherton, C.L., McCrossan, M.C., Denyer, M., Ponnambalam, S., Armstrong, J., Takamatsu, H.H. and Wileman, T.E. (2006) African swine fever virus causes microtubule-dependent dispersal of the trans-golgi network and slows delivery of membrane protein to the plasma membrane. J Virol 80(22), 11385-92.
Neufeld, E.B., Stonik, J.A., Demosky, S.J., Jr., Knapper, C.L., Combs, C.A., Cooney, A., Comly, M., Dwyer, N., Blanchette-Mackie, J., Remaley, A.T., Santamarina-Fojo, S. and Brewer, H.B., Jr. (2004) The ABCA1 transporter modulates late endocytic trafficking: insights from the correction of the genetic defect in Tangier disease. J Biol Chem 279(15), 15571-8.
Nguyen, D.G., Wolff, K.C., Yin, H., Caldwell, J.S. and Kuhen, K.L. (2006) "UnPAKing" human immunodeficiency virus (HIV) replication: using small interfering RNA screening to identify novel cofactors and elucidate the role of group I PAKs in HIV infection. J Virol 80(1), 130-7.
Nicola, A.V., Hou, J., Major, E.O. and Straus, S.E. (2005) Herpes simplex virus type 1 enters human epidermal keratinocytes, but not neurons, via a pH-dependent endocytic pathway. J Virol 79(12), 7609-16.
Nicola, A.V., McEvoy, A.M. and Straus, S.E. (2003) Roles for endocytosis and low pH in herpes simplex virus entry into HeLa and Chinese hamster ovary cells. J Virol 77(9), 5324-32.
Nicot, A.S., Fares, H., Payrastre, B., Chisholm, A.D., Labouesse, M. and Laporte, J. (2006) The phosphoinositide kinase PIKfyve/Fab1p regulates terminal lysosome maturation in Caenorhabditis elegans. Mol Biol Cell 17(7), 3062-74.
Nogal, M.L., Gonzalez de Buitrago, G., Rodriguez, C., Cubelos, B., Carrascosa, A.L., Salas, M.L. and Revilla, Y. (2001) African swine fever virus IAP homologue inhibits caspase activation and promotes cell survival in mammalian cells. J Virol 75(6), 2535-43.
Nomura, R., Kiyota, A., Suzaki, E., Kataoka, K., Ohe, Y., Miyamoto, K., Senda, T. and Fujimoto, T. (2004) Human coronavirus 229E binds to CD13 in rafts and enters the cell through caveolae. J Virol 78(16), 8701-8.
Novoa, R.R., Calderita, G., Arranz, R., Fontana, J., Granzow, H. and Risco, C. (2005) Virus factories: associations of cell organelles for viral replication and morphogenesis. Biol Cell 97(2), 147-72.
Nunes, J.F., Vigario, J.D. and Terrinha, A.M. (1975) Ultrastructural study of African swine fever virus replication in cultures of swine bone marrow cells. Arch Virol 49(1), 59-66.

O'Doherty, U., Swiggard, W.J. and Malim, M.H. (2000) Human immunodeficiency virus type 1 spinoculation enhances infection through virus binding. J Virol 74(21), 10074-80.
O'Donnell, V., LaRocco, M., Duque, H. and Baxt, B. (2005) Analysis of foot-and-mouth disease virus internalization events in cultured cells. J Virol 79(13), 8506-18.
Odorizzi, G. (2006) The multiple personalities of Alix. J Cell Sci 119(Pt 15), 3025-32.
Odorizzi, G., Babst, M. and Emr, S.D. (1998) Fab1p PtdIns(3)P 5-kinase function essential for protein sorting in the multivesicular body. Cell 95(6), 847-58.
Oh, J. and Hegele, R.A. (2007) HIV-associated dyslipidaemia: pathogenesis and treatment. Lancet Infect Dis 7(12), 787-96.
Ohkuma, S. and Poole, B. (1978) Fluorescence probe measurement of the intralysosomal pH in living cells and the perturbation of pH by various agents. Proc Natl Acad Sci U S A 75(7), 3327-31.
Pasqual, G., Rojek, J.M., Masin, M., Chatton, J.Y. and Kunz, S. (2011) Old world arenaviruses enter the host cell via the multivesicular body and depend on the endosomal sorting complex required for transport. PLoS Pathog 7(9), e1002232.
Pattanakitsakul, S.N., Poungsawai, J., Kanlaya, R., Sinchaikul, S., Chen, S.T. and Thongboonkerd, V. (2010) Association of Alix with late endosomal lysobisphosphatidic acid is important for dengue virus infection in human endothelial cells. J Proteome Res 9(9), 4640-8.
Pelkmans, L., Fava, E., Grabner, H., Hannus, M., Habermann, B., Krausz, E. and Zerial, M. (2005) Genome-wide analysis of human kinases in clathrin- and caveolae/raft-mediated endocytosis. Nature 436(7047), 78-86.
Pelkmans, L. and Helenius, A. (2003) Insider information: what viruses tell us about endocytosis. Curr Opin Cell Biol 15(4), 414-22.
Pelkmans, L., Kartenbeck, J. and Helenius, A. (2001) Caveolar endocytosis of simian virus 40 reveals a new two-step vesicular-transport pathway to the ER. Nat Cell Biol 3(5), 473-83.
Pena, L., Yanez, R.J., Revilla, Y., Vinuela, E. and Salas, M.L. (1993) African swine fever virus guanylyltransferase. Virology 193(1), 319-28.
Perez, J., Rodriguez, F., Fernandez, A., Martin de las Mulas, J., Gomez-Villamandos, J.C. and Sierra, M.A. (1994) Detection of African swine fever virus protein VP73 in tissues of experimentally and naturally infected pigs. J Vet Diagn Invest 6(3), 360-5.
Pfeffer, S. and Aivazian, D. (2004) Targeting Rab GTPases to distinct membrane compartments. Nat Rev Mol Cell Biol 5(11), 886-96.
Pizarro-Cerda, J., Bonazzi, M. and Cossart, P. (2010) Clathrin-mediated endocytosis: what works for small, also works for big. Bioessays 32(6), 496-504.
Plowright, W., Parker, J. and Peirce, M.A. (1969) African swine fever virus in ticks (Ornithodoros moubata, murray) collected from animal burrows in Tanzania. Nature 221(185), 1071-3.
Plowright, W., Parker, J. and Staple, R.F. (1968) The growth of a virulent strain of African swine fever virus in domestic pigs. J Hyg (Lond) 66(1), 117-34.
Poh, M.K., Shui, G., Xie, X., Shi, P.Y., Wenk, M.R. and Gu, F. (2011) U18666A, an intra-cellular cholesterol transport inhibitor, inhibits dengue virus entry and replication. Antiviral Res 93(1), 191-8.
Poh, M.K., Shui, G., Xie, X., Shi, P.Y., Wenk, M.R. and Gu, F. (2012) U18666A, an intra-cellular cholesterol transport inhibitor, inhibits dengue virus entry and replication. Antiviral Res 93(1), 191-8.
Polo-Jover, F. and Sánchez-Botija, C. (1961) La Peste porcina africana en España. Bull Off Int Epizoot 55, 107-147.
Poteryaev, D., Datta, S., Ackema, K., Zerial, M. and Spang, A. (2010) Identification of the switch in early-to-late endosome transition. Cell 141(3), 497-508.

Quetglas, J.I., Hernaez, B., Galindo, I., Munoz-Moreno, R., Cuesta-Geijo, M.A. and Alonso, C. (2012) Small rho GTPases and cholesterol biosynthetic pathway intermediates in african Swine Fever virus infection. J Virol 86(3), 1758-67.

Raiborg, C., Bache, K.G., Gillooly, D.J., Madshus, I.H., Stang, E. and Stenmark, H. (2002) Hrs sorts ubiquitinated proteins into clathrin-coated microdomains of early endosomes. Nat Cell Biol 4(5), 394-8.

Raiborg, C., Rusten, T.E. and Stenmark, H. (2003) Protein sorting into multivesicular endosomes. Curr Opin Cell Biol 15(4), 446-55.

Raiborg, C. and Stenmark, H. (2009) The ESCRT machinery in endosomal sorting of ubiquitylated membrane proteins. Nature 458(7237), 445-52.

Ramiro-Ibanez, F., Escribano, J.M. and Alonso, C. (1995) Application of a monoclonal antibody recognizing protein p30 to detect African swine fever virus-infected cells in peripheral blood. J Virol Methods 55(3), 339-45.

Ramiro-Ibanez, F., Ortega, A., Brun, A., Escribano, J.M. and Alonso, C. (1996) Apoptosis: a mechanism of cell killing and lymphoid organ impairment during acute African swine fever virus infection. J Gen Virol 77 (Pt 9), 2209-19.

Ramiro-Ibanez, F., Ortega, A., Ruiz-Gonzalvo, F., Escribano, J.M. and Alonso, C. (1997) Modulation of immune cell populations and activation markers in the pathogenesis of African swine fever virus infection. Virus Res 47(1), 31-40.

Raychaudhuri, S. and Prinz, W.A. (2010) The diverse functions of oxysterol-binding proteins. Annu Rev Cell Dev Biol 26, 157-77.

Rink, J., Ghigo, E., Kalaidzidis, Y. and Zerial, M. (2005) Rab conversion as a mechanism of progression from early to late endosomes. Cell 122(5), 735-49.

Rivera, J., Abrams, C., Hernaez, B., Alcazar, A., Escribano, J.M., Dixon, L. and Alonso, C. (2007) The MyD116 African swine fever virus homologue interacts with the catalytic subunit of protein phosphatase 1 and activates its phosphatase activity. J Virol 81(6), 2923-9.

Rocha, N., Kuijl, C., van der Kant, R., Janssen, L., Houben, D., Janssen, H., Zwart, W. and Neefjes, J. (2009) Cholesterol sensor ORP1L contacts the ER protein VAP to control Rab7-RILP-p150 Glued and late endosome positioning. J Cell Biol 185(7), 1209-25.

Rodriguez, J.M., Garcia-Escudero, R., Salas, M.L. and Andres, G. (2004) African Swine Fever Virus Structural Protein p54 Is Essential for the Recruitment of Envelope Precursors to Assembly Sites. J Virol 78(8), 4299-1313.

Rodriguez, J.M., Salas, M.L. and Vinuela, E. (1992) Genes homologous to ubiquitin-conjugating proteins and eukaryotic transcription factor SII in African swine fever virus. Virology 186(1), 40-52.

Rodriguez, J.M., Salas, M.L. and Vinuela, E. (1996) Intermediate class of mRNAs in African swine fever virus. J Virol 70(12), 8584-9.

Roger, F., Ratovonjato, J., Vola, P. and Uilenber, G. (2001) Ornithodoros porcinus ticks, bushpigs, and African swine fever in Madagascar. Exp Appl Acarol 25(3), 263-9.

Rohn, W.M., Rouille, Y., Waguri, S. and Hoflack, B. (2000) Bi-directional trafficking between the trans-Golgi network and the endosomal/lysosomal system. J Cell Sci 113 (Pt 12), 2093-101.

Rojo, G., Chamorro, M., Salas, M.L., Vinuela, E., Cuezva, J.M. and Salas, J. (1998) Migration of mitochondria to viral assembly sites in African swine fever virus-infected cells. J Virol 72(9), 7583-8.

Rojo, G., Garcia-Beato, R., Vinuela, E., Salas, M.L. and Salas, J. (1999) Replication of African swine fever virus DNA in infected cells. Virology 257(2), 524-36.

Romero-Brey, I., Merz, A., Chiramel, A., Lee, J.Y., Chlanda, P., Haselman, U., Santarella-Mellwig, R., Habermann, A., Hoppe, S., Kallis, S., Walther, P., Antony, C., Krijnse-Locker, J. and Bartenschlager, R. (2012) Three-dimensional architecture and biogenesis of membrane structures associated with hepatitis C virus replication. PLoS Pathog 8(12), e1003056.

Rothberg, K.G., Heuser, J.E., Donzell, W.C., Ying, Y.S., Glenney, J.R. and Anderson, R.G. (1992) Caveolin, a protein component of caveolae membrane coats. Cell 68(4), 673-82.
Rothwell, C., Lebreton, A., Young Ng, C., Lim, J.Y., Liu, W., Vasudevan, S., Labow, M., Gu, F. and Gaither, L.A. (2009) Cholesterol biosynthesis modulation regulates dengue viral replication. Virology 389(1-2), 8-19.
Rouiller, I., Brookes, S.M., Hyatt, A.D., Windsor, M. and Wileman, T. (1998) African swine fever virus is wrapped by the endoplasmic reticulum. J Virol 72(3), 2373-87.
Rudge, S.A., Anderson, D.M. and Emr, S.D. (2004) Vacuole size control: regulation of PtdIns(3,5)P2 levels by the vacuole-associated Vac14-Fig4 complex, a PtdIns(3,5)P2-specific phosphatase. Mol Biol Cell 15(1), 24-36.
Rust, M.J., Lakadamyali, M., Zhang, F. and Zhuang, X. (2004) Assembly of endocytic machinery around individual influenza viruses during viral entry. Nat Struct Mol Biol 11(6), 567-73.
Rusten, T.E., Rodahl, L.M., Pattni, K., Englund, C., Samakovlis, C., Dove, S., Brech, A. and Stenmark, H. (2006) Fab1 phosphatidylinositol 3-phosphate 5-kinase controls trafficking but not silencing of endocytosed receptors. Mol Biol Cell 17(9), 3989-4001.
Sachse, M., Urbe, S., Oorschot, V., Strous, G.J. and Klumperman, J. (2002) Bilayered clathrin coats on endosomal vacuoles are involved in protein sorting toward lysosomes. Mol Biol Cell 13(4), 1313-28.
Salas, J., Salas, M.L. and Vinuela, E. (1988) Effect of inhibitors of the host cell RNA polymerase II on African swine fever virus multiplication. Virology 164(1), 280-3.
Salas, M.L., Kuznar, J. and Vinuela, E. (1981) Polyadenylation, methylation, and capping of the RNA synthesized in vitro by African swine fever virus. Virology 113(2), 484-91.
Salas, M.L., Kuznar, J. and Vinuela, E. (1983) Effect of rifamycin derivatives and coumermycin A1 on in vitro RNA synthesis by African swine fever virus. Brief report. Arch Virol 77(1), 77-80.
Salas, M.L., Rey-Campos, J., Almendral, J.M., Talavera, A. and Vinuela, E. (1986) Transcription and translation maps of African swine fever virus. Virology 152(1), 228-40.
Sanchez-Torres, C., Gomez-Puertas, P., Gomez-del-Moral, M., Alonso, F., Escribano, J.M., Ezquerra, A. and Dominguez, J. (2003) Expression of porcine CD163 on monocytes/macrophages correlates with permissiveness to African swine fever infection. Arch Virol 148(12), 2307-23.
Sanchez, E.G., Quintas, A., Perez-Nunez, D., Nogal, M., Barroso, S., Carrascosa, A.L. and Revilla, Y. (2012) African swine fever virus uses macropinocytosis to enter host cells. PLoS Pathog 8(6), e1002754.
Sapp, M. and Bienkowska-Haba, M. (2009) Viral entry mechanisms: human papillomavirus and a long journey from extracellular matrix to the nucleus. FEBS J 276(24), 7206-16.
Sbrissa, D., Ikonomov, O.C., Fenner, H. and Shisheva, A. (2008) ArPIKfyve homomeric and heteromeric interactions scaffold PIKfyve and Sac3 in a complex to promote PIKfyve activity and functionality. J Mol Biol 384(4), 766-79.
Sbrissa, D. and Shisheva, A. (2005) Acquisition of unprecedented phosphatidylinositol 3,5-bisphosphate rise in hyperosmotically stressed 3T3-L1 adipocytes, mediated by ArPIKfyve-PIKfyve pathway. J Biol Chem 280(9), 7883-9.
Schelhaas, M., Malmstrom, J., Pelkmans, L., Haugstetter, J., Ellgaard, L., Grunewald, K. and Helenius, A. (2007) Simian Virus 40 depends on ER protein folding and quality control factors for entry into host cells. Cell 131(3), 516-29.
Scherer, J. and Vallee, R.B. (2011) Adenovirus recruits dynein by an evolutionary novel mechanism involving direct binding to pH-primed hexon. Viruses 3(8), 1417-31.
Schmid, E.M. and McMahon, H.T. (2007) Integrating molecular and network biology to decode endocytosis. Nature 448(7156), 883-8.

Schmitt, L. and Tampe, R. (2002) Structure and mechanism of ABC transporters. Curr Opin Struct Biol 12(6), 754-60.
Sexton, R.C., Panini, S.R., Azran, F. and Rudney, H. (1983) Effects of 3 beta-[2-(diethylamino)ethoxy]androst-5-en-17-one on the synthesis of cholesterol and ubiquinone in rat intestinal epithelial cell cultures. Biochemistry 22(25), 5687-92.
Shen, D., Wang, X. and Xu, H. (2011) Pairing phosphoinositides with calcium ions in endolysosomal dynamics: phosphoinositides control the direction and specificity of membrane trafficking by regulating the activity of calcium channels in the endolysosomes. Bioessays 33(6), 448-57.
Shisheva, A. (2008) PIKfyve: Partners, significance, debates and paradoxes. Cell Biol Int 32(6), 591-604.
Sidorkiewicz, M., Jozwiak, B., Durys, B., Majda-Stanislawska, E., Piekarska, A., Kosciuk, N., Ciechowicz, J., Majewska, E. and Bartkowiak, J. (2009) Mevalonate pathway modulation is associated with hepatitis C virus RNA presence in peripheral blood mononuclear cells. Virus Res 145(1), 141-4.
Sieczkarski, S.B. and Whittaker, G.R. (2002) Influenza virus can enter and infect cells in the absence of clathrin-mediated endocytosis. J Virol 76(20), 10455-64.
Sieczkarski, S.B. and Whittaker, G.R. (2003) Differential requirements of Rab5 and Rab7 for endocytosis of influenza and other enveloped viruses. Traffic 4(5), 333-43.
Simon-Mateo, C., Andres, G., Almazan, F. and Vinuela, E. (1997) Proteolytic processing in African swine fever virus: evidence for a new structural polyprotein, pp62. J Virol 71(8), 5799-804.
Simon-Mateo, C., Andres, G. and Vinuela, E. (1993) Polyprotein processing in African swine fever virus: a novel gene expression strategy for a DNA virus. Embo J 12(7), 2977-87.
Sirena, D., Lilienfeld, B., Eisenhut, M., Kalin, S., Boucke, K., Beerli, R.R., Vogt, L., Ruedl, C., Bachmann, M.F., Greber, U.F. and Hemmi, S. (2004) The human membrane cofactor CD46 is a receptor for species B adenovirus serotype 3. J Virol 78(9), 4454-62.
Smit, J.M., Bittman, R. and Wilschut, J. (1999) Low-pH-dependent fusion of Sindbis virus with receptor-free cholesterol- and sphingolipid-containing liposomes. J Virol 73(10), 8476-84.
Smith, A.E. and Helenius, A. (2004) How viruses enter animal cells. Science 304(5668), 237-42.
Smith, G.A. and Enquist, L.W. (2002) Break ins and break outs: viral interactions with the cytoskeleton of Mammalian cells. Annu Rev Cell Dev Biol 18, 135-61.
Smith, J.L., Campos, S.K. and Ozbun, M.A. (2007) Human papillomavirus type 31 uses a caveolin 1- and dynamin 2-mediated entry pathway for infection of human keratinocytes. J Virol 81(18), 9922-31.
Snyers, L., Zwickl, H. and Blaas, D. (2003) Human rhinovirus type 2 is internalized by clathrin-mediated endocytosis. J Virol 77(9), 5360-9.
Sobo, K., Le Blanc, I., Luyet, P.P., Fivaz, M., Ferguson, C., Parton, R.G., Gruenberg, J. and van der Goot, F.G. (2007) Late endosomal cholesterol accumulation leads to impaired intra-endosomal trafficking. PLoS ONE 2(9), e851.
Sodeik, B. (2000) Mechanisms of viral transport in the cytoplasm. Trends Microbiol 8(10), 465-72.
Sorkin, A. (2004) Cargo recognition during clathrin-mediated endocytosis: a team effort. Curr Opin Cell Biol 16(4), 392-9.
Steele-Mortimer, O., Meresse, S., Gorvel, J.P., Toh, B.H. and Finlay, B.B. (1999) Biogenesis of Salmonella typhimurium-containing vacuoles in epithelial cells involves interactions with the early endocytic pathway. Cell Microbiol 1(1), 33-49.
Stefanovic, S., Windsor, M., Nagata, K.I., Inagaki, M. and Wileman, T. (2005) Vimentin rearrangement during African swine fever virus infection involves retrograde transport along microtubules and phosphorylation of vimentin by calcium calmodulin kinase II. J Virol 79(18), 11766-75.

Stein, M.P., Feng, Y., Cooper, K.L., Welford, A.M. and Wandinger-Ness, A. (2003) Human VPS34 and p150 are Rab7 interacting partners. Traffic 4(11), 754-71.
Stenmark, H. (2009) Rab GTPases as coordinators of vesicle traffic. Nat Rev Mol Cell Biol 10(8), 513-25.
Stuart, A.D. and Brown, T.D. (2006) Entry of feline calicivirus is dependent on clathrin-mediated endocytosis and acidification in endosomes. J Virol 80(15), 7500-9.
Sturley, S.L., Patterson, M.C., Balch, W. and Liscum, L. (2004) The pathophysiology and mechanisms of NP-C disease. Biochim Biophys Acta 1685(1-3), 83-7.
Subramanian, K. and Balch, W.E. (2008) NPC1/NPC2 function as a tag team duo to mobilize cholesterol. Proc Natl Acad Sci U S A 105(40), 15223-4.
Suikkanen, S., Antila, M., Jaatinen, A., Vihinen-Ranta, M. and Vuento, M. (2003) Release of canine parvovirus from endocytic vesicles. Virology 316(2), 267-80.
Sun, X., Yau, V.K., Briggs, B.J. and Whittaker, G.R. (2005) Role of clathrin-mediated endocytosis during vesicular stomatitis virus entry into host cells. Virology 338(1), 53-60.
Syed, G.H., Amako, Y. and Siddiqui, A. (2010) Hepatitis C virus hijacks host lipid metabolism. Trends Endocrinol Metab 21(1), 33-40.
Tabares, E. and Sanchez Botija, C. (1979) Synthesis of DNA in cells infected with African swine fever virus. Arch Virol 61(1-2), 49-59.
Taksir, T.V., Johnson, J., Maloney, C.L., Yandl, E., Griffiths, D., Thurberg, B.L. and Ryan, S. (2012) Optimization of a histopathological biomarker for sphingomyelin accumulation in acid sphingomyelinase deficiency. J Histochem Cytochem 60(8), 620-9.
Taylor, M.J., Lampe, M. and Merrifield, C.J. (2012) A Feedback Loop between Dynamin and Actin Recruitment during Clathrin-Mediated Endocytosis. PLoS Biol 10(4), e1001302.
Taylor, M.J., Perrais, D. and Merrifield, C.J. (2011) A high precision survey of the molecular dynamics of mammalian clathrin-mediated endocytosis. PLoS Biol 9(3), e1000604.
Teo, H., Gill, D.J., Sun, J., Perisic, O., Veprintsev, D.B., Vallis, Y., Emr, S.D. and Williams, R.L. (2006) ESCRT-I core and ESCRT-II GLUE domain structures reveal role for GLUE in linking to ESCRT-I and membranes. Cell 125(1), 99-111.
Teodoro, J.G. and Branton, P.E. (1997) Regulation of apoptosis by viral gene products. J Virol 71(3), 1739-46.
Thomson, G.R. (1985) The epidemiology of African swine fever: the role of free-living hosts in Africa. Onderstepoort J Vet Res 52(3), 201-9.
Thomson, G.R., Gainaru, M.D. and Van Dellen, A.F. (1980) Experimental infection of warthos (Phacochoerus aethiopicus) with African swine fever virus. Onderstepoort J Vet Res 47(1), 19-22.
Thorley, J.A., McKeating, J.A. and Rappoport, J.Z. (2010) Mechanisms of viral entry: sneaking in the front door. Protoplasma 244(1-4), 15-24.
Toei, M., Saum, R. and Forgac, M. (2010) Regulation and isoform function of the V-ATPases. Biochemistry 49(23), 4715-23.
Townsley, A.C., Weisberg, A.S., Wagenaar, T.R. and Moss, B. (2006) Vaccinia virus entry into cells via a low-pH-dependent endosomal pathway. J Virol 80(18), 8899-908.
Traub, L.M. (2009) Tickets to ride: selecting cargo for clathrin-regulated internalization. Nat Rev Mol Cell Biol 10(9), 583-96.
Trombetta, E.S. and Mellman, I. (2005) Cell biology of antigen processing in vitro and in vivo. Annu Rev Immunol 23, 975-1028.
Tsai, B. (2007) Penetration of nonenveloped viruses into the cytoplasm. Annu Rev Cell Dev Biol 23, 23-43.
Umata, T., Moriyama, Y., Futai, M. and Mekada, E. (1990) The cytotoxic action of diphtheria toxin and its degradation in intact Vero cells are inhibited by bafilomycin A1, a specific inhibitor of vacuolar-type H(+)-ATPase. J Biol Chem 265(35), 21940-5.

Valdeira, M.L., Bernardes, C., Cruz, B. and Geraldes, A. (1998) Entry of African swine fever virus into Vero cells and uncoating. Vet Microbiol 60(2-4), 131-40.
Valdeira, M.L. and Geraldes, A. (1985) Morphological study on the entry of African swine fever virus into cells. Biol Cell 55(1-2), 35-40.
Van Aelst, L. and D'Souza-Schorey, C. (1997) Rho GTPases and signaling networks. Genes Dev 11(18), 2295-322.
van der Goot, F.G. and Gruenberg, J. (2006) Intra-endosomal membrane traffic. Trends Cell Biol 16(10), 514-21.
van der Schaar, H.M., Rust, M.J., Chen, C., van der Ende-Metselaar, H., Wilschut, J., Zhuang, X. and Smit, J.M. (2008) Dissecting the cell entry pathway of dengue virus by single-particle tracking in living cells. PLoS Pathog 4(12), e1000244.
Vazquez-Calvo, A., Saiz, J.C., McCullough, K.C., Sobrino, F. and Martin-Acebes, M.A. (2012) Acid-dependent viral entry. Virus Res 167(2), 125-37.
Veiga, E. and Cossart, P. (2005) Listeria hijacks the clathrin-dependent endocytic machinery to invade mammalian cells. Nat Cell Biol 7(9), 894-900.
Vicinanza, M., D'Angelo, G., Di Campli, A. and De Matteis, M.A. (2008) Function and dysfunction of the PI system in membrane trafficking. Embo J 27(19), 2457-70.
Vitelli, R., Santillo, M., Lattero, D., Chiariello, M., Bifulco, M., Bruni, C.B. and Bucci, C. (1997) Role of the small GTPase Rab7 in the late endocytic pathway. J Biol Chem 272(7), 4391-7.
Vitner, E.B., Dekel, H., Zigdon, H., Shachar, T., Farfel-Becker, T., Eilam, R., Karlsson, S. and Futerman, A.H. (2010a) Altered expression and distribution of cathepsins in neuronopathic forms of Gaucher disease and in other sphingolipidoses. Hum Mol Genet 19(18), 3583-90.
Vitner, E.B., Platt, F.M. and Futerman, A.H. (2010b) Common and uncommon pathogenic cascades in lysosomal storage diseases. J Biol Chem 285(27), 20423-7.
Vonderheit, A. and Helenius, A. (2005) Rab7 associates with early endosomes to mediate sorting and transport of Semliki forest virus to late endosomes. PLoS Biol 3(7), e233.
White, J., Kartenbeck, J. and Helenius, A. (1980) Fusion of Semliki forest virus with the plasma membrane can be induced by low pH. J Cell Biol 87(1), 264-72.
White, J., Matlin, K. and Helenius, A. (1981) Cell fusion by Semliki Forest, influenza, and vesicular stomatitis viruses. J Cell Biol 89(3), 674-9.
Whitley, P., Reaves, B.J., Hashimoto, M., Riley, A.M., Potter, B.V. and Holman, G.D. (2003) Identification of mammalian Vps24p as an effector of phosphatidylinositol 3,5-bisphosphate-dependent endosome compartmentalization. J Biol Chem 278(40), 38786-95.
Wickham, T.J., Mathias, P., Cheresh, D.A. and Nemerow, G.R. (1993) Integrins alpha v beta 3 and alpha v beta 5 promote adenovirus internalization but not virus attachment. Cell 73(2), 309-19.
Yanez, R.J., Rodriguez, J.M., Nogal, M.L., Yuste, L., Enriquez, C., Rodriguez, J.F. and Vinuela, E. (1995) Analysis of the complete nucleotide sequence of African swine fever virus. Virology 208(1), 249-78.
Yoshimori, T., Yamamoto, A., Moriyama, Y., Futai, M. and Tashiro, Y. (1991) Bafilomycin A1, a specific inhibitor of vacuolar-type H(+)-ATPase, inhibits acidification and protein degradation in lysosomes of cultured cells. J Biol Chem 266(26), 17707-12.
Zaitseva, E., Yang, S.T., Melikov, K., Pourmal, S. and Chernomordik, L.V. (2010) Dengue virus ensures its fusion in late endosomes using compartment-specific lipids. PLoS Pathog 6(10), e1001131.
Zerial, M. and McBride, H. (2001) Rab proteins as membrane organizers. Nat Rev Mol Cell Biol 2(2), 107-17.
Zhang, F., Moon, A., Childs, K., Goodbourn, S. and Dixon, L.K. (2010) The African swine fever virus DP71L protein recruits the protein phosphatase 1 catalytic subunit to

dephosphorylate eIF2alpha and inhibits CHOP induction but is dispensable for these activities during virus infection. J Virol 84(20), 10681-9.
Zsak, L., Lu, Z., Burrage, T.G., Neilan, J.G., Kutish, G.F., Moore, D.M. and Rock, D.L. (2001a) African swine fever virus multigene family 360 and 530 genes are novel macrophage host range determinants. J Virol 75(7), 3066-76.
Zsak, L., Lu, Z., Kutish, G.F., Neilan, J.G. and Rock, D.L. (1996) An African swine fever virus virulence-associated gene NL-S with similarity to the herpes simplex virus ICP34.5 gene. J Virol 70(12), 8865-71.
Zsak, L., Sur, J.H., Burrage, T.G., Neilan, J.G. and Rock, D.L. (2001b) African Swine Fever virus (asfv) multigene families 360 and 530 genes promote infected macrophage survival. ScientificWorldJournal 1(1 Suppl 3), 97.

Anexo

CITOTOXICIDAD DE LOS DIFERENTES INHIBIDORES UTILIZADOS

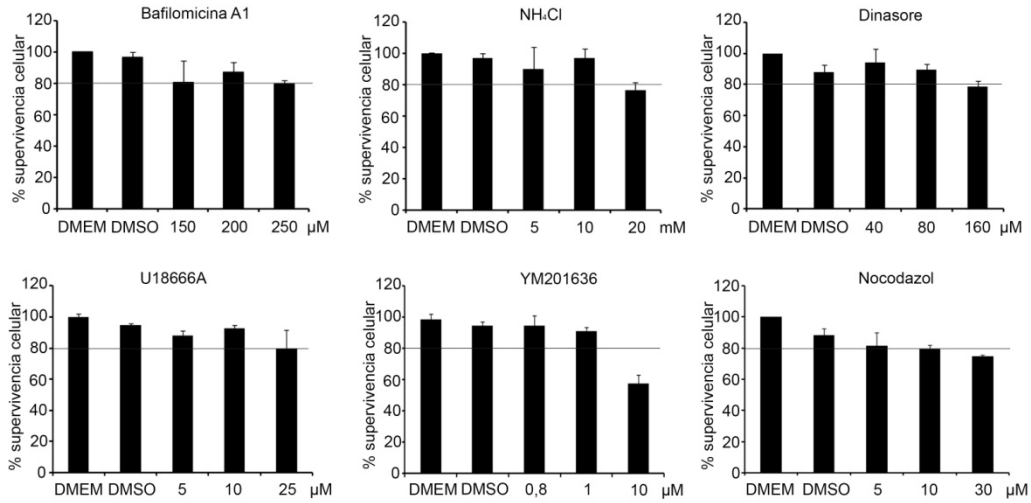

PUBLICACIONES A LAS QUE HA DADO LUGAR ESTA TESIS DOCTORAL

OPEN ACCESS Freely available online

PLOS ONE

Endosomal Maturation, Rab7 GTPase and Phosphoinositides in African Swine Fever Virus Entry

Miguel A. Cuesta-Geijo, Inmaculada Galindo, Bruno Hernáez, Jose Ignacio Quetglas, Inmaculada Dalmau-Mena, Covadonga Alonso*

Departamento de Biotecnologia, Instituto Nacional de Investigacion y Tecnologia Agraria y Alimentaria (INIA), Madrid, Spain

Abstract

Here we analyzed the dependence of African swine fever virus (ASFV) infection on the integrity of the endosomal pathway. Using confocal immunofluorescence with antibodies against viral capsid proteins, we found colocalization of incoming viral particles with early endosomes (EE) during the first minutes of infection. Conversely, viral capsid protein was not detected in acidic late endosomal compartments, multivesicular bodies (MVBs), late endosomes (LEs) or lysosomes (LY). Using an antibody against a viral inner core protein, we found colocalization of viral cores with late compartments from 30 to 60 minutes postinfection. The absence of capsid protein staining in LEs and LYs suggested that virus desencapsidation would take place at the acid pH of these organelles. In fact, inhibitors of intraluminal acidification of endosomes caused retention of viral capsid staining virions in Rab7 expressing endosomes and more importantly, severely impaired subsequent viral protein production. Endosomal acidification in the first hour after virus entry was essential for successful infection but not thereafter. In addition, altering the balance of phosphoinositides (PIs) which are responsible of the maintenance of the endocytic pathway impaired ASFV infection. Early infection steps were dependent on the production of phosphatidylinositol 3-phosphate (PtdIns3P) which is involved in EE maturation and multivesicular body (MVB) biogenesis and on the interconversion of PtdIns3P to phosphatidylinositol 3, 5-biphosphate (PtdIns(3,5)P_2). Likewise, GTPase Rab7 activity should remain intact, as well as processes related to LE compartment physiology, which are crucial during early infection. Our data demonstrate that the EE and LE compartments and the integrity of the endosomal maturation pathway orchestrated by Rab proteins and PIs play a central role during early stages of ASFV infection.

Citation: Cuesta-Geijo MA, Galindo I, Hernáez B, Quetglas JI, Dalmau-Mena I, et al. (2012) Endosomal Maturation, Rab7 GTPase and Phosphoinositides in African Swine Fever Virus Entry. PLoS ONE 7(11): e48853. doi:10.1371/journal.pone.0048853

Editor: Jieru Wang, National Jewish Health, United States of America

Received May 5, 2012; **Accepted** October 2, 2012; **Published** November 1, 2012

Funding: The present work was supported by grants from the Welcome Trust Foundation WT075813, UE EPIZONE FOOD-CT2006-016236 and from the Ministerio de Economia y Competitividad of Spain Consolider CSD2006-00007, AGL2009-09209 and AGL2012-34533. The funders had no role in study design, data collection and analysis, decision to publish, or preparation of the manuscript.

Competing Interests: The authors have declared that no competing interests exist.

* E-mail: calonso@inia.es

Introduction

Many animal viruses have evolved to exploit endocytosis to enter host cells after initial attachment of virions to specific cell surface receptors. African swine fever virus (ASFV), the only known member of the *Asfarviridae* family, is a nucleo-cytoplasmic double-stranded DNA enveloped virus [1]. ASFV particles, with an overall icosahedral shape and an average diameter of 200 nm, are composed of several concentric domains: an internal core consisting of a central DNA-containing nucleoid coated by a thick protein layer referred to as core shell, an inner lipid envelope, and an icosahedral protein capsid [2,3,4]. The extracellular virions usually contain an additional external membrane acquired by budding from the plasma membrane [5] and both intracellular and extracellular mature virions are infectious [6,7]. The viral capsid that surrounds the internal membrane is composed by the major viral capsid protein p72 and protein pE120R [1]. The core shell protein composition consists in a 220 kDa protein that is cleaved to give four structural proteins (p150, p37, p14 and p34) and the two products of a 62 kDa protein [8]. Also, two DNA binding proteins, pA78R and p10 are found in virions. Early mRNA synthesis begins in the cytoplasm immediately after virus entry and is regulated by enzymes and factors packaged in the virus core. Virus DNA replication starts at 6 hours postinfection (hpi) and assembly takes place in perinuclear factory areas [1]. Early genes are expressed prior to DNA replication but some early genes continue to be synthesized throughout infection (e.g. p30 protein encoding gene). The expression of late genes takes place after viral DNA replication. Several structural proteins accumulate in viral factories where virus morphogenesis takes place (p.e. structural proteins p54, major capsid protein p72, etc.) [6,7]. Most of these studies on viral cycle characterization were performed in the Vero cell line infected with the cell culture adapted isolate ASFV BA71.

Using this model, early studies on ASFV entry demonstrated that the internalization of viral particles is a temperature-, energy-, and low pH-dependent process, since it is inhibited at 4°C and in the presence of inhibitors of cellular respiration or lysosomotropic agents [9,10]. More recent analysis of major endocytic routes for cell entry indicate that the ASFV moves into Vero cells by clathrin-mediated endocytosis, which requires the activity of the GTPase dynamin [11]. All these features are consistent with a receptor-mediated endocytosis mechanism of entry. Also, the presence of cholesterol in cellular membranes, but not lipid rafts or caveolae, was found to be essential for productive ASFV infection

during initial stages. Alternative pathways of entry, such as macropinocytosis have been proposed for cells of the monocyte/macrophage lineage [12] however, these studies encounter the problem that these cells have a heterogeneous surface marker profile and only restricted macrophage subpopulations are susceptible to ASFV [13,14,15]. Given that macropinocytosis would also drive to the endocytic pathway at some stage [16], we focused this work on further steps in endocytosis that remain unexplored.

Once a virus has entered the endocytic pathway, it must temporally and physiologically pass through distinct endosome populations to achieve successful infection; however, it is still unknown whether ASFV follows this pathway. Early endosomes (EEs) generally serve as sorting vesicles for incoming ligands, such as epidermal growth factor (EGF) or transferrin. The mode of entry of these ligands by clathrin-mediated endocytosis is very fast and efficient and recruitment of the necessary molecules to clathrin vesicle scission have been determined to occur within a 30–100 seconds (s) time frame [17,18]. EEs can progress to recycling endosomes (REs), which deliver endocytosed material back to the cell surface, or progress and mature to late endosomes (LEs). LEs have a significantly lower pH compared to that of EEs [19] and may fuse with lysosomes (LYs) for degradation. Multivesicular bodies (MVBs) form through invagination of small intraluminal vesicles (ILVs) and thus EE become MVBs. The development of these vessels requires the endosome-specific lipid phosphatidylinositol 3-phosphate (PtdIns3P) [20]. As EEs undergo maturation, the lumen (pH of 6.5) is gradually acidified to reach a pH of 6–5 in MVBs and mature to Rab7-expressing LEs. After the fusion of LEs with LYs, which are characterized by Lamp1 expression, a pH of 5–4.5 is reached.

Endosome maturation requires a coordinated function of lipids and proteins in membrane bending, elongation and fission processes. These cellular factors are hallmarks of the steps followed by viruses to traffic through the cytoplasm. Members of the Rab family of small GTPases are regulators of the host endocytic pathway and each Rab member localizes to a specific compartment [21]. By interacting with one or more effector proteins, Rab proteins create membrane subdomains to regulate specific downstream functions, such as membrane transport and fusion by recruiting tethering and docking factors [22]. Rab5 regulates fusion between EEs and the motility of these compartments along microtubules. In contrast, Rab7 acts more downstream in the endocytic pathway and, it controls transport to LEs and regulates the transport of and fusion between LEs and LYs [23].

Regulation of the endosomal pathway by Rab GTPases is achieved in coordination with the lipid composition of the endosomal membrane in phosphoinositides (PIs). This regulates the traffic and maturation of the endosome since these molecules allow the specific incorporation of binding proteins to a given membrane. PIs, which are the phosphorylated forms of phosphatidylinositol (PtdIns) are tightly regulated both spatially and temporally through the many phosphoinositide kinases (PIKs) and phosphatases by rapid metabolic interconversions. The regulatory actions of PIs in many cellular functions are the result of their capacity to control the subcellular localization and activation of various effector proteins that carry PI-binding domains, such as the PH (Pleckstrin homology), FYVE (Fab1p, YOTB, Vac1 and EEA1), and PX (Phox homology) domains [24,25]. All these cellular factors may be required for virus traffic through the endocytic pathway.

Viruses have evolved to exploit the endocytic pathway for cell entry and transport. Members of subgroup B of Adenovirus (Ad), serotypes 3 and 7, have relatively long residence times inside endosomes. The endosomal pathway was identified as the route used by Ad7, as virions were observed to colocalize with LE and LY marker proteins, including Rab7 and Lamp1, during viral entry and before viral egress from this compartment [26]. Despite trafficking through this pathway, Ad7 escapes degradation in these organelles. This virus traffics through the low lysosomal pH and the Ad fiber protein confers the property of low pH escape of the Ad7 capsid to the cytoplasm. Colocalization studies of the influenza virus using defined endosomal markers and Rab mutants, confirmed the traffic of this virus through EEs and LEs at distinct times during infection. The HA glycoprotein of the influenza virus has been described to undergo membrane fusion at a pH of 5.5. Analysis with conformation-specific antibodies against HA indicates that the fusion peptide is not exposed until late in entry, approximately at the time when virus is concentrated in LEs [27].

Here we studied the endocytosis of ASFV as it traffics through the cytoplasm during early infection. ASFV required functional EEs and LEs during early steps for successful infection, together with Rab5 and Rab7 GTPases – master regulators of the endocytic pathway – and membrane PI signaling. We analyzed the temporal passage of the virus through the different endosomal compartments and studied the impact of endosome maturation processes on ASFV entry into the host cell.

Results

Relevance of endosomal compartments during ASFV infection

To study how ASFV gains access to the host cell through the endocytic pathway, we examined the virus association with early and late endosomal compartments as it traffics to reach its replication site at the microtubule organizing center (MTOC). The colocalization of ASFV proteins detected in virions such as p72 major capsid protein and pE120R with endosome markers was analyzed by confocal immunomicroscopy of fixed cells.

Vero cells were infected with ASFV BA71V isolate at a multiplicity of infection (moi) of 10 pfu/cell. This experiment was performed at a high moi in order to visualize several viral particles per cell. After virus adsorption at 4°C for 90 min, medium was replaced by warm medium at 37°C, and cells were then fixed at the indicated time points starting from 1 min post-infection (mpi) to 60 mpi. To detect EEs, MVBs, LEs and LYs, we used antibodies against EEA1, CD63, Rab7 and Lamp1, respectively (Fig. 1 left panel). Confocal microscopy analysis of cells infected with ASFV showed increasing colocalization of viral capsid protein with EEA1 from 1 to 30 mpi, to decrease thereafter (Fig. 1 A, E). In contrast, p72/pE120R viral capsid proteins showed a very low colocalization level with CD63, Rab7 and Lamp1 (Fig. 1 B–E). The absence of capsid protein staining in late endosomes and lysosomes suggested that desencapsidation of virions could occur at the acid pH of these compartments. Then, we labeled virions with an antibody against p150 viral core protein. Staining for inner viral core protein p150 corresponding to desencapsidated virions, was found in over 60% Rab7 positive endosomes at 45 min after infection (Fig. 1 F, G and G1–4). In contrast, viral core protein colocalization was reduced to ca. 15% with Lamp1 between 30–60 mpi (Fig. 1 H). This fact, could suggest that the virus uncoating and egress to the cytosol occurred rapidly from LEs and few viral cores colocalized with lysosomes expressing Lamp1.

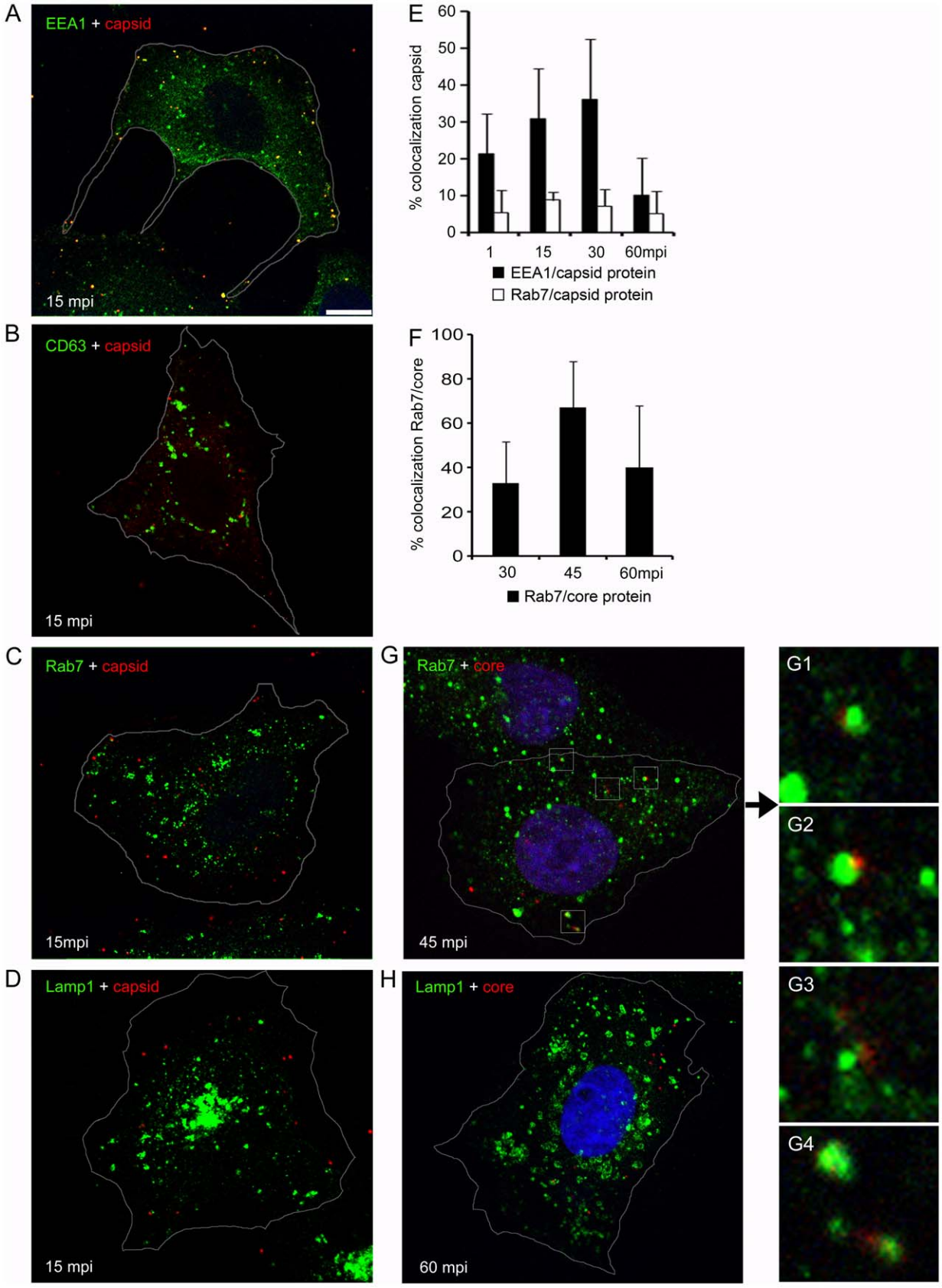

Figure 1. Viral colocalization with endosomes at early infection. Representative confocal micrographs of Vero cells infected with ASFV and immunostained for viral capsid proteins p72 and pE120R (shown in red), and in green, EE marker EEA1 (**A**), MVB marker CD63 (**B**), LE marker Rab7 (**C**) and LY marker Lamp1 (**D**) at 15 minutes postinfection (mpi). Scale bars, 10 μm. Cells were infected at a moi of 10 pfu/cell and adsorption was

maintained at 4°C for 90 min. Unbound virus was then washed, cells were shifted to 37°C and infection was allowed to progress for indicated times. (**E**) Percentages of colocalization events of p72 capsid protein with EE or LE marker are expressed as means and relativized to the total cell-associated virus particles per individual cell at each time point in 10 cells in duplicates. (**F**) Percentages of colocalization events of p150 inner core protein with LE marker expressed as means and relativized to the total cell-associated virus particles per individual cell at each time point in 10 cells in duplicates. (**G**) Representative confocal micrograph of the colocalization of viral cores with Rab7 positive endosomes. Nuclei were stained with TOPRO3. (**G1–4**) Detail of colocalization between viral cores and LE in high magnification of the boxed areas in (G). (**H**) Colocalization of viral core protein p150 with Lamp1 marker.
doi:10.1371/journal.pone.0048853.g001

Low intraluminal pH and Endocytosis are required for ASFV infectivity

To study the possibility that the virus desencapsidation occurred at the acid pH of LEs, we analyzed the effects of inhibitors known to raise the luminal pH of endosomes. As EEs undergo maturation, the lumen (pH of 6.5) is gradually acidified to reach a pH of 6–5 in MVBs and mature to Rab7-expressing LEs. After the fusion of LEs with LYs, which are characterized by Lamp1 expression, a pH of 5–4.5. The acidic pH of the late compartment stages of the endosomal pathway in contrast to EEs was shown in Vero cells using a pH sensitive dye (lysotracker; Fig. S1 A–D). The vacuolar ATPase (V-ATPase) is required for acidifying endosomes and LYs [28]. Treatment of Vero cells with V-ATPase inhibitor bafilomycin A1 (Baf) caused a rapid alkalinization of these organelles as monitored with the pH sensitive dye which resulted in a rapid reduction in lysotracker fluorescence (Fig. 2 A).

The inhibition of acidification would thus impair viral particles uncoating in LEs and could eventually stop further progress of viral infection. Nevertheless, the presence of viral particles in the cytoplasm could not be representative of their capacity to pursue a successful infection. Hence, in order to evaluate the actual impact on a productive infection we addressed the following infection step corresponding to early viral protein synthesis.

We treated cells with 200 nM Baf to inhibit endosome acidification. Cells were infected at 1 pfu/cell and after a brief adsorption period (90 min) at 4°C, medium was replaced and temperature was shifted to 37°C (time 0). Thereafter, a pulse of acid pH medium at 5.4 for 1 h was performed when indicated, followed by washing. Infection was then allowed to proceed for 6 hpi with medium at pH 7.4. Then, acid pH pulsed, Baf treated and control cells were collected and early protein p30 expression was evaluated by Western blot and flow cytometry. P30 is a viral protein that is expressed early post infection and during the complete viral cycle. Under Baf treatment, early protein expression decreased indicating the relevance of the intraluminal low pH and this effect could not be reversed by weak acid treatment of the cells (Fig. 2 B, D).

Conversely, we assayed whether acid pH could allow infection in absence of endocytosis. ASFV was allowed to adsorb to Vero cells in presence of dynamin inhibitor dynasore (Dyn) at 80 μM concentration and then medium was replaced with medium at pH 5.4 (1 h acid pH pulse) or pH 7.4 and dimethyl sulfoxide (DMSO) control. After 6 hpi, cells were collected and early protein p30 expression evaluated by western blot and flow cytometry (Fig. 2 C and E, respectively). Acid media conditions did not allow infectivity recovery in the presence of endocytosis inhibitor Dyn.

Time-dependent effect of lysosomotropic drugs on ASFV infectivity

In order to address the temporal relevance of low endosomal pH, we treated cells with NH_4Cl at 10 mM concentration or 200 nM Baf to inhibit endosome acidification at several post-infection times. Blockage of acidification within the first hour of infection had a strong negative impact on early viral protein synthesis, as shown by p30 expression using both drug inhibitors (Fig. 3 A). Conversely, when added at later times (3 hpi), both Baf- and NH_4Cl-treated cells produced p30 levels similar to control cells. Taken together, these results suggest that luminal endosomal acidification is a major determinant for allowing the virus to gain entry to the cytosol. LE passage would be required for ASFV uncoating and the low pH in this endosomal compartment resulted necessary within the first hour of infection when ASFV desencapsidation and viral egress take place.

The next question was whether endosomal acidification inhibition resulted in a demonstrable observation of viral capsid protein p72 in LEs, as would be expected from the inhibition of virus desencapsidation and release from this compartment. For this purpose, we examined the association of viral particles with LE marker Rab7 in these inhibitory acidic conditions. To this end, cells were treated for 20 min with 200 nM of Baf and then infected at 10 pfu/cell, after an adsorption period of 90 min at 4°C. Medium was then replaced with fresh medium containing Baf at 37°C, and these cells were compared with untreated infected cells in the same conditions. Infections were allowed to progress for 3 h in the presence of this agent. Cells were then fixed, immunolabeled with anti-Rab7 and anti-p72 and then analyzed using confocal microscopy.

Colocalization events between p72 and Rab7 increased significantly under inhibited acidification as shown at a higher magnification of Rab7-positive vesicles and associated viral particles (Fig. 3 B). Percentages of virions colocalizing with Rab7 per cell in control and in Baf-treated conditions are shown in graphics (Fig. 3 C). Increased percentages of p72 colocalization events with Rab7 when acidification was inhibited, strongly suggest that virion desencapsidation was blocked in a Rab7 staining LE compartment. Taken together, these observations are consistent with the notion that ASFV uses the endosomal pathway for infection and that an increase in the pH of acidic organelles can cause infection blockage, as shown by the retention of encapsidated viral particles in LEs in Baf-treated cells. These results would support that virus uncoating occurs through a transient step from the LE compartment.

These observations pointed to a crucial role of the LE compartment during the viral uncoating and egress from the endosome.

Relevance of the late endosome compartment in ASFV infection

The relevance of the LE compartment in infection was further evaluated on infectivity and viral protein expression by transient expression of Rab7 dominant negative (DN) mutant (GFP-Rab7 DN; T22N) in COS-7 cells 24 h after transfection. This cell line was used in this experiment because it shows higher transfection efficiency than Vero cells.

Fluorescence-expressing cells were then sorted and isolated for subsequent infection, which was allowed to progress to complete viral cycle at 24 hpi. At this time point infected cells show a characteristic viral factory at the MTOC where viral proteins and viral DNA accumulate for the assembly of newly formed virions. Fig. 4 A shows the percentages of sorted transfected cells.

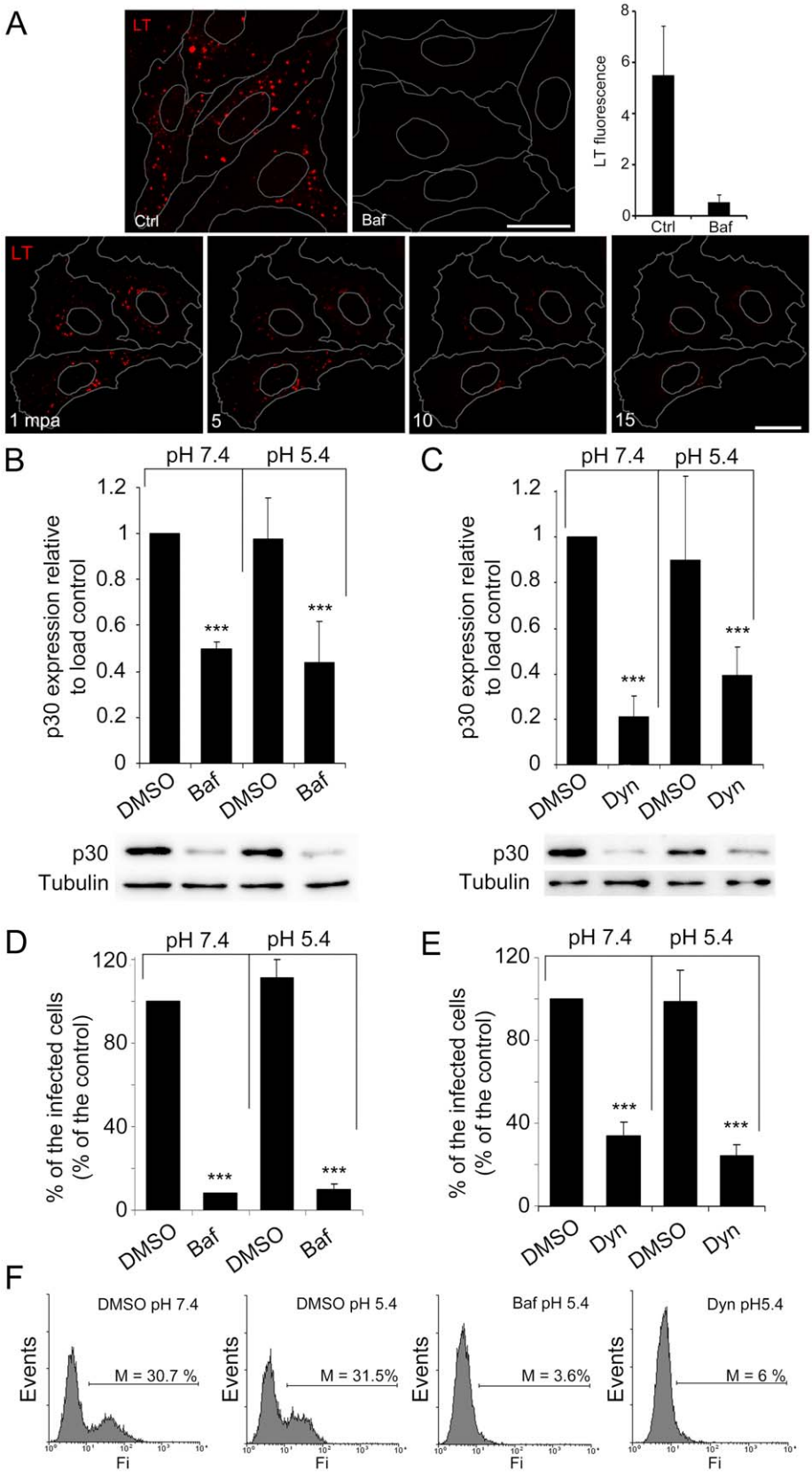

Figure 2. Low intraluminal pH and Endocytosis are required for ASFV infectivity. (**A**) Inhibition of intraluminal acidification of endosomes by Baf in a time dependent manner is shown using the pH sensitive dye lysotracker red. Bar 25 μm; mpa: minutes after Baf addition. (**B–E**) Inhibition of intraluminal acidification of endosomes with Baf and inhibition of endocytosis with Dyn impaired virus infectivity and neither Baf nor Dyn inhibition of early infection could be recovered with acid pH medium. (**B**) Early viral protein p30 expression in cells pretreated with 200 nM Baf or

DMSO and pulsed for 1 h with ph 5.4 medium postadsorption or maintained at pH 7.4 for 6 hpi. Western blot with specific antibodies was quantified and normalized to protein load control values. Low early viral protein expression with Baf was not recovered by acid pH medium treatment. (**C**) Quantification of viral protein p30 expression at 6 hpi as determined by Western blot in cells pretreated with 80 μM Dyn or DMSO and maintained in presence of medium at pH 7.4 or pulsed at pH 5.4 for 1 h post-adsorption. (**D**) Flow cytometry of Vero cells pretreated with Baf and infected in medium at pH 7.4 or pulsed at pH 5.4 for 1 h post-adsorption. Infected cells were then detected by FACS and data normalized to infection rates in DMSO treated cells. (**E**) Flow cytometry of Vero cells pretreated with Dyn and infected in medium at pH 7.4 or pulsed at pH 5.4 for 1 h. Asterisks denote sadistically significant differences (*** $P<0.001$). (**F**) Representative FACS profiles obtained during the analysis are shown.
doi:10.1371/journal.pone.0048853.g002

Indirect immunofluorescence assay revealed that, from total counts of 400 cells per experiment, the infected cell number detected with a mouse monoclonal anti-p72 decreased from 43.5% for Rab7 WT-expressing cells to 1.65% for cells transfected with Rab7 DN plasmid (Fig. 4 B left and right panel, respectively).

Indirect fluorescent immunoassays (IFI) demonstrated that the expression of Rab7 DN decreased infectivity. Taken together, these data indicate that ASFV requires functional LE trafficking for infection, thereby suggesting that this step is necessary for successful viral infection. We propose that the LE environment provides the correct pH for ASFV uncoating and virus egress from the endosome to the cytosol.

ASFV entry depends on endosomal membrane phosphoinositides

PIs are required for the maturation of endosomes as they progress along the endosomal pathway. To further study the relevance of the endocytic pathway in viral traffic, we then analyzed the role of endosomal membrane PIs. There are two main PIs involved in the regulation of the endosomes, PtdIns3P and phosphatidylinositol 3, 5 bisphosphate (PtdIns(3,5)P_2).

PtdIns3P itself and most if not all PtdIns3P-binding proteins that have been characterized, are present on early endosomes. Examples of those are the Rab5 effectors such as EEA1. PtdIns3P is found in a complex with Rab5 and EEA1, and the latter bridges the complex by binding PtdIns3P directly through its FYVE domain and Rab5 through its Rab5-binding domain. PtdIns3P therefore plays a fundamental role in endosomal trafficking as the

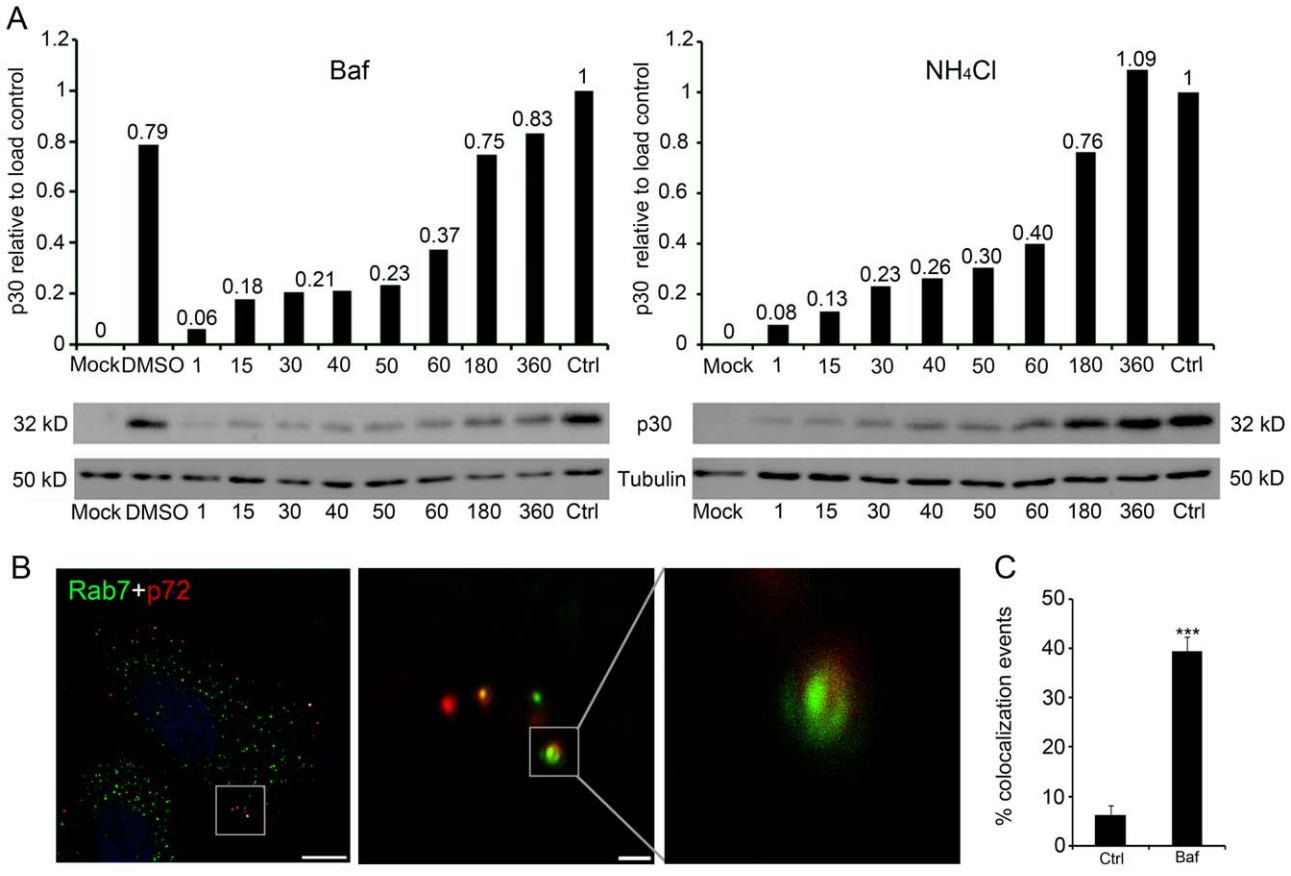

Figure 3. Acid pH of the late endosome is required at early stages of ASFV infection. (**A**) Early viral protein p30 expression determined at 8 hpi by Western blotting with specific antibodies, quantified and normalized to protein load control values. Acid pH requirement was evidenced by the effect of lysosomotropic drug addition at any time point within the first hpi but not thereafter. (**B**) Representative confocal micrograph of Baf-pretreated cells fixed after 3 hpi and immunostained for major viral capsid protein p72 (red) and LE marker Rab7 (green); Bar 10 μm. Detail of colocalization between viral capsids and LEs in Baf-treated cells; Insets are magnifications of the boxed areas in the previous image, bar 1 μm. (**C**) Quantification of colocalization events relativized to the total number of cell-associated virions per individual cell, performed in 130 virions and expressed as means and standard deviations from two independent experiments. Asterisks denote statistically significant differences (***$P<0.001$).
doi:10.1371/journal.pone.0048853.g003

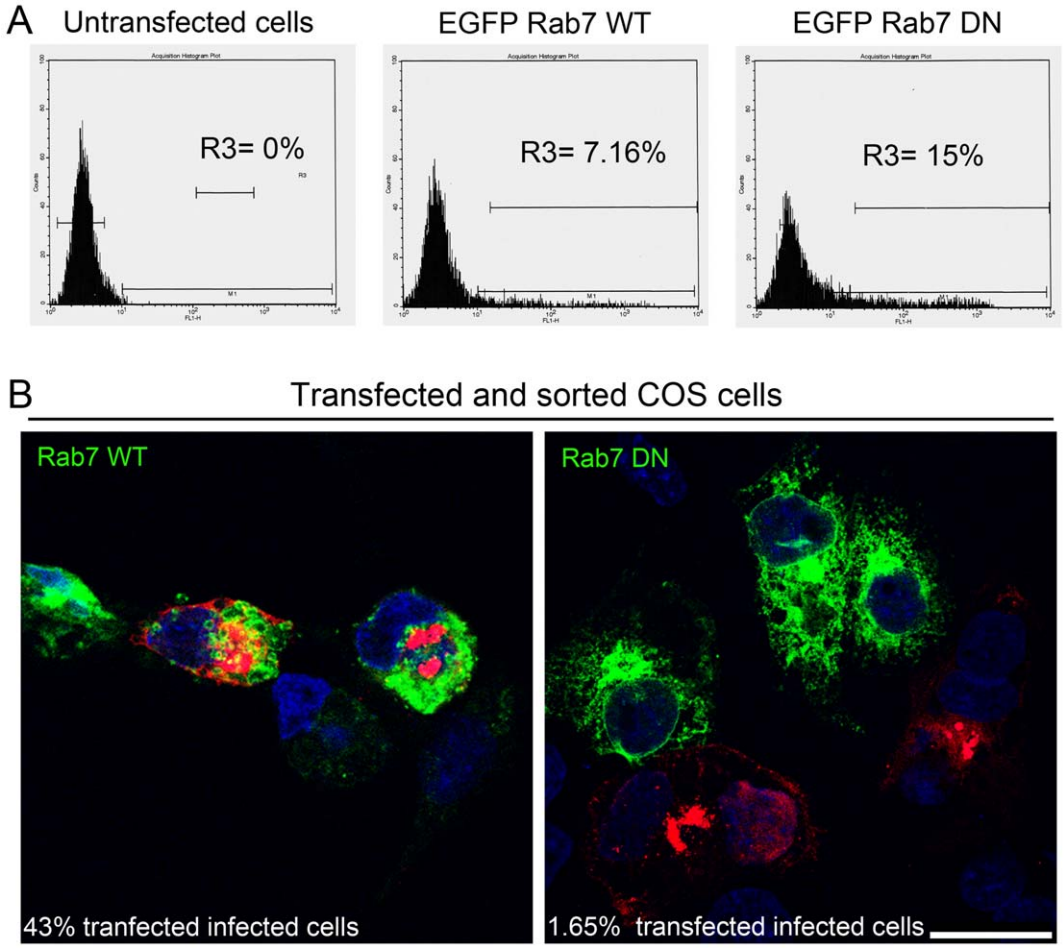

Figure 4. Late endosomal compartment relevance for ASFV infection. (**A**) Representative FACS profiles obtained during sorter analysis of COS-7 cells transfected with GFP-Rab7-wild type (Rab7 WT) and dominant negative mutant (GFP-Rab7-DN, T22N). R3 represents transfected cells expressing GFP to be sorted. (**B**) Representative confocal micrographs of transfected, sorted cells after isolation, infected with ASFV at a moi of 1 for 24 hpi and immunostained for major viral capsid protein p72 (red). Percentages of transfected infected cells decreased from 43.5% in cells expressing Rab7 WT to 1.65% in cells expressing Rab7 DN. Bar 25 μm.
doi:10.1371/journal.pone.0048853.g004

anchoring element of protein complexes. Then, we first addressed the relevance of phosphoinositide 3 kinase (PI3K) in ASFV infection with the inhibitor drug wortmannin. Non-toxic concentrations were determined and low working concentrations (ranging from 0–10 μM) were used to avoid undesirable effects (Fig. 5 A). The addition of this inhibitor had a significant negative effect on infectivity in a dose-dependent manner, as shown by percentages of infected cells detected by p30 expression at 3 hpi, which corresponds to an early time point after virus entry but before replication (Fig. 5 B). The presence of low doses of wortmannin during the complete infection cycle reduced virus production in a dose-dependent manner; conversely, few changes were found when the drug was added after 3 hpi (Fig. 5 C). Viral protein production also decreased dramatically with the PI3K inhibitor (Fig. 5 D). Moreover, PtdIns(3,5)P_2 is essential in LE/LY dynamics, with a distinct function from that of the small GTPase Rab7 [29,30]. YM201636 is a potent inhibitor of the mammalian class III phosphatidylinositol phosphate kinase (PIKfyve), which synthesizes PtdIns(3,5)P_2 from PtdIns3P. Then, we further evaluated the relevance of the correct maintenance of balance in the degradative pathway by analyzing the role of PIKfyve in ASFV infection using the inhibitor of this kinase. A working concentration of 1 μM of PIKfyve inhibitor was selected, this amount being non-toxic but active, as the characteristic swollen vesicle phenotype could be readily identified in cells (Fig. 6 C).

We studied whether the inhibition of PIKfyve activity before infection interferes with virus production. Cells were treated with 1 μM of YM201636 or equivalent volumes of DMSO at indicated times: 2 h prior to infection, at the time of infection (time 0) and at 2 hpi. The medium was then replaced with medium containing the drug at the indicated concentrations. Cells were infected at a moi of 1 pfu/cell and infection was allowed to proceed for 24 h. Statistically significant reductions in ASFV infectivity after YM201636 treatment correlated with a time-dependent decrease in viral production, with a maximum reduction of 90% in viral production in cells treated 2 h before infection with respect to DMSO control (Fig. 6 A).

We also examined the effect of PIKfyve inhibition on viral infectivity. To this end, 1 μM of YM201636 was added 1 h before or at several times after infection with ASFV at 1 pfu/cell. Controls without drug and equivalent volumes of DMSO were carried out. Infection was allowed to proceed for 6 h, an early time point that allows detecting early viral protein expression before viral replication occurs. IFI assays revealed a dramatic reduction

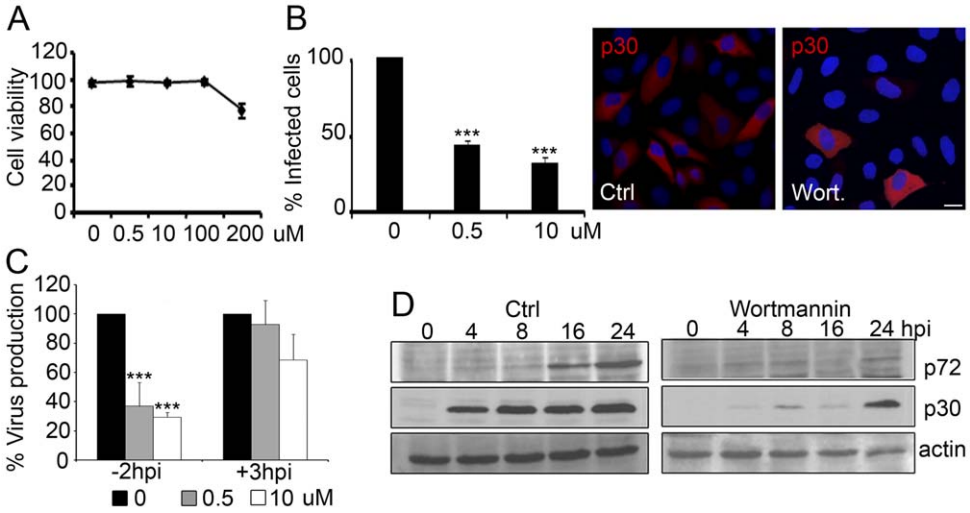

Figure 5. ASFV entry depends on endosomal membrane phosphoinositides. (**A**) Quantification of cell viability at 24 h by Trypan blue exclusion to determine the working concentration of PI3K inhibitor wortmannin. (**B**) Quantification of ASFV infectivity at 3 hpi (moi of 0.5 pfu/cell) in the presence of increasing concentrations of wortmannin. Data are expressed as percentages of infected cells from 30 random fields in triplicates and are means ± SD from three independent experiments. Asterisks denote statistically significant differences ***$P<0.001$. Representative confocal micrographs of cells immunostained for early viral protein p30 in red are shown in the right panels. Bar 20 μm. (**C**) Quantification of virus production in Vero cells untreated, treated with increasing concentrations of wortmannin from 2 h before adsorption during the whole infection cycle, or treated after 3 hpi. Cells were infected with ASFV at a moi of 0.5 pfu/cell for 24 hpi. Data are expressed as virus titers and are means ± SD from three independent experiments. Asterisks denote statistically significant differences ***$P<0.001$. (**D**) Viral protein expression at a range of post-infection times as determined by Western blot in cells to which 10 μM wortmannin was added 2 h before virus adsorption and maintained or left untreated.
doi:10.1371/journal.pone.0048853.g005

of ASFV infectivity in cells treated with YM201636 from 1 h before infection and up to 4 hpi, but not thereafter (Fig. 6 B).

Due to the altered equilibrium between the respective PI levels towards PtdIns3P enrichment with respect to PtdIns(3,5)P_2 after PIKfyve inhibition, there was a characteristic alteration in fusion dynamics and impaired maturation of endosomes. Morphologically, this alteration was characterized by the widespread appearance of large swollen vacuoles in most cytoplasmic areas of YM201636-treated cells (Fig. 6 C). YM201636-treated and infected cells at 16 hpi did not show this vacuolar pattern in 100% of those cells which were infected, as shown by a recognizable viral replication site that retained its characteristic morphology and location. This observation contrasted with the typical vacuolar

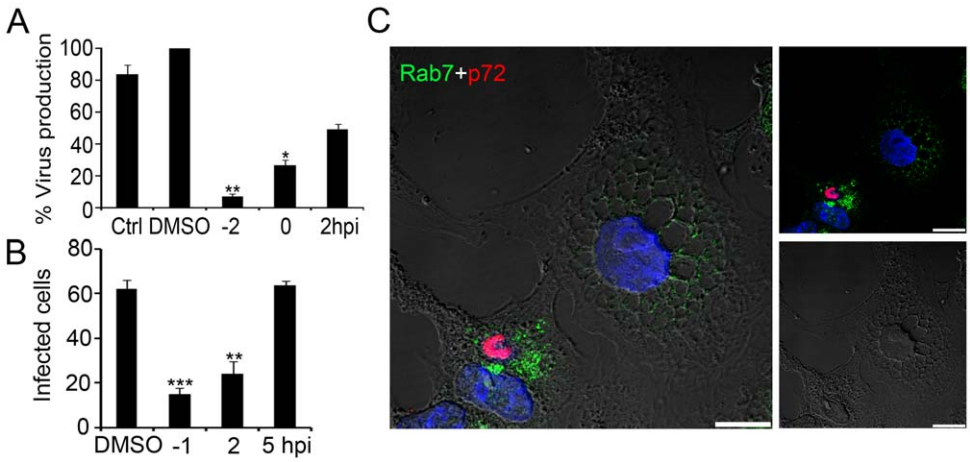

Figure 6. Phosphoinositide interconversion and related late endosome fusion events in ASFV infection. (**A**) Quantification of virus production in cells untreated, treated with 1 μM PIKfyve inhibitor YM201636 or treated with DMSO. Data are expressed as virus titers and are means ± SD from three independent experiments. Asterisks denote statistically significant differences **$P<0.01$; *$P<0.05$ (**B**) Infected cell numbers in cells treated with PIKfyve inhibitor (YM201636) at several time points or an equivalent volume of DMSO. Data are expressed as the number of infected cells at 6 hpi (moi of 1 pfu/cell) from 20 random fields and are means ± SD from two independent experiments. Asterisks denote statistically significant differences (***$P<0.001$ and **$P<0.01$). (**C**) Representative confocal micrographs of infected and non-infected PIKfyve-treated cells, immunostained for Rab7 (green) and viral protein p72 (red). The characteristic phenotype of cytoplasmic vacuoles due to impaired endosome fusion was readily found in uninfected cells. Infected cells are recognized in the image as those harboring viral factories in red and lacked cytoplasmic vacuolization phenotype. Bar 10 μm.
doi:10.1371/journal.pone.0048853.g006

pattern found in neighboring uninfected cells and the origin of this difference is not known (Fig. 6C).

Discussion

ASFV enters Vero cells by endocytosis, through a dynamin-dependent and clathrin-mediated process [11]. However, the subsequent early steps followed by incoming virions to reach the virus replication site close to the MTOC are largely unknown. To identify the endosomal compartment/s involved in early steps of ASFV infection, we first searched for characteristic proteins of the EE, namely EEA1, and LE compartments; CD63 for MBVs, GTPase Rab7 for LEs and Lamp1 for LYs. EEA1 is a Rab5 GTPase effector that regulates the traffic and fusion events of EEs [21] while Rab7 GTPase controls the transport and fusion of LEs. ASFV virions stained with an antibody against major capsid protein p72 colocalized at high percentages with EEs within the first 30 min of infection, while colocalization with CD63, Rab7 and Lamp1 was very low at this time point. As the endosome associated with the incoming virus matures, the colocalization of viral particles with LEs would be expected; however, this colocalization was absent. We postulated that the virus desencapsidation occurs very rapidly in acidic endosomes and consequently it was difficult to observe colocalization of virions with LEs. This hypothesis is consistent with previous electron microscopy observations of viral cores in the cytoplasm of ASFV infected cells 60 min after adsorption corresponding to viral particles without their capsid, although it was not possible to observe the uncoating process itself [31]. In fact, using an antibody against a viral inner core protein (p150), it was possible to observe colocalization of viral cores with LEs while major viral capsid protein was not detected in this acidic late compartment.

We have shown here that endosomal acidification was a major determinant for allowing the virus to gain entry to the cytosol and pursue a productive infection. Inhibitors of intraluminal acidification of endocytic organelles were found to inhibit infection at any time point previous to 1 hpi but not thereafter. Endosomal intraluminal low pH was an important switch for incoming virions to progress into subsequent infection steps, as impaired ASFV infectivity by Baf could not be restored with acid pH treatment of cells. Moreover, the requirement for endocytosis was reinforced by the fact that dynamin inhibitor Dyn mediated infectivity inhibition and it was not possible to bypass this blockage by extracellular acid medium replacement. Similarly, it was previously reported that fusion of the cellular membrane artificially induced by lowering the pH of the medium [9] was not followed by successful ASFV infection in cells treated with other lysosomotropic drugs [10].

We found staining of viral capsid in LEs at intraluminal alkaline conditions, which confirmed the requirement of acidic pH, distinctive of the LE, for viral desencapsidation and further endosomal egress, which take place within the first hour post-infection in this virus model. This observation is consistent with previous results on the accessibility of viral DNA to nuclease and the timing of early viral RNA and protein synthesis of ASFV [31]. Similarly, a recent report on Simian virus 40 (SV40) showed that elevation of vacuolar pH blocks SV40 infection using acidification inhibitors Baf and NH_4Cl [32]. SV40 intracellular traffic includes passage through EEs, maturing hybrid endosomes, LEs with the properties of MVBs, and finally endolysosomes. Agents that raise the pH of endocytic organelles were found to inhibit infection and the internalized virus fraction (about 20%) failed to move beyond Rab5-positive EEs in the presence of Baf and beyond LEs in the presence of monensin.

Under Baf-treatment desencapsidation would be stopped in Rab7-positive late endosomes, thus blocking viral infection progression. After reaching LE acid pH and uncoating would eventually egress from the endosome and the viral cores could be free in the cytosol to start replication at the perinuclear area. There is a close relationship between endosomal maturation and movement. One of the steps required for endosomal maturation includes endosome progression towards the perinuclear area [33], which is achieved through microtubules [30,34]. Endosomal trafficking of ASFV relies on microtubules and previous reports have shown that this virus requires functional microtubules for successful infection [35]. Furthermore, Rac1 activation, which triggers microtubule acetylation and stabilization, is crucial for infection at early time points [36].

The specific low pH of the LE is required for many virus infections, such as the influenza A virus [32] and bunyavirus [37]. Also, most adenovirus (Ad) serotypes enter cells by clathrin-mediated endocytosis, and then the pH inside the endosomes plays an essential role by inducing conformational changes in the viral particle. Ad5 exposed to acidic pH levels shows a clear enhancement in dynein binding through intermediate and light intermediate chains. These data provide physiological evidence of the relevance of adenovirus exposure to endosomal pH for efficient infection [38]. Similarly, rhinovirus enters the cell via clathrin-dependent or -independent endocytosis or via macropinocytosis. Triggered by the low pH of endosomes, the virions undergo conformational alterations and the viral RNA genome is then released through an opening at one of the axes of the icosahedral capsid [39]. Also, Dengue virus uses the unusual lipid composition of the LE membrane for low pH-dependent virus fusion, which determines the timing and site of viral genome release into the cytosol [40].

We have demonstrated that Rab7 GTPase from the LE compartment is essential for successful infection. Rab7 GTPase is characteristic of LEs since the formation of this compartment is preceded by the generation of Rab7 domain, but this protein is scarce on the limiting membrane of EEs [33]. Transient expression of Rab7 DN severely affected ASFV infection outcome, as occurs with other enveloped viruses, such as the influenza virus [41]. After infection of sorted Rab7 WT and DN-transfected cells, ASFV infectivity decreased dramatically compared to cells expressing Rab7 WT.

Altering the balance in PI interconversion would disrupt the endocytic pathway. The small GTPase Rab5 and PtdIns3P are present on classical EEs where they coordinate the assembly of crucial effector complexes for the function and further maturation of these organelles. Efficient recruitment of some of these effectors, such as EEA1 between others, is based on their simultaneous binding to Rab5 and PtdIns3P [23]. As shown above, ASFV requires maturation of the EE to LE, and this process is upregulated by PI3K since the component of switch interconversion Rab5-Rab7, Sand1/Mon1, requires PtdIns3P for endosome binding [42]. Also, the formation of a functional MVB requires the biosynthesis of the membrane lipid PtdIns3P by PI3K [43]. The inhibition of PtdIns3P synthesis impaired ASFV infection, as expected, but not when it was inhibited after the early internalization steps. Thus, PtdIns3P concentration on endosomes regulates the timing of Rab conversion and endosome maturation, which directly affect the very early stages of ASFV infection before endosomal egress. Other viruses such as Kaposi-sarcoma, are also affected by wortmannin treatment [44]. Similar observations have recently been reported for parvoviruses [45], human rhinovirus serotype 2 (HRV2) [46], Influenza A and bunyavirus, all of these late-penetrating viruses [37].

Moreover, PtdIns3P is a precursor for the generation of PtdIns(3,5)P_2 and is distinct from that of the small GTPase Rab7 [47] as it binds the FYVE domain containing PIKfyve [29]. The PIKfyve inhibitor YM201636 affects conversion from PtdIns3P to PtdIns(3,5)P_2 [48], thereby triggering disruption of the degradative pathway and imbalance of fusion endosome dynamics [49], resulting in endosome enlargement and profound vacuolation in mammalian cells [19,49,50,51]. We found that both PIKfyve and acidification inhibition had a strong negative impact on ASFV infection. This inhibitor decreased infectivity and viral production when YM201636 was added before infection but not after 2 hpi. These results with PIKfyve inhibitor are consistent with ASFV requirements for pH acidification during early infection stages since efflux of cations such as Ca^2+ affects acidification [30,52]. PIKfyve may directly regulate the activity of calcium channels and enable the efflux of Ca^2+ allowing the regulation of membrane trafficking pathways in a spatiotemporal manner [53,54].

In conclusion, the profound alteration of the maturation of the LE compartment caused by PIKfyve inhibition deeply affects ASFV infection, as occurs with other pathogens which are dependent on the LE compartment [55]. Conversely, after infection, when the stage of viral replication site formation is reached, it was not possible to further inhibit LE maturation by PIKfyve inhibition.

This is the first report on the requirement for endosomal maturation up to LEs for early ASFV infection. Our results have been achieved using several approaches, namely by blocking pH acidification, impairing the function of the regulatory GTPase of the LE compartment Rab7, and finally by impairing the synthesis of regulatory PIs that have an indisputable role in endosomal maturation.

Taken together, our findings support a model where both EEs and LEs are required for successful ASFV infection (Fig. 7). The incoming virus would gain access to the EE immediately after entering the cell from the clathrin-coated vesicle. Upon EE maturation, the virus would be incorporated into MVBs, progressing to reach the LE and due to the acidic pH of these organelles, desencapsidation would take place. This step was found to be essential for further infection progress. This proposed model includes central roles for small GTPase Rab7 and also membrane PIs, PtdIns3P and PtdIns(3,5)P_2, which orchestrate the maintenance of homeostasis along the pathway. In conclusion, we propose that the integrity of the endocytic pathway maturation process mediated by PIs play a central role during early stages of ASFV infection.

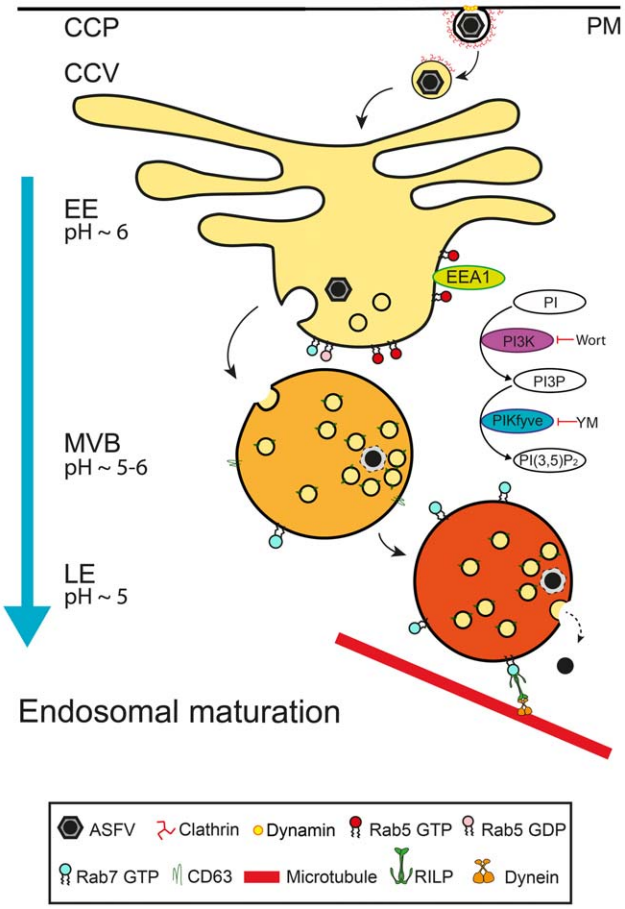

Figure 7. Model of ASFV infection progress through the endosomal pathway. ASFV enters the host cell by clathrin-coated vesicles (CCVs) from clathrin-coated pits (CCPs) and clathrin molecules are recycled to the plasma membrane (PM) as the virus progresses to the endosomal pathway. First, virions gain access to EEs from PM. The EE compartment is characterized by the presence of Rab5 and EEA1. ASFV is then directed from the vacuolar domain of the EE to the acidic late compartments. Subsequently, the virions reach CD63 enriched membranes of MVBs. Under the acid intraluminal pH of these endosomes, viral capsid would be degraded and viral cores would reach LE which depends on the presence of Rab7. At this stage, viral cores could egress to the cytosol to reach their replication site at the perinuclear area. In this process, the PIs composition of the endosomal membrane seemed to be crucial. PtdIns3P is synthesized by PI3K and this process is inhibited by PI3K inhibitor wortmannin and PtdIns(3,5)P_2, which is synthesized by the enzyme PIKfyve, a process blocked by the inhibitor YM201636. These PIs interconversions on the endosomal membrane are necessary for a successful infection.
doi:10.1371/journal.pone.0048853.g007

Materials and Methods

Cells, virus and infections

Vero and COS-7 cells were obtained from ATCC and grown at 37°C in a 5% CO2 atmosphere in Dulbecco's Modified Eagle's Medium (DMEM) supplemented with 5% and 10% fetal bovine serum (FBS), respectively. Cells were grown on chamber slides (Lab-Tek; Nunc), approximately 1.5×10^4 cells/chamber and mock-infected or infected with ASFV-BA71V isolate or recombinant ASFV B54GFP-2 [56] at a multiplicity of infection (moi) of 1 or 10 pfu/ml when indicated. High moi was used to visualize several incoming virus particles/cell.

ASFV stocks from culture supernatants were clarified and semi-purified from vesicles by ultracentrifugation at 40,000 *g* through a 40% (wt/vol) sucrose cushion in phosphate-buffered saline (PBS) for 1 h at 4°C. Purified ASFV stocks were sonicated on ice once for 1 min and stored at −80°C. When synchronization of infection was required, cells were chilled at 4°C for 15 min before viral inoculum addition and virus was then added. Virus adsorption was performed for 90 min at 4°C, and after cold washing, cells were rapidly shifted to 37°C with fresh pre-warmed media.

Indirect immunofluorescence and confocal microscopy

Cells were grown on glass coverslips and fixed in PBS–3.8% paraformaldehyde for 15 min and permeabilized with PBS–0.1% Triton X-100 for 10 min. Following cell fixation, aldehyde fluorescence was quenched by incubation of cells with 50 mM NH4Cl in PBS for 10 min. A monoclonal antibody against major virus capsid protein p72 and against viral core protein p150

(Ingenasa) were used at a working dilution of 1:1000, an anti-p30 antibody at 1:100 [57] and a rabbit serum raised against ASFV structural capsid protein pE120R at 1:500 dilution. Experiments conducted to detect viral capsids were performed with antibodies against both capsid proteins p72 and pE120R and to detect viral cores the antibody against p150 was used. EE were labeled with conjugated anti-mouse EEA1-FITC (BD Biosciences Pharmingen), EEA1 being a Rab5 GTPase effector, and anti-rabbit Rab7 (Cell Signalling) was used to label LEs both at 1:50 dilution. MVBs were labeled with anti CD63 (Developmental Studies Hybridoma Bank, University of Iowa, clone H5C6), a characteristic protein of this compartment, at 1:200 dilution. LYs were labeled with anti-Lamp1 (Abcam) at 1:50 dilution. The secondary antibodies used were anti-mouse immunoglobulin G (IgG) antibody conjugated to Alexa Fluor 594 and anti-rabbit IgG antibody conjugated to Alexa Fluor 488. Secondary antibodies were purchased from Molecular Probes and diluted 1:200. Specificity of labeling and absence of signal crossover were determined by examination of single labeled control samples.

Confocal microscopy was carried out in a Leica TCS SPE confocal microscope using a 63X immersion oil objective, and image analyses were performed with Leica Application Suite advanced fluorescence software (LAS AF). Colocalization events between viral and endosome markers in each cell were counted and relativized to the number of total cell-associated virions and expressed in percentages. Graphics in figures depict means of this percentages and the number of cells counted in each case are expressed in figure legends.

Lysotracker assays

Acid endosomal compartments were labeled by incubation of cells with 75 nM LysoTracker Red DND-99 (Molecular Probes) for 30 min at 37°, then Vero cells were prepared for IFI assay, double labeling endosomal compartments as above described.

To analyze the effect of Baf on LysoTracker staining, pretreated cells were incubated with Baf 200 nM and *in vivo* imaged at several times after Baf addition (1, 5, 10, 15 mpa or minutes after Baf addition), or IFI assays were performed. Fluorescence Intensity in arbitrary units was measured with LAS AF in three maximum points of fluorescence (three similar ROIs, 30×30 μm) per image and background was subtracted. 32 images per condition were analyzed.

Inhibition of endosomal acidification

Stock solution of Baf (Sigma) was dissolved in DMSO at 100uM and stored at −20°C. A working concentration of 200 nM Baf [58,59] was prepared freshly in DMEM. Stock solution of NH4Cl (Sigma) was made in PBS 1 M and the 10 mM working solution [10] was prepared freshly in DMEM. Stock solution of Dyn (Calbiochem) was prepared at 10 mM in DMSO. Cells were seeded at 70% confluence. The culture medium was replaced by cold medium and cells were placed at 4°C during 15 min. ASFV (moi of 1 pfu/ml) was then added on cold medium and the adsorption step was followed for 90 min at 4°C. After cold washing, cells were rapidly shifted to 37°. At the different times post-infection analyzed, culture medium was replaced by pre-warmed medium containing Baf or NH4Cl or DMSO solvent. At 8 hpi, cells were harvested for SDS-PAGE analysis.

For the acid-pH treatment experiments, cells were pretreated with 200 nM Baf, 80 μM Dyn or solvent DMSO. Following, cells were rapidly chilled to 4°C before the addition of the virus. After 90 min adsorption at 4°C, cells were washed and pulsed with pH 5.4 DMEM for 1 h followed by washing and incubation for 6 h at 37°C with pH 7.4 DMEM.

For IFI assays, cells were untreated or pretreated with cold medium containing either Baf or an equivalent volume of DMSO for 20 min. Virus was then added at a moi over 10, followed by an adsorption step of 90 min at 4°C. After washing, culture medium was replaced with fresh pre-warmed medium with or without Baf or an equivalent volume of DMSO. Infection was allowed to progress for 3 h and prepared for IFI assay.

Flow Cytometry

Cells were pretreated for 1 h with 80 μM Dyn or 200 nM Baf followed by cold synchronized infections with 1 pfu/ml ASFV and then washed with ice-cold DMEM to remove unattached virus before incubation with either an hour pulse of pH 5.4 DMEM followed by washing or pH 7.4 DMEM in the presence of inhibitor for the duration of the experiment. At 6 hpi cells were washed with PBS and harvested by trypsinization. After washing with fluorescence-activated cell sorter (FACS) buffer (PBS, 0.01% sodium azide, and 0.1% bovine serum albumin [BSA]), cells were fixed and permeabilized with Perm2 (BD Sciences) for 10 min at room temperature. Detection of infected cells was performed by incubation with anti-p30 monoclonal antibody (diluted 1:100 in FACS buffer) for 30 min at 4°C, followed by incubation with phycoerythrin (PE)-conjugated antimouse immunoglobulins (1:50, diluted in FACS buffer [Dako]) for 30 min at 4°C. After extensive washing, 10000 cells per time point were scored and analyzed in a FACSCalibur flow cytometer (BD Sciences) to determine the percentage of infected cells under these conditions. Infection rates obtained were normalized to infected cell percentages found in control plates.

Viral protein expression analysis

Infected Vero cells were harvested at various times, washed in PBS, and disrupted in Laemmli sample buffer reducing agent (Bio-Rad) containing lithium dodecyl sulfate sample buffer. Lysates were sonicated and incubated at 100°C for 5 min and resolved by sodium dodecyl sulfate-polyacrylamide gel electrophoresis (SDS-PAGE) in a 10% gel. Proteins were transferred to a nitrocellulose membrane and blocked with PBS supplemented with 5% non-fat dried milk for 1 h at room temperature or overnight (ON) at 4°C. To detect p30 protein and α-tubulin, the latter used as a protein load control, membranes were incubated with an anti-p30 monoclonal antibody diluted 1:1000 as previously described [57] and α-tubulin antibody diluted 1:2000. As secondary antibody we used horseradish peroxidase (HRP)-coupled anti-mouse antibodies diluted 1:5000 (GE Healthcare). Precision Protein StrepTactin-HRP Conjugate (Bio-Rad) was used to reveal the ladder Precision Plus Protein WesternC (Bio-Rad).

Western blots were analyzed using Immun-Star WesternC Kit (Bio-Rad) on Molecular Imager Chemidoc XRSplus Imaging System. Bands were quantified by densitometry and data were normalized to control values using Image lab software (Bio-Rad).

Transfections and sorter analysis

Wild-type GFP-tagged human Rab7 and dominant-negative mutant (Rab7 T22N) plasmid constructs cloned as N-terminal GFP fusions in the pGreenLantern vector (Gibco-BRL, Grand Island NY, USA) were kindly provided by Dr, Craig Roy, Yale University, USA. Transfections were performed by using the Fugene HD Transfection Reagent from Roche and following the manufacturer's recommendations. Briefly, COS cells were grown in T-75 flasks, in DMEM 10% serum with 1% streptomycin, penicillin and 1% glutamine until 80% confluence was reached and they were then transfected. After 6 h, the transfection mixture was removed and fresh medium containing 10% serum and 1%

antibiotics and glutamine was added. Transfection was allowed to progress for 24 h. After 24 h post-transfection (hpt), cells were treated with trypsin for 1 min. Trypsin was then carefully removed and detached transfected cells were resuspended in DMEM 5% with 100 μg/μL gentamycin.

1.2×10^8 cells were analyzed for each transfected vector in a Coulter flow cytometer with an argon laser at 488 nm. Cells expressing EGFP fluorescence were counted and seeded into 4-well plates for 12 h. The next day, cells were infected with ASFV at a moi of 1 and analyzed by IFI assay.

Phosphoinositide interconversion inhibitors

Wortmannin, an inhibitor of phosphoinositide 3 kinase (PI3K), which impairs PtdIns3P production, was purchased from Stressgen. The inhibitor did not affect cell viability, as tested by Trypan blue staining. Cells were treated with the drug following three protocols. First, drug treatment was maintained during the entire experiment (24 h). Second, the drug was added before infection and maintained along viral adsorption (cells were rinsed with fresh media after adsorption to remove the drug). Finally, in the third protocol we added the drug 3 h after viral adsorption and maintained it throughout the experiment.

PIKfyve Inhibitor YM201636, which impairs PtdIns(3,5)P_2 production from PtdIns3P, was purchased from Symansis (Cell Signaling Science). A stock solution was diluted in DMSO at 0.8 mM concentration and stored at -20°. A cytotoxicity assay "Cell titter 96" from Promega was used to determine the working concentration of 1 μM as the lowest non-cytotoxic concentration inducing a characteristic swollen vesicle phenotype in the cytoplasm after 30 min incubation. Cells were treated with YM201636 2 hours before infection or at the times indicated and maintained during the whole infection cycle or at the post-infection times indicated in each case.

Supporting Information

Figure S1 Staining of the different endosomal compartments with pH sensitive dye. (**A**) Absence of lysotracker red staining in the EE demonstrates the alkaline intraluminal pH of these organelles. (**B**) MVBs showed lower pH and lysotracker red labeling of these organelles is shown in yellow in the merged image. Similarly, LEs (**C**) and LYs (**D**) intraluminal acid pH is shown by lysotracker staining. Bar 10 μm.
(TIF)

Acknowledgments

We thank Dr. Craig Roy from Yale University, USA, for the GFP-Rab7 and GFP-Rab7 T22N plasmid constructs and Dr. Jean Gruenberg, Dpt. Biochemistry, University of Geneva for useful comments and discussions.

Author Contributions

Conceived and designed the experiments: CA MACG. Performed the experiments: MACG IG BH JIQ IDM. Analyzed the data: MACG IG BH JIQ CA. Contributed reagents/materials/analysis tools: BH JIQ IDM. Wrote the paper: CA MACG IG BH.

References

1. Dixon L, Costa JV, Escribano JM, Rock DL, Vinuela E, et al (2000) Asfarviridae. New York: Academic Press. 159–165 p.
2. Andres G, Simon-Mateo C, Vinuela E (1997) Assembly of African swine fever virus: role of polyprotein pp220. J Virol 71: 2331–2341.
3. Andres G, Garcia-Escudero R, Simon-Mateo C, Vinuela E (1998) African swine fever virus is enveloped by a two-membraned collapsed cisterna derived from the endoplasmic reticulum. J Virol 72: 8988–9001.
4. Carrascosa AL, del Val M, Santaren JF, Vinuela E (1985) Purification and properties of African swine fever virus. J Virol 54: 337–344.
5. Breese SS Jr., DeBoer CJ (1966) Electron microscope observations of African swine fever virus in tissue culture cells. Virology 28: 420–428.
6. Andres G, Garcia-Escudero R, Vinuela E, Salas ML, Rodriguez JM (2001) African swine fever virus structural protein pE120R is essential for virus transport from assembly sites to plasma membrane but not for infectivity. J Virol 75: 6758–6768.
7. Rodriguez JM, Garcia-Escudero R, Salas ML, Andres G (2004) African Swine Fever Virus Structural Protein p54 Is Essential for the Recruitment of Envelope Precursors to Assembly Sites. J Virol 78: 4299–1313.
8. Suarez C, Gutierrez-Berzal J, Andres G, Salas ML, Rodriguez JM (2010) African swine fever virus protein p17 is essential for the progression of viral membrane precursors toward icosahedral intermediates. J Virol 84: 7484–7499.
9. Valdeira ML, Geraldes A (1985) Morphological study on the entry of African swine fever virus into cells. Biol Cell 55: 35–40.
10. Valdeira ML, Bernardes C, Cruz B, Geraldes A (1998) Entry of African swine fever virus into Vero cells and uncoating. Vet Microbiol 60: 131–140.
11. Hernaez B, Alonso C (2010) Dynamin- and clathrin-dependent endocytosis in African swine fever virus entry. J Virol 84: 2100–2109.
12. Sanchez EG, Quintas A, Perez-Nunez D, Nogal M, Barroso S, et al. (2012) African swine fever virus uses macropinocytosis to enter host cells. PLoS Pathog 8: e1002754.
13. Sanchez-Torres C, Gomez-Puertas P, Gomez-del-Moral M, Alonso F, Escribano JM, et al. (2003) Expression of porcine CD163 on monocytes/macrophages correlates with permissiveness to African swine fever infection. Arch Virol 148: 2307–2323.
14. McCullough KC, Schaffner R, Fraefel W, Kihm U (1993) The relative density of CD44-positive porcine monocytic cell populations varies between isolations and upon culture and influences susceptibility to infection by African swine fever virus. Immunol Lett 37: 83–90.
15. McCullough KC, Basta S, Knotig S, Gerber H, Schaffner R, et al. (1999) Intermediate stages in monocyte-macrophage differentiation modulate phenotype and susceptibility to virus infection. Immunology 98: 203–212.
16. Zoncu R, Perera RM, Balkin DM, Pirruccello M, Toomre D, et al. (2009) A phosphoinositide switch controls the maturation and signaling properties of APPL endosomes. Cell 136: 1110–1121.
17. Taylor MJ, Perrais D, Merrifield CJ (2011) A high precision survey of the molecular dynamics of mammalian clathrin-mediated endocytosis. PLoS Biol 9: e1000604.
18. Taylor MJ, Lampe M, Merrifield CJ (2012) A Feedback Loop between Dynamin and Actin Recruitment during Clathrin-Mediated Endocytosis. PLoS Biol 10: e1001302.
19. Lin SX, Mallet WG, Huang AY, Maxfield FR (2004) Endocytosed cation-independent mannose 6-phosphate receptor traffics via the endocytic recycling compartment en route to the trans-Golgi network and a subpopulation of late endosomes. Mol Biol Cell 15: 721–733.
20. Roppenser B, Grinstein S, Brumell JH (2012) Modulation of host phosphoinositide metabolism during Salmonella invasion by the type III secreted effector SopB. Methods Cell Biol 108: 173–186.
21. Stenmark H (2009) Rab GTPases as coordinators of vesicle traffic. Nat Rev Mol Cell Biol 10: 513–525.
22. Jordens I, Marsman M, Kuijl C, Neefjes J (2005) Rab proteins, connecting transport and vesicle fusion. Traffic 6: 1070–1077.
23. Zerial M, McBride H (2001) Rab proteins as membrane organizers. Nat Rev Mol Cell Biol 2: 107–117.
24. Lemmon MA (2008) Membrane recognition by phospholipid-binding domains. Nat Rev Mol Cell Biol 9: 99–111.
25. Vicinanza M, D'Angelo G, Di Campli A, De Matteis MA (2008) Function and dysfunction of the PI system in membrane trafficking. Embo J 27: 2457–2470.
26. Miyazawa N, Crystal RG, Leopold PL (2001) Adenovirus serotype 7 retention in a late endosomal compartment prior to cytosol escape is modulated by fiber protein. J Virol 75: 1387–1400.
27. Sieczkarski SB, Brown HA, Whittaker GR (2003) Role of protein kinase C betaII in influenza virus entry via late endosomes. J Virol 77: 460–469.
28. Toei M, Saum R, Forgac M (2010) Regulation and isoform function of the V-ATPases. Biochemistry 49: 4715–4723.
29. de Lartigue J, Polson H, Feldman M, Shokat K, Tooze SA, et al. (2009) PIKfyve regulation of endosome-linked pathways. Traffic 10: 883–893.
30. Huotari J, Helenius A (2011) Endosome maturation. Embo J 30: 3481–3500.
31. Alcami A, Carrascosa AL, Vinuela E (1989) The entry of African swine fever virus into Vero cells. Virology 171: 68–75.
32. Engel S, Heger T, Mancini R, Herzog F, Kartenbeck J, et al. (2011) Role of endosomes in simian virus 40 entry and infection. J Virol 85: 4198–4211.
33. Rink J, Ghigo E, Kalaidzidis Y, Zerial M (2005) Rab conversion as a mechanism of progression from early to late endosomes. Cell 122: 735–749.
34. Gruenberg J (2009) Viruses and endosome membrane dynamics. Curr Opin Cell Biol 21: 582–588.
35. Alonso C, Miskin J, Hernaez B, Fernandez-Zapatero P, Soto L, et al. (2001) African swine fever virus protein p54 interacts with the microtubular motor complex through direct binding to light-chain dynein. J Virol 75: 9819–9827.

36. Quetglas JI, Hernaez B, Galindo I, Munoz-Moreno R, Cuesta-Geijo MA, et al. (2012) Small rho GTPases and cholesterol biosynthetic pathway intermediates in african Swine Fever virus infection. J Virol 86: 1758–1767.
37. Lozach PY, Mancini R, Bitto D, Meier R, Oestereich L, et al. (2010) Entry of bunyaviruses into mammalian cells. Cell Host Microbe 7: 488–499.
38. Scherer J, Vallee RB (2011) Adenovirus recruits dynein by an evolutionary novel mechanism involving direct binding to pH-primed hexon. Viruses 3: 1417–1431.
39. Fuchs R, Blaas D (2010) Uncoating of human rhinoviruses. Rev Med Virol 20: 281–297.
40. Zaitseva E, Yang ST, Melikov K, Pourmal S, Chernomordik LV (2010) Dengue virus ensures its fusion in late endosomes using compartment-specific lipids. PLoS Pathog 6: e1001131.
41. Sieczkarski SB, Whittaker GR (2003) Differential requirements of Rab5 and Rab7 for endocytosis of influenza and other enveloped viruses. Traffic 4: 333–343.
42. Poteryaev D, Datta S, Ackema K, Zerial M, Spang A (2010) Identification of the switch in early-to-late endosome transition. Cell 141: 497–508.
43. Raiborg C, Rusten TE, Stenmark H (2003) Protein sorting into multivesicular endosomes. Curr Opin Cell Biol 15: 446–455.
44. Naranatt PP, Akula SM, Zien CA, Krishnan HH, Chandran B (2003) Kaposi's sarcoma-associated herpesvirus induces the phosphatidylinositol 3-kinase-PKC-zeta-MEK-ERK signaling pathway in target cells early during infection: implications for infectivity. J Virol 77: 1524–1539.
45. Brabec M, Blaas D, Fuchs R (2006) Wortmannin delays transfer of human rhinovirus serotype 2 to late endocytic compartments. Biochem Biophys Res Commun 348: 741–749.
46. Harbison CE, Lyi SM, Weichert WS, Parrish CR (2009) Early steps in cell infection by parvoviruses: host-specific differences in cell receptor binding but similar endosomal trafficking. J Virol 83: 10504–10514.
47. Sbrissa D, Ikonomov OC, Shisheva A (2002) Phosphatidylinositol 3-phosphate-interacting domains in PIKfyve. Binding specificity and role in PIKfyve. Endomenbrane localization. J Biol Chem 277: 6073–6079.
48. Jefferies HB, Cooke FT, Jat P, Boucheron C, Koizumi T, et al. (2008) A selective PIKfyve inhibitor blocks PtdIns(3,5)P(2) production and disrupts endomembrane transport and retroviral budding. EMBO Rep 9: 164–170.
49. Johnson EE, Overmeyer JH, Gunning WT, Maltese WA (2006) Gene silencing reveals a specific function of hVps34 phosphatidylinositol 3-kinase in late versus early endosomes. J Cell Sci 119: 1219–1232.
50. Griffiths G, Matteoni R, Back R, Hoflack B (1990) Characterization of the cation-independent mannose 6-phosphate receptor-enriched prelysosomal compartment in NRK cells. J Cell Sci 95 (Pt 3): 441–461.
51. Rohn WM, Rouille Y, Waguri S, Hoflack B (2000) Bi-directional trafficking between the trans-Golgi network and the endosomal/lysosomal system. J Cell Sci 113 (Pt 12): 2093–2101.
52. Marshansky V, Futai M (2008) The V-type H+-ATPase in vesicular trafficking: targeting, regulation and function. Curr Opin Cell Biol 20: 415–426.
53. Dong XP, Shen D, Wang X, Dawson T, Li X, et al. (2010) PI(3,5)P(2) controls membrane trafficking by direct activation of mucolipin Ca(2+) release channels in the endolysosome. Nat Commun 1: 38.
54. Shisheva A (2008) PIKfyve: Partners, significance, debates and paradoxes. Cell Biol Int 32: 591–604.
55. Kerr MC, Wang JT, Castro NA, Hamilton NA, Town L, et al. (2010) Inhibition of the PtdIns(5) kinase PIKfyve disrupts intracellular replication of Salmonella. Embo J 29: 1331–1347.
56. Hernaez B, Escribano JM, Alonso C (2006) Visualization of the African swine fever virus infection in living cells by incorporation into the virus particle of green fluorescent protein-p54 membrane protein chimera. Virology 350: 1–14.
57. Hernaez B, Escribano JM, Alonso C (2008) African swine fever virus protein p30 interaction with heterogeneous nuclear ribonucleoprotein K (hnRNP-K) during infection. FEBS Lett 582: 3275–3280.
58. Umata T, Moriyama Y, Futai M, Mekada E (1990) The cytotoxic action of diphtheria toxin and its degradation in intact Vero cells are inhibited by bafilomycin A1, a specific inhibitor of vacuolar-type H(+)-ATPase. J Biol Chem 265: 21940–21945.
59. Stuart AD, Brown TD (2006) Entry of feline calicivirus is dependent on clathrin-mediated endocytosis and acidification in endosomes. J Virol 80: 7500–7509.

Virus Research 173 (2013) 42–57

Contents lists available at SciVerse ScienceDirect

Virus Research

journal homepage: www.elsevier.com/locate/virusres

Review

African swine fever virus-cell interactions: From virus entry to cell survival

Covadonga Alonso*, Inmaculada Galindo, Miguel Angel Cuesta-Geijo, Marta Cabezas, Bruno Hernaez[1], Raquel Muñoz-Moreno

Dpto. de Biotecnología, INIA, Instituto Nacional de Investigación y Tecnología Agraria y Alimentaria, Ctra. de la Coruña Km 7.5, 28040 Madrid, Spain

ARTICLE INFO

Article history:
Available online 20 December 2012

Keywords:
African swine fever virus
ASFV
Virus entry
Endocytosis
Clathrin
Dynamin
Macropinocytosis
Early endosome
Late endosome
Rab GTPases
PI3K
PIKfyve
ER stress
Unfolded protein response
Caspases
Apoptosis
Bcl2
PP1
eIF2α
HDAC6
Autophagy
Beclin1
Cholesterol

ABSTRACT

Viruses have adapted to evolve complex and dynamic interactions with their host cell. The viral entry mechanism determines viral tropism and pathogenesis. The entry of African swine fever virus (ASFV) is dynamin-dependent and clathrin-mediated, but other pathways have been described such as macropinocytosis. During endocytosis, ASFV viral particles undergo disassembly in various compartments that the virus passes through en route to the site of replication. This disassembly relies on the acid pH of late endosomes and on microtubule cytoskeleton transport. ASFV interacts with several regulatory pathways to establish an optimal environment for replication. Examples of these pathways include small GTPases, actin-related signaling, and lipid signaling. Cellular cholesterol, the entire cholesterol biosynthesis pathway, and phosphoinositides are central molecular networks required for successful infection. Here we report new data on the conformation of the viral replication site or viral factory and the remodeling of the subcellular structures. We review the virus-induced regulation of ER stress, apoptosis and autophagy as key mechanisms of cell survival and determinants of infection outcome. Finally, future challenges for the development of new preventive strategies against this virus are proposed on the basis of current knowledge about ASFV-host interactions.

Contents

* Corresponding author. Tel.: +34 91 3476896; fax: +34 91 3478771.
E-mail addresses: calonso@inia.es (C. Alonso), galindo@inia.es (I. Galindo), cuesta.miguel@inia.es (M.A. Cuesta-Geijo), marta.cabezas@inia.es (M. Cabezas), bhernaez@cbm.uam.es, hernaez@inia.es (B. Hernaez), munoz.raquel@inia.es (R. Muñoz-Moreno).
[1] Present address: Centro de Biología Molecular Severo Ochoa, CSIC-UAM (CBMSO), C\ Nicolas Cabrera 1, Cantoblanco, 28049 Madrid, Spain.

0168-1702/$ – see front matter © 2012 Elsevier B.V. All rights reserved.
http://dx.doi.org/10.1016/j.virusres.2012.12.006

1. Entry of African swine fever virus

The entry of a virus into host cells is not only the first step that initiates infection, but also a key determinant of viral tropism and pathogenesis. For an intracellular pathogen, the crucial issue is not merely the crossing of the cytoplasmic membrane since the entry pathway determines whether a productive infection takes place or not. There is also a substantial degree of complexity associated with the entry pathways of large DNA viruses. ASFV interaction with cellular receptor/s promotes subsequent entry steps involving the activation of signaling and endocytosis. However, early studies on ASFV entry in Vero cells and porcine macrophages characterized this event as a low pH- and temperature-dependent process consistent with saturable and specific receptor-mediated endocytosis (Alcami et al., 1989a,b; Alcami et al., 1990; Valdeira and Geraldes, 1985). An interesting observation was that the virus entered the macrophages of another species (rabbit), thus leading to an abortive infection when using a different mechanism mediated by non-saturable or non-specific receptors. These data are consistent with clathrin-mediated entry. In fact, early electron microscopy observations found ASFV particles frequently adsorbed to invaginations similar to clathrin-coated pits (Alcami et al., 1989a).

1.1. ASFV entry is dynamin-dependent and clathrin-mediated

Clathrin-mediated endocytosis is regulated by a network of proteins and lipids that are recruited in a dynamic temporal sequence. These molecules take part in membrane bending and elongation, and final fission of the endocytic vesicle (Fig. 1) (Merrifield et al., 2005; Taylor et al., 2011). The cell invaginates the plasma membrane, thus giving rise to a small intracellular vesicle composed by a clathrin coat with adaptor proteins, Epsin15 (Ede1), and dynamin. The latter recruits BAR domain proteins, which in turn recruit actin-related signaling molecules (Merrifield et al., 2002; Traub, 2009). Dynamin and actin nucleation at the base and the neck of the vesicle would propel the membrane inward and promote scission of the clathrin-coated pit (Taylor et al., 2012). Epidermal growth factor receptor (EGFR) and transferrin are characteristic proteins that are internalized through this endocytic pathway.

Biochemical and molecular analysis of ASFV entry, using the specific dynamin inhibitor dynasore, but also a dominant-negative mutant of dynamin-2, have revealed that viral endocytosis depends on dynamin GTPase, which participates in vesicle fission from the plasma membrane (Hernaez and Alonso, 2010). Clathrin-assembly inhibitors, such as chlorpromazine, and also knock-out of clathrin-adaptor Epsin15 by expression of a dominant-negative mutant, profoundly affect virus infectivity and subsequent virus production. This was shown using a highly adapted virus isolate (BV71V), a low passage one in Vero cells, and also in the WSL cell line, derived from wild boar lung cells (Hernaez and Alonso, 2010). Moreover, at very early post-infection times, virions colocalize with clathrin-heavy-chain antibodies on the cell surface. Jointly, these findings led to the conclusion that ASFV entry involves dynamin-dependent and clathrin-mediated endocytosis (Hernaez and Alonso, 2010). In addition, this entry mechanism requires cholesterol (Bernardes et al., 1998) as it is sensitive to membrane cholesterol depletion by cyclodextrin. Conversely, it is insensitive to nystatin, a drug that disorganizes cholesterol in lipid rafts without reducing cholesterol levels (Hernaez and Alonso, 2010). These data are not consistent with a caveolae-dependent pathway for entry, which is another dynamin-dependent endocytic route. Other information about the relevance of the cholesterol biosynthesis pathway for virus entry is discussed below.

Although it is tempting to exclude clathrin-mediated endocytosis because of the large size of ASFV particles (200 nm), there is increasing scientific evidence that the direct participation of actin in membrane dynamics during clathrin-mediated endocytosis promotes the efficient internalization of large viruses, such as vesicular stomatitis virus (70 × 200 nm) (Cureton et al., 2009, 2010), and even bacteria (Pizarro-Cerda et al., 2010; Veiga and Cossart, 2005) and fungi (Moreno-Ruiz et al., 2009). This may be the case of ASFV.

1.2. Entry by macropinocytosis. The role of actin

Recent studies on ASFV entry, using BA71V or E70 isolates either in Vero or IPAM cells, have demonstrated the activation of the small Rho-GTPase Rac1 immediately after infection (Quetglas et al., 2012; Sanchez et al., 2012). Rac1 has been implicated in the modulation of actin dynamics and in the stabilization of microtubules by acetylation. Disruption of actin cytoskeleton with cytochalasin D alters infectivity (Sanchez et al., 2012), in contrast with others reporting scarce effects on infectivity using jasplakinolide and latrunculin A (Hernaez and Alonso, 2010). Field emission scanning electron microscopy has revealed that actin is involved in

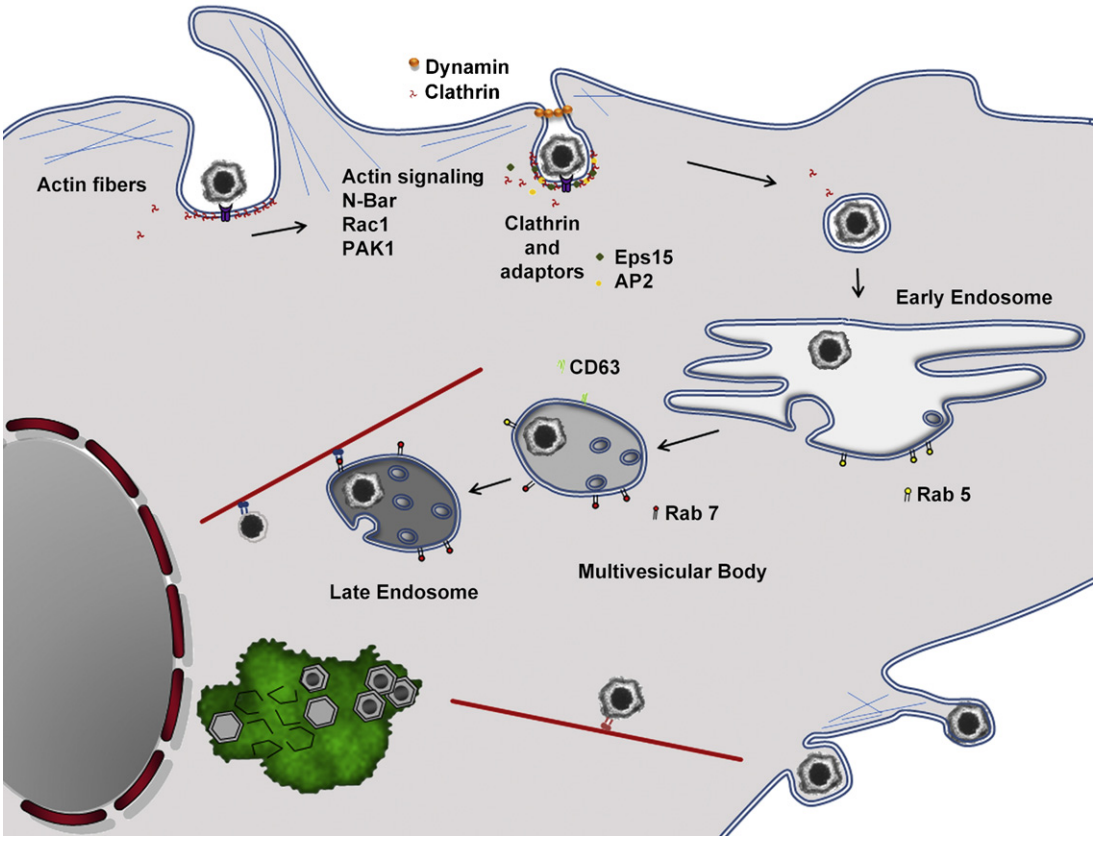

Fig. 1. Replication cycle of ASFV and first interactions with the host cell upon entry. The proposed model for virus entry would include dynamin and clathrin-mediated endocytosis and macropinocytosis. Clathrin-mediated endocytosis could be aided by actin reorganization and blebbing during macropinocytosis. Clathrin and adaptor molecules Eps15 and AP2 at clathrin-coated pits on the membrane promote actin nucleation (N-BAR) and recruit temporally successive modules of lipids and proteins necessary for the invagination and elongation of the vesicle. Finally, dynamin and actin induce constriction at the tail and neck produce final scission of the vesicle to the cytosol. In a few seconds, Rab5 and related molecules on the vesicle membrane give rise to the early endosome (EE). Further maturation of the early endosome requires acidification of the pH, phosphoinositide interconversions mediated by PI3K and PIKfyve, and finally Rab7 GTPase activation. Acidic late endosomal compartments produce virion desencapsidation, which will take place within the first 30–45 mpi.

the induction of the ruffles and blebs observed during the first hour post-infection (hpi). Sanchez et al. (2012) reported that ASFV infection is impaired by EIPA-amiloride, a potent inhibitor of the sodium/proton exchanger (Na^+/H^+), which has traditionally been used as a hallmark of macropinocytosis. On the basis of these data, they concluded that ASFV-induced macropinocytosis was a mechanism of virus entry, as previously described for vaccinia virus (VACV) (Mercer and Helenius, 2008). Nevertheless, macropinocytosis is recognized to be dynamin-independent. This conclusion contrasts with other reports (Cuesta-Geijo et al., 2012; Hernaez and Alonso, 2010).

Analysis of the mechanisms of entry in macrophages, the natural host cells of ASFV, is hindered by the fact that these cells have a heterogeneous surface marker profile and only restricted macrophage subpopulations are susceptible to this virus (McCullough et al., 1993, 1999; Sanchez-Torres et al., 2003). Moreover, permissive macrophage cell lines with the appropriate marker profile are not available (de Leon et al., 2012). Therefore, experimental approaches have frequently used the well-established laboratory model of ASFV BA71V isolate infection in Vero cells. In a wide analysis of various cell lines, it was shown that permissiveness for ASFV infection reaches different levels depending on the cell line analyzed and the restriction was found at the entry level or at later steps (Carrascosa et al., 1999).

Porcine CD163 scavenger receptor participates in the natural host cell infection (Sanchez-Torres et al., 2003). Expressed on most tissue macrophages but not on other myeloid cells, CD163 is one of the most reliable markers for cells of the monocyte macrophage lineage (Peréz et al., 2008). Nevertheless, some reports have shown how ASFV and other pathogens enter macrophages by fluid-phase uptake during macropinocytosis or by means of phagocytosis (Basta et al., 2010), which are receptor-independent.

Hence, the proposed routes of entry reported for the virus in the target cell include phagocytosis (Basta et al., 2010), macropinocytosis (Sanchez et al., 2012) and receptor-mediated endocytosis (Alcami et al., 1989a; Cuesta-Geijo et al., 2012; Hernaez and Alonso, 2010; Hernaez et al., 2012a). Nevertheless, these routes might not be equally effective to initiate infection. To evaluate infectivity, Sanchez et al. (2012) used p72 capsid protein expression at 1 hpi as measured by flow cytometry. This method does not discriminate viruses that entered the cytoplasm from those retained in membrane grooves. Virions that successfully entered the endocytic pathway and desencapsidated as a result of the acid pH of the late endosome are not detectable with p72 antibodies, as discussed below (Cuesta-Geijo et al., 2012). The dependence of infection on acid pH and endocytosis indicates that only desencapsidated virions will develop a productive infection. Thus, virions entering by pathways other than receptor-mediated endocytosis are not able to escape endosomes which is a crucial step for infection.

As occurs in poxviruses, ASFV mature intracellular virions (MVs) and extracellular virions (EVs) are infective (Andres et al., 2001). However, ASFV entry presents quite distinct features with respect to its mode of entry. VACV and Kaposi's sarcoma-associated herpesvirus use macropinocytosis and require this process for host cell entry and internalization (Mercer and Helenius, 2009; Raghu et al., 2009). Other viruses, such as species C Adenovirus (Ad) 2

and 5 and rubella virus, require macropinocytosis for entry but not for internalization. For Ad 2, macropinocytosis is required for the penetration of endosomal membranes after clathrin-mediated endocytosis (Meier et al., 2002).

VACV entry by macropinocytosis is followed by fusion of the viral membrane with the plasma membrane, which results in deposition of the viral core into the cytosol (Carter et al., 2005; Schmidt et al., 2012). Acid media treatment is sufficient to induce VACV membrane fusion (by removal of A25/A26 proteins); however, the need of endocytic passage is variable for MVs and EVs (Schmidt et al., 2011). Macropinosomes can undergo homo- and hetero-typic fusion and acidification but their relationship with endosomes and lysosomes remains elusive (Schmidt et al., 2012). Nevertheless, ASFV does not enter host cells by fusion at the plasma membrane, nor does it undergo acidic media-induced fusion, and it cannot circumvent the passage through acidic endosomes as shown by Cuesta-Geijo et al. (2012). Coincident with previous reports (Alcami et al., 1989a,b; Alcami et al., 1990; Valdeira and Geraldes, 1985), those authors concluded that both acid pH and endocytosis requirements are crucial for ASFV entry.

1.3. Open questions

Nevertheless, many questions regarding the ASFV entry mechanism remain unresolved. Could dynamin/clathrin-mediated endocytosis and macropinocytosis be alternative or even cooperative mechanisms of entry? If they are alternative, do they both lead to productive infection? Are both mechanisms consistent with saturable and specific receptor-mediated endocytosis? Could an alternative entry mechanism involve clathrin and some of the features described for macropinocytosis, such as actin-cytoskeleton and Rac1-dependent signaling? In this regard, it is conceivable that the activation of actin signaling elicited by macropinocytosis enhances clathrin-mediated endocytosis of the virus. A proposed model for the co-existence of both mechanisms is shown in Fig. 1.

Future research should clarify some of these questions, including the entry mechanism used in macrophages. However, after crossing the cell membrane, the next step for the virus involves the endocytic pathway.

2. ASFV at the endosomal pathway

2.1. Endocytosis maturation stages

Once the virus is internalized in primary endocytic vesicles, the intracellular pathways followed by incoming viruses are the same as those used by physiological cargoes. In a few seconds, various protein modules are recruited to clathrin-coated structures to enter the endocytic pathway (Taylor et al., 2011). Endosomal maturation requires the presence of some lipids, such as phosphoinositides, on the endosomal membrane for the specific incorporation of proteins involved in traffic and maturation termed Rab GTPases. Rab GTPases are regulators of the endocytic pathway, and each Rab protein incorporates to a specific compartment (Jordens et al., 2005). Shortly after the clathrin-coated vesicle pinches off the membrane, Rab5 effectors and Rab5 itself are recruited to the newly formed early endosome (EE) (Taylor et al., 2011). From this compartment, cargoes can be recycled to the membrane or progress and mature to late endosomes (LEs), which may fuse with lysosomes (LYs) for degradation. This pathway involves gradual acidification of the endosomal lumen, starting from the pH 6.5 of the EE, which, through invagination of small intraluminal vesicles (ILVs), becomes the multivesicular bodies (MVBs). These bodies then mature to Rab7-expressing LEs at pH between 6 and 5 (Huotari and Helenius, 2011). After fusion of LEs with LYs, which are characterized by Lamp1 expression, the pH drops to 5–4.5.

Many viruses have evolved to use the endocytic pathway for cell entry and transport (Mercer et al., 2010). For example, adenovirus (Ad) serotypes 3 and 7 have relatively long residence times in endosomes. The endosomal pathway was identified as the route used by Ad7, as virions were observed to colocalize with LE and LY marker proteins, including Rab7 and Lamp1, during viral entry and before viral egress from this compartment (Miyazawa et al., 2001). Despite trafficking through this pathway, Ad7 escapes degradation in these organelles. This virus traffics through low lysosomal pH, and the Ad fiber protein confers the Ad7 capsid the capacity to escape to the cytoplasm at low pH escape.

2.2. Virus entry is dependent on endosomal intraluminal acid pH

The dependence of ASFV infection on endosomal acid pH was reported several years ago (Valdeira and Geraldes, 1985) as infection was sensitive to a number of lysosomotropic agents (Alcami et al., 1989a). Fusion with the cell membrane artificially induced by lowering the pH of the medium was not followed by successful infection in cells treated with lysosomotropic drugs. This observation implied that this membrane fusion does not bypass the endocytic pathway for viral entry and that these virions are degraded in the cytoplasm (Valdeira et al., 1998). More recent studies showed that ASFV infectivity was severely decreased by drugs that block endosomal intraluminal acidification such as bafilomycin A1 (Baf) and ammonium chloride (Cuesta-Geijo et al., 2012). In fact, this blockage could not be reversed by exposure of the cells to an acidic medium. Similarly, an acidic medium cannot reverse dynasore-induced inhibition of endocytosis (Cuesta-Geijo et al., 2012). In conclusion, both endocytosis and intraluminal acidification of the endosome are required for successful ASFV infection. These results are summarized in Fig. 1.

2.3. ASFV desencapsidation occurs at late endosomes

The requirement for endosomal acidification was observed to be relevant before the first hour post-infection (30–45 mpi), but not thereafter. At this time, virions in the endosomes undergo desencapsidation, a necessary step for uncoating prior to egress to the cytosol to start replication.

ASF virions are *ca.* 200 nm in diameter and consist of a DNA-containing central nucleoid surrounded by core shell proteins derived by processing of viral polypeptides, pp220 and p62 (Salas and Andres, 2012). The ASF viral genome is protected by a protein shell termed capsid. The capsid has an icosahedral structure, which is composed of many subunits of structural protein p72. The capsid surrounds the inner envelope. The outer viral envelope is obtained by virus budding through the plasma membrane but is dispensable for infection (Andres et al., 2001).

Viral structure undergoes major conformational changes for an eventual release of genomic information, a stepwise process termed uncoating. It is crucial that uncoating does not prematurely expose the viral genome, since this would lead to degradation and/or failed transport to the replication site. Incoming virion capsids detected with antibodies against viral capsid proteins (p72 or pE120R) colocalize with early endosomes within the first minutes of infection (1–15 mpi) but not with other mature acidic compartments (Cuesta-Geijo et al., 2012). In fact, the inhibition of endosomal acidification with Baf impedes both acidification and viral desencapsidation, as shown by the detection of viral capsid protein staining in LEs expressing Rab7 exclusively under these conditions. Instead, viral core protein p150 colocalize with Rab7-positive LEs lacking viral capsid staining in control conditions (Cuesta-Geijo et al., 2012). Protein p150 is one of the products

obtained from the proteolytic cleavage of ASFV pp220 core shell protein (Salas et al., 2012; this issue). Moreover, recent electron microscopy studies showed that endocytic traffic through LEs is accompanied by changes in virion ultrastructure, these leading to the desencapsidation of genome-containing cores (Hernaez et al., 2012a).

All together, these data indicate that viral desencapsidation occurs in the acid pH of LE compartments between 30 mpi and 45 mpi. Moreover, this desencapsidation is a key step to ensure that the virion progresses through uncoating and egress in order to start replication. These data imply that ASFV belongs to the category of late-penetrating viruses (Brabec et al., 2006; Lozach et al., 2010; Mercer et al., 1996; Sieczkarski and Whittaker, 2003).

Moreover, Rab7 GTPase activity is crucial for ASFV infectivity, as shown with knock-out function dominant-negative mutants (Cuesta-Geijo et al., 2012). Similarly, the interconversion of phosphoinositides, which coordinate the assembly of effectors to allow endosomal maturation, is required for successful ASFV infection. The inhibition of enzymes that mediate this interconversion, such as phosphoinositide-3-kinase (PI3K), by wortmannin (Sanchez et al., 2012) and inhibitors of PIKfyve, an enzyme that mediates the conversion from phosphatidylinositol 3 phosphate (PtdIns3P) to phosphatidylinositol-3,5-bisphosphate (PtdIns(3,5)P_2) (Jefferies et al., 2008), profoundly impairs fusion endosome dynamics and consequently ASFV infection (Cuesta-Geijo et al., 2012). In conclusion, the early steps of ASFV infection are strongly dependent on endosomal pathway maturation. Future research should be conducted to identify the viral components involved in the further steps required to complete uncoating after desencapsidation and to determine the fate of other internal membranes and the precise mechanism of viral egress from the endosome before virus replication starts.

3. Microtubules during ASFV entry

Incoming ASFV virions reach the replication site in the perinuclear area, close to the microtubule organizing center (MTOC; Alonso et al., 2001). One of the steps required for endosomal maturation includes endosome progression toward the perinuclear area through microtubules (Huotari and Helenius, 2011). In fact microtubule depolymerizing agents, such as nocodazole, impair virus trafficking (Alonso et al., 2001; de Matos and Carvalho, 1993; Heath et al., 2001). Trafficking of ASFV relies on microtubules, and previous reports have shown that this virus requires functional microtubules for successful infection. Moreover, the activation of Rac1, a molecule that also triggers microtubule stabilization, is crucial during early infection (Quetglas et al., 2012).

3.1. ASFV p54 interaction with microtubule motor dynein

One of the major structural proteins of ASFV, p54, interacts directly with the 8-kDa light chain of the microtubule motor protein dynein (dynein light chain 1 or DLC1) (Alonso et al., 2001). Cytoplasmic dynein is a minus-end-directed microtubule motor protein that mediates a wide range of functions, including the transport of organelles, proteins and viruses to defined subcellular sites of action (Vallee et al., 2012). Binding of dynein to p54 is a high affinity chemical interaction that forms a stable-molecular-weight-complex *in vitro*. A putative p54 binding surface on DLC1 has been defined by nuclear magnetic resonance (NMR) spectroscopy (Hernaez et al., 2010). A short peptide sequence mimicking the viral protein DLC1-binding domain binds and competes for the binding of the viral protein. The relevance of the p54-dynein interaction in infected cells is highlighted by the observation that the use of this short sequence to compete with this interaction in infected Vero cells results in a marked decrease in virus infectivity, viral replication and finally virus production (Hernaez et al., 2010).

Interestingly, sera from pigs surviving infection presented antibodies against p54 DLC1-binding domain (DBD) and immune mice sera raised to this domain reduced virus infection plaques in neutralization assays (Escribano et al., 2012; this issue). These observations led to the conclusion that p54 DBD is implicated in antibody-mediated virus neutralization.

Moreover, other functions have been postulated for p54 at late stages of infection. This protein is important for virus morphogenesis, and it participates in the recruitment of viral membranes to assembly sites, as shown with the inducible mutant vE183Li (Rodriguez et al., 2004). This mutant triggers virus assembly arrest, and this phenotype is partially reversible when p54 expression is induced at 12 hpi, as would be expected for a p54 function exerted at late times after infection.

Interestingly, exposure of viral particles to an acidic medium can induce substantial changes that are relevant for transport linked to microtubules. Most Ad serotypes enter cells by clathrin-mediated endocytosis, and the pH inside the endosomes plays a crucial role by inducing conformational changes in a viral protein. Ad5 hexon protein exposed to an acid pH enhances dynein binding through intermediate and light-intermediate chains (Scherer and Vallee, 2011). These data provide physiological evidence of the relevance of Ad exposure to endosomal pH and dynein binding for efficient infection.

In contrast, ASFV p54 expressed in *E. coli* interacts with dynein at basic pH *in vitro*. ASFV p54 is located on the internal membrane of the virion and can be externally exposed between capsomers when the capsid is intact (Rodriguez et al., 2004). Nevertheless, further studies are required to clarify whether desencapsidation of the virus in acidic endosomes facilitates p54 interaction with dynein motor protein, thus driving desencapsidated virions to the MTOC to start virus replication. In fact, in several virus models, the low pH of endosomes is relevant for genome release by a number of mechanisms (Fuchs and Blaas, 2010; Zaitseva et al., 2010).

3.2. Open questions

Further structural studies are probably required in order to relate these results with the successive uncoating steps of the virion in order to establish at which step p54 may access to microtubules and motors. Future research should focus on the early steps of ASFV infection before replication takes place, as these phases are essential targets in the design of intervention strategies against the disease.

4. ASFV at the nucleus

Early ASFV transcription start using processing enzymes packaged in the virion core (Dixon et al., 2012). These enzymes required for DNA replication are expressed immediately following virus entry into the cytoplasm from partially uncoated core particles. ASFV site of viral replication is predominantly cytoplasmic in defined perinuclear factories as characterized by early ultrastructural studies (Breese and DeBoer, 1966). However, ASFV DNA replication presents an initial stage at the nucleus (Garcia-Beato et al., 1992; Tabares and Sanchez Botija, 1979). Like other viruses belonging to the nucleocytoplasmic large DNA virus superfamily such as poxviruses, ASFV requires intact nuclei for replication (Dixon et al., 2012; Ortin and Vinuela, 1977). Nevertheless, while poxviruses only require nucleus-derived cellular factors, ASFV DNA is detected in the nucleus and cytoplasmic replication sites by *in situ* hybridization and radioactive labeling (Ballester et al., 2010; Garcia-Beato et al., 1992; Rojo et al., 1999). Short viral DNA nuclear

fragments are synthesized in the proximity of the nuclear membrane and then, transported to the cytoplasmic replication factory (Garcia-Beato et al., 1992). ASFV DNA found in mature viral particles is derived from both nuclear and cytoplasmic fragments (Ortin et al., 1979; Rojo et al., 1999)

Moreover, viral proteins p37 and p14 can be targeted to the nucleus (Eulalio et al., 2004). These proteins are products of polyprotein pp220, a component of the ASFV core shell (Salas and Andres, 2012). ASFV p37 is transported to the nucleus and exported to the cytoplasm, independent of the CRM1-mediated nuclear import, and therefore, it may be involved in ASFV DNA nucleocytoplasmic transport (Eulalio et al., 2006, 2007). Recent studies reported that ASFV infection disrupts nuclear organization at an early stage of infection (Ballester et al., 2011). Increased lamin A/C phosphorylation is found at 4 hpi, followed by lamina network disassembly in the proximity of the replication site. Other nuclear elements that are redistributed include RNA polymerase II, the splicing speckle SC35 marker, and the B23 nucleolar marker. The impact of nuclear disorganization is reflected by the presence of lamin and other nuclear envelope markers in the cytoplasm at late infection stages (Ballester et al., 2011; Basta et al., 2010).

5. Viral factory formation

5.1. Aggresomes and HDAC6

ASFV specifically binds dynein and migrates toward MTOC to reach perinuclear viral replication sites and form structures known as viral factories (VFs) or the viral replication organelle. Similarities between aggresomes and ASFV VFs described several years ago (Heath et al., 2001) raised the possibility that ASFV uses the aggresome pathway to concentrate cellular and viral proteins, thus facilitating replication and assembly (Wileman, 2007). Cytoplasmic histone deacetylase 6 (HDAC6), through its simultaneous interaction with ubiquitinated proteins and dynein motors (Fig. 2F), is a key element that mediates the selective disposal of protein aggregates and cytotoxic misfolded proteins by sequestering activity in cellular "storage bins" called aggresomes (Boyault et al., 2007b; Rodriguez-Gonzalez et al., 2008). HDAC6 is a major cytoplasmic tubulin-deacetylase, a specific member of class II HDACs (Hubbert et al., 2002; Matsuyama et al., 2002; Zhang et al., 2003). HDAC6 binds to both mono- and poly-ubiquitinated proteins (Boyault et al., 2007a) and dynein proteins, thereby recruiting protein cargo to dynein motors in order to transport misfolded proteins on the microtubule cytoskeleton to aggresomes (Kawaguchi et al., 2003). Many cellular trafficking compartments are organized by microtubule motor proteins such as dynein, and they tend to cluster in the MTOC adjacent to the nucleus.

We report new results that suggest that HDAC6 is not involved in the formation of the ASFV VF. Inhibition of HDAC6 function was performed using the reversible inhibitor tubacin, which impedes the specific interaction of HDAC6 with dynein (Hideshima et al., 2005). Cells were pretreated for 3 h with tubacin at the indicated concentrations in growth medium at 37 °C, followed by cold synchronized infections with a m.o.i. of 1 pfu/cell the Ba71V or of the recombinant fluorescent virus B54GFP (Hernaez et al., 2006). The inhibitor was present throughout the experiment. At 24 hpi, cells were harvested by trypsinization for FACs analysis or lysed for Western blot. Infectivity rates obtained in tubacin-treated cells were normalized to the values in infected control cells. Concentrations of 1–2 μM tubacin (Ding et al., 2008) efficiently increased acetylated tubulin in Vero cells (over 4-fold starting 1 h after addition and reaching a peak at 16 h, as detected by Western blot (Fig. 2A) and confocal laser scanning microscopy (not shown). Nevertheless, at the same doses that increased microtubule acetylation, tubacin did not modify infected cell percentages, as shown by immunostaining for ASFV proteins p30 at 6 hpi and p72 at 16 hpi (Fig. 2B). Nor did this inhibitor alter the detection of infected cells with the recombinant virus B54GFP by flow cytometry (Fig. 2C). Moreover, tubacin did not change early or late viral protein expression (p30 or p72), as shown by Western blot (Fig. 2D). Similarly, viral production was not modified under tubacin-induced HDAC6 inhibition (not shown). Furthermore, confocal microscopy revealed that inhibition of HDAC6 did not alter the formation of VFs and their number, morphology and location were preserved under these conditions. Also, the characteristic vimentin cage was formed around the factory (Fig. 2E). Hence, although the morphology of the ASFV VF is similar to that of aggresomes, the mechanism of viral factory formation is apparently not related with the canonical aggresome pathway mediated by HDAC6 (Fig. 2F).

5.2. Time-lapse imaging of viral factory formation

VFs comprise a robust collection of newly synthesized viral proteins and viral DNA and are located at the perinuclear area corresponding to the MTOC. The formation of these factories remains intriguing. When the first recombinant ASFV expressing GFP fused to viral protein p54 (B54GFP) was used as a tool for live-imaging of the viral infection, the GFP fusion protein was observed to accumulate in a few discrete spots at the perinuclear area about 8 hpi (Hernaez et al., 2006). These multiple VFs or early factories are motile around the nucleus and coalesce in a single location coincident with the MTOC at subsequent time points. We have generated other fluorescent recombinant viruses, these expressing p12-GFP (B12GFP) under p72 promoter control, and p54-mCherry fluorescent protein (B54ChFP) under p54 promoter control, following a similar procedure to that described in Hernaez et al. (2006). These viral fusion proteins exhibited VF localization.

5.3. Morphometric analysis of the ASFV replication organelle

We report on the use of these recombinant fluorescent ASFVs to study the location, morphology and size of VFs in Vero cells and in WSL, a cell line of wild swine origin (Fig. 3). No significant differences in VF size were observed in cells infected with the different recombinant viruses in either cell line ($N_{Vero} = 140$, $N_{WSL} = 50$; ns, $p > 0.05$; Fig. 3A). Moreover, these recombinant viruses showed almost complete superposition in their distribution at the VF (Fig. 3B). VFs showed intense fluorescence as a result of the high amount of proteins accumulated in these replication and assembly areas (Fig. 3B and 4A–C). However, viral DNA, detected by TOPRO3 staining did not show a complete superposition in VFs. These observations suggest an organization with segregated functions for DNA replication and viral protein synthesis in VFs (Fig. 4C).

VFs are well-defined structures with a major axis size (X) *ca.* 5 μm at 16 hpi in Vero cells and *ca.* 6 μm in WSL cells (Fig. 4E). The only differences between these two cell lines were found in the size of VFs. The major axis of the factories was significantly larger in WSL than in Vero cells ($^{***}p < 0.001$ and $^{**}p < 0.01$; Fig. 4E).

At this time point, 34 and 39% of Vero and WSL infected cells, respectively, presented a marked cytopathic effect. Also, in 25% of infected Vero and in 12% of WSL cells, we found multiple VFs as several independent organelle-shaped fluorescent spots prior to coalescence (Fig. 4B and C). These infected cells bearing multiple VFs did not show a marked cytopathic effect in 83% of infected Vero or in 87.5% of WSL cells.

We also addressed organelle organization in Vero cells infected with recombinant viruses B12GFP and B54GFP at 16 hpi. VFs were characteristically devoid of organelle markers. ER staining in infected cells was disperse in the cytoplasm, and sometimes maintained an empty halo around the factory (Fig. 5). Consistent with

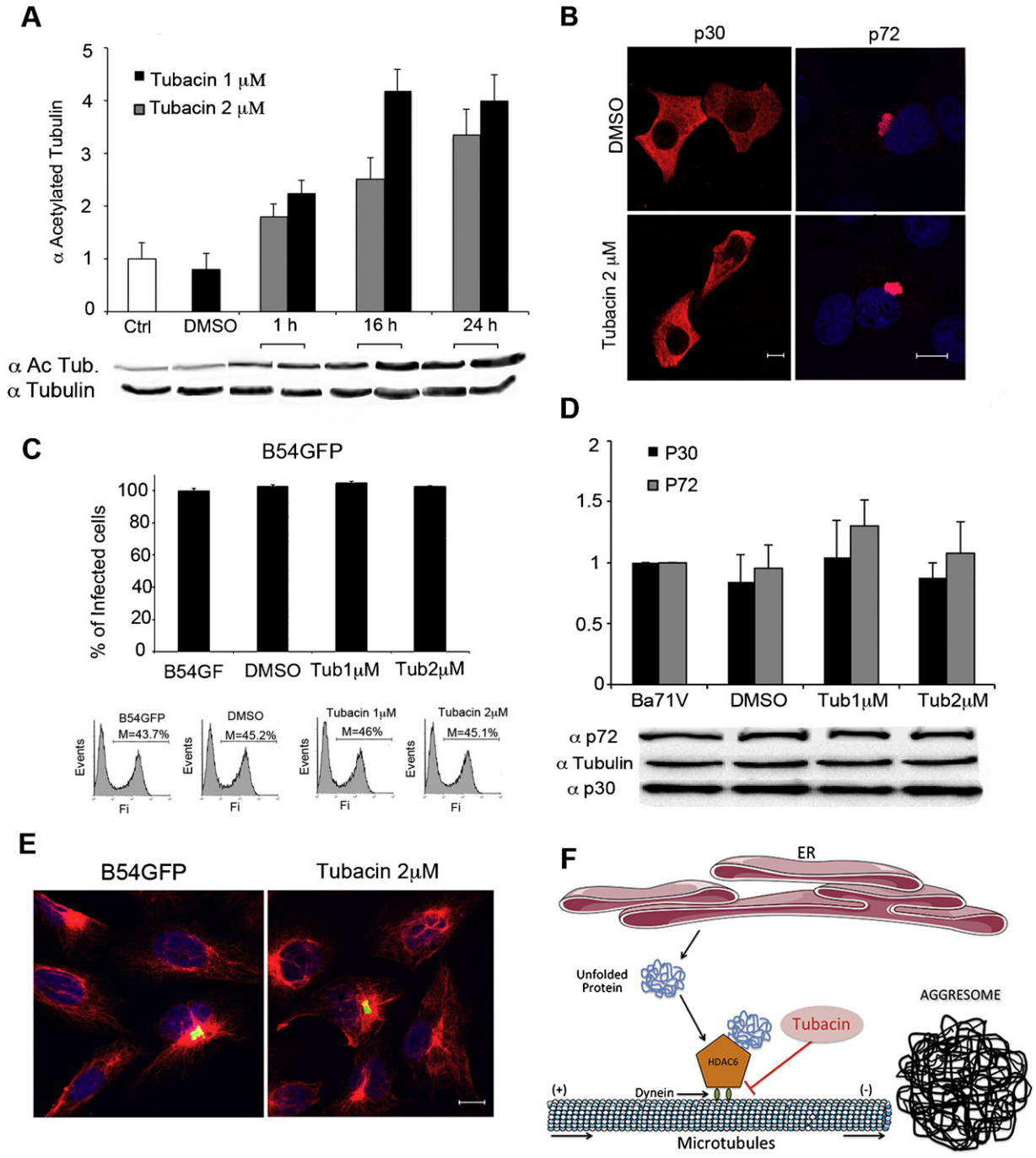

Fig. 2. HDAC6 participation in the viral factory formation. (A) Acetylated tubulin levels in Vero cells treated with HDAC6 inhibitor tubacin, as shown by Western blot. (B) Infectivity was analyzed by immunofluorescence using antibodies against ASFV proteins p30 and p72 to evaluate infected cell numbers. Representative micrographs of p30 (6 hpi) or p72 (16 hpi) in Vero cells infected with BA71V ASFV isolate (m.o.i. of 1 pfu/cell) and treated with tubacin. (C) Flow cytometry analysis of infectivity in Vero cells infected with recombinant B54GFP (m.o.i. of 5 pfu/cell) and treated with tubacin. (D) Western blot analysis of p30 and p72 viral protein expression of tubacin-treated infected cells or controls. (E) Vimentin-cage formation around the viral factories. Vimentin staining of Vero cells treated with tubacin and infected with B54GFP. Bar 10 μm. F. Role of HDAC6 in the canonical pathway of aggresome formation.

previous reports (Rojo et al., 1998), mitochondria were organized around the VFs and the Golgi complex disassembled following microtubules (Netherton et al., 2006), until the signal almost disappeared (Fig. 5). One of the consequences of trans-Golgi network dispersal is that the delivery of membrane protein to the plasma membrane is slowed down.

With respect to cytoskeleton organization, intermediate filaments stained with anti-vimentin antibody proliferated in the cytoplasm forming a robust vimentin cage around the factories (Fig. 5) (Stefanovic et al., 2005). Acetylated tubulin filaments were reduced, and actin cytoskeleton was progressively disassembled, as shown by the faint staining of the few remaining polymerized actin filaments (Fig. 5). Disorganization of cytoskeleton after 24 hpi could affect viral transport to the membrane itself. In fact, extracellular virus production was considerably lower when compared to the intracellular fraction in BA71V Vero infected cells at 24 hpi. This observation could be a consequence of less efficient virus exocytosis.

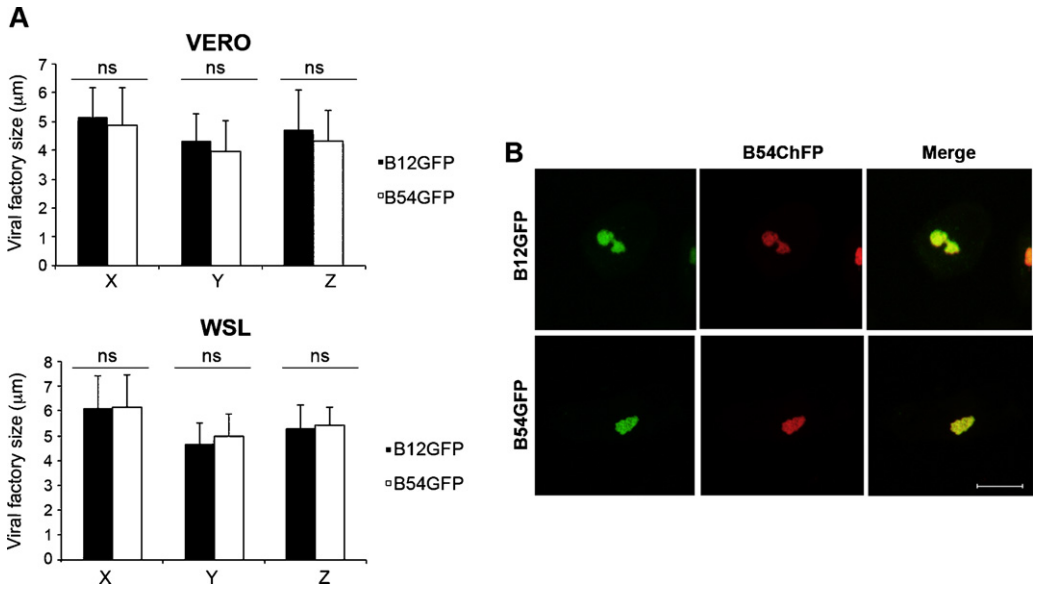

Fig. 3. Recombinant ASFV expressing fluorescent proteins. (A) Comparison of the size of the virus factories in Vero and WSL cells infected with recombinant viruses B12GFP and B54GFP (N_{Vero} = 140, N_{WSL} = 50; ns $p > 0.05$). (B) Representative confocal micrographs of Vero cells infected with the recombinant viruses in (A) and B54ChFP. The merged images show almost complete superposition of these fusion proteins at the viral factories. Bar 10 μm.

5.4. Host factors in viral factory formation

VF formation is governed by several cellular determinants. For example, depolymerization of microtubules results in the dispersal of VFs (de Matos and Carvalho, 1993; Heath et al., 2001). Findings that Rho GTPase inhibitors impair virus morphogenesis, thus resulting in abnormally large VFs (Quetglas et al., 2012), indicate that Rho GTPases have an essential role in the formation of these factories. Transmission electron microscopy (TEM) revealed the accumulation of envelope precursors and immature virions at these enlarged VFs and fewer ribosomes. Also, in cells treated with a Rho GTPase inhibitor, instead of normal virion budding by filopodia, we observed the accumulation of immature virions at the plasma membrane and the absence of filopodia. Actin filopodia formation was described by Jouvenet et al. (2006). Rho-GTPase signaling inhibition may impede cortical actin regulation, thus explaining the absence of filopodia. However, we cannot exclude that mature ASFV particles are required for filopodia formation, as reported for VACV-induced actin tails (Smith et al., 2002).

In fact, host protein lipid modifications, such as the prenylation of small GTPases, are crucial for infection outcome (Quetglas et al., 2012). These post-translational modifications are required for the normal function of small GTPases belonging to the Ras superfamily. Isoprenoids are prenyl donors synthesized as intermediates of the cholesterol biosynthesis pathway. ASFV infection requires the integrity of the entire cholesterol biosynthesis pathway. Statins are potent drug inhibitors of 3-hydroxy-3-methylglutaryl-coenzyme A (HMG-CoA) reductase, the enzyme that catabolizes the conversion of HMG-CoA to mevalonate. Statins are widely used as cholesterol-lowering drugs in humans and can be used as antivirals. Statin treatment (Lovastatin) decreased ASFV progeny and infectivity in Vero cells. This effect is fully reversed by the addition of early precursor mevalonate. Isoprenoids generated in the cholesterol biosynthesis pathway, geranygeranyl pyrophosphate (GGPP) and farnesyl pyrophosphate (FPP), are prenyl donors for protein posttranslational modifications. Farnesylation or geranylgeranylation of cellular and viral proteins are required at several infection steps. Intact pools of GGPP and FPP are required for viral replication (Quetglas et al., 2012). Rac1 is a geranylgeranylated protein that is important during early stages of infection (Quetglas et al., 2012), and its relevance has been discussed above.

ASFV encodes a transprenyltransferase (ORF *B318L*), which is an essential and late gene (Alejo et al., 1997). FPP and GGPP are formed in the reaction catalyzed by the viral enzyme. This enzyme has the unique characteristic that it is associated with precursor viral membranes derived from the ER at the viral assembly sites (Alejo et al., 1999; Andres et al., 1997). GGPP synthesized by B318L product serves as a substrate for protein prenylation, required during virus replication and morphogenesis.

6. ER stress and unfolded protein response

6.1. Overexpression of chaperones and ER stress caspase 12 activation

As obligate intracellular pathogens, viruses have evolved to exploit cellular responses to support viral replication. Viral infection leads to the modification of numerous signaling pathways including antagonizing or activating of specific cellular targets at distinct stages of the replication cycle. Several of these pathways belong to antiviral defense mechanisms such as cellular stress and/or host antiviral innate immune response.

By means of two-dimensional electrophoresis and matrix-assisted laser desorption/ionization peptide mass fingerprinting (MALDI PMF), a wide proteomic analysis of the cellular proteins that modify their expression upon ASFV infection led to identification of the overexpression of several chaperones, such as heat shock proteins 70, 27 and prohibitin, especially after 10–24 hpi (Alfonso et al., 2004). The high level of viral protein production at the ER saturates the protein folding capacity of chaperones. This saturation disturbs ER homeostasis, thereby inducing the so called Unfolded Protein Response (UPR).

ER stress after ASFV infection is reflected by the activation of caspase 12, which follows similar temporal dynamics to mitochondrial caspase 9 and effector caspase 3 activation. Also chaperones, calnexin and calreticulin, but not ERp57 or BiP, are over expressed after infection (Galindo et al., 2012).

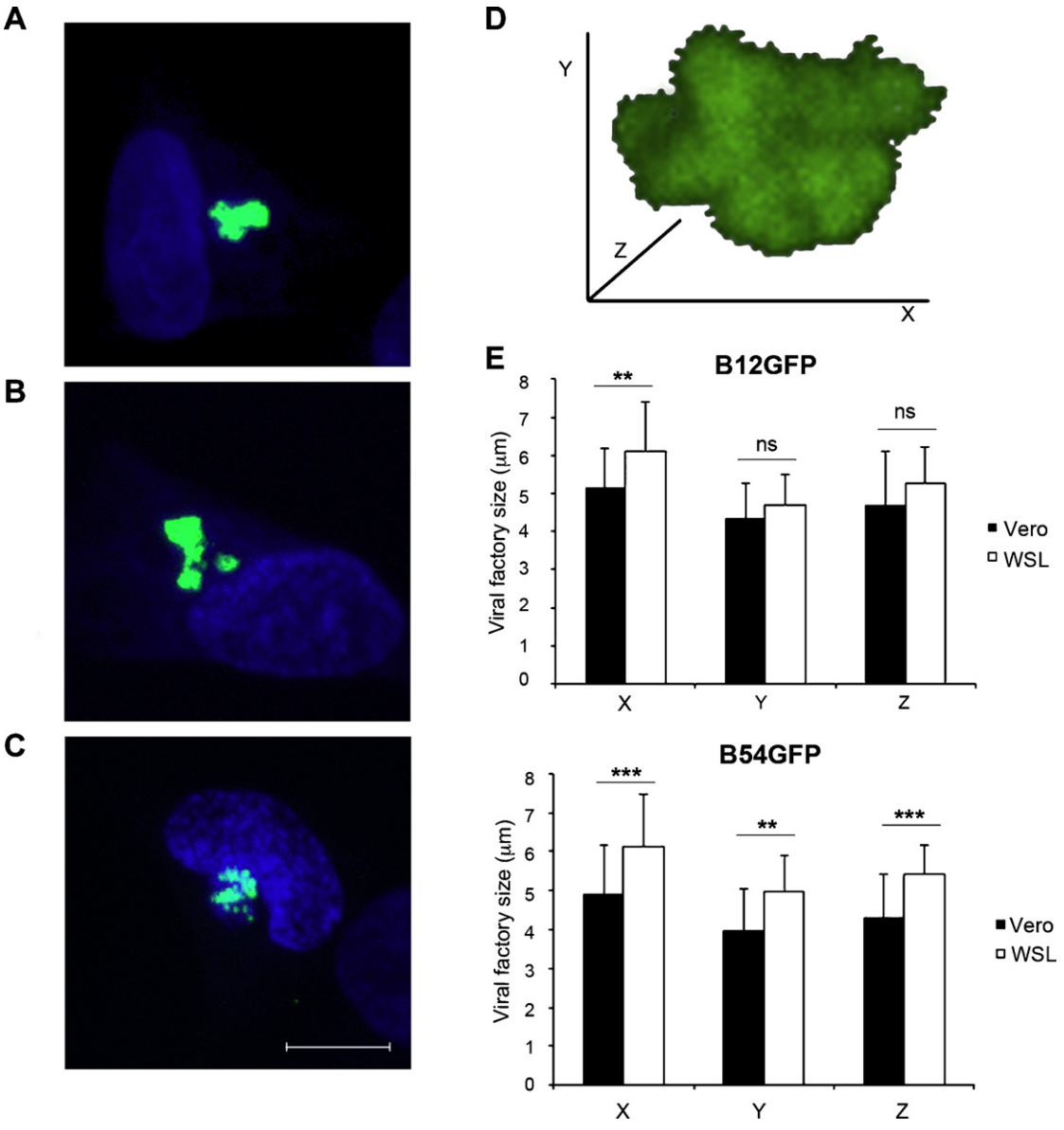

Fig. 4. Morphology of the ASFV viral factory. (A)–(C) are representative confocal micrographs of viral factories; as a typical single compact fluorescent spot (A) or as multiple viral factories (B) and (C). Bar 10 μm. (D) Three-axis dimensions of the viral factories in Vero and WSL cells infected with recombinant viruses B12GFP and B54GFP at 16 hpi were analyzed. Image acquisition of 13 *Z*-stacks per viral factory from $N_{Vero} = 140$ and $N_{WSL} = 50$ cells infected with these recombinant viruses was performed by confocal laser scanning microscope (Leica) and tridimensional reconstruction, and image analysis was done with the Leica Application Suite Advanced software. E. Graphics show means and standard deviations of *X*, *Y* and *Z* axis in μm. Major axis (*X*) was significantly larger in WSL cells when compared to Vero cells $^{***}p < 0.001$ or $^{**}p < 0.01$.

6.2. UPR pathways control and ATF6 translocation

Three ER transmembrane proteins function as UPR sensors, namely protein kinase-like ER resident kinase (PERK), inositol-requiring enzyme 1 (IRE1) and activated transcription factor 6 (ATF6). In their steady state these proteins are associated with the chaperone BiP/Grp78, which prevents their aggregation and further activation. Under misfolded protein accumulation, BiP is released, thereby leading to the UPR (Fig. 6). UPR pathways transcriptionally activate a number of genes involved in protein degradation (Fig. 6). Nevertheless, according to previous data, several of these genes lack apparent activation (Galindo et al., 2012; Netherton et al., 2004).

ATF6 is activated and translocated from the ER to the nucleus and VFs (Galindo et al., 2012). Activation of the ATF6 branch and its transcriptional activation of chaperone-encoding genes might benefit the virus by assisting the folding of accumulated proteins and preventing protein aggregation (Fig. 6). It is relevant to mention here that VACV infection induces the sequester of crucial translation initiation factors within VFs in order to increase the efficiency of virus transcription and translation "on site". This is yet another mechanism by which viral gene expression is promoted (Katsafanas and Moss, 2007).

Furthermore, Bap31 is not activated by the fragmentation of p20 in ASFV-infected cells. This observation indicates the absence of pro-apoptotic signaling between the ER and mitochondria. Interestingly, a serine protease inhibitor that impairs ATF6 activation abolishes both virus infectivity and virus production. This compound inhibits ASFV-induced activation of caspase 12, 3 and 9 but not staurosporine-induced caspase 3 activation. These findings reveal that this effect was highly specific for the virus infection. Conversely, inhibition of caspase 12 activation is not relevant for virus infection (Galindo et al., 2012).

Selective regulation of the UPR has been described for other double-stranded-DNA viruses, such as the cytomegalovirus (CMV)

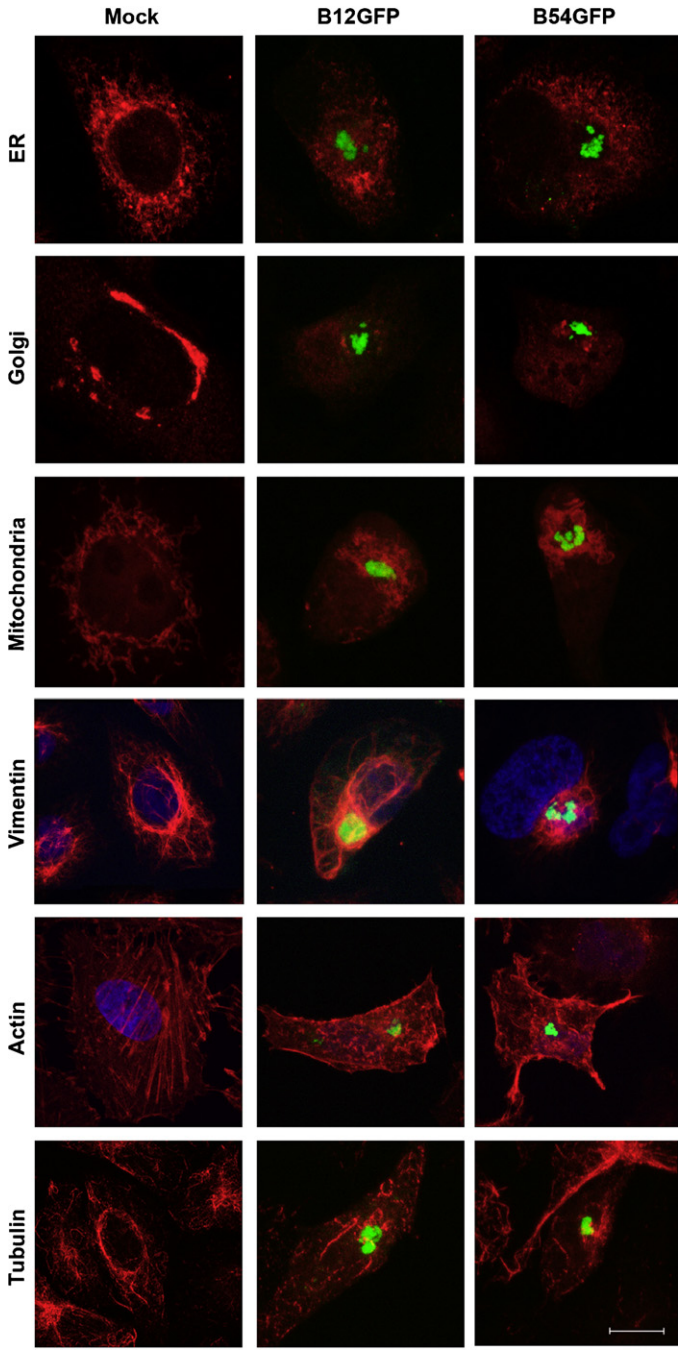

Fig. 5. Viral factories, cellular organelles and cytoskeleton. Intracellular structures in Vero cells infected with ASFV recombinant viruses B12GFP and B54GFP (m.o.i. of 1 pfu/cell) at 16 hpi and stained for ER (α-PDI), Golgi (α-TGN46), mitochondria (Mitotracker CMXRos), α-Vimentin-Cy3, AF594 phalloidin for actin and α-acetylated tubulin AF594. No labeling for any organelles inside the viral factories was observed. At this time point, ER staining was dispersed, Golgi apparatus had virtually disappeared, and mitochondria were organized around the viral factory. Vimentin filaments proliferated and accumulated in the viral factory forming a vimentin cage, along with actin cytoskeleton fiber disassembly. Acetylated tubulin lost its organization and accumulated around the viral factories. Bar 10 μm.

(Isler et al., 2005) and herpes simplex virus 1 (HSV-1) (Cheng et al., 2005). In fact, ASFV protein DP71L is involved in ATF4 downregulation and CHOP inhibition (Zhang et al., 2010). Future research should identify other possible viral protein candidates to mediate such regulation.

7. ASFV and apoptosis

7.1. Membrane blebbing and virus dissemination

Among the diverse ASFV-cell interactions, the manipulation of cell death and survival pathways is a key factor by which the cell lifetime is lengthened in order to ensure completion of viral replication. ASFV induces apoptosis in the target cell at relatively late times after infection (24–48 hpi) (Ramiro-Ibanez et al., 1996). The dynamics of caspase expression shows a late profile, starting with ER stress caspase 12 and mitochondrial upstream caspase 9 activation at 16 hpi, followed by executor caspase 3 activation at 48 hpi (Galindo et al., 2012). The activation of executor caspases causes proteolysis of DNA repair enzymes, DNA replication factors and cytoskeleton regulators, and cleavage of lamina, thus leading to final DNA fragmentation and chromatin condensation. Also, at the cytoplasm, cleavage of gelsolin, fodrin, and actin causes cytoplasmic vacuolization. Shortly after, the apoptotic cell starts to lose contacts with neighboring cells (Hernaez et al., 2006). At the end of an apoptotic process of any origin, caspase activation of Rock-I GTPase and myosin-actin contractile force generation produce the characteristic cytoplasmic membrane blebbing. Finally, cell shrinkage occurs, accompanied by the formation of membrane vesicles filled with fragmented nucleus, referred to as apoptotic bodies. The apoptotic bodies and vesicles derived from ASFV-infected cells are filled with viral particles and this has been postulated to be an efficient system for virus spread (Hernaez et al., 2006). In fact, Rock-I implication in membrane blebbing in ASFV-infected cells was demonstrated by using Rock-I and myosin-II ATPase inhibitors (Galindo et al., 2012). Moreover, we found that the inhibition of membrane blebbing reduces extracellular virus production (Galindo et al., 2012). Blebbing suppression at late infection, either using a Rock-I inhibitor (Y-27632) or a myosin-II ATPase inhibitor (Blebbistatin), reduces the extracellular virus fraction but does not modify total virus production. In comparison with common virus exocytosis, the process of membrane blebbing is crucial for efficient virus spread, especially at late post-infection times, when the microtubule and actin cytoskeleton are severely impaired.

7.2. ASFV induction of apoptosis

Cell death regulation by ASFV (Fig. 7) is a complex equilibrium between induction and inhibition signals (Reviewed in Hernaez et al., 2004). Although the execution of apoptosis in the target cell is a relatively late event, the signal triggering this process has been reported to occur early after virus interaction with the host cell. The apoptosis initiation signal occurs after virus binding but prior to ASFV early protein synthesis and virus replication (Carrascosa et al., 2002). Some viruses induce apoptosis solely by interaction with the cell membrane (Brojatsch et al., 1996). However, this was not found to be the case for ASFV, as UV-inactivated virus failed to induce caspase expression or apoptosis. ASFV uncoating is required to trigger apoptosis and is inhibited with lysosomotropic drugs that impair endosomal acidification (Carrascosa et al., 2002). VACV also induces apoptosis at a post-binding step associated with cell entry (Ramsey-Ewing and Moss, 1998). It has been proposed that the interaction of p54 with microtubule motor protein DLC1 during early virus transport competes for pro-apoptotic Bim binding to DLC1. This would free Bim in the cytosol to exert its apoptotic function at the mitochondrial membrane (Hernaez et al., 2004).

7.3. Apoptosis inhibitor ASFV genes

Despite this early trigger, ASFV-infected macrophages undergo apoptosis at late stages of infection, thus indicating that other virus genes negatively regulate apoptosis (Ramiro-Ibanez et al., 1996).

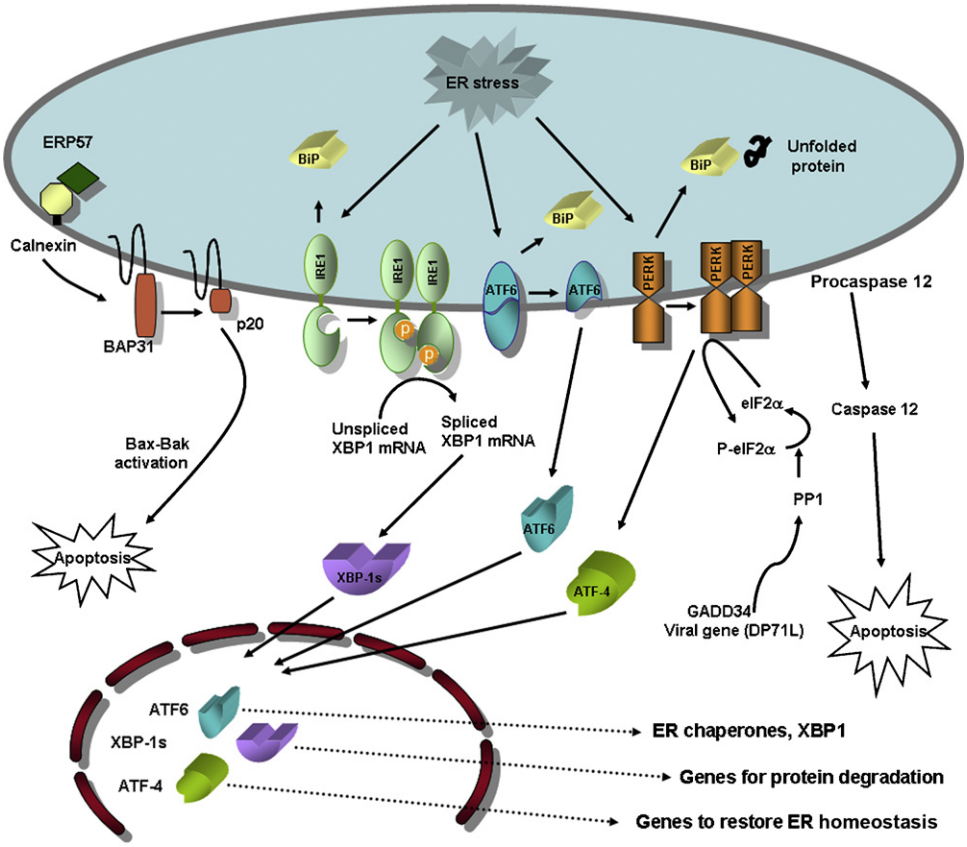

Fig. 6. ER stress and unfolded protein response pathways. When misfolded-proteins accumulate at the ER, sensor GRP78/BiP dissociates from the three endoplasmic reticulum stress receptors. Activated PERK blocks general protein synthesis by phosphorylating eukaryotic initiation factor 2 (eIF2a) and enables translation of ATF4, a transcription factor. ATF4 translocates to the nucleus and induces the transcription of genes required to restore ER homeostasis. ATF6 is activated by proteolysis and regulates the expression of ER chaperones and XBP1, another transcription factor. The spliced form of XBP1 protein, carried out by IRE1, controls the transcription of genes involved in protein degradation. Calnexin acts as a scaffold for the cleavage of the ER transmembrane protein Bap31 and thus for the generation of the pro-apoptotic p20 under ER stress. The Bap31 p20 fragment directs pro-apoptotic crosstalk between the ER and mitochondria. Caspase 12 is also cleaved to an active form in response to ER stress. ASFV-induced expression of caspase 12 and ATF6 is translocated to the nucleus and the viral factories while other UPR pathways can be tightly controlled by the virus.

To prevent premature cell death and ensure virus replication, ASFV, like other large DNA viruses, encodes for several apoptosis inhibitor genes (Fig. 7). The viral Bcl2 homolog (vBcl2) *A179L/5HL* is a conserved, essential gene encoding a 19-kDa protein named p21 (Neilan et al., 1993; Revilla et al., 1997). *A179L* protects cells from apoptosis, even when expressed in heterologous systems such as VACV or baculovirus (Brun et al., 1996, 1998). This vBcl2 contains the highly conserved domains of cellular Bcl2 (cBcl2)-related proteins, BH1, BH2 and BH3, but lacks the Bcl2 transmembrane domain (Afonso et al., 1996; Brun et al., 1996). *A179L* BH1 domain is conserved and functionally similar to cBcl2, including the relevant Gly-85 (Gly-145 in cBcl2), whose single mutation to Ala abrogates its capacity to protect cells from apoptosis (Revilla et al., 1997). vBcl2 *A179L* is expressed both at early and late times after infection, thus supporting the notion that this protein plays a crucial role in cell survival at various steps of the ASFV life cycle.

A179L product inhibits the action of several pro-apoptotic BH3-only proteins, known to be rapid inducers of apoptosis, such as activated Bid, BimL, BimS, BimEL, Bad, Bmf, Bik, Puma, and DP5 (Galindo et al., 2008). It also interacts at the mitochondrial membrane, A179L action is exerted on key pro-apoptotic Bcl2 family members, such as Bax and Bak (Fig. 7). Interestingly, A179L interacts only with active forms of Bid, not with the non-cleaved full-length Bid protein. Thus, A179L is a highly selective inhibitor.

Also, the late ASFV gene homolog to IAP proteins inhibits caspase 3 (Nogal et al., 2001) and activates NFkB (Rodriguez et al., 2002). Lectin-like E153R protein, which acts in the p53 pathway, was the first ASFV protein described with anti-apoptotic activity (Hurtado et al., 2004; Neilan et al., 1999). A238L is an early-late multifunctional protein that inhibits nuclear factors involved in immune responses NFkB (Powell et al., 1996), and the nuclear factor of activated T cells NFAT (Miskin et al., 1998). A238L inhibits NFkB interaction with the p65 subunit of NFkB (Revilla et al., 1998) by inhibiting CBP/p300 co-activators (Granja et al., 2006). A238L binds to calcineurin, thus impairing its phosphatase activity, which regulates NFAT (Abrams et al., 2008; Miskin et al., 2000). And NFAT modulates COX-2/PGE2 pro-inflammatory responses (Granja et al., 2004). The complex functions of this gene have been reviewed by Revilla et al. (this issue).

Moreover, ASFV encodes a homolog of the neurovirulence factor ICP34.5 of HSV-1 and the cellular gene *GADD34*. This homolog is the *DP71L* (*23NL/MyD 88*) gene (Zsak et al., 1996). The cytoprotective effect of *DP71L* is exerted by binding the catalytic subunit of protein phosphatase 1 (PP1). This binding causes the dephosphorylation of eukaryotic translation initiation factor 2α (eIF2α), thereby preventing the inhibition of protein synthesis produced by ER stress and the UPR (Rivera et al., 2007).

The prevention of the protein synthesis inhibition caused by eIF2α phosphorylation is an important virus-host interaction that ensures viral protein synthesis and cell survival in several virus models. HSV-1 ICP34.5 (He et al., 1997), papilloma virus (Kazemi et al., 2004), and coronavirus (Cruz et al., 2011) follow a similar strategy to that used by ASFV to overcome protein synthesis inhibition during its adaptation to the host. Moreover, a number of viruses have evolved mechanisms to inhibit viral nucleic acid sensing by interferon-inducible protein kinase (PKR) and activation of eIF2α,

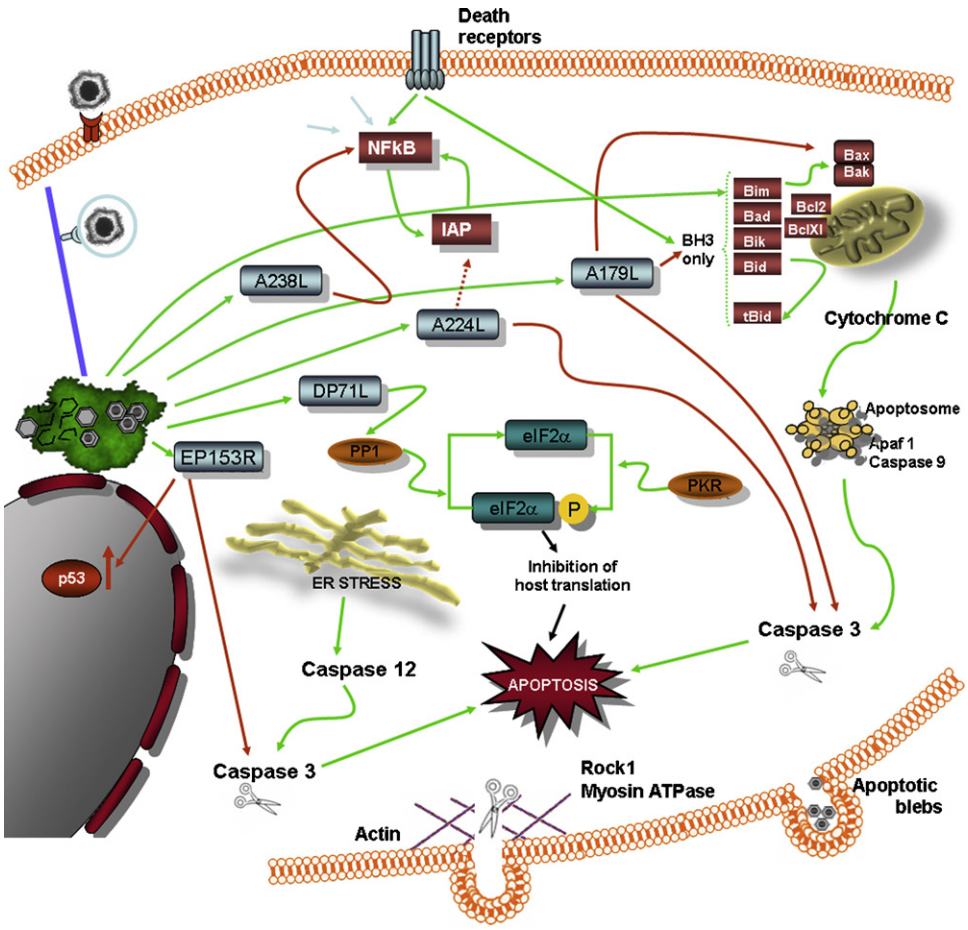

Fig. 7. Apoptosis pathways in ASFV infection. Major pathways of apoptosis activation (green) or inhibition (red) are summarized in this diagram. ASFV induces the activation of mitochondrial caspase 9, caspase 12 and executor caspase 3. The virus encodes several apoptosis inhibitor genes, namely *A238L, A224L, EP153R, DP71L* and *A179L*. Some of their functions are summarized. The function of these genes is required to prevent premature cell death, an event that would impair viral replication. Finally, late execution of apoptosis produces nuclear fragmentation, cytoplasmic vacuolization and membrane blebbing, giving rise to apoptotic bodies as cytoplasmic remnants surrounded by plasma membrane and filled with virus. These bodies are efficient vehicles for virus dissemination.

the latter promoting cell death (Domingo-Gil et al., 2011; Ramelot et al., 2002). The prevention of PKR-mediated translational arrest is shared by VACV (Sharp et al., 1997), HSV-1 protein Us11 (Poppers et al., 2000), and hepatitis C virus (He et al., 1997), among others.

Interestingly, deletion of DP71L from a virulent ASFV (isolate E70) reduces the virulence of the virus in pigs (Zsak et al., 1996); however, this effect was not reproducible for the highly pathogenic Malawi isolate. Moreover, deletion of this gene does not modify eIF2α phosphorylation. This observation thus suggests the presence of alternative mechanisms to prevent eIF2α phosphorylation (Zhang et al., 2010), as described for other DNA viruses (*e.g.* HSV-1). Also, DP71L inhibits the early induction of ATF4 and its downstream target CHOP (Zhang et al., 2010), a transcription factor that is commonly up-regulated as a result of the UPR, but not in ASFV infection (Galindo et al., 2012; Netherton et al., 2004).

Other functions undertaken by the HSV-1-homologous gene, such as the inhibition of autophagy by means of Beclin-1 inhibition (Orvedahl et al., 2007); do not occur in ASFV DP71L, as described below.

7.4. ASFV regulation of cell survival

In general, the controversial effects of viruses on cell homeostasis are well illustrated in the host systems with which ASFV interacts. This virus encodes for several apoptosis inhibitor genes but finally induces the death of the infected cell. Also, most UPR genes are not activated upon infection; however, ASFV induces ER stress, casapase 12 activation and the UPR. Similarly, ASFV inhibits pro-inflammatory gene transcription; however, this infection induces the secretion of many cytokines both *in vitro* and *in vivo* that underlie the pathogenesis of this virus (Zhang et al., 2010). All together, these observations highlight that several cell responses to virus sensing are strongly counteracted by viruses.

8. ASFV and autophagy

Macroautophagy has the capacity to remove a wide variety of intracellular components, ranging from protein aggregates to whole organelles such as mitochondria, by sequestration and degradation (Mizushima et al., 2008). Cytoplasmic targets are captured within double membrane structures called autophagosomes, which subsequently fuse with lysosomes where the engulfed target is degraded or eliminated. The physiological functions of autophagy include the provision of a source of energy and amino acids by self-digestion in response to cellular stress or nutritional deprivation (starvation). Autophagy integrates with other cell stress responses upon nutrient deprivation, and the presence of reactive oxygen species, DNA damage, protein aggregates and intracellular pathogens (Fig. 8). Autophagy prevents cell death or senescence caused by the accumulation of damaged organelles and large macromolecular aggregates. Interestingly, autophagy may

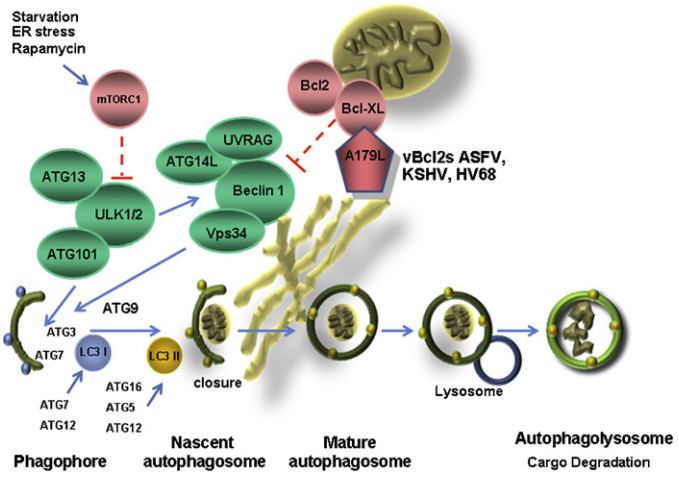

Fig. 8. Autophagic pathways and ASFV A179L Bcl2 homolog regulation. Autophagy is induced by starvation, ER stress, pathogen-associated molecular patterns, redox stress and mitochondrial damage. ULK1 and ULK2 play a key role in autophagy induction, acting downstream of mTORC1. Upon mTORC1 inhibition, for example by starvation, mTORC1 dissociates from the ULK complex, thus leading to its catalytic activation. ULK1 can phosphorylate Ambra1. Beclin1 is a multiprotein complex formed by the allosteric activation of the class III PI3K Vps34 to generate PI3P, which recruits FYVE proteins to mediate the initial stages of the isolation membrane nucleation and autophagosome formation. Anti-apoptotic Bcl2 family members are important regulators of autophagy that interact with Beclin1. Similarly, ASFV A179L homolog inhibits autophagy through interaction of its BH3-binding domain with the BH3 domain of Beclin1. The mammalian LC3 (ortholog of yeast Atg8) is translocated to the initiation membrane of the autophagosome and conjugated with lipids by means of different Atg proteins. This conjugation leads to the conversion of the soluble form of LC3 (LC3-I) to the lipidated LC3-II form. LC3-II is associated with the autophagic vesicle and its biochemical and microscopic detection is used to measure cellular autophagy.

constitute a cellular defense mechanism for virion degradation and it participates in innate immunity.

8.1. Regulation of autophagosome formation

Autophagy begins with the formation of an isolation membrane or phagophore (Fig. 8) and involves several molecules called authophagy proteins (atg). The Atg1/ULK (unc-51-like kinase) complex is downstream of the mammalian target of rapamycin (mTOR) complex 1 (mTORC1) and it plays a key role in autophagy induction (Fig. 8). Upon mTORC1 inhibition, as by starvation, mTORC1 dissociates from the ULK complex, thus causing its dephosphorylation (Mizushima, 2010). Other key molecular complexes in this pathway include Atg6/Beclin1, class III phosphatidylinositol 3-kinase (PI3K), Atg9, and ubiquitin-like proteins Atg12 and Atg8/LC3 conjugation systems.

8.2. DNA viruses control of autophagy

Several DNA viruses keep autophagy under control, probably to prevent the degradation of replicating or newly assembled virions by lysosomal fusion. HSV-1 ICP34.5 targets Beclin1 autophagy protein and inhibits autophagy-dependent virion degradation (Alexander et al., 2007; Orvedahl et al., 2007). Viral Bcl2 homologs encoded by Kaposi's sarcoma herpesvirus (KSHV; (Pattingre et al., 2005) and murine γ-herpesvirus 68 (HV68); (Ku et al., 2008) also inhibit autophagy by a mechanism involving direct interaction with Beclin1. Therefore, there are at least two potential candidates by which to achieve Beclin1 regulation in ASFV, namely the viral homolog to HSV1 ICP34.5 DP71L, and the vBcl2 A179L.

We have shown that A179L interacts directly with Beclin1 while DP71L does not and that the A179L BH3 domain is required for binding (Hernaez et al., 2012b). Transient expression of A179L in HeLa cells inhibits starvation-induced autophagosome formation. Transient expression assays with A179L-GFP showed colocalization with both mitochondria and ER. This subcellular distribution makes it conceivable that A179L plays a dual role, on the one hand interacting with pro-apoptotic BH3-only proteins (Bim, aBid, Bad, Bmf, Bik, Puma, *etc.*) and Bax and Bak at the mitochondrial membrane, and on the other hand, with Beclin1 at the ER. In fact, cellular Bcl2 inhibits apoptosis at the mitochondrial membrane and also suppresses autophagy by interacting with Beclin1 at the ER. The UPR, the major ER stress pathway, is a potent stimulus of autophagy (Buchberger et al., 2010), hence this dual function of Bcl2 points to a close relationship between the two cascades.

In contrast, most RNA viruses have been reported to induce autophagy in infected cells, and in several cases autophagy may enhance viral replication (Reviewed in (Dreux and Chisari, 2010). A number of viruses replicate in multi-membrane vesicles that closely resemble autophagosomes (de Haan and Reggiori, 2008). Given the nature and location of these structures, autophagosomes may serve as sites of viral replication during some infections. Also, membranes associated with viral replication sites are often derived from the ER, which is a potential source for the autophagosomal membrane (Mijaljica et al., 2006). Nevertheless, VACV infection, which uses double-membrane vesicles, is not impaired in autophagy-deficient mice (Zhang et al., 2006). In other viral models, controversial results suggest that the impact of inhibition autophagy on viral infection varies depending on the cell type or the stage of the viral life cycle considered.

We found that ASFV does not induce autophagy in infected cells. ASFV infection did not induce LC3 activation or autophagosome formation in Vero cells infected with the ASFV BA71V isolate (Hernaez et al., 2012b). However, ASFV infection is strongly inhibited by lysosomotropic drugs because of its endosomal-dependent entry mechanism. This is a limitation when studying autophagic flux during infection in the presence of bafilomycin or protease inhibitors. Interestingly, induction of autophagy by starvation and rapamycin prior to ASFV infection reduces viral infectivity. This decrease could be due to the consumption of yet unknown factor/s from the core autophagic pathway required at an early stage of ASFV infection. This notion, together with the interconnection between autophagy regulation and its crosslinks with cell stress and apoptosis in ASFV infection, awaits further investigation.

9. Virus-cell interaction-based analysis of potential therapeutic intervention targets

9.1. Potential applications of antivirals

This chapter has reviewed some key ASFV interactions with the host cell that are crucial for the virus to start and complete productive infection. Several of these molecular systems are viewed as potential targets to consider in a rational vaccine design–something that continues to be an unmet need. Also, some of these systems are sensitive to antivirals. A possible application of antivirals would be to prolong survival in experimental infections with virulent ASFV isolates in order to gain further insight into the pathogenesis of this disease. Longer survival may change the acute course of the disease and eventually allow the swine host to generate an immune response against the virus. In addition, the combination antivirals with experimental vaccination protocols could be useful for the analysis of immune response required for effective protection against the disease. These antiviral/vaccine protocols should be further developed to refine the targets to be selected and to clarify the major obstacles that hinder achievement of a protective immune response against the virus.

9.2. "Druggable" targets at the virus-cell interface

Cholesterol-lowering drugs called statins effectively inhibit ASFV infection *in vitro* (Quetglas et al., 2012). These drugs are of generalized use in humans and their safety is widely proven. Valproic acid, which is used for treatment of neurological disorders, was found to have a potent antiviral effect against a number of enveloped viruses, including ASFV (Vazquez-Calvo et al., 2011) Also, resveratrol and other phytoalexins produced by plants effectively inhibit virus replication (Galindo et al., 2011). Together with extracts from marine microalgae (Fabregas et al., 1999), these plant compounds are antivirals derived from natural sources and they can be administered to animals as a dietary supplement. Other inhibitors that are used in oncological therapy in humans are effective antivirals against ASFV at different infection stages. Examples include serine protease inhibitors (Galindo et al., 2012), PI3K and/or PIKfyve inhibitors (Cuesta-Geijo et al., 2012) and microtubule-depolymerizing drugs (Basta et al., 2010).

Using our knowledge of ASFV-cell interactions, together with insights gained from NMR structure-based design, researchers face the challenge of further developing antiviral treatments and preventive strategies. Antiviral compounds targeting virus-host interactions are already under development. One example is an antiviral peptide that impairs infectivity and viral replication in cultured cells by competing with p54 binding to its cellular target dynein (Hernaez et al., 2010). Like the above-mentioned antivirals targeting cellular mechanisms, this peptide could be used to shed light on unknown cellular mechanisms targeted by ASFV infection and on the induction of protection.

Acknowledgments

This study was supported by grant WT075813 Wellcome Trust Foundation, grant UE EPIZONE FOOD-CT2006-016236 and the grants Consolider CSD2006-00007, AGL2009-09209 and AGL2012-34533, awarded by the *Ministerio de Economia y Competitividad* of Spain.

References

Abrams, C.C., Chapman, D.A., Silk, R., Liverani, E., Dixon, L.K., 2008. Domains involved in calcineurin phosphatase inhibition and nuclear localisation in the African swine fever virus A238L protein. Virology 374 (2), 477–486.

Afonso, C.L., Neilan, J.G., Kutish, G.F., Rock, D.L., 1996. An African swine fever virus Bc1-2 homolog, 5-HL, suppresses apoptotic cell death. Journal of Virology 70 (7), 4858–4863.

Alcami, A., Carrascosa, A.L., Vinuela, E., 1989a. The entry of African swine fever virus into Vero cells. Virology 171 (1), 68–75.

Alcami, A., Carrascosa, A.L., Vinuela, E., 1989b. Saturable binding sites mediate the entry of African swine fever virus into Vero cells. Virology 168 (2), 393–398.

Alcami, A., Carrascosa, A.L., Vinuela, E., 1990. Interaction of African swine fever virus with macrophages. Virus Research 17 (2), 93–104.

Alejo, A., Andres, G., Vinuela, E., Salas, M.L., 1999. The African swine fever virus prenyltransferase is an integral membrane trans-geranylgeranyl-diphosphate synthase. Journal of Biological Chemistry 274 (25), 18033–18039.

Alejo, A., Yanez, R.J., Rodriguez, J.M., Vinuela, E., Salas, M.L., 1997. African swine fever virus trans-prenyltransferase. Journal of Biological Chemistry 272 (14), 9417–9423.

Alexander, D.E., Ward, S.L., Mizushima, N., Levine, B., Leib, D.A., 2007. Analysis of the role of autophagy in replication of herpes simplex virus in cell culture. Journal of Virology 81 (22), 12128–12134.

Alfonso, P., Rivera, J., Hernaez, B., Alonso, C., Escribano, J.M., 2004. Identification of cellular proteins modified in response to African swine fever virus infection by proteomics. Proteomics 4 (7), 2037–2046.

Alonso, C., Miskin, J., Hernaez, B., Fernandez-Zapatero, P., Soto, L., Canto, C., Rodriguez-Crespo, I., Dixon, L., Escribano, J.M., 2001. African swine fever virus protein p54 interacts with the microtubular motor complex through direct binding to light-chain dynein. Journal of Virology 75 (20), 9819–9827.

Andres, G., Garcia-Escudero, R., Vinuela, E., Salas, M.L., Rodriguez, J.M., 2001. African swine fever virus structural protein pE120R is essential for virus transport from assembly sites to plasma membrane but not for infectivity. Journal of Virology 75 (15), 6758–6768.

Andres, G., Simon-Mateo, C., Vinuela, E., 1997. Assembly of African swine fever virus: role of polyprotein pp220. Journal of Virology 71 (3), 2331–2341.

Ballester, M., Galindo-Cardiel, I., Gallardo, C., Argilaguet, J.M., Segales, J., Rodriguez, J.M., Rodriguez, F., 2010. Intranuclear detection of African swine fever virus DNA in several cell types from formalin-fixed and paraffin-embedded tissues using a new in situ hybridisation protocol. Journal of Virological Methods 168 (1–2), 38–43.

Ballester, M., Rodriguez-Carino, C., Perez, M., Gallardo, C., Rodriguez, J.M., Salas, M.L., Rodriguez, F., 2011. Disruption of nuclear organization during the initial phase of African swine fever virus infection. Journal of Virology 85 (16), 8263–8269.

Basta, S., Gerber, H., Schaub, A., Summerfield, A., McCullough, K.C., 2010. Cellular processes essential for African swine fever virus to infect and replicate in primary macrophages. Veterinary Microbiology 140 (1–2), 9–17.

Bernardes, C., Antonio, A., Pedroso de Lima, M.C., Valdeira, M.L., 1998. Cholesterol affects African swine fever virus infection. Biochimica et Biophysica Acta 1393 (1), 19–25.

Boyault, C., Sadoul, K., Pabion, M., Khochbin, S., 2007a. HDAC6, at the crossroads between cytoskeleton and cell signaling by acetylation and ubiquitination. Oncogene 26 (37), 5468–5476.

Boyault, C., Zhang, Y., Fritah, S., Caron, C., Gilquin, B., Kwon, S.H., Garrido, C., Yao, T.P., Vourc'h, C., Matthias, P., Khochbin, S., 2007b. HDAC6 controls major cell response pathways to cytotoxic accumulation of protein aggregates. Genes and Development 21 (17), 2172–2181.

Brabec, M., Blaas, D., Fuchs, R., 2006. Wortmannin delays transfer of human rhinovirus serotype 2 to late endocytic compartments. Biochemical and Biophysical Research Communications 348 (2), 741–749.

Breese Jr., S.S., DeBoer, C.J., 1966. Electron microscope observations of African swine fever virus in tissue culture cells. Virology 28 (3), 420–428.

Brojatsch, J., Naughton, J., Rolls, M.M., Zingler, K., Young, J.A., 1996. CAR1, a TNFR-related protein, is a cellular receptor for cytopathic avian leukosis-sarcoma viruses and mediates apoptosis. Cell 87 (5), 845–855.

Brun, A., Rivas, C., Esteban, M., Escribano, J.M., Alonso, C., 1996. African swine fever virus gene A179L, a viral homologue of bcl-2, protects cells from programmed cell death. Virology 225 (1), 227–230.

Brun, A., Rodriguez, F., Escribano, J.M., Alonso, C., 1998. Functionality and cell anchorage dependence of the African swine fever virus gene A179L, a viral bcl-2 homolog, in insect cells. Journal of Virology 72 (12), 10227–10233.

Buchberger, A., Bukau, B., Sommer, T., 2010. Protein quality control in the cytosol and the endoplasmic reticulum: brothers in arms. Molecular Cell 40 (2), 238–252.

Carrascosa, A.L., Bustos, M.J., Galindo, I., Vinuela, E., 1999. Virus-specific cell receptors are necessary, but not sufficient, to confer cell susceptibility to African swine fever virus. Archives of Virology 144 (7), 1309–1321.

Carrascosa, A.L., Bustos, M.J., Nogal, M.L., Gonzalez de Buitrago, G., Revilla, Y., 2002. Apoptosis induced in an early step of African swine fever virus entry into vero cells does not require virus replication. Virology 294 (2), 372–382.

Carter, G.C., Law, M., Hollinshead, M., Smith, G.L., 2005. Entry of the vaccinia virus intracellular mature virion and its interactions with glycosaminoglycans. Journal of General Virology 86 (Pt 5), 1279–1290.

Cruz, J.L., Sola, I., Becares, M., Alberca, B., Plana, J., Enjuanes, L., Zuniga, S., 2011. Coronavirus gene 7 counteracts host defenses and modulates virus virulence. PLoS Pathogens 7 (6), e1002090.

Cuesta-Geijo, M.A., Galindo, I., Hernáez, B., Quetglas, J.I., Dalmau-Mena, I., Alonso, C., 2012. Endosomal maturation Rab7 GTPase and Phosphoinositides in African Swine Fever Virus entry. PLoS ONE 7 (11), e48853.

Cureton, D.K., Massol, R.H., Saffarian, S., Kirchhausen, T.L., Whelan, S.P., 2009. Vesicular stomatitis virus enters cells through vesicles incompletely coated with clathrin that depend upon actin for internalization. PLoS Pathogens 5 (4), e1000394.

Cureton, D.K., Massol, R.H., Whelan, S.P., Kirchhausen, T., 2010. The length of vesicular stomatitis virus particles dictates a need for actin assembly during clathrin-dependent endocytosis. PLoS Pathogens 6 (9), e1001127.

Cheng, G., Feng, Z., He, B., 2005. Herpes simplex virus 1 infection activates the endoplasmic reticulum resident kinase PERK and mediates eIF-2alpha dephosphorylation by the gamma(1)34.5 protein. Journal of Virology 79 (3), 1379–1388.

de Haan, C.A., Reggiori, F., 2008. Are nidoviruses hijacking the autophagy machinery? Autophagy 4 (3), 276–279.

de Leon, P., Bustos, M.J., Carrascosa, A.L., 2012. Laboratory methods to study African swine fever virus. Virus Research, http://dx.doi.org/10.1016/j.virusres.2012.09.013, This issue.

de Matos, A.P., Carvalho, Z.G., 1993. African swine fever virus interaction with microtubules. Biologie Cellulaire 78 (3), 229–234.

Ding, H., Dolan, P.J., Johnson, G.V., 2008. Histone deacetylase 6 interacts with the microtubule-associated protein tau. Journal of Neurochemistry 106 (5), 2119–2130.

Dixon, L.K., Chapman, D.D., Netherton, C.L., Upton, C., 2012. African swine fever virus replication and genomics. Virus Research, http://dx.doi.org/10.1016/j.virusres.2012.10.020, This issue.

Domingo-Gil, E., Toribio, R., Najera, J.L., Esteban, M., Ventoso, I., 2011. Diversity in viral anti-PKR mechanisms: a remarkable case of evolutionary convergence. PLoS ONE 6 (2), e16711.

Dreux, M., Chisari, F.V., 2010. Viruses and the autophagy machinery. Cell Cycle 9 (7), 1295–1307.

Eulalio, A., Nunes-Correia, I., Carvalho, A.L., Faro, C., Citovsky, V., Salas, J., Salas, M.L., Simoes, S., de Lima, M.C., 2006. Nuclear export of African swine fever virus p37 protein occurs through two distinct pathways and is mediated by three independent signals. Journal of Virology 80 (3), 1393–1404.

Eulalio, A., Nunes-Correia, I., Carvalho, A.L., Faro, C., Citovsky, V., Simoes, S., Pedroso de Lima, M.C., 2004. Two African swine fever virus proteins derived from a

common precursor exhibit different nucleocytoplasmic transport activities. Journal of Virology 78 (18), 9731–9739.
Eulalio, A., Nunes-Correia, I., Salas, J., Salas, M.L., Simoes, S., Pedroso de Lima, M.C., 2007. African swine fever virus p37 structural protein is localized in nuclear foci containing the viral DNA at early post-infection times. Virus Research 130 (1–2), 18–27.
Fabregas, J., Garcia, D., Fernandez-Alonso, M., Rocha, A.I., Gomez-Puertas, P., Escribano, J.M., Otero, A., Coll, J.M., 1999. In vitro inhibition of the replication of haemorrhagic septicaemia virus (VHSV) and African swine fever virus (ASFV) by extracts from marine microalgae. Antiviral Research 44 (1), 67–73.
Fuchs, R., Blaas, D., 2010. Uncoating of human rhinoviruses. Reviews in Medical Virology 20 (5), 281–297.
Galindo, I., Hernaez, B., Berna, J., Fenoll, J., Cenis, J.L., Escribano, J.M., Alonso, C., 2011. Comparative inhibitory activity of the stilbenes resveratrol and oxyresveratrol on African swine fever virus replication. Antiviral Research 91 (1), 57–63.
Galindo, I., Hernaez, B., Diaz-Gil, G., Escribano, J.M., Alonso, C., 2008. A179L, a viral Bcl-2 homologue, targets the core Bcl-2 apoptotic machinery and its upstream BH3 activators with selective binding restrictions for Bid and Noxa. Virology 375 (2), 561–572.
Galindo, I., Hernaez, B., Munoz-Moreno, R., Cuesta-Geijo, M.A., Dalmau-Mena, I., Alonso, C., 2012. The ATF6 branch of unfolded protein response and apoptosis are activated to promote African swine fever virus infection. Cell Death & Disease 3, e341.
Garcia-Beato, R., Salas, M.L., Vinuela, E., Salas, J., 1992. Role of the host cell nucleus in the replication of African swine fever virus DNA. Virology 188 (2), 637–649.
Granja, A.G., Nogal, M.L., Hurtado, C., Del Aguila, C., Carrascosa, A.L., Salas, M.L., Fresno, M., Revilla, Y., 2006. The viral protein A238L inhibits TNF-alpha expression through a CBP/p300 transcriptional coactivators pathway. Journal of Immunology 176 (1), 451–462.
Granja, A.G., Nogal, M.L., Hurtado, C., Salas, J., Salas, M.L., Carrascosa, A.L., Revilla, Y., 2004. Modulation of p53 cellular function and cell death by African swine fever virus. Journal of Virology 78 (13), 7165–7174.
He, B., Gross, M., Roizman, B., 1997. The gamma(1)34.5 protein of herpes simplex virus 1 complexes with protein phosphatase 1alpha to dephosphorylate the alpha subunit of the eukaryotic translation initiation factor 2 and preclude the shutoff of protein synthesis by double-stranded RNA-activated protein kinase. Proceedings of the National Academy of Sciences of the United States of America 94 (3), 843–848.
Heath, C.M., Windsor, M., Wileman, T., 2001. Aggresomes resemble sites specialized for virus assembly. Journal of Cell Biology 153 (3), 449–455.
Hernaez, B., Alonso, C., 2010. Dynamin- and clathrin-dependent endocytosis in African swine fever virus entry. Journal of Virology 84 (4), 2100–2109.
Hernaez, B., Cabezas, M., Muñoz-Moreno, R., Galindo, I., Cuesta-Geijo, M.A., Alonso, C., 2012b. A179L, a new viral Bcl2 homolog targeting Beclin 1 autophagy related protein. Current Molecular Medicine 7.
Hernaez, B., Diaz-Gil, G., Garcia-Gallo, M., Ignacio Quetglas, J., Rodriguez-Crespo, I., Dixon, L., Escribano, J.M., Alonso, C., 2004. The African swine fever virus dynein-binding protein p54 induces infected cell apoptosis. FEBS Letters 569 (1-3), 224–228.
Hernaez, B., Escribano, J.M., Alonso, C., 2006. Visualization of the African swine fever virus infection in living cells by incorporation into the virus particle of green fluorescent protein-p54 membrane protein chimera. Virology 350 (1), 1–14.
Hernaez, B., Guerra, M., Salas, M.L., Andres, G., 2012a. New insights on African swine fever virus entry. In: Poster Communication. XIX International Poxvirus, Asfarvirus & Iridovirus Conference, Salamanca, Spain.
Hernaez, B., Tarrago, T., Giralt, E., Escribano, J.M., Alonso, C., 2010. Small peptide inhibitors disrupt a high-affinity interaction between cytoplasmic dynein and a viral cargo protein. Journal of Virology 84 (20), 10792–10801.
Hideshima, T., Bradner, J.E., Wong, J., Chauhan, D., Richardson, P., Schreiber, S.L., Anderson, K.C., 2005. Small-molecule inhibition of proteasome and aggresome function induces synergistic antitumor activity in multiple myeloma. Proceedings of the National Academy of Sciences of the United States of America 102 (24), 8567–8572.
Hubbert, C., Guardiola, A., Shao, R., Kawaguchi, Y., Ito, A., Nixon, A., Yoshida, M., Wang, X.F., Yao, T.P., 2002. HDAC6 is a microtubule-associated deacetylase. Nature 417 (6887), 455–458.
Huotari, J., Helenius, A., 2011. Endosome maturation. EMBO Journal 30 (17), 3481–3500.
Hurtado, C., Granja, A.G., Bustos, M.J., Nogal, M.L., Gonzalez de Buitrago, G., de Yebenes, V.G., Salas, M.L., Revilla, Y., Carrascosa, A.L., 2004. The C-type lectin homologue gene (EP153R) of African swine fever virus inhibits apoptosis both in virus infection and in heterologous expression. Virology 326 (1), 160–170.
Isler, J.A., Skalet, A.H., Alwine, J.C., 2005. Human cytomegalovirus infection activates and regulates the unfolded protein response. Journal of Virology 79 (11), 6890–6899.
Jefferies, H.B., Cooke, F.T., Jat, P., Boucheron, C., Koizumi, T., Hayakawa, M., Kaizawa, H., Ohishi, T., Workman, P., Waterfield, M.D., Parker, P.J., 2008. A selective PIKfyve inhibitor blocks PtdIns(3,5)P(2) production and disrupts endomembrane transport and retroviral budding. EMBO Reports 9 (2), 164–170.
Jordens, I., Marsman, M., Kuijl, C., Neefjes, J., 2005. Rab proteins, connecting transport and vesicle fusion. Traffic 6 (12), 1070–1077.
Jouvenet, N., Windsor, M., Rietdorf, J., Hawes, P., Monaghan, P., Way, M., Wileman, T., 2006. African swine fever virus induces filopodia-like projections at the plasma membrane. Cellular Microbiology 8 (11), 1803–1811.
Katsafanas, G.C., Moss, B., 2007. Colocalization of transcription and translation within cytoplasmic poxvirus factories coordinates viral expression and subjugates host functions. Cell Host & Microbe 2 (4), 221–228.
Kawaguchi, Y., Kovacs, J.J., McLaurin, A., Vance, J.M., Ito, A., Yao, T.P., 2003. The deacetylase HDAC6 regulates aggresome formation and cell viability in response to misfolded protein stress. Cell 115 (6), 727–738.
Kazemi, S., Papadopoulou, S., Li, S., Su, Q., Wang, S., Yoshimura, A., Matlashewski, G., Dever, T.E., Koromilas, A.E., 2004. Control of alpha subunit of eukaryotic translation initiation factor 2 (eIF2 alpha) phosphorylation by the human papillomavirus type 18 E6 oncoprotein: implications for eIF2 alpha-dependent gene expression and cell death. Molecular and Cellular Biology 24 (8), 3415–3429.
Ku, B., Woo, J.S., Liang, C., Lee, K.H., Hong, H.S., E, X., Kim, K.S., Jung, J.U., Oh, B.H., 2008. Structural and biochemical bases for the inhibition of autophagy and apoptosis by viral BCL-2 of murine gamma-herpesvirus 68. PLoS Pathogens 4 (2), e25.
Lozach, P.Y., Mancini, R., Bitto, D., Meier, R., Oestereich, L., Overby, A.K., Pettersson, R.F., Helenius, A., 2010. Entry of bunyaviruses into mammalian cells. Cell Host Microbe 7 (6), 488–499.
Matsuyama, A., Shimazu, T., Sumida, Y., Saito, A., Yoshimatsu, Y., Seigneurin-Berny, D., Osada, H., Komatsu, Y., Nishino, N., Khochbin, S., Horinouchi, S., Yoshida, M., 2002. In vivo destabilization of dynamic microtubules by HDAC6-mediated deacetylation. EMBO Journal 21 (24), 6820–6831.
McCullough, K.C., Basta, S., Knotig, S., Gerber, H., Schaffner, R., Kim, Y.B., Saalmuller, A., Summerfield, A., 1999. Intermediate stages in monocyte-macrophage differentiation modulate phenotype and susceptibility to virus infection. Immunology 98 (2), 203–212.
McCullough, K.C., Schaffner, R., Fraefel, W., Kihm, U., 1993. The relative density of CD44-positive porcine monocytic cell populations varies between isolations and upon culture and influences susceptibility to infection by African swine fever virus. Immunology Letters 37 (1), 83–90.
Meier, O., Boucke, K., Hammer, S.V., Keller, S., Stidwill, R.P., Hemmi, S., Greber, U.F., 2002. Adenovirus triggers macropinocytosis and endosomal leakage together with its clathrin-mediated uptake. Journal of Cell Biology 158 (6), 1119–1131.
Mercer, A.A., Fraser, K.M., Esposito, J.J., 1996. Gene homology between orf virus and smallpox variola virus. Virus Genes 13 (2), 175–178.
Mercer, J., Helenius, A., 2008. Vaccinia virus uses macropinocytosis and apoptotic mimicry to enter host cells. Science 320 (5875), 531–535.
Mercer, J., Helenius, A., 2009. Virus entry by macropinocytosis. Nature Cell Biology 11 (5), 510–520.
Mercer, J., Schelhaas, M., Helenius, A., 2010. Virus entry by endocytosis. Annual Review of Biochemistry 79, 803–833.
Merrifield, C.J., Feldman, M.E., Wan, L., Almers, W., 2002. Imaging actin and dynamin recruitment during invagination of single clathrin-coated pits. Nature Cell Biology 4 (9), 691–698.
Merrifield, C.J., Perrais, D., Zenisek, D., 2005. Coupling between clathrin-coated-pit invagination, cortactin recruitment, and membrane scission observed in live cells. Cell 121 (4), 593–606.
Mijaljica, D., Prescott, M., Devenish, R.J., 2006. Endoplasmic reticulum and Golgi complex: contributions to, and turnover by, autophagy. Traffic 7 (12), 1590–1595.
Miskin, J.E., Abrams, C.C., Dixon, L.K., 2000. African swine fever virus protein A238L interacts with the cellular phosphatase calcineurin via a binding domain similar to that of NFAT. Journal of Virology 74 (20), 9412–9420.
Miskin, J.E., Abrams, C.C., Goatley, L.C., Dixon, L.K., 1998. A viral mechanism for inhibition of the cellular phosphatase calcineurin. Science 281 (5376), 562–565.
Miyazawa, N., Crystal, R.G., Leopold, P.L., 2001. Adenovirus serotype 7 retention in a late endosomal compartment prior to cytosol escape is modulated by fiber protein. Journal of Virology 75 (3), 1387–1400.
Mizushima, N., 2010. The role of the Atg1/ULK1 complex in autophagy regulation. Current Opinion in Cell Biology 22 (2), 132–139.
Mizushima, N., Tsukamoto, S., Kuma, A., 2008. Autophagy in embryogenesis and cell differentiation. Tanpakushitsu Kakusan Koso 53 (Suppl. 16), 2170–2174.
Moreno-Ruiz, E., Galan-Diez, M., Zhu, W., Fernandez-Ruiz, E., d'Enfert, C., Filler, S.G., Cossart, P., Veiga, E., 2009. Candida albicans internalization by host cells is mediated by a clathrin-dependent mechanism. Cellular Microbiology 11 (8), 1179–1189.
Neilan, J.G., Borca, M.V., Lu, Z., Kutish, G.F., Kleiboeker, S.B., Carrillo, C., Zsak, L., Rock, D.L., 1999. An African swine fever virus ORF with similarity to C-type lectins is non-essential for growth in swine macrophages in vitro and for virus virulence in domestic swine. Journal of General Virology 80 (Pt 10), 2693–2697.
Neilan, J.G., Lu, Z., Afonso, C.L., Kutish, G.F., Sussman, M.D., Rock, D.L., 1993. An African swine fever virus gene with similarity to the proto-oncogene bcl-2 and the Epstein-Barr virus gene BHRF1. Journal of Virology 67 (7), 4391–4394.
Netherton, C.L., McCrossan, M.C., Denyer, M., Ponnambalam, S., Armstrong, J., Takamatsu, H.H., Wileman, T.E., 2006. African swine fever virus causes microtubule-dependent dispersal of the trans-golgi network and slows delivery of membrane protein to the plasma membrane. Journal of Virology 80 (22), 11385–11392.
Netherton, C.L., Parsley, J.C., Wileman, T., 2004. African swine fever virus inhibits induction of the stress-induced proapoptotic transcription factor CHOP/GADD153. Journal of Virology 78 (19), 10825–10828.
Nogal, M.L., Gonzalez de Buitrago, G., Rodriguez, C., Cubelos, B., Carrascosa, A.L., Salas, M.L., Revilla, Y., 2001. African swine fever virus IAP homologue inhibits caspase activation and promotes cell survival in mammalian cells. Journal of Virology 75 (6), 2535–2543.

Ortin, J., Enjuanes, L., Vinuela, E., 1979. Cross-links in African swine fever virus DNA. Journal of Virology 31 (3), 579–583.
Ortin, J., Vinuela, E., 1977. Requirement of cell nucleus for African swine fever virus replication in Vero cells. Journal of Virology 21 (3), 902–905.
Orvedahl, A., Alexander, D., Talloczy, Z., Sun, Q., Wei, Y., Zhang, W., Burns, D., Leib, D.A., Levine, B., 2007. HSV-1 ICP34.5 confers neurovirulence by targeting the Beclin 1 autophagy protein. Cell Host & Microbe 1 (1), 23–35.
Pattingre, S., Tassa, A., Qu, X., Garuti, R., Liang, X.H., Mizushima, N., Packer, M., Schneider, M.D., Levine, B., 2005. Bcl-2 antiapoptotic proteins inhibit Beclin 1-dependent autophagy. Cell 122 (6), 927–939.
Peréz, C., Ortuño, E., Gómez, N., García-Briones, M., Álvarez, B., Martinez de la Riva, P., Alonso, F., Revilla, C., Dominguez, J., Ezquerra, A., 2008. Cloning and expression of porcine CD163: its use for characterization of monoclonal antibodies to porcine. Spanish Journal of Agricultural Research 6, 59–72.
Pizarro-Cerda, J., Bonazzi, M., Cossart, P., 2010. Clathrin-mediated endocytosis: what works for small, also works for big. Bioessays 32 (6), 496–504.
Poppers, J., Mulvey, M., Khoo, D., Mohr, I., 2000. Inhibition of PKR activation by the proline-rich RNA binding domain of the herpes simplex virus type 1 Us11 protein. Journal of Virology 74 (23), 11215–11221.
Powell, P.P., Dixon, L.K., Parkhouse, R.M., 1996. An IkappaB homolog encoded by African swine fever virus provides a novel mechanism for downregulation of proinflammatory cytokine responses in host macrophages. Journal of Virology 70 (12), 8527–8533.
Quetglas, J.I., Hernaez, B., Galindo, I., Munoz-Moreno, R., Cuesta-Geijo, M.A., Alonso, C., 2012. Small rho GTPases and cholesterol biosynthetic pathway intermediates in African swine fever virus infection. Journal of Virology 86 (3), 1758–1767.
Raghu, H., Sharma-Walia, N., Veettil, M.V., Sadagopan, S., Chandran, B., 2009. Kaposi's sarcoma-associated herpesvirus utilizes an actin polymerization-dependent macropinocytic pathway to enter human dermal microvascular endothelial and human umbilical vein endothelial cells. Journal of Virology 83 (10), 4895–4911.
Ramelot, T.A., Cort, J.R., Yee, A.A., Liu, F., Goshe, M.B., Edwards, A.M., Smith, R.D., Arrowsmith, C.H., Dever, T.E., Kennedy, M.A., 2002. Myxoma virus immunomodulatory protein M156R is a structural mimic of eukaryotic translation initiation factor eIF2alpha. Journal of Molecular Biology 322 (5), 943–954.
Ramiro-Ibanez, F., Ortega, A., Brun, A., Escribano, J.M., Alonso, C., 1996. Apoptosis: a mechanism of cell killing and lymphoid organ impairment during acute African swine fever virus infection. Journal of General Virology 77 (Pt 9), 2209–2219.
Ramsey-Ewing, A., Moss, B., 1998. Apoptosis induced by a postbinding step of vaccinia virus entry into Chinese hamster ovary cells. Virology 242 (1), 138–149.
Revilla, Y., Callejo, M., Rodriguez, J.M., Culebras, E., Nogal, M.L., Salas, M.L., Vinuela, E., Fresno, M., 1998. Inhibition of nuclear factor kappaB activation by a virus-encoded IkappaB-like protein. Journal of Biological Chemistry 273 (9), 5405–5411.
Revilla, Y., Cebrian, A., Baixeras, E., Martinez, C., Vinuela, E., Salas, M.L., 1997. Inhibition of apoptosis by the African swine fever virus Bcl-2 homologue: role of the BH1 domain. Virology 228 (2), 400–404.
Rivera, J., Abrams, C., Hernaez, B., Alcazar, A., Escribano, J.M., Dixon, L., Alonso, C., 2007. The MyD116 African swine fever virus homologue interacts with the catalytic subunit of protein phosphatase 1 and activates its phosphatase activity. Journal of Virology 81 (6), 2923–2929.
Rodriguez-Gonzalez, A., Lin, T., Ikeda, A.K., Simms-Waldrip, T., Fu, C., Sakamoto, K.M., 2008. Role of the aggresome pathway in cancer: targeting histone deacetylase 6-dependent protein degradation. Cancer Research 68 (8), 2557–2560.
Rodriguez, C.I., Nogal, M.L., Carrascosa, A.L., Salas, M.L., Fresno, M., Revilla, Y., 2002. African swine fever virus IAP-like protein induces the activation of nuclear factor kappa B. Journal of Virology 76 (8), 3936–3942.
Rodriguez, J.M., Garcia-Escudero, R., Salas, M.L., Andres, G., 2004. African swine fever virus structural protein p54 is essential for the recruitment of envelope precursors to assembly sites. Journal of Virology 78 (8), 4299-1313.
Rojo, G., Chamorro, M., Salas, M.L., Vinuela, E., Cuezva, J.M., Salas, J., 1998. Migration of mitochondria to viral assembly sites in African swine fever virus-infected cells. Journal of Virology 72 (9), 7583–7588.
Rojo, G., Garcia-Beato, R., Vinuela, E., Salas, M.L., Salas, J., 1999. Replication of African swine fever virus DNA in infected cells. Virology 257 (2), 524–536.
Salas, M.L., Andres, G., 2012. African swine fever virus morphogenesis. Virus Research, http://dx.doi.org/10.1016/j.virusres.2012.09.016, This issue.
Sanchez-Torres, C., Gomez-Puertas, P., Gomez-del-Moral, M., Alonso, F., Escribano, J.M., Ezquerra, A., Dominguez, J., 2003. Expression of porcine CD163 on monocytes/macrophages correlates with permissiveness to African swine fever infection. Archives of Virology 148 (12), 2307–2323.
Sanchez, E.G., Quintas, A., Perez-Nunez, D., Nogal, M., Barroso, S., Carrascosa, A.L., Revilla, Y., 2012. African swine fever virus uses macropinocytosis to enter host cells. PLoS Pathogens 8 (6), e1002754.
Scherer, J., Vallee, R.B., 2011. Adenovirus recruits dynein by an evolutionary novel mechanism involving direct binding to pH-primed hexon. Viruses 3 (8), 1417–1431.
Schmidt, F.I., Bleck, C.K., Helenius, A., Mercer, J., 2011. Vaccinia extracellular virions enter cells by macropinocytosis and acid-activated membrane rupture. EMBO Journal 30 (17), 3647–3661.
Schmidt, F.I., Bleck, C.K., Mercer, J., 2012. Poxvirus host cell entry. Current Opinion in Virology 2 (1), 20–27.
Sharp, T.V., Witzel, J.E., Jagus, R., 1997. Homologous regions of the alpha subunit of eukaryotic translational initiation factor 2 (eIF2alpha) and the vaccinia virus K3L gene product interact with the same domain within the dsRNA-activated protein kinase (PKR). European Journal of Biochemistry 250 (1), 85–91.
Sieczkarski, S.B., Whittaker, G.R., 2003. Differential requirements of Rab5 and Rab7 for endocytosis of influenza and other enveloped viruses. Traffic 4 (5), 333–343.
Smith, G.L., Vanderplasschen, A., Law, M., 2002. The formation and function of extracellular enveloped vaccinia virus. Journal of General Virology 83 (Pt 12), 2915–2931.
Stefanovic, S., Windsor, M., Nagata, K.I., Inagaki, M., Wileman, T., 2005. Vimentin rearrangement during African swine fever virus infection involves retrograde transport along microtubules and phosphorylation of vimentin by calcium calmodulin kinase II. Journal of Virology 79 (18), 11766–11775.
Tabares, E., Sanchez Botija, C., 1979. Synthesis of DNA in cells infected with African swine fever virus. Archives of Virology 61 (1–2), 49–59.
Taylor, M.J., Lampe, M., Merrifield, C.J., 2012. A feedback loop between dynamin and actin recruitment during clathrin-mediated endocytosis. PLoS Biology 10 (4), e1001302.
Taylor, M.J., Perrais, D., Merrifield, C.J., 2011. A high precision survey of the molecular dynamics of mammalian clathrin-mediated endocytosis. PLoS Biology 9 (3), e1000604.
Traub, L.M., 2009. Tickets to ride: selecting cargo for clathrin-regulated internalization. Nature Reviews Molecular Cell Biology 10 (9), 583–596.
Valdeira, M.L., Bernardes, C., Cruz, B., Geraldes, A., 1998. Entry of African swine fever virus into Vero cells and uncoating. Veterinary Microbiology 60 (2-4), 131–140.
Valdeira, M.L., Geraldes, A., 1985. Morphological study on the entry of African swine fever virus into cells. Biologie Cellulaire 55 (1-2), 35–40.
Vallee, R.B., McKenney, R.J., Ori-McKenney, K.M., 2012. Multiple modes of cytoplasmic dynein regulation. Nature Cell Biology 14 (3), 224–230.
Vazquez-Calvo, A., Saiz, J.C., Sobrino, F., Martin-Acebes, M.A., 2011. Inhibition of enveloped virus infection of cultured cells by valproic acid. Journal of Virology 85 (3), 1267–1274.
Veiga, E., Cossart, P., 2005. Listeria hijacks the clathrin-dependent endocytic machinery to invade mammalian cells. Nature Cell Biology 7 (9), 894–900.
Wileman, T., 2007. Aggresomes and pericentriolar sites of virus assembly: cellular defense or viral design? Annual Review of Microbiology 61, 149–167.
Zaitseva, E., Yang, S.T., Melikov, K., Pourmal, S., Chernomordik, L.V., 2010. Dengue virus ensures its fusion in late endosomes using compartment-specific lipids. PLoS Pathogens 6 (10), e1001131.
Zhang, F., Hopwood, P., Abrams, C.C., Downing, A., Murray, F., Talbot, R., Archibald, A., Lowden, S., Dixon, L.K., 2006. Macrophage transcriptional responses following in vitro infection with a highly virulent African swine fever virus isolate. Journal of Virology 80 (21), 10514–10521.
Zhang, F., Moon, A., Childs, K., Goodbourn, S., Dixon, L.K., 2010. The African swine fever virus DP71L protein recruits the protein phosphatase 1 catalytic subunit to dephosphorylate eIF2alpha and inhibits CHOP induction but is dispensable for these activities during virus infection. Journal of Virology 84 (20), 10681–10689.
Zhang, Y., Li, N., Caron, C., Matthias, G., Hess, D., Khochbin, S., Matthias, P., 2003. HDAC-6 interacts with and deacetylates tubulin and microtubules in vivo. EMBO Journal 22 (5), 1168–1179.
Zsak, L., Lu, Z., Kutish, G.F., Neilan, J.G., Rock, D.L., 1996. An African swine fever virus virulence-associated gene NL-S with similarity to the herpes simplex virus ICP34.5 gene. Journal of Virology 70 (12), 8865–8871.

Available online at www.sciencedirect.com
ScienceDirect
Virology 375 (2008) 561–572
VIROLOGY
www.elsevier.com/locate/yviro

A179L, a viral Bcl-2 homologue, targets the core Bcl-2 apoptotic machinery and its upstream BH3 activators with selective binding restrictions for Bid and Noxa

Inmaculada Galindo [1], Bruno Hernaez [1], Gema Díaz-Gil [1,2], Jose M. Escribano, Covadonga Alonso *

Departamento de Biotecnología, Instituto Nacional de Investigación y Tecnología Agraria y Alimentaria (INIA), Autopista A6 Km 7, 28040 Madrid, Spain

Received 21 December 2007; returned to author for revision 7 January 2008; accepted 24 January 2008
Available online 10 March 2008

Abstract

Several large DNA viruses encode Bcl-2 protein homologues involved in the regulation of the cellular apoptosis cascade. This regulation often involves the interaction of these viral proteins with diverse cellular Bcl-2 family members. We have identified the specific interactions of A179L, an African swine fever virus (ASFV) Bcl-2 homologue, with the active forms of the porcine BH3-only Bid protein (truncated Bid p13 and p15). Transient expression of ASFV A179L gene in Vero cells prevented apoptosis induced by these active forms of Bid protein. Interestingly, A179L protein was able to interact, also with the main core Bcl-2 proapoptotic proteins Bax and Bak, and with several BH3-only proteins with selective binding restrictions for full length Bid and Noxa. These results suggest a fine regulation for A179L action in the suppression of apoptosis in infected cells which is essential for efficient virus replication.

Keywords: Apoptosis; Bid; Virus–cell interaction; African swine fever virus

Introduction

Some of the best studied cellular apoptosis regulators belong to the Bcl-2 family, which include both proapoptotic and antiapoptotic effectors (Korsmeyer, 1995; White, 1996). Members of Bcl-2 family have common conserved regions, designated Bcl-2 homology regions 1, 2, 3 and 4 (BH1, BH2, BH3 and BH4). Bcl-2 protein is the prototypical member that negatively regulates apoptosis and contains all the Bcl-2 domains. This protein preserves mitochondrial integrity by interacting with Bcl-2 family proapoptotic members (Petros et al., 2004). Apoptosis inducer members include BH3-only proteins, which are cellular damage sensors that initiate rapidly the death process, and Bax-like proteins that act downstream of BH3-only proteins to permeabilise the mitochondrial outer membrane (Bouillet and Strasser, 2002).

The apoptosis cascade may be initiated by pathogenic agents such as viruses and is considered as part of the cellular defensive mechanism. Viruses have adapted numerous ways of circumventing this host defensive response, including regulation of endogenous host death receptors and ligands, expression of caspase activation inhibitors, regulation of host Bcl-2 proteins, and expression of viral homologues of Bcl-2 (vBcl-2s) (Benedict et al., 2002; Polster et al., 2004).These viral genes encoding proteins with amino acid sequence similarity to cellular Bcl-2 apoptosis inhibitors have been identified in several viral models including Epstein–Barr virus (EBV) (Bellows et al., 2002; Henderson et al., 1993), human herpes virus 8 (HHV8) (Cheng et al., 1997) and African swine fever virus (ASFV) (Afonso et al., 1996) between others. The role of these vBcl-2s in diverse aspects of the viral cell-cycle and their mechanism of action has been gradually emerging (Everett and McFadden, 1999; Hardwick and Bellows, 2003). VBcl-2s mediate inhibition of apoptosis in infected cells and prevent premature death of the host cell which would impair virus replication and might have also a role in the development of persistent infection (Cuconati and White, 2002).

Abbreviations: vBcl-2, viral Bcl-2; cBcl-2, cellular Bcl-2; ORF, open reading frame; HA, hemagglutinin tag; Bid, BH3 interacting domain death agonist; tBid, truncated Bid; ASFV, African swine fever virus.

* Corresponding author. Fax: +34 91 3573107.
E-mail address: calonso@inia.es (C. Alonso).
[1] The first three authors contributed equally to this work.
[2] Present address: Facultad Ciencias de la Salud, Universidad Rey Juan Carlos, 28922, Madrid, Spain.

0042-6822/$ - see front matter © 2008 Elsevier Inc. All rights reserved.
doi:10.1016/j.virol.2008.01.050

African swine fever virus (ASFV) is a double stranded large DNA virus that induces an acute disease of swine in which apoptosis plays a central role in pathogenesis. Virus infection induces apoptosis in target and immune defence cells (Oura et al., 1998; Ramiro-Ibanez et al., 1996). This programmed cell death induction in the target cell has been recently tracked in vivo in living cells as infection progresses and the execution phase of apoptosis becomes evident at late infection times (Hernaez et al., 2006). In fact, ASFV encodes for various apoptosis inhibitor genes, one of these sharing high sequence similarity to cellular Bcl-2, the ASFV A179L gene (Revilla et al., 1997; Yanez et al., 1995). This gene encodes for a 21 kDa protein which is expressed at early and late times after infection and is essential for virus replication throughout the infection cycle (Brun et al., 1996; Neilan et al., 1993). A179L is highly conserved in most ASFV isolates, both in pathogenic and cell-cultured adapted isolates. In comparison to other viral Bcl-2s, its sequence is very similar to the cellular protein containing all the characteristic Bcl-2 homology domains (BH1, BH2, BH3 and BH4), but lacking the transmembrane region (Afonso et al., 1996). A179L is involved in the suppression of apoptosis in ASFV infected cells (Brun et al., 1996) and prolongs host cell survival until the replication of the large viral genome is completed. Prolonged cell survival could be relevant facilitating a persistent infection (Afonso et al., 1996; Brun et al., 1996). Moreover, given the fact that immune defence entails cytotoxic T lymphocytes attack against infected cells by TNFα, FasL or TRAIL, A179L could play a role in the infected cell escape to premature death due to cytokine signalling. Mutations in the BH1 domain of A179L abrogate its death-repressor activity (Revilla et al., 1997). Interestingly, this protein is functional and prevents virus induced apoptosis not only in mammalian cells but also in insect cells (Brun et al., 1998), indicating a very low degree of species-specificity, as would be required of a viral protein that should exert its function in both, mammals and the arthropod vector (White, 1996). The ASFV arthropod vectors are ticks of the *Ornithodorus* genus (Plowright et al., 1969).

However, the precise mechanism of action of A179L remains undefined. Some evidences suggest that most vBcl-2s might target the core cellular proapoptotic machinery for inhibition (Bellows et al., 2002; Nava et al., 1997), but also redundant actions on specific, short BH3 proapoptotic members have been described (Boyd et al., 1995; Han et al., 1996b) probably directed to secure apoptosis inhibition in the infected cell.

The aim of this work was to characterize the biochemical mechanisms by which the A179L protein suppresses apoptosis. Active forms of Bid protein from *Sus scrofa* were first identified as A179L interacting proteins. A179L blocked Bid-induced apoptosis when transfected in Vero cells, pointing out that A179L action may take place downstream of caspase 8 or granzyme B cleavage. In this work, we have shown that A179L protein interacted specifically with both BH3-only proapoptotic proteins and the core cellular proapoptotic machinery suggesting a central role for this protein in the inhibition of apoptosis induced by a wide variety of stimuli.

Results

Interaction of ASFV A179L protein with p13 truncated Bid protein

Although previous results demonstrated that ASVF A179L protects cells from programmed cell death, the molecular mechanisms supporting this biological effect remain to be determined. To elucidate the role of the virus Bcl-2 homologue, the yeast two hybrid system was used to screen a porcine macrophage cDNA library with full-length A179L as bait, searching for cellular interacting proteins. Two yeast clones were identified to induce the expression of the three reporter genes (*HIS3*, *LEU2*, *TRIP1*), as indicated by growth on SD medium and blue staining in the presence of X-α-Gal. These two cDNA clones were characterized by nucleotide sequence analysis. One of these clones was not included in these studies because the sequence revealed no significant homology to any known gene or translated product at the NCBI data base. Another cDNA clone was found to encode a porcine protein with high percentage homology (65%) to tBid-p13 protein from *Homo sapiens*. TBid-p13 protein corresponds to the carboxy-terminal fragment of Bid protein, named truncated Bid (tBid).

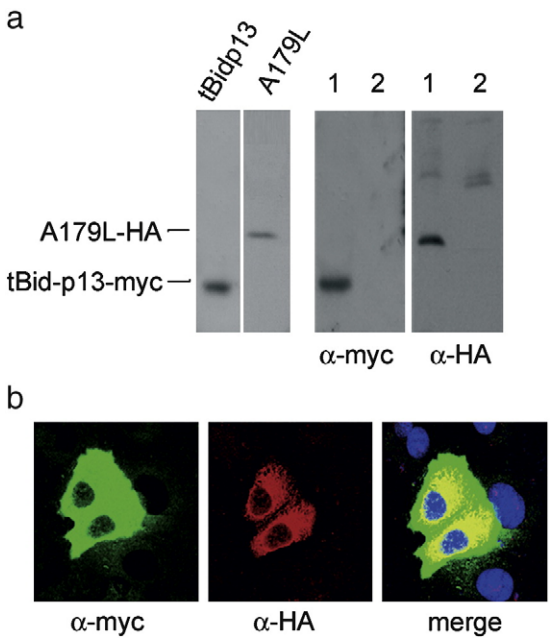

Fig. 1. ASFV A179L interaction with porcine tBid-p13 in mammalian cells by affinity chromatography and confocal microscopy. (a) Total cell lysates from single transfected cells with either tBid-p13–myc or A179L–HA were blotted for anti-myc or anti-HA (left panel). Interaction of A179L with tBid-p13 was confirmed by immunoprecipitation of HA-tagged A179L and myc-tagged tBid-p13, from Vero cells transfected with the corresponding expression constructs. The immunoprecipitates were analyzed by SDS-PAGE and subjected to immunoblotting with antibodies against myc or HA. Lane 1, immunoprecipitation with a mAb against HA. Lane 2, immunoprecipitation with normal mouse serum (right panel). (b) Vero cells were transiently transfected with pCMVA179L–HA and pCMVtBid-p13–myc plasmids. Colocalization of A179L and tBid-p13 was assayed by confocal microscopy. A179L was detected with anti-HA-Alexa 594 (red) and tBid-p13 with anti-myc-FITC (green). Nuclei were stained with Hoechst 33258 (blue). Colocalization areas are depicted in yellow.

This protein is related with apoptosis mediated by death receptors and results from post-transductional cleavage of full length Bid by caspase 8 or granzyme B (Li et al., 1998; Luo et al., 1998). The resulting protein of 13 kDa has been found to be one of the active forms of Bid protein inducing apoptosis (Gross et al., 1999a,b; Stoka et al., 2001).

To further confirm the interaction of tBid-p13 and ASVF A179L we tested the association of both proteins by immunoprecipitation. Protein extracts from Vero cells expressing A179L–HA or tBid-p13–myc protein were incubated with protein A-sepharose, previously conjugated with anti-HA antibody or with an irrelevant rabbit serum. After extensive

a

```
   ATG GAT TCT AAG GTC AGC AAC GGT TCC AGC CTC CAG GAC GAG CGC ATC
 1  M   D   S   K   V   S   N   G   S   S   L   Q   D   E   R   I  16

   ACA AAC CTA CTG GTG TTT GGC TTC CTC CAA AGC TGC CCC CAT GCC AGT
17  T   N   L   L   V   F   G   F   L   Q   S   C   P   H   A   S  32

   TTC CAC AAG GAG CTG GAG GTG CTG GGC CAC GAG CTG CCT GTG CAC ACT
33  F   H   K   E   L   E   V   L   G   H   E   L   P   V   H   T  48

   TCG GGC AGT GAC GAG CTG CAG ACA GAC GGC AAT CGA TGC AGC TAC TTC
49  S   G   S   D   E   L   Q   T   D   G   N   R   C   S   Y   F  64

   ATG GAG GAC GCG GCG GAG ACA GAT TCT GAG AGC CAG GAG GCA GTC ATT
65  M   E   D   A   A   E   T   D   S   E   S   Q   E   A   V   I  80

   CGG GAC ATT GCC AGG CAT CTC GCC CGA ATA GGG GAC AGG ATG GAG TAT
81  R   D   I   A   R   H   L   A   R   I   G   D   R   M   E   Y  96

   GGC ATC CGC CCA GGG CTG GTG GAT AGC CTG GCC GCA CAG TTC AGG AAC
97  G   I   R   P   G   L   V   D   S   L   A   A   Q   F   R   N 112

   CAG AGC CTG TCG GAG GAG GAC AGA CGG CAG GGC CTG GCT GCT GTG CTG
113 Q   S   L   S   E   E   D   R   R   Q   G   L   A   A   V   L 128

   CAG CAG CTC GTG CAC TCC TAC CCT GCA GAC ATG GGC CAG GAG AAG ACC
129 Q   Q   L   V   H   S   Y   P   A   D   M   G   Q   E   K   T 144

   CTG CTT GTG CTG ACT ATG CTC CTG GCC AGA AAG GTG GCT GAA CAC TCG
145 L   L   V   L   T   M   L   L   A   R   K   V   A   E   H   S 160

   CCG GCC TTG CTC CGG GAT GTC TTT CAC ACA ACG GTG AAC TTC ATC AAC
161 P   A   L   L   R   D   V   F   H   T   T   V   N   F   I   N 176

   CAG AAC CTC CTC ACC TAC TTG CGC AAC TTA GTC CAA AGT GAG ATG GAC
177 Q   N   L   L   T   Y   L   R   N   L   V   Q   S   E   M   D 192

   TGA
193 *
```

b

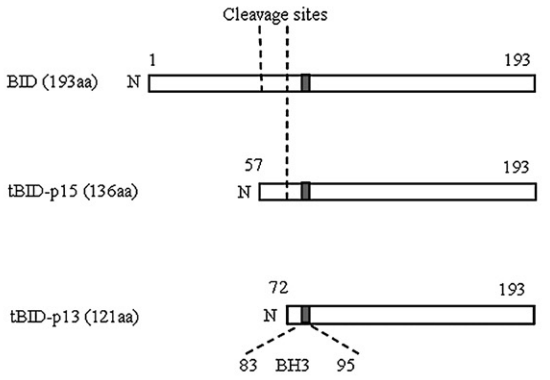

c

Homologue (NCBI accession number)	(%) Identity/Similarity to Bid porcine	
	BH3	Full ORF
Human Bid (P55957)	69/92	64/77
Mouse Bid (P70444)	76/92	59/74
Rat Bid (NM_022684)	61/84	59/73
Avian Bid (AY112660)	72/81	34/54

Fig. 2. Complete sequence of porcine Bid protein. (a) Full length Bid open reading frame (ORF) cDNA clone and its predicted amino acid sequence. A conserved BH3 domain (bold) and putative cleavage sites (underlined) are indicated. (b) Schematic structure of porcine Bid isoforms, pointing out BH3 and protease cleavage domains. (c) Homology to other annotated Bid proteins. The identity/similarity values (%) were obtained from ClustalW program (http://www.ebi.ac.uk/clustalw/). Percentages of similarity for BH3 domain were calculated including in each BH3 domain the following amino acid residues: Human Bid aa 86–98, mouse Bid 85–97, rat Bid 87–99, avian Bid 87–99 and porcine Bid 83–95. For full open reading frame (ORF) comparation, the full-length protein for each species analyzed was included from the start codon to the stop codon.

washing, bound proteins were analyzed by immunoblotting with anti-myc or anti-HA antibodies (Fig. 1a). Results showed that tBid-p13–myc was coimmunoprecipitated with A179L–HA by the anti-HA antibody, confirming the interaction between these two proteins (Fig. 1a, lane 1). As expected, tBid-p13–myc was not immunoprecipitated by the irrelevant rabbit serum (Fig. 1a, lane 2).

To gain further insight into the interaction between A179L and p13 truncated form of Bid protein, confocal microscopy assays were also performed in Vero cells transiently expressing both proteins. In agreement with the results found with the two-hybrid assay, we found colocalization of both proteins, A179L and p13 truncated form of Bid (Fig. 1b). The subcellular localization of porcine tBid, diffusely distributed throughout the cytoplasm, was similar to that of other reported Bid proteins (Wang et al., 1996). A179L stained diffusely the cytoplasm with a significant proportion accumulating in the perinuclear space. Colocalization of both proteins, A179L and tBid-p13, was found mainly in the perinuclear region as it is shown in the overlay (colocalization percentage over 72%). The above results indicate an interaction between ASFV A179L and porcine truncated Bid protein not only in vitro but also in vivo.

Isolation and sequence analysis of cDNA encoding porcine Bid

On the basis of the information from NCBI data base, where the A179L interacting sequence showed a high degree of homology with one of the truncated forms of human Bid protein, a RACE-PCR was performed to obtain the complete sequence for porcine Bid protein. The full length sequence generated of porcine Bid gene was deposited at GenBank under accession no DQ087226.

This sequence predicts an open reading frame of 579 nucleotides encoding for a protein of 192 amino acids. The protein contains a BH3 domain from amino acid 83 to amino acid 95. Moreover, similarly to the human Bid sequence, the analysis of the porcine sequence indicated the presence of two potential cleavage sites present in the full length protein (Fig. 2a). The primary site (LQTDG), at 54–57 amino acids, is the putative caspase 8 and 1 cleavage sites which generate a 15 kDa truncated form of Bid protein (tBid-p15 protein). The secondary site (AETD) at residues 69–72, would be recognized by both caspase 8 and granzyme B, generating tBid-p13 protein. A third cleavage site generating tBid-p11 protein, described in *H. sapiens* as an inactive form of Bid (Gross et al., 1999a,b), was not found in the porcine Bid sequence however (Fig. 2b).

A comparison between the deduced amino acid sequences of porcine Bid with those from other organisms was performed using the computer analysis tool ClustalW. The porcine Bid sequence exhibited high identity with every annotated sequence from mammalian origin Bid proteins (Fig. 2c): *H. sapiens* (64%), *Mus musculus* (59%) and *Rattus novergicus* (59%). In contrast, porcine Bid was less closely related to avian Bid protein (*Gallus gallus*), with an identity of 34%. Alignment of Bid amino acid sequences indicates that the BH3 domain is highly conserved between species, sharing 75–60% identity (Fig. 2c). Cleavage sites were also conserved, particularly, primary cleavage site (LQTD) which was identical in all five species examined (100%). Secondary cleavage site (AETD) yielded lower identity percentage (50%) between the porcine Bid site and the homologue mammalian sequences.

Apoptosis induction by porcine Bid truncated isoforms in Vero cells

On the basis of its homology with human and murine Bid proteins, we predicted that porcine Bid protein would also function as a proapoptotic protein. To investigate the proapoptotic activity of porcine Bid protein, as well as its truncated forms activities, we transfected Vero cells with either pCMVBid–myc, pCMVtBid-p13–myc, pCMVtBid-p15–myc or empty pCMV–HA (negative control) constructs and examined by immunofluorescence microscopy.

As described in other species, Vero cells expressing full length porcine Bid did not show evident apoptosis features or morphological changes up to 24 h after transfection. In contrast, characteristic nuclear features of apoptosis were found in those cells expressing tBid-p13 and tBid-p15. Condensation and fragmentation of chromatin, leading to typically small or shrunken nuclei were found in cells expressing truncated forms of Bid protein, whereas cells transfected with control vector and full length Bid exhibited intact round-shaped nuclei with diffuse bright blue fluorescence with Hoechst 33258 staining (Fig. 3a). In the same way, cells transiently expressing truncated forms of Bid, but not complete Bid, showed activation of caspase 3 (Fig. 3b). In order to further characterize apoptosis induced by the active forms of Bid protein, a potential-sensitive dye (CMXRos) was used to determine mitochondrial changes. Mitochondria stained finely distributed along the cytoplasm in healthy non-transfected cells. Nevertheless, cells transfected with the active forms of Bid proteins changed dramatically this distribution, presenting accumulation and irregular clumping (Fig. 3c). In these transfected cells, either tBid-p13 or tBid-p15, was found localizing with mitochondria. These morphological changes were easily observed in 96 and 92% of the cells transiently expressing tBid-p13–myc and tBid-p15–myc, respectively, from a total of 50 transfected cells examined.

Jointly, these results showed the proapoptotic activity of truncated porcine Bid proteins rapidly inducing apoptosis after transient transfection. In addition, the absence of proapoptotic

Fig. 3. Proapoptotic activity of truncated Bid isoforms in Vero cells. (a) Vero cells were tranfected with either pCMV–myc (negative control), pCMVBid–myc, pCMVtBid-p13–myc or pCMVtBid-p15–myc. Full length and truncated forms of Bid, were detected using anti-myc-FITC (green). DNA was stained with Hoechst 33258 (blue). Cells transfected with active Bid forms showed nuclear features characteristic of apoptosis: nuclear size reduction, condensation and irregular chromatin pattern. In contrast, full length Bid transfection did not result in altered nuclear morphology. (b) Expression of truncated forms of Bid in transfected cells induced activation of caspase 3. (c) Vero cells expressing Bid truncated forms presented irregular mitochondrial clumping using a mitochondrial membrane potential-sensitive dye (CMXRos, orange). The finely reticular mitochondrial pattern is evident in non-transfected cells (arrows).

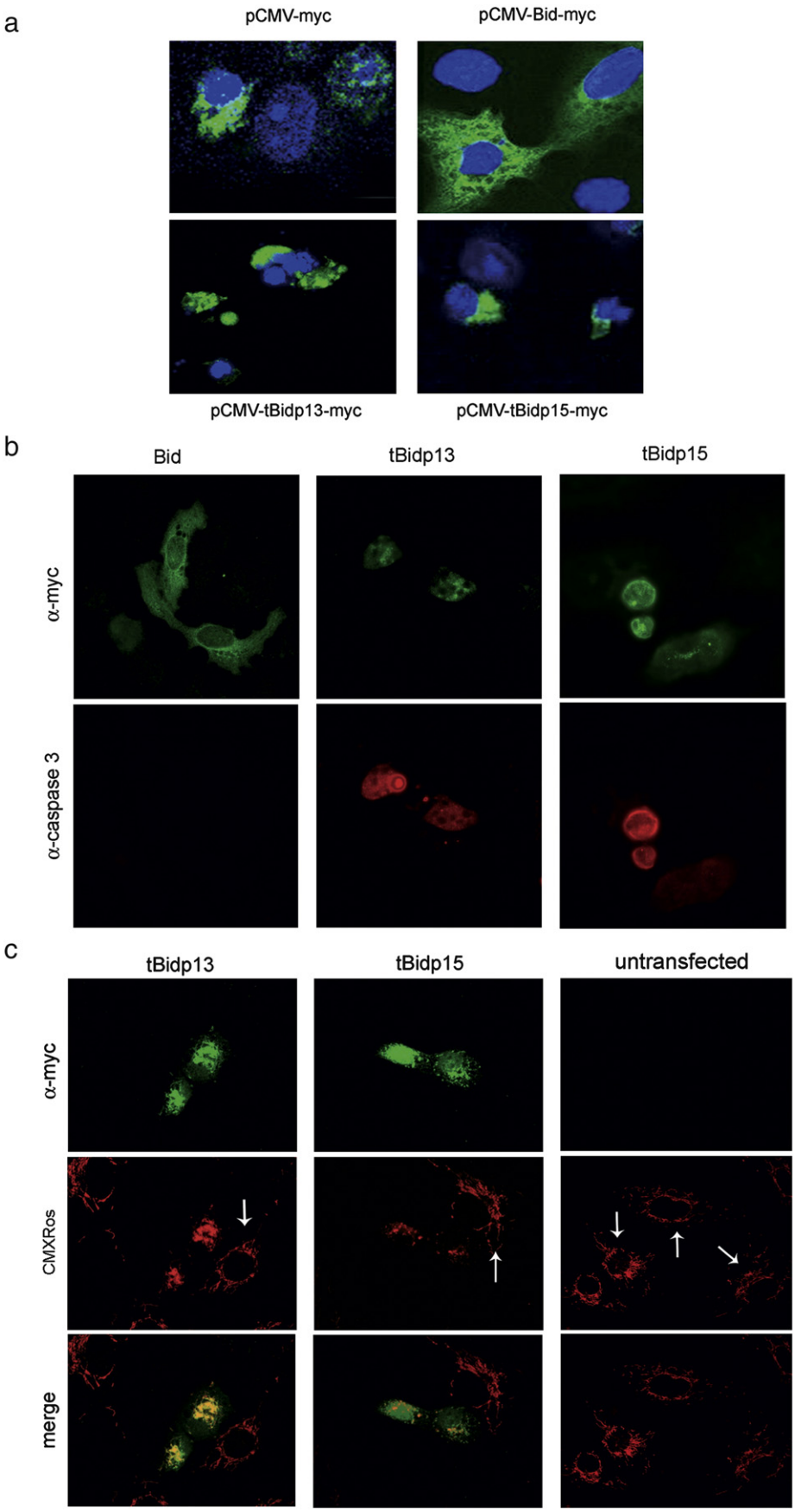
a
pCMV-myc
pCMV-Bid-myc
pCMV-tBidp13-myc
pCMV-tBidp15-myc
b
Bid
tBidp13
tBidp15
α-myc
α-caspase 3
c
tBidp13
tBidp15
untransfected
α-myc
CMXRos
merge

Table 1
Interaction of ASVF proteins A179L, p30, p54 and MyD with mammalian Bax, Bak and BH3 only proteins, as judged by yeast two hybrid assays

	A179L	p54	p30	MyD
Bid (Ss)	−	−	−	−
tBid-p15 (Ss)	+	−	−	−
tBid-p13 (Ss)	+	−	−	−
Bid (Mm)	−	−	−	−
Bad (Mm)	+	−	−	−
Bmf (Mm)	+	−	−	−
Noxa (Hs)	−	−	−	−
Puma (Hs)	+	−	−	−
DP5 (Mm)	+	−	−	−
Bik (Hs)	+	−	−	−
Biklk (Mm)	+	−	−	−
Bim S (Mm)	+	−	−	−
Bim L (Mm)	+	−	−	−
Bim EL (Mm)	+	−	−	−
Bax (Hs)	+	−	−	−
Bak (Hs)	+	−	−	−

Plasmids expressing viral proteins A179L, p30, p54 or MyD fused to GAL4 DNA-binding domain were cotransfected with plasmids expressing each Bcl-2 proapoptotic members fused to the GAL4 transcriptional activation domain. Protein-protein interaction (+) resulted in growth of yeast in absence of leucine, trytophan and histidine and blue staining in presence of X-Gal. Interaction was negative (−) with full length Bid, Noxa and irrelevant viral proteins included as controls. Ss: *Sus scrofa*, Mm: *Mus musculus*; Hs, *Homo sapiens*.

activity of full length porcine Bid protein is in agreement with the notion that only caspase 8 or granzyme B post-transductional processing render this protein active.

Inhibition of proapoptotic activity of truncated forms of Bid by specific interaction with A179L

Although sequence analysis and functional experiments showed that there are at least three isoforms of porcine Bid protein, only tBid-p13 protein, was at first identified as an ASFV A179L interacting protein when a yeast two hybrid screening was conducted using a porcine macrophage library. To determine if A179L was also able to interact with others forms of porcine Bid protein (full length Bid and tBid-p15), we performed a series of direct yeast two hybrid assays. Y190 yeast strain was cotransformed with pGBT9–A179L vector and pATC2 vector containing Bid, tBid-p13 or tBid-p15. The results (Table 1) indicated that A179L selectively interacts with active forms of Bid protein, tBid-p13 and tBid-p15, and failed to associate with full length Bid, the inactive form of Bid protein.

Once the interaction between A179L protein and the active forms of porcine Bid protein was found, we investigated the functional role of these interactions and whether A179L binding to truncated forms of Bid could interfere with the death signal mediated by these proteins. We first tested proapoptotic activity mediated by active Bid isoforms alone. For this purpose, Vero cells were cotransfected with pCMV–A179L–HA and pCMVtBid-p13–myc or pCMVtBid-p15–myc and were then analyzed by laser confocal microscopy. As it was shown above (Fig. 3), 24 h post-transfection, expression of tBid proteins induced apoptosis features. In contrast, every cell transiently expressing A179L and either tBid-p13 or tBid-p15 did not show apoptosis features; that is, double positive cells exhibited healthy cellular morphology (Fig. 4). DNA pattern evaluation in those single transfected cells expressing truncated Bid proteins revealed nuclei condensation and chromatin fragmentation (Fig. 4, indicated by arrows). Moreover, these cells exhibited rounding and nuclear size reduction. Jointly, these results suggest that A179L is able to impact on apoptotic pathway mediated by the BH3-only protein Bid, which is a central actor in the death receptor apoptosis pathway, protecting the host cell against programmed cell death.

Interaction of A179L with Bcl-2 proapoptotic proteins

Many of the viral Bcl-2 homologues have been shown to inhibit apoptosis induced by a variety of cell death stimuli (Cuconati and White, 2002). Nevertheless, different death stimuli seem to activate different BH3-only effectors. To further investigate which pathways were inhibited by A179L, we tested if this protein was able to interact with other proapoptotic Bcl-2 family proteins (Table 1). Several mammalian BH3-only proteins, including murine Bid were cloned into pATC2 vector to be used in a yeast two-hybrid assay. Three isoforms of Bim (Bim S, Bim L and Bim EL) were analyzed, since differences in the proapoptotic potential activity of these isoforms have been previously described (Marani et al., 2002). *H. sapiens* Bik and its murine homologue (Biklk) were tested to analyze possible species specific differences.

All clones cotransformed with pGBT9-A179L and pATC2-BH3-only proteins, except those containing pATC2-Bid or pATC2-Noxa, were able to grow to form blue-stained colonies

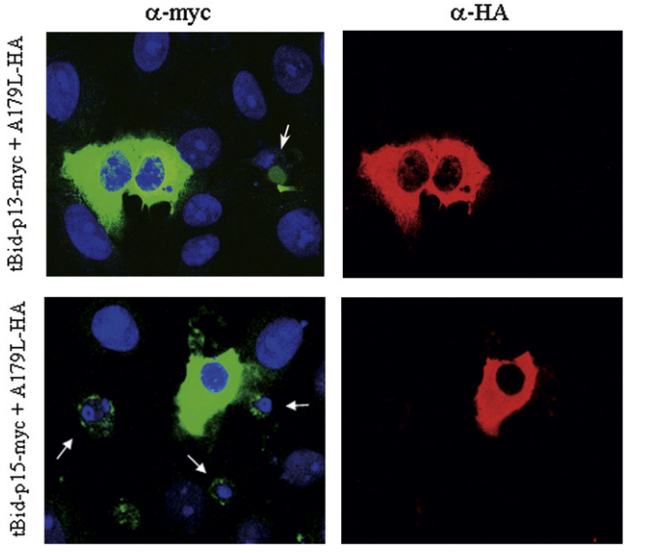

Fig. 4. Proapoptotic activity in Vero cells expressing simultaneously ASVF A179L and truncated Bid proteins. Plasmids expressing pCMVtBid-p13–myc or pCMVtBid-p15–myc were cotransfected alternatively in Vero cells together with pCMVA179L–HA. An antibody against the myc epitope tag FITC conjugated (green) and anti-HA antibody conjugated with Alexa 594 (red) were used to detect truncated Bid and *A179L* proteins, respectively and Hoechst 33258 DNA dye stained nuclei in blue. Single transfected cells with truncated Bid underwent typical apoptosis changes with a marked size reduction (arrows) while cotransfected cells conserved normal morphology.

on synthetic media lacking three amino acids (Trp, Leu, His) and adenine. These results suggest that, as other apoptosis suppressors which are members of Bcl-2 family, A179L mediates inhibition through heterodimerization with BH3-only proteins. However, A179L failed to associate with murine complete Bid and human Noxa proteins. This result confirms previous data obtained for porcine Bid, indicating that A179L interacts only with active forms of Bid protein. Interestingly, this viral gene failed to associate with Noxa suggesting that A179L is not involved in the apoptosis pathway mediated by this BH3-only protein.

BH3-only proteins are not the only targets described for viral Bcl-2 homologues. Interactions with the core cellular proapoptotic machinery, represented by Bax and Bak have been identified for adenoviruses and herpesviruses among others (Cuconati and White, 2002). Thus, to determine if the mechanisms responsible for A179L mediated inhibition of apoptosis were related with the core cellular proapoptotic machinery, yeast two hybrid assays were performed using Bax and Bak as preys. As indicated in Table 1, A179L was found to interact with these two proteins.

To characterize the specificity of the A179L interactions, the ability of other ASFV proteins to interact with these Bcl-2 propapoptotic members was also determined. ASFV p30 (Afonso et al., 1992), p54 (Rodriguez et al., 1994) and MyD (Rivera et al., 2007) were chosen since these are major viral proteins upon infection. None of these three virus proteins were able to interact with Bcl-2 propapoptotic members in the yeast two hybrid assays.

These results indicated that A179L selectively interacts with functionally related Bcl-2 family members to inhibit apoptosis. Hence, mechanisms underlying this *A179L* inhibition seem to be related to heterodimerization with both the core apoptotic machinery and its upstream regulators, the BH3-only proteins.

To confirm the interactions between A179L and the Bcl-2 proapoptotic proteins, previously identified by yeast two hybrid assays, we tested most of these interactions *in vitro* using recombinant proteins. A recombinant vaccinia virus expressing A179L protein fused to glutathione *S*-transferase (GST–A179L) was constructed. Several Bcl-2 proapoptotic proteins were expressed in *Escherichia coli* as fusion proteins with polyhistidine tag (His–BH3-only proteins). Expression levels of His–BH3-only proteins in *E.coli* were assessed by Western blot (data not shown). Equal amounts, as judged by Coomassie blue staining, of recombinant GST–A179L and GST were immobilized on glutathione-sepharose beads and incubated with bacterial cell extracts containing the His–BH3-only proteins. After extensive washing, bound proteins to the G-Sepharose beads were separated by SDS-PAGE and visualized by Western blotting with a monoclonal antibody recognizing the His-tag. A179L interacted with BimS, BimL, BimEL, Bad, Bmf, Bik and Biklk. An interaction between A179L and Noxa was not detected, confirming previous results obtained in yeast two hybrid assay. An estimation of the percentages of BH3-only proteins interacting with A179L and relative to BimS is shown in Fig. 5. The control experiments showed that GST alone did not interact with the Bcl-2 proapoptotic proteins analyzed.

Discussion

Apoptosis represents an important innate cellular mechanism for curtailing virus infection, and many viruses have in turn, developed strategies for inhibiting or delaying this cellular response (Benedict et al., 2002). This represents a mechanism used by the host immune system and the infected host cell itself as part of the antiviral response but often contributes to pathogenesis (Barber, 2001; Hardwick, 2001). For a successful replication, viruses must modulate apoptotic pathways to extend the lifespan of their host cell and encode homologues of antiapoptotic Bcl-2 proteins to this end (Hardwick and Bellows, 2003). A179L is one of those viral Bcl-2 homologues that protect cell from programmed cell death (Brun et al., 1996). Various viral Bcl-2 homologues have been demonstrated to interact with the core cellular proapoptotic machinery for inhibition, but it was also proposed that these virus genes may target BH3-only proteins, perhaps to secure a broad spectrum of apoptosis inhibition to the infected cell. Recently, vaccinia virus N1 protein, a novel Bcl-2-like antiapoptotic protein, has been shown to interact with Bid, Bad and Bax (Cooray et al., 2007). Alternatively, it may be so critically important to block

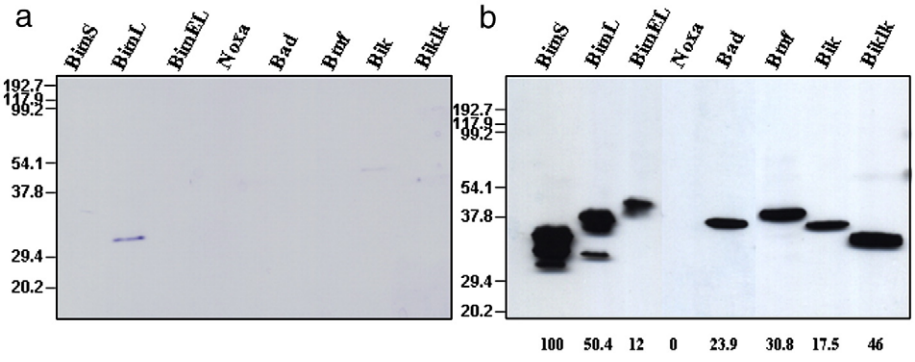

Fig. 5. A179L interaction with BimS, BimL, BimEL, Bad, Bmf, Bik and Biklk but not with Noxa, by GST-pull down assays. Bacterial cell lysates containing His-tagged BimS, BimL, BimEL, Bad, Bmf, Bik, Biklk or Noxa were incubated with equal amounts of GST (a) or GST–A179L (b) attached to glutathione matrix beads. After extensive washing, proteins bound to beads were resolved by SDS-PAGE and inmunoblotted for anti His. The positions in Kilodaltons of protein standards are shown to the left of the gel. Bands were quantified by densitometry using TINA software package (Raytest) and the percentage of protein in each lane, relative to BimS, is shown below.

apoptosis by death receptor ligands that viruses encode redundant inhibitory mechanisms to ensure survival of the infected cell. The first indication that the adenovirus Bcl-2 E1B 19K protein functions similarly to cellular Bcl-2 emerged when a yeast two-hybrid screening using E1B 19K as bait, identified Bax and Bak as interacting proteins (Farrow et al., 1995; Han et al., 1996a,b). Nevertheless, searches in databases do not reveal homology between adenovirus E1B 19K and Bcl-2. On this basis, E1B 19K is referred to as a "functional homologue" of Bcl-2 and the three dimensional structure revealed a folded structure similar to Bcl-2 (Polster et al., 2004). Some other viral Bcl-2 homologues share low amino acid sequence similarity with cellular Bcl-2 such as murine γ-herpes virus 68 (γHV68) M11 protein (Wang et al., 1999). Viral Bcl-2 homologues sharing the four homology domains BH1–BH4 include human herpes virus 8 Bcl-2 (Cheng et al., 1997), fowl poxvirus (FPV039) (Banadyga et al., 2007) and ASFV A179L (Neilan et al., 1993). The last one, lacking a putative membrane-spanning region (Afonso et al., 1996).

Although the role of most of these viral Bcl-2 homologues in infection have been gradually emerging (Cuconati and White, 2002), the biology of Bcl-2 homologue encoded by African swine fever virus is poorly understood. This is related in part to the complex genetic manipulation of this virus and the lack of convenient cell culture system and/or animal models (Hardwick and Bellows, 2003). In this work, using a porcine macrophage cDNA library, by yeast two-hybrid screening with the A179L protein as bait, we identified a truncated form of porcine Bid as the first cellular interacting protein characterized. It is known that after death receptors activation, the BH3-only Bid protein is proteolysed by caspase 8 (Li et al., 1998), whereas Bid is proteolysed by granzyme B during granule-mediated cytotoxic T lymphocyte cell killing (Heibein et al., 2000). These post-transductional modifications are necessary for function and then truncated products are translocated to the mitochondria where they promote the exit of cytochrome *c* (Fleischer et al., 2003). We have described *S. scrofa* Bid and its truncated forms encoding sequences, and according to the reported data for human Bid only these truncated forms resulted proapoptotic. Putative cleavage sites for caspase 8 and granzyme B were found in the porcine Bid sequence that would generate two carboxy-terminal fragments of 15 kDa (tBid-p15) and 13 kDa (tBid-p13), similarly to human Bid. According to previous results (Fleischer et al., 2003; Zha et al., 2000) we have shown that only truncated Bid forms caused an efficient Bid-mediated cell death, demostrating that a viral Bcl-2 is able to prevent this process. Moreover, Bid is constitutively phosporylated and must be dephosphorylated for inducing apoptosis. Several residues of Bid are phosphorylation targets for casein kinases I and II, being then insensitive to caspase 8 cleavage (Desagher et al., 2001). Similarly to previously described Bid proteins, serine residues present at porcine Bid protein also suggests a similar regulation by phosphorylation status.

An intriguing fact was to find that full length Bid failed to interact with A179L, given that the BH3 region is present in the linear sequence of this protein. The solution structure of the Bid protein was determined using NMR spectroscopy (Chou et al., 1999; McDonnell et al., 1999). The structure of full-length Bid in solution consists of eight α-helices arranged with two central somewhat more hydrophobic helices forming the core of the molecule. The third helix, which contains the BH3 domain, is connected to the first two helices by a long flexible loop, which includes the caspase-8 cleavage site. After caspase cleavage, the activated fragment, tBid, lacks the first helix, the small additional helix, and part of the unstructured loop. Since the first α-helix of Bid has hydrophobic interactions with the BH3 region in the native protein, removal of this helix would expose a large hydrophobic surface on the BH3 helix, making it accessible for binding by other Bcl-2 family members (Gong et al., 2004; Petros et al., 2004).

Bid is the first molecule likely to be involved in A179L pathway since we showed that, in transfected cells, A179L is able to prevent Bid-induced apoptosis. This result indicates that ASFV possibly inhibits the death receptor apoptosis pathway downstream of caspase 8 or granzyme B activation which would cleave Bid in its active forms and suggests then that one possible function of A179L could be to prevent death of the infected cell due to signaling by death cytokines. There are several examples of inhibition of death receptor signaling by vBcl-2 proteins. The BHRF1 and Balf1 proteins of EBV are capable of inhibiting TNF-α and FasL induced cell death (Foghsgaard and Jaattela, 1997; Marshall et al., 1999). The M11 protein of γHV68 can inhibit TNF-α and FasL induced cell death (Wang et al., 1999) and the vBcl-2 of herpes virus saimiri (HVS) blocks Fas signalling in a cell-type dependent manner (Derfuss et al., 1998; Feng et al., 2004). Those examples indicate how crucial is for infected cells to escape the attack of cytokine signaling triggered by cytotoxic T cells. The presence of redundant antiapoptotic functions in many viral genomes makes unclear what is the overall contribution of vBcl-2 proteins in the inhibition of cytokine death signaling during infection.

Interestingly, A179L is also capable of interacting with Bax and Bak proapoptotic proteins and with most of the BH3-only proteins described. This suggests that A179L protein acts as a receptor for the BH3 domain of proapoptotic Bcl-2 family proteins and is able to antagonize their function. In doing this, the ASFV Bcl-2 homologue is predicted to function by similar biochemical mechanisms to cellular Bcl-2 (cBcl-2), namely by interacting with other family members, and by either promoting or antagonizing the function of its binding partner (Gross et al., 1999a). These protein–protein interactions rely on the BH3 domain of one protein, interacting with the hydrophobic cleft created by BH1–BH3 domains of cBcl-2 (Sattler et al., 1997). This may explain why BH1 domain mutations in ASFV Bcl-2 homologue eliminate its proapoptotic activity (Revilla et al., 1997).

Thus, cellular and viral Bcl-2 and perhaps other viral antiapoptotic proteins could act both by inhibiting Bak/Bax and by sequestering BH3-only death molecules. However, the physiological context of these activities still remains to be determined. It has been postulated that a possible preference of viral Bcl-2 homologues for Bak and Bax versus BH3-only proteins may vary their regulation and expression in different cell types (Cuconati and White, 2002). As Polster et al. suggest (Polster et al., 2004), it is difficult to conclude that vBcl-2

proteins primarily target the core apoptotic machinery rather than their upstream BH3 activators, since the majority of the studies to date have been focused on Bax and Bak and rarely covered an extensive study of vBcl-2 interactions with the different BH3-death agonist molecules. Data presented in this work for ASFV, suggest a relevant role for BH3-only molecules as A179L targets. An interesting finding is that full length Bid and Noxa have been the only exceptions which did not interact with A179L. This differential targeting of BH3-only proteins has been reported for the cellular prosurvival Bcl-2 family members similarly, and Noxa also presented a more restrictive binding (Chen et al., 2005). Noxa is highly specific for the antiapoptotic Bcl-2 family members Mcl-1 and Bfl-1/A1 being relevant for a fine tuning of survival/cell death pathways with potential therapeutic applications.

In conclusion, we have shown the direct interaction of ASVF A179L with the active forms of porcine Bid protein (tBid-p15 and p13) and that A179L was able to suppress mitochondrial apoptotic signaling pathway initiated by these active Bid proteins. We have also found A179L interactions with several Bcl-2 family proapoptotic members, suggesting a pivotal role for this virus Bcl-2 homologue in the regulation of apoptosis during virus infection. These results indicate that ASFV A179L protein could block apoptosis through interaction with specific Bcl-2 proapoptotic proteins. As a consequence, the abrogation of death receptor signaling through Bid could allow the infected cell to escape immune surveillance by rendering the cell resistant to the action of TNF-α, for instance. But as with most DNA viruses, the activity of A179L during infection is only part of a multilayered response to apoptosis induction from the different antiapoptotic ASFV genes that apparently act to block a wide spectrum of molecules and at different levels of distinct apoptotic pathways (Hernaez et al., 2004b). Future work will be directed to the elucidation of the role of the many ASFV interactions with cell death related proteins and their relevance along infection.

Materials and methods

Cell culture, viruses and transfection

Vero, BSC-1 and CV-1 cell lines were obtained from the American Type Culture Collection (ATCC). Cells were cultured in Dulbecco's modified Eagle's medium supplemented with 5% calf fetal serum, 100 IU/ml penicillin, and 100 μg/ml streptomycin.

BA71V is the prototype ASFV strain used in our laboratory and represents a high cell-passage number strain. Preparation of viral stocks, titrations, and infection experiments were carried out in Vero cells as previously described (Enjuanes et al., 1976; Hernaez et al., 2004a,b). Viral DNAs preps were extracted from infected Vero cells. Vaccinia virus vRB12 was made available by R. Blasco. Vaccinia virus infections were performed with 2% FBS in BSC-1 cells.

Vero cells grown to 40–50% confluence in 6-well culture dishes were transfected using FUGENE6 (Roche) and 2 μg DNA/10^6 (ratio 1:6), following manufacturer's recommendations.

RNA isolation, RT-PCR and DNA RACE-PCR

Total RNA was isolated using Trizol reagent (Invitrogen). Reverse Transcription Polymerase Chain Reaction (RT-PCR) amplification was carried out using Reverse Transcription System (Promega) according to the protocol recommended by manufacture. To obtain the sequence information for porcine Bid, we applied the method of Rapid Amplification of cDNA Ends (RACE) PCR (SMART™ RACE cDNA Amplification Kit, Clontech) following the manufacture's directions. RACE-PCR was carried on using SMART primer (Clontech) and a specific primer based on the 5′ end of porcine Bid protein: 5′-TCAGTCCATCTCACTTTGGACTAAG-3′.

Vectors

Mammalian expression vectors

Plasmids expressing Bid, tBid-p13 or tBid-p15 were generated by RACE-PCR amplification of porcine macrophage total RNA to incorporate restriction sites (Supplementary table), followed by ligation of the amplified cDNA fragments with pCMV–myc plasmid (Clontech). The *A179L* gene was amplified by PCR from purified BA71V DNA, using oligonucleotides containing restrictions sites (supplementary table), and subcloned into pCMV–HA vector (Clontech).

Yeast expression vectors

Full length cDNAs encoding A179L, p54, p30 and MyD ASFV proteins were isolated from purified BA71V DNA and cloned into the pGBT9 vector (Clontech). Bax (GenBank accession no AY217036) and Bak (GenBank accession no NM_001188) cDNA were obtained by RT-PCR from human PBLs total RNA. Full length porcine Bid protein and its truncated forms were cloned into the pATC2 vector (Clontech). DNAs corresponding to BH3-only proteins were obtained from pEFFEE plasmids, kindly provided by Drs. Huang and P. Bouillet (Melbourne, Australia). The PCR products of Bcl-2 proapototic members were digested and cloned into the BamHI/EcoRI sites of pATC2 vector except for pATC2-Bax vector in which SmaI/EcoRI sited were used. Primers used for plasmid generation are listed in the supplementary table. All these constructs were sequenced to ensure that no errors were introduced.

Pull down assays vectors

Plasmid pRBgA179L used for the construction of a recombinant vaccinia virus expressing GST gene fused to the N terminus of the A179L protein was obtained by sequential cloning. The coding sequence of the A179L gene was amplified by PCR, using the genome of BA71V as template and oligonucleotides A179B (5′-AATATAGGGATCCGCTATGGAGGG-3′) (BamHI site underlined) and A179X (5′-GTAAAATCCTGCGCTCGAGCTATATC-3′) (XhoI site underlined). The PCR product was digested with BamHI and XhoI and inserted into BamHI/XhoI digested pGEX4T3 (Amersham Pharmacia Biotech) to generate pGEX-A179L.

The fusion gene GST–A179L was amplified by PCR from plasmid pGEX–A179L with oligonucleotides GSTNhe (5'-

CACACAGGCTAGCGTATTCATGTCC-3') (NheI site underlined) and 179Hin (5'-GTCAGTCACGAAGCTTCCGCTCGA-3') (HindIII site underlined). The PCR product was cut with NheI and HindIII and inserted into NheI/HindIII digested pRB21 plasmid (Blasco and Moss, 1995) to generate pRB21g–A179L.

The coding sequences of the BH3 only proteins were amplified by PCR using the corresponding pATC2–BH3 only proteins vectors as templates and the oligonucleotides in supplementary table. The PCR products were digested and cloned into the NdeI/XhoI sites of Pet-19b vector (Novagen) fused to the C-terminus of the His-tag.

Construction of a vaccinia recombinant virus

Vaccinia recombinant virus was isolated following infection/transfection experiments. CV-1 cells were infected with vRB12 at 0.05 PFU per cell and transfected 1 h later with pRBg-A179L plasmid by use of Fugene6 transfection reagent following the manufacturer's recommendations. Recombinant virus (VVgA179L) was isolated from progeny virus by rounds of plaque purification on BSC-1 cells by selecting large virus plaques following protocols described previously (Blasco and Moss, 1995).

Immunofluorescence

Vero cells seeded in 24-well chamber slides were transfected with pCMV–myc and/or pCMV–HA constructions previously described. At 24 h post transfection, cells were fixed with acetone: methanol 1:1 for 2 min at −20°C. Mouse monoclonal antibodies anti-myc-FITC (Babco) and anti-HA-Alexa 594 (Babco) were used at 1:25 dilution and 1:300 dilution, respectively. Mitochondrial staining was carried out using a potential-sensitive dye, chlorometil rosamine (CMXRos, Molecular Probes) and nuclei were stained with Hoechst 33258 (Sigma). Caspase 3 activation was determined using C8487 rabbit polyclonal antibody (Sigma) which exclusively recognizes the active form of caspase 3. After washing, coverslips were finally mounted on glass plates and cells were observed by confocal laser scanning microscopy in a Radiance 2100 MRC1024 (Bio-Rad) mounted on a Nikon Eclipse 300 microscope. Stadistical analysis of colocalization was performed using Lasersharp Processing 3.2 program (Bio-Rad).

Immunoprecipitation

Twenty four hours post-transfection, Vero cells expressing pCMVtBid-p13–myc or pCMV–A179L–HA were lysed using non denaturing lysis buffer (50 mM Tris–HCl, pH 7.4, 300 mM NaCl, 5 mM EDTA, 0.1% Triton X-100) and a protease inhibitor cocktail (Roche), at 4°C. Cells were scraped, clarified by centrifugation and supernatants were mixed. Previously, Protein-A Sepharose (GE, Healthcare) was conjugated with anti-HA antibody (Babco) or irrelevant rabbit serum as negative control, for 16 h at 4°C. Supernatants were incubated with conjugated beads for 4 h at 4°C and gently washed with non denaturing lysis buffer. Bound proteins were eluted by boiling in SDS sample buffer and resolved on a 10% SDS-PAGE gel. Proteins were transferred onto a polyvinylidene difluoride membrane and probed with monoclonal anti-myc (Clontech) and anti-HA (Babco) antibodies. Proteins were detected using rabbit anti IgG-HRP (Bio-rad) as secondary antibody.

Yeast two hybrid assays

For the yeast two-hybrid system, the plasmids pGBT9 and pATC2 (Clontech) were used as sources of the GAL-4 DNA-binding domain and GAL-4 transcriptional activation domain, respectively. All materials used for the analysis were derived from MATCHMAKER GAL-4 Two-Hybrid System (Clontech). Yeast cells were grown on YPD (1% yeast extract, 2% peptone, 2% dextrose, 2% agar for plates) or in synthetic minimal medium (0.143% yeast nitrogen base, the appropriate auxotrophic supplements) containing 2% of dextrose. Y190 strain carrying *His3* and *lacZ* as reporter genes was transformed with appropriate plasmids by the lithium acetate method (Gietz and Woods, 2006). The transformants were selected on the appropriate synthetic medium (SD/-Trp/-Leu/-His) and tested by colon-lift filter assay β-galactosidase activity with 5-bromo-4-chloro-3-indolyl β-D-galactopyranoside as substrate.

Pull down assays

For preparation of GST, and His-BH3 only proteins *E. coli* strain BL21(DE3) cells, transformed with bacterial expression vectors pGEX-4T3 and Pet-19b–BH3-only proteins, respectively, were grown in LB medium supplemented with 50 μg/ml ampicillin to an OD600 nm of 0.4 to 0.6 at 37 °C. Subsequently, isopropyl-ß-D-thiogalactopyranoside (IPTG) was added to the cell culture at a final concentration of 1 mM, and incubation continued for an additional 4 h. Cells were harvested by centrifugation, suspended in 5 ml of lysis buffer (phosphate-buffered saline [PBS], 1% Triton X-100), and sonicated on ice. For preparation of GST–A179L, BSC1 cells were infected with VVgA179L virus at five PFU per cell. At 24 h postinfection, the cells were scraped and suspended in lysis buffer, sonicated on ice and spun down by centrifugation.

GST–A179L and GST proteins were purified by mixing with glutathione-Sepharose 4B beads (GE, Healthcare) for 2 h at 4 °C. Beads were washed with PBS. For the GST-based interaction assay, equal amounts of GST–A179L or GST, attached to glutathione matrix beads were incubated over-night at 4 °C in a tube rotator with bacterial cell lysate, containing expressed His-tagged BH3-only proteins, in binding buffer (50 mM HEPES, pH 7.5, 50 mM NaCl, 0.1% NP-40 with protease inhibitor mixture (Roche Molecular Biochemical). Beads were extensively washed four times with binding buffer. The glutathione-Sepharose beads immunoprecipitates were resuspended in denaturant buffer, boiled for 5 min at 95 °C, resolved by SDS-PAGE, blotted onto nitrocellulose membranes and probed with mouse monoclonal anti-6×His (catalog no. 8916-1; Clontech) before detection by enhanced chemiluminescence (ECL kit; Amersham).

Acknowledgments

This work was supported by grants from the Welcome Trust Foundation WT 075813 and the Spanish Plan Nacional I+D+I Program Consolider CSD2006-00007, BIO2005-0651 and AGL2002-00668.

We thank to Drs. D. Huang and P. Bouillet for kindly providing pEFFEE plasmids expressing the BH3 proteins indicated in Materials and methods section and Dr. R. Blasco for pRB21 plasmid and vRB12 virus. We also thank to Alberto Alvarez-Barrientos for expert confocal microscopy assistance.

Appendix A. Supplementary data

Supplementary data associated with this article can be found, in the online version, at doi:10.1016/j.virol.2008.01.050.

References

Afonso, C.L., Alcaraz, C., Brun, A., Sussman, M.D., Onisk, D.V., Escribano, J.M., Rock, D.L., 1992. Characterization of p30, a highly antigenic membrane and secreted protein of African swine fever virus. Virology 189 (1), 368–373.

Afonso, C.L., Neilan, J.G., Kutish, G.F., Rock, D.L., 1996. An African swine fever virus Bc1-2 homolog, 5-HL, suppresses apoptotic cell death. J. Virol. 70 (7), 4858–4863.

Banadyga, L., Gerig, J., Stewart, T., Barry, M., 2007. Fowlpox virus encodes a Bcl-2 homologue that protects cells from apoptotic death through interaction with the proapoptotic protein Bak. J. Virol. 81 (20), 11032–11045.

Barber, G.N., 2001. Host defense, viruses and apoptosis. Cell Death Differ. 8 (2), 113–126.

Bellows, D.S., Howell, M., Pearson, C., Hazlewood, S.A., Hardwick, J.M., 2002. Epstein-Barr virus BALF1 is a BCL-2-like antagonist of the herpesvirus antiapoptotic BCL-2 proteins. J. Virol. 76 (5), 2469–2479.

Benedict, C.A., Norris, P.S., Ware, C.F., 2002. To kill or be killed: viral evasion of apoptosis. Nat. Immunol. 3 (11), 1013–1018.

Blasco, R., Moss, B., 1995. Selection of recombinant vaccinia viruses on the basis of plaque formation. Gene 158 (2), 157–162.

Bouillet, P., Strasser, A., 2002. BH3-only proteins — evolutionarily conserved proapoptotic Bcl-2 family members essential for initiating programmed cell death. J. Cell Sci. 115 (Pt 8), 1567–1574.

Boyd, J.M., Gallo, G.J., Elangovan, B., Houghton, A.B., Malstrom, S., Avery, B.J., Ebb, R.G., Subramanian, T., Chittenden, T., Lutz, R.J., et al., 1995. Bik, a novel death-inducing protein shares a distinct sequence motif with Bcl-2 family proteins and interacts with viral and cellular survival-promoting proteins. Oncogene 11 (9), 1921–1928.

Brun, A., Rivas, C., Esteban, M., Escribano, J.M., Alonso, C., 1996. African swine fever virus gene A179L, a viral homologue of bcl-2, protects cells from programmed cell death. Virology 225 (1), 227–230.

Brun, A., Rodriguez, F., Escribano, J.M., Alonso, C., 1998. Functionality and cell anchorage dependence of the African swine fever virus gene A179L, a viral bcl-2 homolog, in insect cells. J. Virol. 72 (12), 10227–10233.

Cooray, S., Bahar, M.W., Abrescia, N.G., McVey, C.E., Bartlett, N.W., Chen, R.A., Stuart, D.I., Grimes, J.M., Smith, G.L., 2007. Functional and structural studies of the vaccinia virus virulence factor N1 reveal a Bcl-2-like anti-apoptotic protein. J. Gen. Virol. 88 (Pt 6), 1656–1666.

Cuconati, A., White, E., 2002. Viral homologs of BCL-2: role of apoptosis in the regulation of virus infection. Genes Dev. 16 (19), 2465–2478.

Chen, L., Willis, S.N., Wei, A., Smith, B.J., Fletcher, J.I., Hinds, M.G., Colman, P.M., Day, C.L., Adams, J.M., Huang, D.C., 2005. Differential targeting of prosurvival Bcl-2 proteins by their BH3-only ligands allows complementary apoptotic function. Mol. Cell 17 (3), 393–403.

Cheng, E.H., Nicholas, J., Bellows, D.S., Hayward, G.S., Guo, H.G., Reitz, M.S., Hardwick, J.M., 1997. A Bcl-2 homolog encoded by Kaposi sarcoma-associated virus, human herpesvirus 8, inhibits apoptosis but does not heterodimerize with Bax or Bak. Proc. Natl. Acad. Sci. U. S. A. 94 (2), 690–694.

Chou, J.J., Li, H., Salvesen, G.S., Yuan, J., Wagner, G., 1999. Solution structure of BID, an intracellular amplifier of apoptotic signaling. Cell 96 (5), 615–624.

Derfuss, T., Fickenscher, H., Kraft, M.S., Henning, G., Lengenfelder, D., Fleckenstein, B., Meinl, E., 1998. Antiapoptotic activity of the herpesvirus saimiri-encoded Bcl-2 homolog: stabilization of mitochondria and inhibition of caspase-3-like activity. J. Virol. 72 (7), 5897–5904.

Desagher, S., Osen-Sand, A., Montessuit, S., Magnenat, E., Vilbois, F., Hochmann, A., Journot, L., Antonsson, B., Martinou, J.C., 2001. Phosphorylation of bid by casein kinases I and II regulates its cleavage by caspase 8. Mol. Cell 8 (3), 601–611.

Enjuanes, L., Carrascosa, A.L., Moreno, M.A., Vinuela, E., 1976. Titration of African swine fever (ASF) virus. J. Gen. Virol. 32 (3), 471–477.

Everett, H., McFadden, G., 1999. Apoptosis: an innate immune response to virus infection. Trends Microbiol. 7 (4), 160–165.

Farrow, S.N., White, J.H., Martinou, I., Raven, T., Pun, K.T., Grinham, C.J., Martinou, J.C., Brown, R., 1995. Cloning of a bcl-2 homologue by interaction with adenovirus E1B 19K. Nature 374 (6524), 731–733.

Feng, P., Scott, C., Lee, S.H., Cho, N.H., Jung, J.U., 2004. Manipulation of apoptosis by herpes viruses (Kaposi's sarcoma pathogenesis). Prog. Mol. Subcell. Biol. 36, 191–205.

Fleischer, A., Rebollo, A., Ayllon, V., 2003. BH3-only proteins: the lords of death. Arch. Immunol. Ther. Exp. (Warsz) 51 (1), 9–17.

Foghsgaard, L., Jaattela, M., 1997. The ability of BHRF1 to inhibit apoptosis is dependent on stimulus and cell type. J. Virol. 71 (10), 7509–7517.

Gietz, R.D., Woods, R.A., 2006. Yeast transformation by the LiAc/SS Carrier DNA/PEG method. Methods Mol. Biol. 313, 107–120.

Gong, X.M., Choi, J., Franzin, C.M., Zhai, D., Reed, J.C., Marassi, F.M., 2004. Conformation of membrane-associated proapoptotic tBid. J. Biol. Chem. 279 (28), 28954–28960.

Gross, A., McDonnell, J.M., Korsmeyer, S.J., 1999a. BCL-2 family members and the mitochondria in apoptosis. Genes Dev. 13 (15), 1899–1911.

Gross, A., Yin, X.M., Wang, K., Wei, M.C., Jockel, J., Milliman, C., Erdjument-Bromage, H., Tempst, P., Korsmeyer, S.J., 1999b. Caspase cleaved BID targets mitochondria and is required for cytochrome *c* release, while BCL-XL prevents this release but not tumor necrosis factor-R1/Fas death. J. Biol. Chem. 274 (2), 1156–1163.

Han, J., Sabbatini, P., Perez, D., Rao, L., Modha, D., White, E., 1996a. The E1B 19K protein blocks apoptosis by interacting with and inhibiting the p53-inducible and death-promoting Bax protein. Genes Dev. 10 (4), 461–477.

Han, J., Sabbatini, P., White, E., 1996b. Induction of apoptosis by human Nbk/Bik, a BH3-containing protein that interacts with E1B 19K. Mol. Cell. Biol. 16 (10), 5857–5864.

Hardwick, J.M., 2001. Apoptosis in viral pathogenesis. Cell Death Differ. 8 (2), 109–110.

Hardwick, J.M., Bellows, D.S., 2003. Viral versus cellular BCL-2 proteins. Cell Death Differ. 10 (Suppl. 1), S68–S76.

Heibein, J.A., Goping, I.S., Barry, M., Pinkoski, M.J., Shore, G.C., Green, D.R., Bleackley, R.C., 2000. Granzyme B-mediated cytochrome *c* release is regulated by the Bcl-2 family members bid and Bax. J. Exp. Med. 192 (10), 1391–1402.

Henderson, S., Huen, D., Rowe, M., Dawson, C., Johnson, G., Rickinson, A., 1993. Epstein-Barr virus-coded BHRF1 protein, a viral homologue of Bcl-2, protects human B cells from programmed cell death. Proc. Natl. Acad. Sci. U. S. A. 90 (18), 8479–8483.

Hernaez, B., Diaz-Gil, G., Garcia-Gallo, M., Ignacio Quetglas, J., Rodriguez-Crespo, I., Dixon, L., Escribano, J.M., Alonso, C., 2004a. The African swine fever virus dynein-binding protein p54 induces infected cell apoptosis. FEBS Lett. 569 (1-3), 224–228.

Hernaez, B., Escribano, J.M., Alonso, C., 2004b. Switching on and off the cell death cascade: African swine fever virus apoptosis regulation. In: Alonso, C. (Ed.), "Viruses and Apoptosis". Springer, Berlin, pp. 57–70.

Hernaez, B., Escribano, J.M., Alonso, C., 2006. Visualization of the African swine fever virus infection in living cells by incorporation into the virus particle of green fluorescent protein-p54 membrane protein chimera. Virology 350 (1), 1–14.

Korsmeyer, S.J., 1995. Regulators of cell death. Trends Genet. 11 (3), 101–105.

Li, H., Zhu, H., Xu, C.J., Yuan, J., 1998. Cleavage of BID by caspase 8 mediates the mitochondrial damage in the Fas pathway of apoptosis. Cell 94 (4), 491–501.

Luo, X., Budihardjo, I., Zou, H., Slaughter, C., Wang, X., 1998. Bid, a Bcl2 interacting protein, mediates cytochrome *c* release from mitochondria in response to activation of cell surface death receptors. Cell 94 (4), 481–490.

Marani, M., Tenev, T., Hancock, D., Downward, J., Lemoine, N.R., 2002. Identification of novel isoforms of the BH3 domain protein Bim which directly activate Bax to trigger apoptosis. Mol. Cell. Biol. 22 (11), 3577–3589.

Marshall, W.L., Yim, C., Gustafson, E., Graf, T., Sage, D.R., Hanify, K., Williams, L., Fingeroth, J., Finberg, R.W., 1999. Epstein-Barr virus encodes a novel homolog of the bcl-2 oncogene that inhibits apoptosis and associates with Bax and Bak. J. Virol. 73 (6), 5181–5185.

McDonnell, J.M., Fushman, D., Milliman, C.L., Korsmeyer, S.J., Cowburn, D., 1999. Solution structure of the proapoptotic molecule BID: a structural basis for apoptotic agonists and antagonists. Cell 96 (5), 625–634.

Nava, V.E., Cheng, E.H., Veliuona, M., Zou, S., Clem, R.J., Mayer, M.L., Hardwick, J.M., 1997. Herpesvirus saimiri encodes a functional homolog of the human bcl-2 oncogene. J. Virol. 71 (5), 4118–4122.

Neilan, J.G., Lu, Z., Afonso, C.L., Kutish, G.F., Sussman, M.D., Rock, D.L., 1993. An African swine fever virus gene with similarity to the proto-oncogene bcl-2 and the Epstein-Barr virus gene BHRF1. J. Virol. 67 (7), 4391–4394.

Oura, C.A., Powell, P.P., Parkhouse, R.M., 1998. African swine fever: a disease characterized by apoptosis. J. Gen. Virol. 79 (Pt 6), 1427–1438.

Petros, A.M., Olejniczak, E.T., Fesik, S.W., 2004. Structural biology of the Bcl-2 family of proteins. Biochim. Biophys. Acta 1644 (2–3), 83–94.

Plowright, W., Parker, J., Peirce, M.A., 1969. African swine fever virus in ticks (*Ornithodoros moubata*, murray) collected from animal burrows in Tanzania. Nature 221 (185), 1071–1073.

Polster, B.M., Pevsner, J., Hardwick, J.M., 2004. Viral Bcl-2 homologs and their role in virus replication and associated diseases. Biochim. Biophys. Acta 1644 (2–3), 211–227.

Ramiro-Ibanez, F., Ortega, A., Brun, A., Escribano, J.M., Alonso, C., 1996. Apoptosis: a mechanism of cell killing and lymphoid organ impairment during acute African swine fever virus infection. J. Gen. Virol. 77 (Pt 9), 2209–2219.

Revilla, Y., Cebrian, A., Baixeras, E., Martinez, C., Vinuela, E., Salas, M.L., 1997. Inhibition of apoptosis by the African swine fever virus Bcl-2 homologue: role of the BH1 domain. Virology 228 (2), 400–404.

Rivera, J., Abrams, C., Hernaez, B., Alcazar, A., Escribano, J.M., Dixon, L., Alonso, C., 2007. The MyD116 African swine fever virus homologue interacts with the catalytic subunit of protein phosphatase 1 and activates its phosphatase activity. J. Virol. 81 (6), 2923–2929.

Rodriguez, F., Alcaraz, C., Eiras, A., Yanez, R.J., Rodriguez, J.M., Alonso, C., Rodriguez, J.F., Escribano, J.M., 1994. Characterization and molecular basis of heterogeneity of the African swine fever virus envelope protein p54. J. Virol. 68 (11), 7244–7252.

Sattler, M., Liang, H., Nettesheim, D., Meadows, R.P., Harlan, J.E., Eberstadt, M., Yoon, H.S., Shuker, S.B., Chang, B.S., Minn, A.J., Thompson, C.B., Fesik, S.W., 1997. Structure of Bcl-xL-Bak peptide complex: recognition between regulators of apoptosis. Science 275 (5302), 983–986.

Stoka, V., Turk, B., Schendel, S.L., Kim, T.H., Cirman, T., Snipas, S.J., Ellerby, L.M., Bredesen, D., Freeze, H., Abrahamson, M., Bromme, D., Krajewski, S., Reed, J.C., Yin, X.M., Turk, V., Salvesen, G.S., 2001. Lysosomal protease pathways to apoptosis. Cleavage of bid, not pro-caspases, is the most likely route. J. Biol. Chem. 276 (5), 3149–3157.

Wang, K., Yin, X.M., Chao, D.T., Milliman, C.L., Korsmeyer, S.J., 1996. BID: a novel BH3 domain-only death agonist. Genes Dev. 10 (22), 2859–2869.

Wang, G.H., Garvey, T.L., Cohen, J.I., 1999. The murine gammaherpesvirus-68 M11 protein inhibits Fas- and TNF-induced apoptosis. J. Gen. Virol. 80 (Pt 10), 2737–2740.

White, E., 1996. Life, death, and the pursuit of apoptosis. Genes Dev. 10 (1), 1–15.

Yanez, R.J., Rodriguez, J.M., Nogal, M.L., Yuste, L., Enriquez, C., Rodriguez, J.F., Vinuela, E., 1995. Analysis of the complete nucleotide sequence of African swine fever virus. Virology 208 (1), 249–278.

Zha, J., Weiler, S., Oh, K.J., Wei, M.C., Korsmeyer, S.J., 2000. Posttranslational N-myristoylation of BID as a molecular switch for targeting mitochondria and apoptosis. Science 290 (5497), 1761–1765.

Citation: Cell Death and Disease (2012) 3, e341; doi:10.1038/cddis.2012.81

www.nature.com/cddis

The ATF6 branch of unfolded protein response and apoptosis are activated to promote African swine fever virus infection

I Galindo[1], B Hernáez[1], R Muñoz-Moreno[1], MA Cuesta-Geijo[1], I Dalmau-Mena[1] and C Alonso*,[1]

African swine fever virus (ASFV) infection induces apoptosis in the infected cell; however, the consequences of this activation on virus replication have not been defined. In order to identify the role of apoptosis in ASFV infection, we analyzed caspase induction during the infection and the impact of caspase inhibition on viral production. Caspases 3, 9 and 12 were activated from 16 h post-infection, but not caspase 8. Indeed, caspase 3 activation during the early stages of the infection appeared to be crucial for efficient virus exit. In addition, the inhibition of membrane blebbing reduced the release of virus particles from the cell. ASFV uses the endoplasmic reticulum (ER) as a site of replication and this process can trigger ER stress and the unfolded protein response (UPR) of the host cell. In addition to caspase 12 activation, indicators of ER stress include the upregulation of the chaperones calnexin and calreticulin upon virus infection. Moreover, ASFV induces transcription factor 6 signaling pathway of the UPR, but not the protein kinase-like ER kinase or the inositol-requiring enzyme 1 pathways. Thus, the capacity of ASFV to regulate the UPR may prevent early apoptosis and ensure viral replication.
Cell Death and Disease (2012) **3,** e341; doi:10.1038/cddis.2012.81; published online 5 July 2012
Subject Category: Experimental Medicine

African swine fever virus (ASFV) is a double-stranded large DNA virus that induces an acute disease of swine in which apoptosis has a central role in pathogenesis. Virus infection elicits apoptosis in target and immune defense cells.[1] The large repertoire of anti-apoptotic proteins encoded by the virus reflects the relevance of apoptosis in limiting viral replication in host cells. Many DNA viruses encode structural and functional homologs of anti-apoptotic Bcl-2 proteins, named viral Bcl2, including the *A179L* gene of ASFV.[2] In common with other viruses, ASFV has several strategies to block apoptotic pathways in order to complete virus replication. ASFV encodes proteins involved in apoptosis inhibition, thereby delaying the final execution step of the apoptotic pathway, which occurs only at late post-infection times. Programmed cell death itself may be relevant for the final release of virus particles within apoptotic bodies, which would provide this virus with a mechanism to spread, thus evading the immune system. The central component of the apoptotic machinery is the caspase proteolytic system. There are two groups of caspases: upstream initiator caspases, such as caspases 8 and 9, which cleave and activate other caspases; and downstream effector caspases, including caspase 3, which cleave a variety of cellular substrates, thereby disassembling cellular structures or inactivating enzymes.[3]

Caspase 12 is associated with the cytoplasmic face of the endoplasmic reticulum (ER) and it cleaves to an active form in response to ER stress.[4] The ER stress response, also called the unfolded protein response (UPR), is mediated by three transmembrane proteins: (i) the protein kinase-like ER resident kinase (PERK); (ii) the activating transcription factor 6 (ATF6); and (iii) the inositol-requiring enzyme 1 (IRE1).[5] These three proteins are associated with the ER chaperone BiP/Grp78, which prevents their aggregation and further activation. However, when misfolded proteins accumulate, BiP is released, thus allowing UPR activation. Activated PERK phosphorylates the eukaryotic initiation factor 2α (eIF2α), thus resulting in translation attenuation to counterbalance enhanced protein accumulation. This counterbalancing effect includes the upregulation of the pro-apoptotic mRNA CHOP (c/EBP homologous protein) and mRNA encoding GADD34 (growth arrest and DNA-damage-inducible protein-34), whose association with the protein phosphatase 1 (PP1) leads to the dephosphorylation of eIF2α.[5] Activated IRE1 removes 26 nucleotides from X-box binding protein-1 (XBP1) mRNA, thereby altering the open reading frame and causing the translation of an active transcription factor.[6] The spliced form of XBP1 protein (sXBP1) is involved in the transcriptional activation of a number of genes,

[1]Departamento de Biotecnología, Instituto Nacional de Investigación y Tecnología Agraria y Alimentaria (INIA), Madrid, Spain
*Corresponding author: C Alonso, Departamento de Biotecnología, Instituto Nacional de Investigación y Tecnología Agraria y Alimentaria (INIA), Ctra. de la Coruña Km 7.5, Madrid 28040, Spain. Tel: +34 91 347 6896; Fax: +34 91 347 8771; E-mail: calonso@inia.es
Keywords: unfolded protein response; ER stress; ATF6; chaperones; caspase 12; African swine fever virus
Abbreviations: ATF6, activating transcription factor 6; ASFV, African swine fever virus; UPR, unfolded protein response; ER, endoplasmic reticulum; PERK, protein kinase-like ER resident kinase; IRE1, inositol-requiring enzyme 1; BiP/Grp78, binding immunoglobulin protein/glucose-regulated protein 78; CHOP/GADD153, c/EBP homologous protein/DNA-damage-inducible gene 153; eIF2α, eukaryotic initiation factor 2α; GADD34, growth arrest and DNA-damage-inducible protein-34; PP1, protein phosphatase 1; XBP1, X-box binding Protein-1; EDEM, ER degradation enhancing α-mannosidase-like protein; HCV, hepatitis C virus; BVDV, bovine viral diarrhea virus; JEV, Japanese encephalitis virus; CMV, cytomegalovirus; SARS-CoV, severe acute respiratory syndrome virus; AEBSF, 4-(2-aminoethyl)-benzenesulfonyl fluoride
Received 08.12.11; revised 10.5.12; accepted 29.5.12; Edited by M Piacentini

including the ER mannosidase-like protein EDEM, which participates in protein degradation. Finally, activated ATF6 exits ER compartment to migrate to the Golgi apparatus where it is cleaved by proteases.[7] ATF6 cytosolic fragment is a transcription factor responsible for the transcriptional induction of XBP1 as well as many ER chaperone-encoding genes.[5] However, when cells are unable to recover from ER stress, apoptosis occurs.

The ER is an essential organelle for viral replication and maturation; in the course of productive infection, a large number of viral proteins are synthesized in infected cells, where unfolded or misfolded proteins activate the ER stress response. It is therefore not surprising that viruses have evolved various mechanisms to counteract these responses that limit or inhibit viral replication. For instance, BiP is induced in cells infected with respiratory syncytial virus,[8] hanta viruses,[9] hepatitis C virus (HCV),[10] bovine viral diarrhea virus (BVDV),[11] Japanese encephalitis virus (JEV),[12] dengue[13] and enterovirus 71.[14] The induction of PERK has also been reported in infection with herpes simplex virus,[15] cytomegalovirus (CMV)[16] and BVDV.[11] The IRE1 pathway has been shown to be activated in cells infected with JEV, dengue[17] and severe acute respiratory syndrome virus,[18] whereas the ATF6 pathway is triggered upon HCV infection[19] and both IRE1 and ATF6 arms are induced during Rotavirus infection.[20] In addition, the activation of all three pathways of the UPR has been reported in infection with West Nile virus[21] and dengue.[22] Furthermore, ASFV encodes the DP71L protein homolog to GADD34,[23] which inhibits the induction of ATF4 and its downstream target CHOP.[24,25] However, the infection does not induce the phosphorylation of PERK or the upregulation of BiP.[24]

Here, we found that ASFV induces caspases 3, 9 and 12 but not caspase 8 in infected cells, as it regulates the three arms of the UPR signaling cascade, thus inhibiting the pathways that hinder viral infection and activating those that are beneficial.

Results

Activation of caspases in ASFV-infected cells. Caspases are key factors in the regulation of apoptotic pathways. These proteins are induced by a variety of apoptotic triggers (stimuli). To identify the apoptotic pathways induced in ASFV-infected cells, we performed caspase activity assays at a range of times after infection (Figure 1). ASFV induced caspases 3 and 9 in Vero (African green monkey kidney) cells from 16 h post-infection (hpi) and increased this activation along infection, with higher levels at 48 hpi and both curves showed a similar pattern (Figures 1a and b). However, caspase 8 activity was not detected in infected Vero cells (Figure 1c). This observation was further confirmed in the infected WSL-R macrophage cell line (Figure 1d); however, caspase 8 activity was found in the specific positive control in both cases.

We also tested the activity of caspase 12, an ER membrane-associated cysteine protease that is activated in response to ER stress.[26] Caspase 12 was undetectable in mock-infected cells or at 6 hpi, but at 16 hpi it was induced and increased threefold until 48 hpi (Figure 1e). The subcellular localization of this caspase in ASFV-infected cells was studied by indirect immunofluorescence (Figure 1f). As a control of induced caspase 12, Vero cells were treated with the ER stress-inducing agent tunicamycin, which activates caspase 12 and translocates it into the nucleus. Caspase 12 was localized in the nucleus in infected cells and in cells incubated with tunicamycin, but not in mock-infected ones.

To study the impact of apoptosis on ASFV infection, we infected Vero cells treated with an inhibitor of caspase 3 activation (Ac-DEVD-CHO) and with a specific inhibitor of myosin II ATPase activity (Blebbistatin). Myosin II ATPase activity, together with the GTPase ROCK-I, is necessary for cell membrane fragmentation into multiple apoptotic bodies in the execution phase of apoptosis. Also, we analyzed the effect of Y-27632, a ROCK-I inhibitor that blocks membrane blebbing. We then compared final infective virus production at 48 hpi when these drugs were added to the cells, either 2 h before infection, or at 6 hpi. Our results showed that neither blebbing nor caspase 3 inhibition modified total virus production (extracellular plus intracellular virus production; Figure 2a). Caspase 3 activation in early stages of the infection was required for virus exit, whereas the inhibition of membrane blebbing reduced the release of virus particles from the cell and this effect was enhanced when the inhibitor was added 6 hpi (Figure 2b). In order to asses a possible role of caspase 12 in caspase 3 and 9 activation, we analyzed the effect of caspase 12 inhibition in infected cells using Z-ATD-FMK. Addition of this inhibitor before infection did not affect percentages of ASFV-infected cells as detected by flow cytometry (fluorescence-activated cell sorter (FACS); Figure 3a). Also, this inhibitor did not cause a decrease in virus production nor in the exit of virus particles (Figure 3b). Moreover, our results showed that neither caspase 3 nor caspase 9 were inhibited by Z-ATD-FMK and only caspase 12 activation was specifically inhibited (Figure 3c).

ASFV infection leads to the induction of ER chaperones. The induction of caspase 12 after ASFV infection suggests that the virus triggers an ER stress response. This response is an autoregulatory program that upregulates a large number of genes, such as ER chaperones and ER-associated degradation (ERAD) components, which increase the folding capacity of the ER.[26] In order to determine whether ASFV infection induces this response, we used western blot analysis to monitor the expression levels of the ER chaperones BiP, calreticulin, calnexin, ERp57 and PDI (protein disulfide isomerase) over the course of the infection. Calreticulin and calnexin were induced upon ASFV infection at 16 hpi (Figure 4a), while only a modest increase in PDI levels was found at 48 hpi. Interestingly, ASFV did not induce the expression of ERp57 or BiP. Chaperone upregulation was coincident with the expression of viral protein p30. Actin levels remained constant during the course of the infection, indicating that chaperone induction was not caused by a global upregulation of protein translation. We also analyzed the expression of BiP by inmunofluorescence. Cells treated with tunicamycin showed a typical ER pattern for BiP, while BiP expression was undetectable in non-treated/non-infected controls and infected cells (Figure 4c). This could be probably due to the low levels of BiP to be detected by the antibody.

Calnexin is an ER resident molecular chaperone that has a key role in the correct folding of membrane proteins. It has

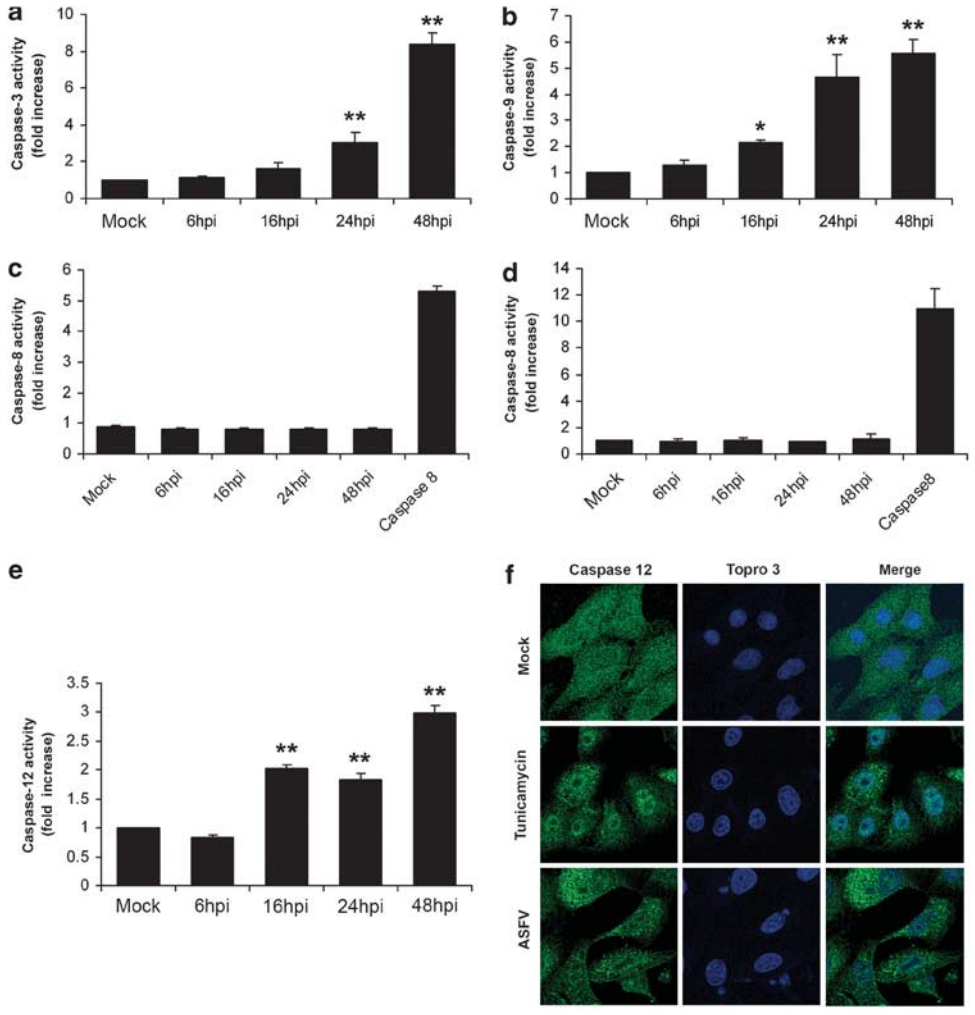

Figure 1 Caspase activities in ASFV-infected cells. Caspase activities were measured in virus-infected cell lysates using specific activity assays at the indicated time points after infection. Data were normalized to the corresponding values for mock-infected cells for each caspase. (**a** and **b**) Caspase 3 and 9 activity of virus-infected Vero cells. (**c** and **d**) Caspase 8 activity of ASFV-infected Vero and WSL-R macrophage cell lines, respectively. (**e**) Caspase 12 activity of ASFV-infected Vero cells. (**f**) Representative confocal micrographs of nuclear localization of caspase 12 in ASFV-infected Vero cells. Cells treated with tunicamycin were used as controls. Statistical significance is indicated by asterisks (*$P<0.05$; **$P<0.01$)

been proposed that calnexin acts as a scaffold for caspase 8-dependent cleavage of the ER transmembrane protein Bap31 and thus for the generation of the pro-apoptotic p20 under ER stress.[27] The Bap31 p20 fragment directs pro-apoptotic crosstalk between the ER and mitochondria.[28] To study whether overexpression of calnexin during the infection is involved in the cleavage of Bap31, we monitored p20 by western blot. Bap31 remained intact during the infection, thereby indicating the absence of pro-apoptotic signals between the ER and mitochondria (Figure 4a).

ASFV infection does not result in an attenuation of protein translation. We studied the expression of UPR markers in virus-infected Vero cells. The activation of the PERK pathway results in the phosphorylation of the eIF2α subunit, leading to translation attenuation.[29] PERK also activates the expression of ATF4, a transcription factor, thus leading to the upregulation of the pro-apoptotic genes *CHOP* and *GADD34*.[30] GADD34 association with the phosphatase PP1 produces the dephosphorylation of eIF2α.[5] Tunicamycin treatment caused an increase in CHOP expression in Vero cells; however, no induction of CHOP was observed in ASFV-infected cells by western blot (Figure 5a). ATF4 expression was detected only in infected cells at 48 hpi. GADD34 protein showed an increase in expression from 16 hpi. Taken together, these results indicate that ASFV inhibits CHOP expression and leads to increased eIF2α dephosphorylation in order to restore protein translation.

ASFV infection does not induce XBP1 splicing in Vero cells. In response to the accumulation of unfolded proteins in the ER, IRE1 is activated by its oligomerization in the membrane, which causes the splicing of the mRNA encoding XBP1 transcription factor. The XBP1 protein encoded by the spliced mRNA is more stable than the unspliced form and is a potent transcription factor of the basic-leucine zipper (bZIP) family and caspase 12 inhibition flow cytometry (FACS ERAD) PDI eIF2α basic-leucine zipper (bZIP) one of the key

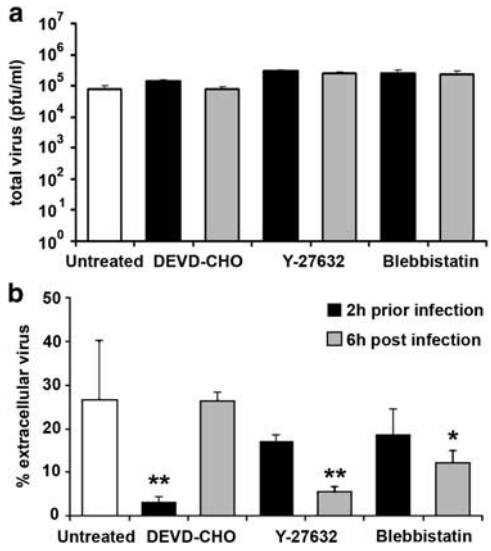

Figure 2 Caspase 3 activation and membrane blebbing enhance ASFV spread. Vero cells treated with DEVD-CHO, Y-27632 or Blebbistatin were infected with ASFV. Drugs were added 2 h before infection or 6 h after, as indicated. At 48 hpi, cells and media were harvested and titrated by plaque assay. Total (**a**) or extracellular virus titers (**b**) are shown. Error bars indicate S.D. from three independent experiments. Statistically significant differences are indicated by asterisks (*$P<0.05$) (**$P<0.01$)

regulators of ER-folding capacity.[31] Using RT-PCR and specific primers to distinguish between the unspliced (inactive) and spliced (active) forms of the XBP1 transcript, we detected XBP1 splicing in Vero cells treated with the UPR inducer tunicamycin but not in ASFV-infected cells at a range of post-infection times (Figure 5c). Therefore, it appears that the infection did not increase levels of active XBP1 mRNA. XBP1 mRNA is spliced by IRE1 but is induced by ATF6 activation.[6] The level of endogenous XBP1 mRNA was measured in infected cells using qRT-PCR analysis of RNAs from ASFV-infected samples. We found an increase in the level of XBP1 transcript in cells treated with tunicamycin or dithiothreitol (DTT) compared with the level of mRNA obtained in mock-infected cells. In contrasts, ASFV results in a gradual decrease in the level of XBP1 mRNA over the course of infection (Figure 5d) indicating the downregulation of this mRNA in ASFV-infected cells.

ASFV infection activates the ATF6 pathway. In response to ER stress, ATF6 exits the ER to the Golgi apparatus, where it is processed by proteases to its active form, which in turn translocates to the nucleus. In order to monitor ATF6 activation by fluorescence microscopy, we used an EGFP (enhanced green fluorescent protein)–ATF6 fusion protein (pCMV short-EGFP-ATF6).[32] This protein was under the control of a shortened CMV promoter, which has a deletion of 430 bp from the 5′ side in order to prevent overexpression, which would modify the localization of the fusion protein itself. The short promoter shows considerably less activity than the full promoter and GFP-ATF6 expressed under the short CMV promoter localizes exclusively to the ER and translocates to the nucleus, in a similar way to endogenous ATF6.[32] Cells transfected with the pCMV short-EGFP-ATF6 plasmid presented a typical ER pattern that relocated to the Golgi apparatus (Figure 6b) or to the nucleus (Figure 6c) in response to tunicamycin treatment. However, this characteristic pattern was modified in infected cells. Cells transfected with this construct and infected with ASFV showed GFP-ATF6 localization either in discrete perinuclear cytoplasmic areas corresponding to viral factories, as indicated by their co-localization with DNA stain (Figures 6d and e), or in the nucleus of infected cells (Figure 6f). This finding indicates that ASFV activates the ATF6 pathway of the UPR. We next studied the effect of a serine protease inhibitor that inhibits ER stress-induced proteolysis of ATF6, AEBSF[33] on ASFV infection. Addition of this inhibitor before infection affected the percentages of ASFV-infected cells in a dose-dependent manner as detected by FACS (Figure 7a). AEBSF also induced a strong inhibition of viral production resulting in 100% reduction of viral titer at 300 μM concentrations of AEBSF (data not shown). We analyzed caspase activation under AEBSF to find that this agent abrogated caspase 3, 9 and 12 activation in infected cells. Inhibition of caspases was dependent of AEBSF effect on infection, given that this serine protease inhibitor did not prevent activation of caspase 3 induced by staurosporine (Figure 7b).

Discussion

Apoptosis is a genetically controlled cell death mechanism involved in the regulation of tissue homeostasis. We analyzed the mechanism by which ASFV induces apoptosis in infected cells and observed that caspases 3 and 9 are activated with similar kinetics as of 16 hpi. However, ASFV-induced apoptosis was independent of caspase 8 activation, a process involved in the extrinsic apoptotic pathways. These results indicated that the virus induces apoptosis through the mitochondrial pathway rather than the death receptor-mediated pathway. ASFV triggers apoptosis in an early stage of the infection process.[34] Nevertheless, extensive apoptosis of infected cells occurs only at late post-infection times. Programmed cell death itself might be relevant for the release of virus particles into apoptotic bodies, which would provide a mechanism to facilitate virus spread and evasion of the immune system. Our results show that caspase 3 activation in early stages of the infection, was relevant for virus exit and that membrane blebbing contributes to virus dissemination, given the fact that the inhibition of the effector caspase 3 reduced the release of virus particles from the cell and this effect was enhanced when the inhibitor was added after 6 hpi. Thus, ASFV takes advantage of an early induction of apoptosis, through caspase 3 activity, while the final execution of programmed cell death in apoptotic blebs contribute to ASFV invasion of host cells and evasion of the immune surveillance. In addition to its critical role in apoptosis, caspase 3 participates in other cellular processes.[35] This could also be the case of ASFV infection, where activation of caspase 3 may be required during early stages of infection to ensure subsequent virus exit from the cell. Another example is the influenza virus infection, in which caspase 3 inhibitors prevent the formation of progeny influenza A virus particles.[36]

We have also shown that ASFV infection in Vero cells induces caspase 12, although this induction is not required for

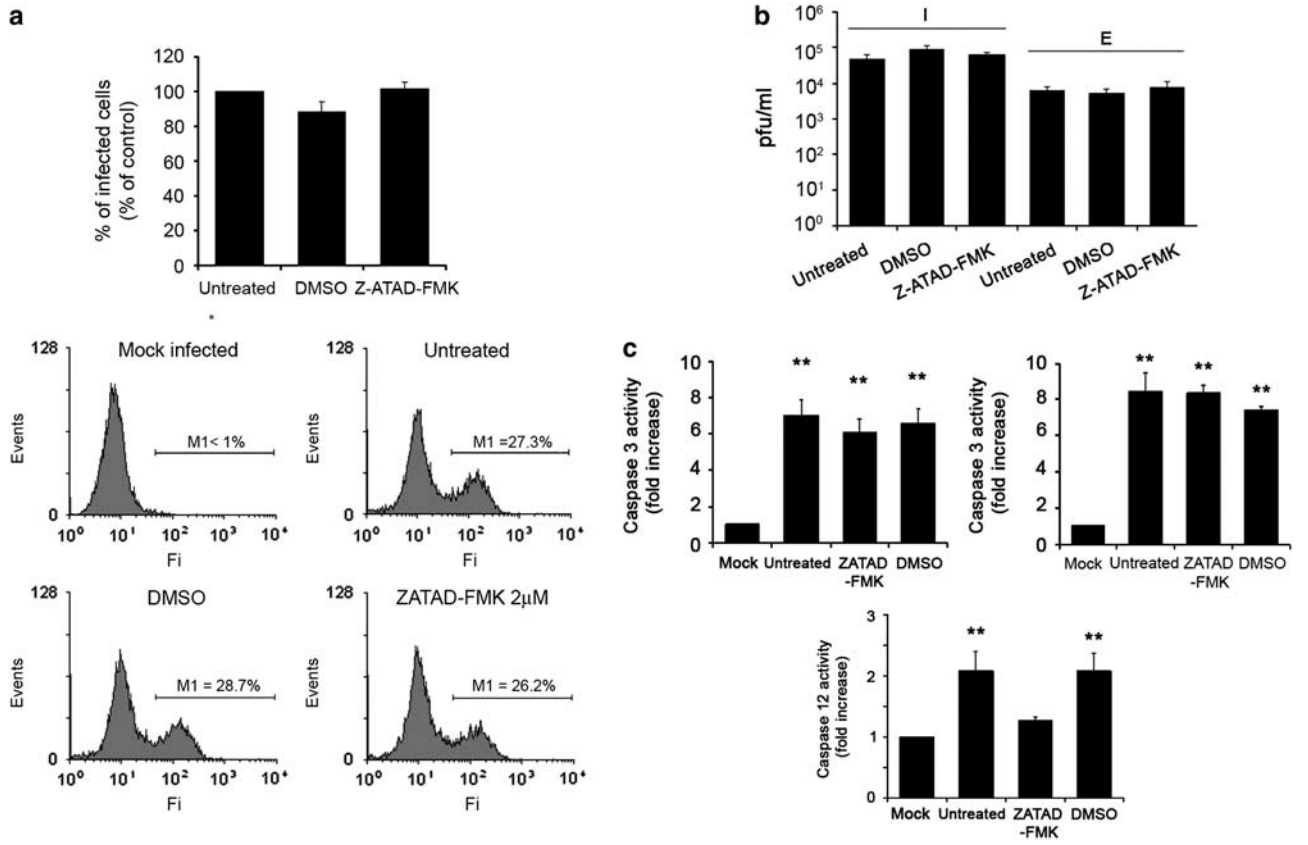

Figure 3 ASFV infection is independent of caspase 12 activation. Vero cells were pretreated with Z-ATAD-FMK and then infected with ASFV. (**a**) Infected cells were detected by FACS and percentages normalized to values in untreated cells. Representative FACS profiles are shown in the graphs below. Infected cells were gated in M1 and expressed as a percentage of total cells analyzed. (**b**) Cells and media were harvested at 48 hpi and titrated by plaque assay. Intracellular (I) or extracellular (E) virus titers in pfu/ml are shown. (**c**) Caspase activities were analyzed at 24 hpi using specific activity assays. Data were normalized to control values. Error bars indicate S.D. from three independent experiments and statistically significant differences are indicated by asterisks (**$P<0.01$)

viral production or for caspases 3 and 9 activation. Caspase 12 is a characteristic ER stress response caspase. Virus assembly begins with the modification of ER membranes, which are subsequently recruited to the viral factories and transformed into viral precursor membranes.[37] Moreover, a large amount of viral proteins are synthesized and accumulated in infected cells, thus overloading the ER-folding capacity. This overload can lead to the activation of the ER stress response of the host cell. Activated caspase 12, a key marker of ER stress-mediated apoptosis, may potentially interact with another pro-apoptotic protein, Bap31, resulting in a feedback mechanism involving the release of cytochrome c elicited through the mitochondrial pathway.[38] However, Bap31 was not activated by the fragmentation of p20 in ASFV-infected cells. This observation indicates the absence of direct pro-apoptotic signals between the ER and mitochondria. Caspase 12 was triggered in ASFV-infected cells but this activation does not necessarily result in apoptosis, because the virus has the capacity to block ER stress at a later step. In general, ER stress starts with the transcriptional induction of ER-localized chaperones as a survival signal. Molecular chaperones are key components of the ER machinery; their main function consists of ensuring the quality of the ER by maintaining newly synthesized proteins in a proper state for folding, and marking misfolded proteins for degradation. Two folding systems have been proposed to contribute to this quality control. One of these is composed of grp78 (BiP), grp94 and PDI. The second system, known as the 'calnexin–calreticulin cycle', includes calnexin, calreticulin and ERp57.[39] Chaperone expression analysis of ASFV-infected cells revealed a marked increase in calnexin and calreticulin expression from 16 hpi, and to a lesser extent, of PDI at 48 hpi. However, ASFV did not induce the expression of ERp57, which, together with calnexin and calreticulin, assists disulfide bond formation in glycoprotein folding. Surprisingly, ASFV did not elicit the expression of grp78 (BiP), thereby indicating that the virus contains the ER stress at this level.

To determine whether ER stress is involved in ASFV-induced cellular responses, we analyzed several ER stress-related proteins, including CHOP, GADD34, XBP1, ATF6 and ATF4. Previous results showed that viral infection in Vero cells inhibits the induction of the ATF4-CHOP signaling arm of the UPR.[24,25] However, we observed expression of ATF4 from 48 hpi when virus is thought to promote programmed cell death in order to spread progeny. The inhibition of this UPR branch results in an attenuation of protein translation. To avoid this, ASFV encodes the *DP71L* gene, a GADD34 homolog that interacts with the catalytic subunit of PP1, and activates its phosphatase activity[40] and that also promotes the expression of cellular GADD34, as shown here.

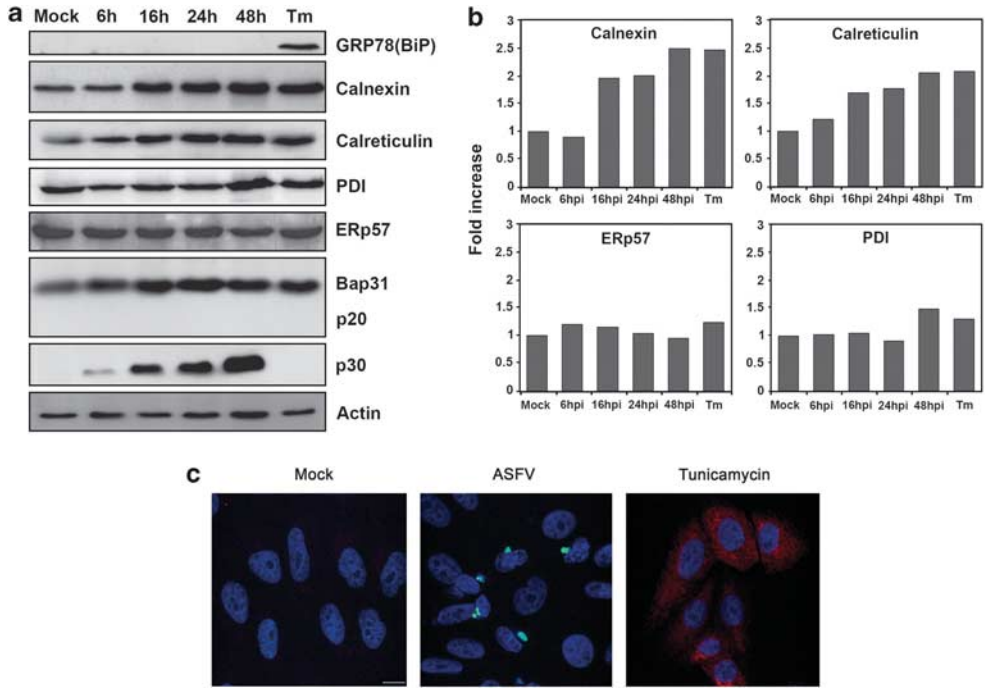

Figure 4 ASFV induces the expression of ER chaperones but not the expression of ERp57 or fragmentation of Bap31. (**a**) Western blot analysis of the ER chaperones in Vero cells infected with ASFV or treated with tunicamycin (Tm). Cell lysates were harvested at the indicated times after infection and then, analyzed. Actin was used as protein load control and viral infection was followed by p30 viral protein expression. (**b**) Quantification of the bands by densitometry corrected to actin data and normalized to control values. (**c**) Representative confocal micrographs of Vero cells grown on glass slides were treated with tunicamycin or infected with B54GFP-2 for 16 hpi. Cells were fixed, stained with anti-BiP plus Alexa Fluor 594-conjugated secondary antibody and incubated with Topro-3 for DNA staining and then analyzed by confocal fluorescence microscopy. Bar 10 μM

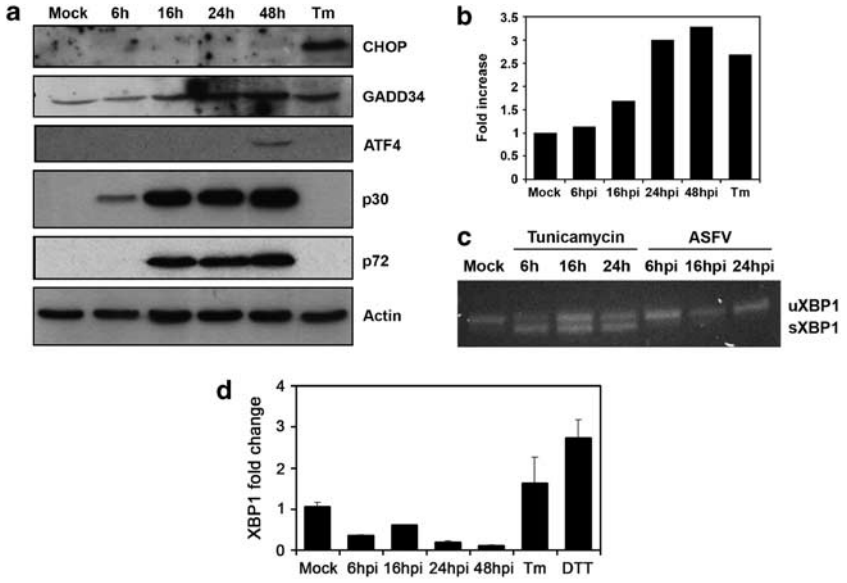

Figure 5 ASFV regulates UPR signaling. (**a**) Western blot analysis of CHOP, GADD34, ATF4, p30 and p72 viral proteins in Vero cells infected with ASFV or treated with tunicamycin, lysated at the indicated times after infection with actin as protein load control. (**b**) Quantification of the bands corresponding to GADD34 by densitometry was corrected to actin data and normalized to control values (**c**) Unspliced (uXBP1) and spliced (sXBP1) bands were RT-PCR-amplified using specific primer pairs. Cells treated with tunicamycin were used as a positive control for the induction of spliced XBP1. (**d**) XBP1 mRNA levels quantified with real-time RT-PCR. Total RNA was isolated from ASFV-infected Vero cells at a range of times post-infection. The XBP1 message was normalized to the 18S ribosomal message and x-fold changes were calculated as described in Materials and Methods. DTT and Tm-treated cells were used as control. Data are means ± S.D. from three independent experiments

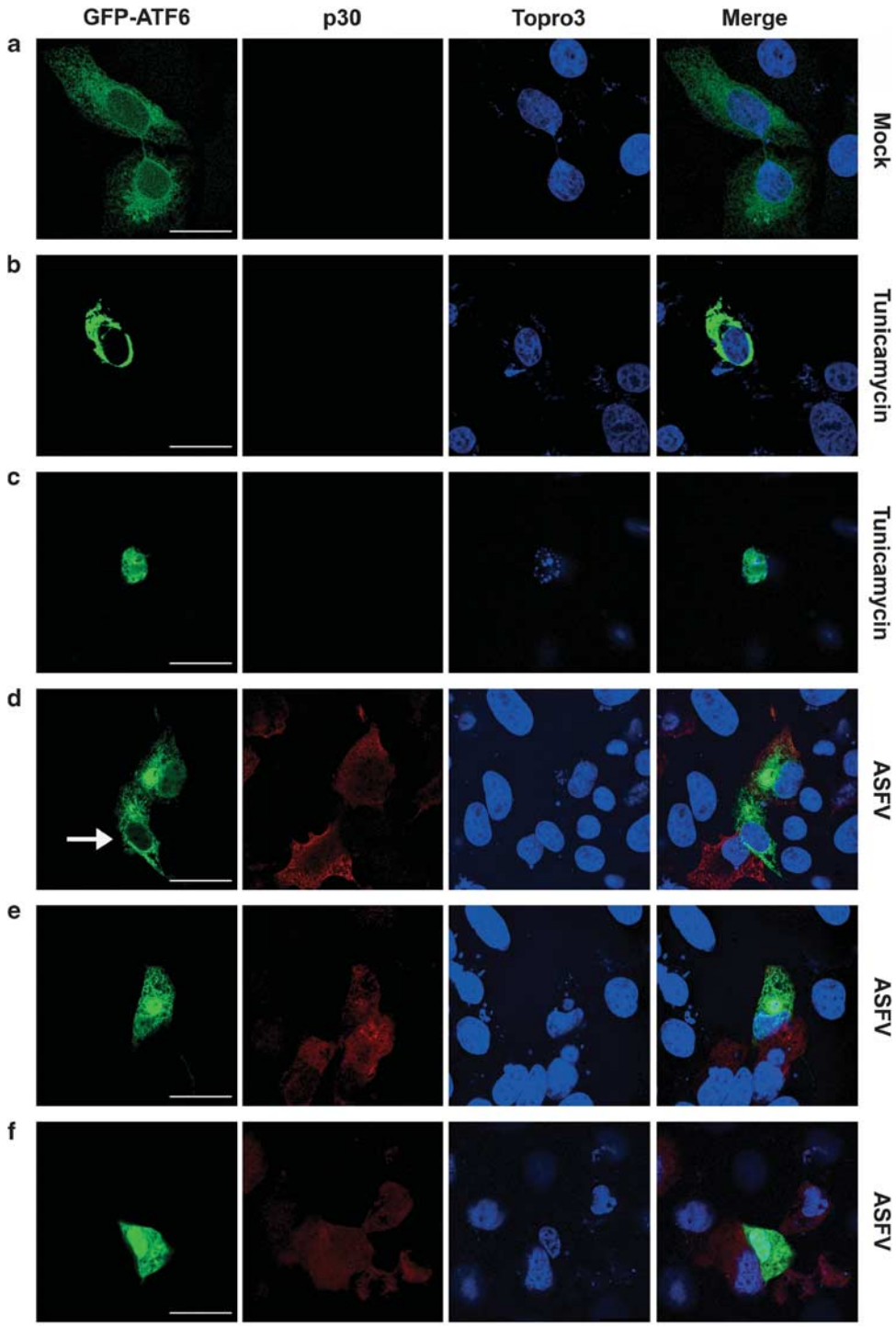

g

%	ER	Golgi	Nucleus	Viral factory
Mock	100	—	—	—
Tunicamycin	7.1	39.3	53.6	—
Infected cells	21	5.3	44.7	29

Figure 6 ASFV infection activates the ATF6 pathway. (**a**) Representative confocal micrographs of Vero cells transfected with the GFP-ATF6 plasmid. After 24 h, untreated cells showed a typical ER pattern, while in cells treated with tunicamicyn, GFP-ATF6 relocated to the Golgi (**b**) and to the nucleus (**c**). (**d–f**) Representative confocal micrographs of ASFV-infected transfected cells. ATF6 translocated to the viral factories and to the nucleus. (**d**, arrow) A neighboring uninfected cell is shown for comparison. Bar 25 μm. (**g**) Percentages of GFP-ATF6 subcellular localization events in infected and tunicamycin treated cells in triplicate experiments calculated in a total of 5×10^4 cells/well

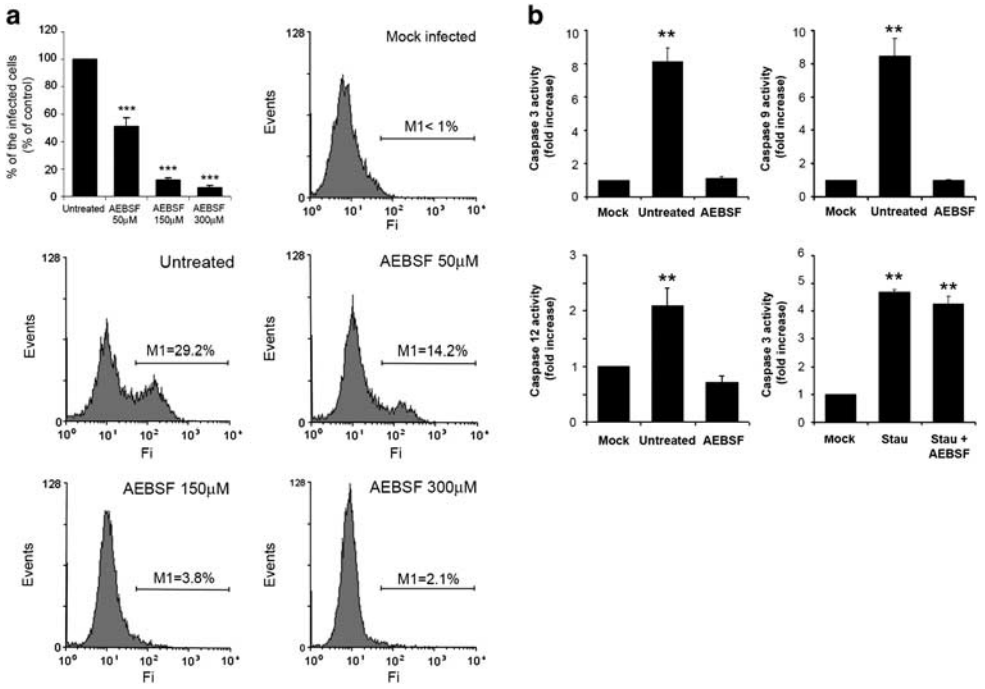

Figure 7 ASFV infection is dependent on ATF6 activation. (**a**) ASFV-infected cell percentages in Vero cells pretreated with AEBSF at the indicated concentrations and then infected. Infected cells were detected by FACS and data normalized to infection rates in untreated cells. Representative FACS profiles obtained during the analysis are shown. Infected cells were gated in M1 and expressed as a percentage of total cell analyzed. (**b**) Caspase activities at 24 hpi in Vero cells pretreated with 300 μM AEBSF and then infected. Data were normalized to mock-infected control values. Cells treated with Staurosporine (Stau) were used as control. Asterisks denote statistically significant differences (**$P<0.01$, ***$P<0.001$)

IRE1-XBP1 is also critical for the UPR, as it stimulates the expression of proteins involved in ER stress-induced protein degradation. Nevertheless, no splicing of XBP1 was detected during ASFV infection. The absence of splicing may favor viral infection as this process would inhibit viral protein degradation induced by ER stress.

The activation of the ATF6 branch and its transcriptional activation of chaperone-encoding genes might benefit the virus by assisting the folding of accumulated proteins and preventing protein aggregation. We demonstrated ATF6 translocation to the nucleus. Activated ATF6 exits the ER to the Golgi apparatus, where it is processed by proteases to its active form, which in turn translocates to the nucleus.[7] We used a short promoter that has considerably lower activity than the full promoter, and GFP-ATF6 expressed under the short CMV promoter localizes exclusively to the ER and translocates to the nucleus in a similar manner to endogenous ATF6.[32] The analysis of ATF6 distribution by confocal microscopy in Vero cells infected with ASFV revealed that this protein was translocated into the nucleus. ATF6 was also located in discrete perinuclear cytoplasmic areas that corresponded to viral factories, as indicated by the co-localization of ATF6 with DNA-containing cytoplasmic foci. Furthermore, ASFV viral replication was blocked by inhibition of the ATF6 translocation to the nucleus by AEBSF. To analyze the transcriptional activity of ATF6 in ASFV infection we examined the expression of XBP1 in ASFV-infected cells by qRT-PCR. Surprisingly, ASFV-infected samples showed a decrease in the induction of XBP1 compared with uninfected samples. Activation of ATF6 was necessary for ASFV replication; however, the virus prevented the transcriptional induction of some ATF6-target genes, such as *XBP1* and *BiP*, but not calnexin or calreticulin. These studies have focused interest in ATF6 pathway in this viral infection and have paved the way for further characterization of ASFV viral gene regulation of these molecules in the UPR.

In conclusion, apoptosis induction, caspase activation and later modulation of the UPR might be advantageous for ASFV as these processes block the effects that are detrimental to the infection, while maintaining those that are beneficial.

Materials and Methods

Cell culture, viruses and plasmids. Vero cell lines were obtained from the American Type Culture Collection (ATCC, Richmond, VA, USA) and cultured at 37 °C in Dulbecco's modified Eagle's medium supplemented with 5% fetal bovine serum (FBS), 100 IU/ml penicillin, 100 μg/ml streptomycin and 2 mM L-glutamine. WSL-R line 379, a macrophage cell line of wild swine origin that was kindly provided by Günther Kiel (Friedrich-Loeffler Institut, Greifswald, Germany), was grown in Iscove's medium (Gibco-BRL, Grand Island, NY, USA) plus F-12 nutrient mixture (Gibco) plus 10% FBS. Where indicated, cells were treated with 1 μg/ml Staurosporine (Sigma-Aldrich, Steinheim, Germany), or with 10 μg/ml tunicamycin (Sigma-Aldrich) or 2.5 mM DTT (Sigma-Aldrich) as a positive control of ER stress.

The Vero-adapted ASFV isolate BA71V was used. For flow cytometry (FACS) analyses we used an infectious recombinant ASFV, B54GFP-2, which expresses and incorporates into the virus particle a chimera of the p54 envelope protein fused to the EGFP.[41] Preparation of viral stocks, titrations and infection experiments were carried out in Vero cells as previously described.[42]

The plasmid pCMVshort-EGFP-ATF6α was kindly provided by Dr. Mori (Kyoto University, Japan)[32] and was transfected into Vero cells using Fugene 6 (Roche Biochemicals, Mannheim, Germany), following the manufacturer's protocols.

Western blotting. Cells seeded in 24-well plates were harvested in Laemmli sample buffer, boiled for 5 min at 95 °C, resolved by SDS-PAGE and transferred to a nitrocellulose membrane (Bio-Rad, Hercules, CA, USA). The non-specific antibody binding sites were blocked with skimmed milk in phosphate buffered saline (PBS) and then incubated with the specific primary and the HRP (Horseradish peroxidase)-conjugated secondary antibody.

Bands obtained after development with ECL reagent (GE Healthcare, Piscataway, NJ, USA) were detected using a Chemidoc XRS imaging system (Bio-Rad).

Antibodies used for western blotting included the following: rabbit polyclonal antibody to calreticulin (ab2907 abcam, Cambridge, UK) at a dilution of 1 : 3000; rabbit polyclonal antibody to calnexin (StressGen, San Diego, CA, USA) 1 : 3000; rabbit polyclonal to Bap31 (ab37120 abcam) 1 : 3000; rabbit polyclonal antibody to ERp57 (ab10287 abcam) 1 : 1000; goat polyclonal to GADD34 (ab9869 abcam) 1 : 1000; rabbit polyclonal antibody GADD153/CHOP (F-168) (Santa Cruz Biotechnology, Santa Cruz, CA, USA) 1 : 200; rabbit polyclonal antibody to GRP78 (BiP) (Santa Cruz Biotechnology) 1 : 200; rabbit polyclonal antibody to ATF4 (ab85049) 1 : 500 mouse monoclonal antibody to PDI (ab2792 abcam) 1 : 1000; anti-β-actin (Sigma, St Louis, MI, USA) 1 : 1500; anti-ASFV p30 monoclonal antibody 1 : 1000; and anti-p72 monoclonal antibody clone 18BG3 (Ingenasa, Madrid, Spain) 1 : 5000. The following secondary antibodies were used: goat anti-rabbit IgG HPR conjugate (Bio-Rad) and sheep anti-mouse IgG HPR conjugate (GE Healthcare), observing the manufacturer's instructions. Band densitometry was performed with TINA image analysis software and data were normalized to control values.

Caspase activity assays. Using fluorimetric caspase 3, 8 and 9 assay kits (Sigma-Aldrich), the activity of caspases 3, 8 and 9, respectively, were measured at a range of times post-infection in Vero cells and in WSL-R cells infected with ASFV at a multiplicity of 1 pfu/cell. Caspase 12 activity was determined using a fluorimetric caspase 12 assay kit (Biovision, Mountain View, CA, USA), following the manufacturer's instructions.

Effect of inhibitors on viral production. Monolayers of Vero cells were infected with ASFV at a multiplicity of infection of 1 pfu/cell and treated with Ac-DEVD-CHO (*N*-acetyl-L-aspartyl-L-α-glutamyl-*N*- (2-carboxyl-1-formylethyl)-L-valinamide) (Sigma-Aldrich), Blebbistatin (Sigma-Aldrich), Y-27632 (Calbiochem, Merck, Darmstadt, Germany), Z-ATAD-FMK (benzyoxycarbonyl-Ala-Thr-Asp-fluoromethylketone) (Biovision) or AEBSF (4-(2-Aminoethyl)-Benzenesulfonyl Fluoride) (Sigma-Aldrich) at final concentrations of 25, 30, 10, 2 and 300 μM, respectively, for 2 h before the infection or 6 hpi. Infection was allowed to proceed for 48 h and then virus titers in cell lysates (intracellular virus) and culture medium (extracelullar virus) were titrated by plaque assay in triplicate samples on cells.

FACS analyses. Vero cells were pretreated with inhibitors at the indicated concentrations in growth medium for 1 h at 37 °C, followed by infection with ASFV B54GFP-2 recombinant virus at a moi of 1 pfu/ml. After 24 hpi cells were washed with PBS, harvested by trypsinization, and then washed with FACS buffer (PBS, 0.01% sodium azide, and 0.1% bovine serum albumin. In order to determine the percentage of infected cells per condition, 10 000 cells/time point were scored and analyzed in a FACSCalibur flow cytometer (BD Sciences, Franklin Lakes, NJ, USA). Untreated control infected cultures yielded 25–30% of infected cells from the total cells examined. Infected cell percentages obtained after drug treatments were normalized to values found in control plates.

Immunofluorescence. Cells seeded on glass coverslips in a 24-well plate were infected with ASFV. At several time points after virus infection, the cells were fixed with 4% paraformaldehyde in PBS for 15 min at room temperature and permeabilized in 0.1% Triton X 100 in PBS for 15 min at room temperature. Cells were consecutively stained with primary and secondary antibodies and then incubated with Topro-3 (Invitrogen, Eugene, OR, USA) 1/1000 in PBS1X for DNA staining. After washing, coverslips were finally mounted on glass plates and cells were observed under a Leica TCS SPE confocal microscope (Leica-Microsystems, Wetzlar, Germany). The primary antibodies used were: rabbit polyclonal antibody to GRP78 (BiP) (Santa Cruz Biotechnology) 1 : 50, rabbit polyclonal antibody to caspase 12 (BioVision) diluted 1 : 25 and anti-ASFV p30 monoclonal antibody 1 : 100. Anti-rabbit IgG Alexa 488 and anti-mouse IgG Alexa 594-conjugated antibodies (Invitrogen) diluted to 1 : 200 were used as secondary antibodies respectively.

RNA preparation and RT-PCR analysis for XBP1. Total RNA from cultured cells was isolated with TRI-Reagent (Sigma-Aldrich) following the manufacturer's instructions. Reverse transcription reactions (RT-PCR) were carried out using the SuperScript One Step RT-PCR (Invitrogen), following the manufacturer's instructions. The primers used were: forward primer: 5′-CCTTGTAGTTGAGAAC CAGG-3′ and reverse primer 5′-GGGGCTTGGTATATATGTGG-3′. Amplification conditions included an initial step of 45 °C for 30 s, followed by a denaturation step of 94 °C for 2 min, 30 cycles of 94 °C for 30 s, 55 °C for 30 s and 70 °C for 30 s. PCR products were resolved by electrophoresis in a 2% agarose gel and stained with SYBR Green.

For quantitative PCR, cDNA was synthesized using the QuantiTect Reverse Trancription kit (Qiagen, Hilden, Germany) following the manufacturer's instructions. After heat inactivation at 95 °C, cDNA levels were quantified by using quantitative PCR (qPCR). Amplification was performed in a Rotor-Gene 3000 (Corbett Life Sciences, Sydney, Australia) using a QuantiTect SYBR Green PCR kit (Qiagen) following the manufacturer's recommendations. Primer sets used for 18S and XBP1 are available from Qiagen (QuantiTect Primer Assay). Fold change was calculated using the $\Delta\Delta$CT method of relative quantification with 18S rRNA as the endogenous control for normalization.[43] Melting curves were used to verify the specificities of products.

Data analysis. One-way analysis of variance was performed using INSTAT 3 for Windows. For multiple comparisons, Dunnet's correction was applied. Data are presented as means ± S.D. Differences were considered statistically significant at a *P*-value of < 0.05.

Conflict of Interest

The authors declare no conflict of interest.

Acknowledgements. We thank K Mori for the GFP-ATF6 construct. This work was supported by grants from the Spanish Ministry of Science and Innovation Program Consolider CSD 2006-00007, AGL2009-09209 and the Wellcome Trust Foundation WT075813.

1. Ramiro-Ibanez F, Ortega A, Brun A, Escribano JM, Alonso C. Apoptosis: a mechanism of cell killing and lymphoid organ impairment during acute African swine fever virus infection. *J Gen Virol* 1996; **77**(Pt 9): 2209–2219.
2. Brun A, Rivas C, Esteban M, Escribano JM, Alonso C. African swine fever virus gene A179L, a viral homologue of bcl-2, protects cells from programmed cell death. *Virology* 1996; **225**: 227–230.
3. Thornberry NA, Lazebnik Y. Caspases: enemies within. *Science* 1998; **281**: 1312–1316.
4. Rao RV, Hermel E, Castro-Obregon S, del Rio G, Ellerby LM, Ellerby HM *et al.* Coupling endoplasmic reticulum stress to the cell death program. Mechanism of caspase activation. *J Biol Chem* 2001; **276**: 33869–33874.
5. Schroder M, Kaufman RJ. The mammalian unfolded protein response. *Annu Rev Biochem* 2005; **74**: 739–789.
6. Yoshida H, Matsui T, Yamamoto A, Okada T, Mori K. XBP1 mRNA is induced by ATF6 and spliced by IRE1 in response to ER stress to produce a highly active transcription factor. *Cell* 2001; **107**: 881–891.
7. Ye J, Rawson RB, Komuro R, Chen X, Dave UP, Prywes R *et al.* ER stress induces cleavage of membrane-bound ATF6 by the same proteases that process SREBPs. *Mol Cell* 2000; **6**: 1355–1364.
8. Bitko V, Barik S. An endoplasmic reticulum-specific stress-activated caspase (caspase-12) is implicated in the apoptosis of A549 epithelial cells by respiratory syncytial virus. *J Cell Biochem* 2001; **80**: 441–454.
9. Li XD, Lankinen H, Putkuri N, Vapalahti O, Vaheri A. Tula hantavirus triggers pro-apoptotic signals of ER stress in Vero E6 cells. *Virology* 2005; **333**: 180–189.
10. Liberman E, Fong YL, Selby MJ, Choo QL, Cousens L, Houghton M *et al.* Activation of the grp78 and grp94 promoters by hepatitis C virus E2 envelope protein. *J Virol* 1999; **73**: 3718–3722.
11. Jordan R, Wang L, Graczyk TM, Block TM, Romano PR. Replication of a cytopathic strain of bovine viral diarrhea virus activates PERK and induces endoplasmic reticulum stress-mediated apoptosis of MDBK cells. *J Virol* 2002; **76**(19): 9588–9599.
12. Su HL, Liao CL, Lin YL. Japanese encephalitis virus infection initiates endoplasmic reticulum stress and an unfolded protein response. *J Virol* 2002; **76**: 4162–4171.
13. Wati S, Soo ML, Zilm P, Li P, Paton AW, Burrell CJ *et al.* Dengue virus infection induces upregulation of GRP78, which acts to chaperone viral antigen production. *J Virol* 2009; **83**: 12871–12880.
14. Jheng JR, Lau KS, Tang WF, Wu MS, Horng JT. Endoplasmic reticulum stress is induced and modulated by enterovirus 71. *Cell Microbiol* 2010; **12**: 796–813.

15. Cheng G, Feng Z, He B. Herpes simplex virus 1 infection activates the endoplasmic reticulum resident kinase PERK and mediates eIF-2alpha dephosphorylation by the gamma (1)34.5 protein. *J Virol* 2005; **79**: 1379–1388.
16. Isler JA, Skalet AH, Alwine JC. Human cytomegalovirus infection activates and regulates the unfolded protein response. *J Virol* 2005; **79**: 6890–6899.
17. Yu CY, Hsu YW, Liao CL, Lin YL. Flavivirus infection activates the XBP1 pathway of the unfolded protein response to cope with endoplasmic reticulum stress. *J Virol* 2006; **80**: 11868–11880.
18. Dediego ML, Nieto-Torres JL, Jimenez-Guardeno JM, Regla-Nava JA, Alvarez E, Oliveros JC *et al.* Severe acute respiratory syndrome coronavirus envelope protein regulates cell stress response and apoptosis. *PLoS Pathog* 2011; **7**: e1002315.
19. Tardif KD, Mori K, Kaufman RJ, Siddiqui A. Hepatitis C virus suppresses the IRE1-XBP1 pathway of the unfolded protein response. *J Biol Chem* 2004; **279**: 17158–17164.
20. Trujillo-Alonso V, Maruri-Avidal L, Arias CF, Lopez S. Rotavirus Infection Induces the Unfolded Protein Response of the Cell and Controls It through the Nonstructural Protein NSP3. *J Virol* 2011; **85**: 12594–12604.
21. Ambrose RL, Mackenzie JM. West Nile virus differentially modulates the unfolded protein response to facilitate replication and immune evasion. *J Virol* 2011; **85**: 2723–2732.
22. Umareddy I, Pluquet O, Wang QY, Vasudevan SG. Chevet E, Gu F. Dengue virus serotype infection specifies the activation of the unfolded protein response. *Virol J.* 2007; **4**: 91.
23. Zsak L, Lu Z, Kutish GF, Neilan JG, Rock DL. An African swine fever virus virulence-associated gene NL-S with similarity to the herpes simplex virus ICP34.5 gene. *J Virol* 1996; **70**: 8865–8871.
24. Netherton CL, Parsley JC, Wileman T. African swine fever virus inhibits induction of the stress-induced proapoptotic transcription factor CHOP/GADD153. *J Virol* 2004; **78**: 10825–10828.
25. Zhang F, Moon A, Childs K, Goodbourn S, Dixon LK. The African swine fever virus DP71L protein recruits the protein phosphatase 1 catalytic subunit to dephosphorylate eIF2alpha and inhibits CHOP induction but is dispensable for these activities during virus infection. *J Virol* 2010; **84**: 10681–10689.
26. Ron D, Walter P. Signal integration in the endoplasmic reticulum unfolded protein response. *Nat Rev Mol Cell Biol* 2007; **8**: 519–529.
27. Delom F, Emadali A, Cocolakis E, Lebrun JJ, Nantel A. Chevet E. Calnexin-dependent regulation of tunicamycin-induced apoptosis in breast carcinoma MCF-7 cells. *Cell Death Differ* 2007; **14**: 586–596.
28. Nguyen M, Breckenridge DG, Ducret A, Shore GC. Caspase-resistant BAP31 inhibits fas-mediated apoptotic membrane fragmentation and release of cytochrome c from mitochondria. *Mol Cell Biol* 2000; **20**: 6731–6740.
29. Harding HP, Calfon M, Urano F, Novoa I, Ron D. Transcriptional and translational control in the Mammalian unfolded protein response. *Annu Rev Cell Dev Biol* 2002; **18**: 575–599.
30. Oyadomari S, Mori M. Roles of CHOP/GADD153 in endoplasmic reticulum stress. *Cell Death Differ* 2004; **11**: 381–389.
31. Calfon M, Zeng H, Urano F, Till JH, Hubbard SR, Harding HP *et al.* IRE1 couples endoplasmic reticulum load to secretory capacity by processing the XBP-1 mRNA. *Nature* 2002; **415**: 92–96.
32. Nadanaka S, Yoshida H, Kano F, Murata M, Mori K. Activation of mammalian unfolded protein response is compatible with the quality control system operating in the endoplasmic reticulum. *Mol Biol Cell* 2004; **15**: 2537–2548.
33. Okada T, Haze K, Nadanaka S, Yoshida H, Seidah NG, Hirano Y *et al.* A serine protease inhibitor prevents endoplasmic reticulum stress-induced cleavage but not transport of the membrane-bound transcription factor ATF6. *J Biol Chem* 2003; **278**: 31024–31032.
34. Carrascosa AL, Bustos MJ, Nogal ML, Gonzalez de Buitrago G, Revilla Y. Apoptosis induced in an early step of African swine fever virus entry into vero cells does not require virus replication. *Virology* 2002; **294**: 372–382.
35. Fernando P, Kelly JF, Balazsi K, Slack RS, Megeney LA. Caspase 3 activity is required for skeletal muscle differentiation. *Proc Natl Acad Sci USA* 2002; **99**: 11025–11030.
36. Wurzer WJ, Planz O, Ehrhardt C, Giner M, Silberzahn T, Pleschka S *et al.* Caspase 3 activation is essential for efficient influenza virus propagation. *Embo J.* 2003; **22**: 2717–2728.
37. Andres G, Garcia-Escudero R, Simon-Mateo C, Vinuela E. African swine fever virus is enveloped by a two-membraned collapsed cisterna derived from the endoplasmic reticulum. *J Virol* 1998; **72**: 8988–9001.
38. Groenendyk J, Michalak M. Endoplasmic reticulum quality control and apoptosis. *Acta Biochem Pol* 2005; **52**: 381–395.
39. Ellgaard L, Molinari M, Helenius A. Setting the standards: quality control in the secretory pathway. *Science* 1999; **286**: 1882–1888.
40. Rivera J, Abrams C, Hernaez B, Alcazar A, Escribano JM, Dixon L *et al.* The MyD116 African swine fever virus homologue interacts with the catalytic subunit of protein phosphatase 1 and activates its phosphatase activity. *J Virol* 2007; **81**: 2923–2929.
41. Hernaez B, Escribano JM, Alonso C. Visualization of the African swine fever virus infection in living cells by incorporation into the virus particle of green fluorescent protein-p54 membrane protein chimera. *Virology* 2006; **350**: 1–14.
42. Enjuanes L, Carrascosa AL, Moreno MA, Vinuela E. Titration of African swine fever (ASF) virus. *J Gen Virol* 1976; **32**: 471–477.
43. Livak KJ, Schmittgen TD. Analysis of relative gene expression data using real-time quantitative PCR and the 2(-Delta Delta C(T)) Method. *Methods* 2001; **25**: 402–408.

Journal of Virology

Small Rho GTPases and Cholesterol Biosynthetic Pathway Intermediates in African Swine Fever Virus Infection

Jose I. Quetglas, Bruno Hernáez, Inmaculada Galindo, Raquel Muñoz-Moreno, Miguel A. Cuesta-Geijo and Covadonga Alonso

J. Virol. **2012, 86(3):1758. DOI: 10.1128/JVI.05666-11.**
Published Ahead of Print 23 November 2011.

JVI Journals.ASM.org

Small Rho GTPases and Cholesterol Biosynthetic Pathway Intermediates in African Swine Fever Virus Infection

Jose I. Quetglas,* Bruno Hernáez, Inmaculada Galindo, Raquel Muñoz-Moreno, Miguel A. Cuesta-Geijo, and Covadonga Alonso

Departamento de Biotecnología–Instituto Nacional de Investigación y Tecnología Agraria y Alimentaria, INIA, Madrid, Spain

The integrity of the cholesterol biosynthesis pathway is required for efficient African swine fever virus (ASFV) infection. Incorporation of prenyl groups into Rho GTPases plays a key role in several stages of ASFV infection, since both geranylgeranyl and farnesyl pyrophosphates are required at different infection steps. We found that Rho GTPase inhibition impaired virus morphogenesis and resulted in an abnormal viral factory size with the accumulation of envelope precursors and immature virions. Furthermore, abundant defective virions reached the plasma membrane, and filopodia formation in exocytosis was abrogated. Rac1 was activated at early ASFV infection stages, coincident with microtubule acetylation, a process that stabilizes microtubules for virus transport. Rac1 inhibition did not affect the viral entry step itself but impaired subsequent virus production. We found that specific Rac1 inhibition impaired viral induced microtubule acetylation and viral intracellular transport. These findings highlight that viral infection is the result of a carefully orchestrated modulation of Rho family GTPase activity within the host cell; this modulation results critical for virus morphogenesis and in turn, triggers cytoskeleton remodeling, such as microtubule stabilization for viral transport during early infection.

The members of Rho family of small GTPases are essential key regulators of diverse critical cellular functions, including cytoskeleton dynamics, cell cycle progression, migration, the generation of reactive oxygen species, and gene expression (16, 29, 35, 53). Like the majority of Ras superfamily proteins, most Rho GTPases function as molecular switches and cycle between an active GTP-bound form and an inactive GDP-bound one. Two types of regulatory proteins control this cycling: guanine nucleotide exchange factors (GEFs) that promote activation of these proteins during signal transduction by exchanging of GDP for GTP molecules and, in contrast, GTPase-activating proteins (GAPs) that promote the hydrolysis of the bound GTP molecules, thus allowing the transfer of the GTPase back to the inactive state (7, 9). In addition, Rho GTPases must often undergo posttranslational prenylation to become functionally active (43). Thus, their localization, insertion into membranes, and protein-protein interactions require covalent incorporation into the carboxy terminus of either farnesyl pyrophosphate (FPP) or geranylgeranyl pyrophosphate (GGPP) (62). Since these prenyl groups are derived from mevalonic acid, which is also the starting material for the cholesterol biosynthesis, statins have been widely used to inhibit the prenylation of Ras-related proteins, particularly the Rho GTPase subfamily (24, 28, 41).

Given the control that the most studied Rho GTPase members (RhoA, Rac1, and Cdc42) exert over cytoskeleton dynamics, vesicle trafficking, and signaling pathways, it has been hypothesized that they make a major contribution to viral entry, replication, and morphogenesis. In this regard, Rac1/Cdc42 regulates actin dynamics and architecture during macropinocytotic entry of diverse large DNA viruses, such as vaccinia virus (42, 45) and adenovirus (40). In addition, during entry into host cells, herpes simplex virus 1 (HSV-1) activates Rac1 and Cdc42, which results in the induction of filopodia and lamellipodia in epithelial cells and fibroblasts (33). Rho GTPases are also implicated in microtubule regulation during capsid trafficking of Kaposi's sarcoma-associated herpesvirus (48). Recently, it has been shown that vaccinia virus F11L protein interacts directly with RhoA to inhibit its downstream signaling (61). This F11L-mediated inhibition of RhoA signaling has been proposed to be required for an efficient virus release from infected cells (4) and also for stimulating virus-induced cell motility (4, 12, 66) and the spreading of infection. RhoA signaling is required for respiratory syncytial virus replication and morphogenesis (26). Moreover, the expression of active Rac1 is increased after hepatitis B virus replication (59).

African swine fever virus (ASFV) is the causative agent of a severe and highly lethal hemorrhagic disease that affects domestic pigs. This large icosahedral and enveloped DNA virus is the only known member of the family *Asfarviridae* (17). It enters host cells by clathrin- and dynamin-dependent endocytosis after attachment to a still unknown cell receptor(s) and requires later fusion between the viral envelope and endosome membrane to deliver DNA into cytoplasm (31, 60). This fusion event requires the characteristic acidic pH of the endosomal environment and also the presence of cholesterol at the plasma membrane of the target cell (6, 22). Like many other viruses, during the early stages of infection ASFV interacts with the microtubule cytoskeleton and requires retrograde dynein-based transport to constitute the perinuclear virus factory (3, 30), where DNA replication and assembly occur. This specialized site, close to the microtubule organizing center, contains mostly viral DNA, most of the viral proteins, immature and mature virions, and also abundant virus-induced membranes. Microtubule motors have also been proposed to be involved in at least three other events that occur in the ASFV replication cycle, namely, vimentin rearrangement into a cage that

Received 13 July 2011 **Accepted** 8 November 2011

Published ahead of print 23 November 2011

Address correspondence to C. Alonso, calonso@inia.es.

* Present address: Division of Gene Therapy, School of Medicine, Center for Applied Medical Research, University of Navarra, Pamplona, Spain.

doi:10.1128/JVI.05666-11

finally surrounds the viral factory (57), the recruitment of virus-targeted membranes to the virus factory (54), and the transport of fully assembled virions to the plasma membrane before their release from an infected cell by budding (36).

Here we explored, for the first time, the relevance of the Rho GTPase subfamily during ASFV infection. We found that a general inhibition of Rho GTPases leads to a decrease in viral yields and deficient viral morphogenesis. Most importantly, since Rac1 resulted activated early during infection and coincident with an increase in microtubule acetylation, the data obtained suggest the involvement of Rac1-mediated signaling on ASFV intracellular transport.

MATERIALS AND METHODS

Cell culture, viruses, and plasmids. Vero cells were obtained from the European Collection of Cell Cultures (ECACC) and maintained in Dulbecco modified Eagle medium supplemented with 5% fetal bovine serum at 37°C and 5% CO_2. The tissue culture-adapted ASFV strain BA71V was used in all experiments (18). Where indicated, a recombinant virus expressing viral protein p54 fused to the green fluorescence protein (GFP) was used (B54GFP-2 [32]) to identify viral factories by confocal microscopy. Cell infections and titrations were carried out as previously described. When indicated, we used highly purified ASFV as described elsewhere (10).

Plasmids (pcDNA3) encoding wild-type (wt), dominant-negative (17N), and constitutively active (Q61L) forms of Rac1 fused to GFP were kindly provided by Ole Gjoerup (58). Constructs expressing the glutathione *S*-transferase (GST)-Rac1/Cdc42 binding domain of Pak1 (GST-PBD) were a generous gift from Keith Burridge (5). Transient expression in Vero cells was achieved by transfection using Fugene HD transfection reagent (Roche) and 2 μg of DNA/10^6 cells (ratio 1:6) according to the manufacturer's instructions.

Antibodies and other reagents. Antibodies against Cdc42 and Rac1 were obtained from BD Transduction Laboratories. Monoclonal antibodies against α-tubulin and acetylated α-tubulin were purchased from Sigma. Jose M. Escribano provided the monoclonal antibody against p30. The monoclonal antibody against p72 clone 18BG3 was purchased from Ingenasa. Rabbit polyclonal serum against ASFV protein pE120R was obtained after immunization with recombinant protein. Anti-rabbit and anti-mouse antibodies conjugated to horseradish peroxidase were purchased from GE Healthcare. Alexa Fluor 488- and Alexa Fluor 594-conjugated anti-mouse IgG antibodies were from Molecular Probes.

Triton X-100, lovastatin (Mevinolin), farnesyl pyrophosphate (FPP), geranylgeranyl pyrophosphate (GGPP), L-mevalonate, cholesterol, β-actin polyclonal antibody, and Hoechst 33258 were purchased from Sigma. *Clostridium difficile* toxin B (CdTB), FTI-277 (farnesyltransferase inhibitor [FTase] inhibitor), GGTI-286 (geranylgeranyltransferase inhibitor [GGTI]), NSC23766 (Rac1 inhibitor), and Fluorsave were obtained from Calbiochem.

Cytotoxicity assay. The cytotoxicity elicited by inhibitors was analyzed by using a lactate dehydrogenase cytotoxicity assay kit (Promega) and by trypan blue exclusion.

Drug treatments and infections. Vero cells were treated with a range of concentrations (1 to 3 μM) of lovastatin (Lov) for 24 or 48 h at 37°C. Add-back of intermediate metabolites was done at the following concentrations: 200 μM mevalonate (Mev), 5 μM GGPP, 5 μM FPP, or 5 μg of cholesterol/ml, together with 1 to 3 μM Lov. In all cases, at 24 h after ASFV infection (BA71V isolate, 0.5 PFU/cell), cells and supernatants were collected to determine virus progeny production by plaque assay, as previously described (25). In a second set of experiments, the cells were incubated with a range of concentrations of GGTI-286 (10 to 30 μM), FTI-277 (10 to 30 μM), or CdTB (25 to 100 ng/ml). These chemical inhibitors were added either 2 h before virus inoculation and removed after viral adsorption or maintained throughout infection, or they were added at 3 h postinfection (hpi) and maintained until the end of the experiment. In order to evaluate the infectivity of ASFV in the presence of these drugs, we infected pretreated cells (2 h before virus inoculation for GGTI-286, FTI-277, or CdTB or 24 and 48 h before virus inoculation when using Lov) and analyzed the number of infected cells at 3 hpi by immunofluorescence detection of viral early protein p30 (see the discussion of immunofluorescence analysis). Where indicated, cells were infected at high multiplicity of infection (MOI), i.e., ~20 PFU/cell.

GTPase activation assays. Serum-starved Vero cells (60% confluence), infected or mock infected with ASFV at an MOI of 5 PFU/cell, were washed with phosphate-buffered saline (PBS) at a range of times postinfection and lysed in a buffer containing 10% glycerol, 50 mM Tris-HCl (pH 7.4), 100 mM NaCl, 1% NP-40, 2 mM $MgCl_2$, and protease inhibitors.

Bacterially expressed and purified GST-PBD (p21-binding domain of Pak1) interacts with activated GTP-bound Rac1 and Cdc42 was used to pull-down GTP-bound forms of Rac1 and Cdc42, as described previously (15, 55). Equal amounts of total protein from cell lysates were incubated for 1 h at 4°C with glutathione-Sepharose 4B beads (GE Healthcare) previously conjugated to GST-PBD. After extensive washing, bound proteins were analyzed by Western blotting with monoclonal antibodies against Rac1 or Cdc42. Previously, lysates were probed with the same antibodies to detect total Rac1 and Cdc42 in the samples. To determine the levels of active GTPases, the intensities of the corresponding bands were measured by densitometry (Tina 2.0) and normalized to values obtained with mock-infected cells.

RhoA, Rac1, and Cdc42 activation was also measured using RhoA-, Rac1-, and Cdc42-specific G-Lisa activation kits (Cytoskeleton, Inc.) according to the manufacturer's instructions. Briefly, Vero cells were seeded in 25-cm^2 flasks for the indicated confluence and serum starved for 24 h prior to BA71V infection (5 PFU/cell). Mock-infected and infected cells were harvested in lysis buffer at the indicated times postinfection. G-Lisa kits used 96-well plates coated with the binding domain of the corresponding GTPase effector protein. GTPase-GDP was removed during washing steps, and GTPase-GTP was detected with specific antibodies, followed by absorbance at 490 nm.

Detection and quantitation of the ASFV genome. DNA from infected or mock-infected Vero cells with ASFV 0.5 PFU/cell was extracted and purified with a DNeasy blood and tissue kit (Qiagen) at 16 hpi. Detection and quantitation of the ASFV genome was achieved by quantitative real-time PCR using specific oligonucleotides and a TaqMan probe, as previously described (38). The amplification reaction was performed in a Rotor-Gene RG3000 (Corbett Research) as follows: 1 cycle at 94°C for 10 min, then 45 cycles at 94°C for 15 s, and finally 45 cycles at 58°C for 1 min. Positive and negative amplification controls (DNA purified from ASFV virions and DNA from mock-infected cells, respectively) were included in the assay, and duplicates from each sample were analyzed.

Western blot analysis. After estimation of total protein in samples by the Bradford method, 30 μg of protein was resolved by SDS-PAGE and transferred to nitrocellulose membranes (Bio-Rad). Membranes were probed for 1 h at room temperature with the corresponding primary antibodies in PBS containing 0.05% Tween 20 (PBS-T; Sigma) at the following dilutions: monoclonal antibody against p30 (1:500), monoclonal antibody anti-p72 (1:5000), mouse monoclonal antibody anti-Rac1 (1:1,000), mouse monoclonal antibody anti-Cdc42 (1:250), mouse monoclonal antibodies anti-α-tubulin (1:4,000), and anti-acetylated α-tubulin (1:2,000). As a protein loading control, we included the detection of actin with polyclonal rabbit anti-β-actin serum diluted 1:250. After an extensive washing with PBS-T, membranes were incubated with anti-mouse IgG antibody (1:5,000) or anti-rabbit IgG (1:4,000), both conjugated to horseradish peroxidase. Finally, bands were developed by using an enhanced chemiluminescence reaction with a Western blot detection reagent (GE Healthcare).

Immunofluorescence analysis. Vero cells (60% confluence) were grown on glass coverslips and then infected with BA71V or B54GFP-2. In

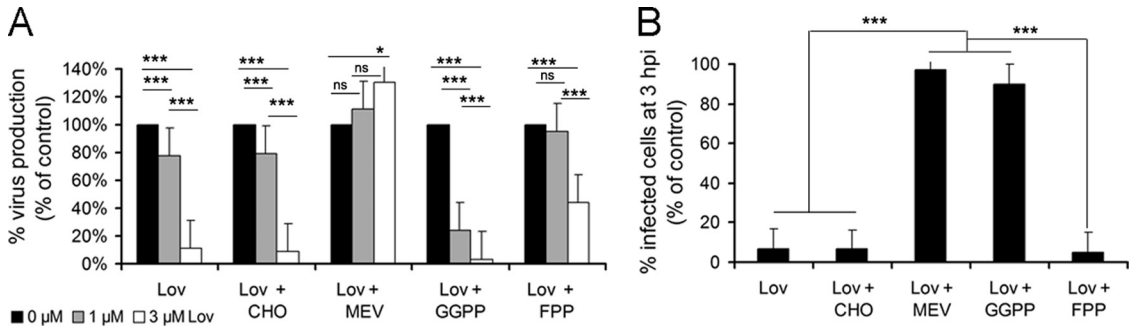

FIG 1 Antiviral effect of lovastatin on ASFV infection. Vero cells were incubated with increasing, but nontoxic, concentrations of lovastatin for 24 h before ASFV infection (0.5 PFU/cell). Where indicated, mevalonate (Mev), cholesterol (CHO), FPP, or GGPP was added to cells. (A) Virus progeny at 24 hpi was analyzed by plaque assay, and virus yields are represented as a percentage of the untreated control cells. (B) Similarly, the number of infected cells (infectivity) at 3 hpi was determined by immunofluorescence in Vero cells treated with 3 μM lovastatin and are represented as a percentage of untreated infected cells. Means and SD correspond to three independent experiments. Values that are significantly different from each other are indicated (***, $P < 0.001$;*, $P < 0.05$).

infectivity assays, at 3 hpi, the cells were rinsed with PBS, fixed with PBS–3.8% paraformaldehyde for 10 min, and permeabilized with 0.2% PBS–Triton X-100 for 15 min. Infected cells at this time were identified by detection of early ASFV protein with monoclonal anti-p30 antibody (1:200). For the viral factory analysis, cells infected with B54GFP-2 were fixed at 16 hpi. Internalized virions in pCDNA-3-transfected cells were detected at 1 hpi with monoclonal antiviral major capsid protein p72 (1:1,000). Rabbit polyclonal serum against pE120R was diluted 1:500. The secondary antibodies used were an anti-mouse IgG antibody conjugated to either Alexa Fluor 488 or Alexa Fluor 549. Nuclei and also DNA in virus factories were identified by staining with Hoechst 33258. Finally, coverslips were mounted onto slides using Fluorsave reagent.

Confocal microscopy was carried out in a Leica confocal microscope TCS SP2-AOBS equipped with ×63 and ×100 objective lenses. The digital images were processed with Adobe Photoshop 8.0.

Electron microscopy. For conventional Epon section analysis, Vero cells, preincubated or not with toxin B, were infected with ASFV at 1 PFU/cell and fixed at 16 hpi with 2.5% glutaraldehyde (Sigma) in PBS for 30 min at room temperature. Postfixation was carried out with 1% OsO_4 in PBS at room temperature for 90 min. The samples were then dehydrated with acetone and embedded in Epon according to standard procedures. Samples were examined at 80 kV in a JEOL JEM 10-10 electron microscope. The digital images were processed with Adobe Photoshop 8.0.

Statistical analysis. All error terms are expressed as standard deviations (SD). Prism software (GraphPad Software, Inc., San Diego, CA) was used for the statistical analysis. A one-way analysis of variance test, followed by Bonferroni's multiple-comparison test, was used to compare different experimental groups. *P* values of <0.05 were considered statistically significant.

RESULTS

ASFV infection requires host protein prenylation at several stages of the infectious cell cycle. To study the relevance of the cholesterol biosynthesis pathway and its precursors during ASFV infection, we used lovastatin (Lov), a powerful inhibitor of 3-hydroxy-3-methylglutaryl-coenzyme A (HMG-CoA) reductase, the enzyme that catabolizes the conversion of HMG-CoA to mevalonate (Mev). Vero cells were incubated with nontoxic concentrations of Lov for 24 or 48 h prior to ASFV infection. Under these conditions, we first analyzed virus production at 24 h postinfection (hpi) by plaque assay. A dramatic reduction of virus progeny was observed in a dose-dependent manner after 24 h of incubation with Lov (Fig. 1A). The addition of the immediate precursor Mev to Lov-treated cells resulted in the recovery of viral yields to reach values similar to those obtained with untreated control cells. This effect was not detected when other intermediate precursors of the cholesterol biosynthesis pathway, such as the isoprenoids GGPP and FPP, were added. Neither was this effect observed with cholesterol add-back. In order to determine whether this reduction in virus progeny correlated with a decrease in ASFV infectivity after Lov treatment, we counted the number of infected cells as early as 3 hpi by indirect immunofluorescence. Lov caused a severe reduction in the number of infected cells (ca. 85%) compared to untreated controls. The effect of Lov on ASFV infectivity was reversed by complementation with Mev or GGPP, but not by the single addition of FPP or cholesterol add-back (Fig. 1B). Similar results were obtained in cells incubated with Lov for 48 hpi (data not shown).

These results indicate a relevant role for cholesterol pathway intermediates and prenyl groups (GGPP and FPP) in posttranslational protein modification during the first stages of ASFV infection. Thus, we evaluated the effect of specific inhibitors of geranylgeranyl transferase I (GGTI-286) and farnesyltransferase I (FTI-277) at various steps of ASFV infection (see Materials and Methods). Inhibition with GGTI-286 resulted in a decrease in the number of infected cells at 3 hpi, which correlated with defective virus production levels independently of the time point at which the inhibitor was added (Fig. 2). These observations are consistent with results from Lov experiments and suggest a role for geranylgeranylation during the first stages of infection, including viral entry. In addition, the reduction of viral yields observed after inhibition of geranylgeranylation with GGTI-286 correlated with a reduction in ASFV DNA replication, as shown by quantitative PCR (Fig. 2C). However, incubation with FTI-277 did not impair ASFV infectivity or virus production when it was added to cells at 3 hpi (Fig. 2). This finding indicates that efficient infection requires farnesylation during the first stages of infection but not after the viral entry into the host cell.

Downregulation of Rho GTPases by toxin B affects ASFV infection but not cell infectivity. Geranylgeranylation promotes activation of many members of the Rho GTPase family that participate in a range of cellular processes, including viral entry into host cells (14, 42, 48). Our data show that geranylgeranylation is relevant during ASFV infection. We thus examined whether Rho GTPases participate in ASFV infection. To this end, we used toxin B from *Clostridium difficile* (CdTB) as a specific inhibitor that

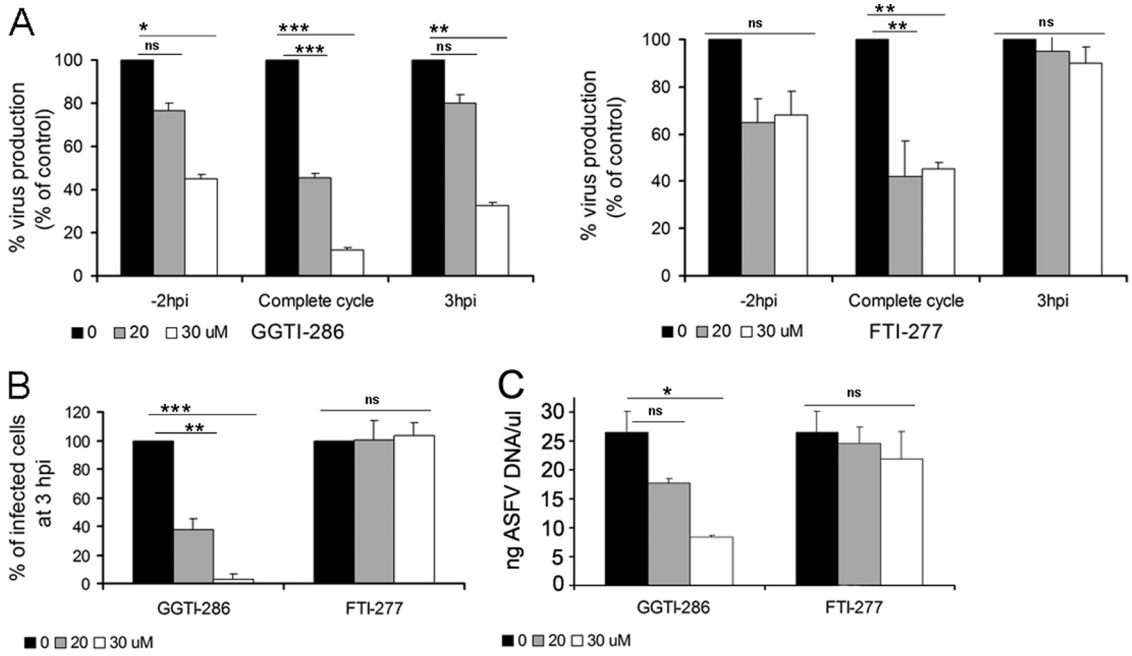

FIG 2 ASFV infection in the presence of prenylation inhibitors. (A) Virus progeny from ASFV-infected cells in the presence of geranylgeranyltransferase I specific inhibitor (GGTI-286) or farnesyltransferase specific inhibitor (FTI-277) at 24 hpi was determined by plaque assay. Inhibitors were added to cells 2 h prior to infection (−2 hpi) or 3 h postinfection (3 hpi) or were present throughout infection. (B) The number of infected cells at 3 hpi in the presence of increasing concentrations of GGTI-286 or FTI-277 was also determined as described previously. (C) ASFV DNA replication at 16 hpi after treatment with increasing concentrations of inhibitors GGTI-286 and FT-277 was analyzed by quantitative PCR. The means and SD correspond to three independent experiments. Values that are significantly different from each other are indicated (***, $P < 0.001$; **, $P < 0.01$; *, $P < 0.05$).

efficiently blocks the interaction of these GTPases with their effectors, resulting in functionally inactive GTPases. The addition of CdTB resulted in rapid depletion of actin stress fibers in Vero cells, which is indicative of successful inhibition of Rho GTPases (data not shown). The incubation of Vero cells with CdTB significantly reduced (ca. 60%) virus titers at 24 hpi compared to untreated cells (Fig. 3A). This effect was detected only when the inhibitor was added to cells before virus inoculation, with no significant differences between removing the inhibitor after virus adsorption and maintaining it throughout the infection. This result raised the question as to whether Rho GTPases contribute to ASFV entry. To study this possibility, we analyzed virus infectivity, as the ratio of infected versus noninfected cells, at 3 hpi in CdTB-treated cells, and we did not find differences in the number of infected cells after CdTB treatment compared to untreated control cells (Fig. 3B). Moreover, we confirmed that viral entry was not affected by the inactivation of Rho GTPases, as shown by the synthesis rates of early (p30) and late (p72) viral proteins detected by immunoblotting of cell lysates at different times of infection, and we did not find significant differences between CdTB treated and untreated cells (Fig. 3C).

ASFV infectivity was not affected by the downregulation of Rho GTPases, thus raising the possibility that the impairment of viral morphogenesis explains the reduction of viral yields observed after CdTB treatment. We next analyzed whether early Rho GTPase inactivation affected the ASFV morphogenesis that takes place at perinuclear viral factories. Vero cells were incubated or not incubated with CdTB, which was removed after virus adsorption. Viral factories were then examined at 16 hpi by confocal microscopy. To identify and analyze these factories, cells were infected with B54GFP-2, a recombinant ASFV expressing enhanced GFP (EGFP) fused to viral protein p54. Cells infected in the presence of CdTB exhibited loose and less compact viral factories (Fig. 3D), and this appearance correlated with larger dimensions (average diameter of 5.56 ± 1.68 μm) than those in nontreated infected cells (average diameter of 4.01 ± 1.25 μm). This observation suggests that an inadequate constitution of the viral assembly site or an incorrect assembly of newly generated virions after Rho GTPase inactivation caused the reduction in viral yields observed after CdTB treatment. In order to confirm this hypothesis, we examined in more detail the effects of CdTB in ASFV-infected cells at 16 hpi by transmission electron microscopy (TEM). Cytoplasmic factories formed in the absence of CdTB contained the expected viral structures (envelope precursors and immature and mature icosahedral particles) (Fig. 4B). In contrast, those that developed after treatment with this inhibitor contained higher ratios of nonicosahedral envelope precursors and immature viral particles and few mature icosahedral viral particles. Consistent with the data from confocal microscopy, an increment in viral factory size was also detected, and this increase appeared to be due to the accumulation of envelope precursors in CdTB-treated cells. Under these conditions, a smaller number of ribosomes were found compared to viral factories from control cells, where ribosomes often appear to be associated with immature or mature virus particles. After infection very few immature particles reach the plasma membrane to be released by budding (8a). However, in infected CdTB-treated cells, abundant immature or defective virus particles reached the plasma membrane. Virus budding occurs by means of filopodial extensions from the plasma membrane, apparently by actin polymerization (11, 37), but after Rho

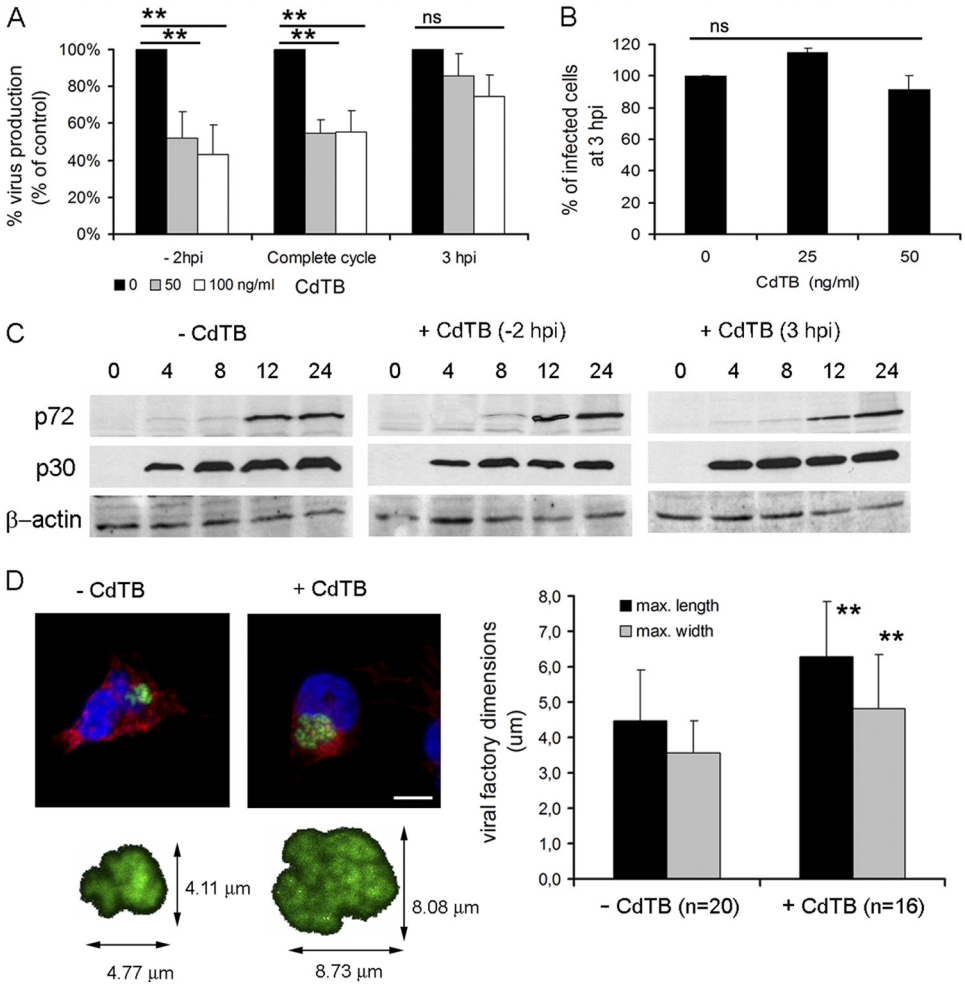

FIG 3 The downregulation of Rho GTPases impairs ASFV infection. Vero cells incubated for a range of times with increasing concentrations of toxin B from *Clostridium difficile* (CdTB) were infected with ASFV at 0.5 PFU/cell. (A) As described in the text, virus titers from infected cells at 24 hpi were determined by plaque assay and are shown as a percentage of untreated infected cells. (B) The number of infected cells at 3 hpi is represented as a percentage of untreated infected cells. The means and SD correspond to three independent experiments. Values that are significantly different from each other are indicated (**, $P < 0.01$; *, $P < 0.05$). (C) The expression of early (p30) and late (p72) viral proteins was analyzed at several time points during infection in cells treated with 100 ng of CdTB/ml 2 h prior to infection or 3 hpi and compared to untreated infected cells. β-Actin was used as a protein load control. (D) Vero cells were infected with B54GFP-2 in the presence or absence of CdTB and examined by confocal microscopy at 16 hpi. Viral factories from 16 to 20 cells were measured, and maximum dimensions are represented as means with the corresponding SD. A representative image is shown, where viral factories were detected by direct visualization of p54-EGFP (green). Nuclei (blue) and actin (red) were detected by Hoechst staining and anti-β actin antibody, respectively. Bar, 10 μm. Values significantly ($P < 0.01$) different from controls are indicated (**).

GTPases inactivation with CdTB no filopodia could be observed by TEM. In summary, these results indicate that early inhibition of Rho GTPase-mediated signaling with CdTB during the first stages of infection negatively affects virus progeny, virion maturation, and virus assembly site composition.

ASFV infection induces the activation of Rac1 GTPase in Vero cells. The requirement of Rho GTPases for efficient virus multiplication at early infection led us to explore the members of this family that are activated during ASFV entry. We specifically examined RhoA, Rac1, and Cdc42, the most extensively characterized members of the Rho GTPase family. All of these GTPases were inhibited by CdTB. RhoA, Rac1, and Cdc42 induction was monitored by an enzyme-linked immunosorbent assay (ELISA)-based assay (G-Lisa) at a range of times within first hour after virus inoculation in Vero cells (Fig. 5D), and the activation of Rac1 and Cdc42 could be also determined by an established affinity precipitation assay using GST-PBD, followed by immunoblot analysis (Fig. 5A to C). No activation of RhoA was observed by G-Lisa assay during the first hour after ASFV infection since active RhoA levels were similar to those obtained for mock-infected cells (Fig. 5D). Likewise, no activation of Cdc42 during first hour postinfection could be detected by G-Lisa and pulldown assay. In contrast, in the same conditions, a gradual increase in Rac1-GTP (the active form of Rac1) was observed during first 30 min of ASFV infection, with maximum activation at 25 min postinfection. At this time point, Rac1 was consistently activated ~3-fold over mock-infected cells (Fig. 5A and C). Interestingly, Rac1-GTP levels were restored to basal levels 5 min later, at 30 min postinfection. The total Rac1 in infected cells was not significantly modified during infection, thereby indicating the specificity of GTP activation. A Rac1-specific G-Lisa assay confirmed a Rac1 activation peak during the first 30 min of infection (Fig. 5D). These results support

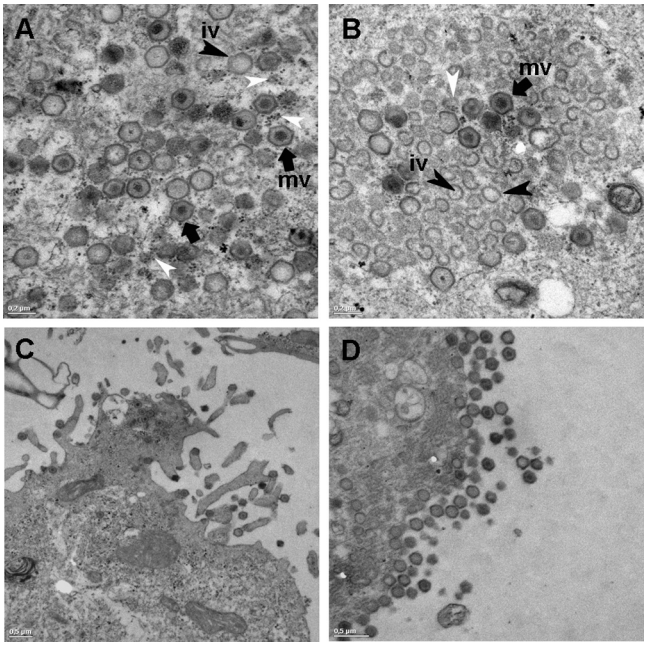

FIG 4 Electron microscopy analysis of ASF viral factory after inhibition of Rho GTPase-mediated signaling. Vero cells were infected with ASFV at 0.5 PFU/cell in the presence or absence of 50 ng of CdTB/ml and fixed at 16 hpi. (A) In the absence of CdTB, viral factories contained envelope precursors and abundant immature (iv, black arrowheads) and mature icosahedral particles (mv, arrows). (B) In contrast, viral factories formed in the presence of CdTB contained high amounts of envelope precursors and low numbers of both mature and immature icosahedral particles. (C) In the absence of CdTB, almost all viral particles that reached the plasma membrane were mature and were found with the characteristic filopodia in exocytosis. This observation contrasts with the abundant immature particles found at the cell membrane in the presence of CdTB and the absence of filopodia formation. (D). Scale bars: A and B, 0.2 μm; C and D, 0.5 μm. White arrowheads indicate ribosomes.

the hypothesis that Rac1 is the member of the Rho-GTPase family that is immediately activated after ASFV entry and that it is crucial for an efficient infection.

Effect of specific inhibition of Rac1 signaling on ASFV infection of Vero cells. To ascertain the specificity of Rac1 action during ASFV infection, we inhibited this GTPase, without affecting the other members of the Rho GTPase family. We used a chemical inhibitor, NSC23766, to prevent the specific activation of Rac1 and analyze impact on virus production (21). Cells were incubated with nontoxic doses of NSC23766 before ASFV infection, and virus progeny was examined at 24 hpi. Virus yields obtained after NSC23766 incubation decreased in a dose-dependent manner (Fig. 6A). Consistent with the CdTB experiments, this effect on virus yields was greater when the inhibitor was added to cells before infection. When we analyzed ASFV infectivity in Rac1-inhibited cells, we could observe a slight but significant decrease in the number of infected cells at 3 hpi compared to untreated control cells (Fig. 6B). Given that Rac1 activation occurred immediately after infection, we next analyzed by confocal microscopy the number of internalized virus particles in infected Vero cells 1 h after virus infection with highly purified ASFV at a high MOI and also their positions with respect to the host cell nucleus. Inhibition of geranylgeranylation with GGTI-286 did not modify the number of internalized virions (ranging between 19.5 and 21.2 PFU/cell). However, we observed a significant decrease in the number of virions exhibiting a perinuclear location at 1 hpi after GGTI-286 treatment.

Similarly, ASFV perinuclear localization, but not virion internalization, was affected after NSC23766 Rac1 inhibition, since the percentage of perinuclear virions was significantly reduced under these conditions (Fig. 6C). These results indicate that Rac1 is the member of Rho GTPase family whose activation after ASFV entry

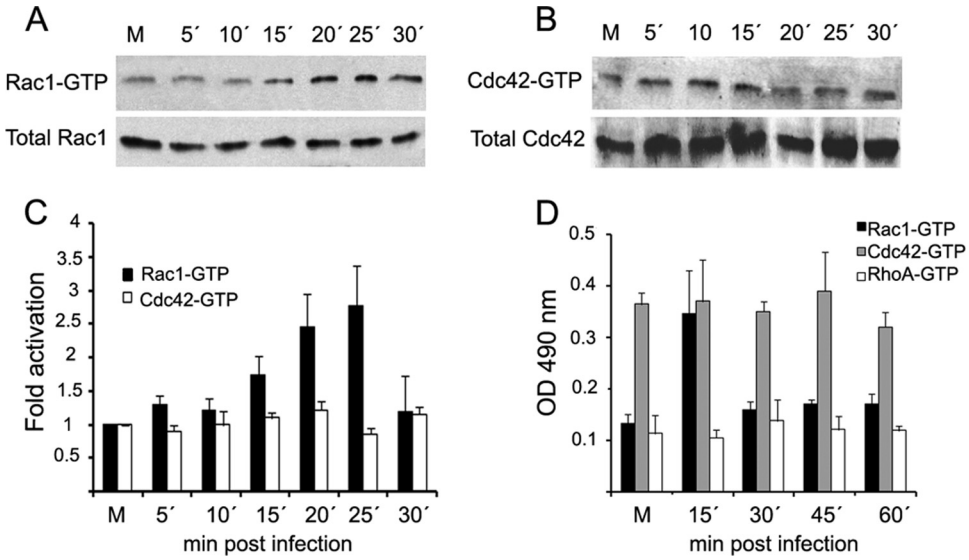

FIG 5 Rac1 is activated during early stages of ASFV infection. Equal amounts of Vero cell lysates from mock-infected cells (M) or ASFV-infected cells (5 PFU/cell) at various time points after infection were used to capture the GTP-bound form of Rac1 and Cdc42 by affinity precipitation with GST-PBD beads. The proteins captured by beads were analyzed by immunoblotting with anti-Rac1 antibody and anti-Cdc42 (top portions of panels A and B, respectively). The bottom portions of panels A and B show normalized cell lysates analyzed for total Rac1 as a protein load control. (C) Bands corresponding to GTP-bound forms of Rac1 and Cdc42 were quantified and normalized to values from total Rac1 and Cdc-42, respectively. The data obtained from mock-infected cells were considered to be activated 1-fold for comparison with infected cells. Representative images are shown from five independent pulldown assays. (D) Activation of Rac1, Cdc42, and RhoA was analyzed by an ELISA-based assay in infected Vero cells at the indicated time points within the first hour of infection. The GTP-bound forms of Rho GTPases were measured with an absorbance set at 490 nm. Each point represents the means ± the SD for three independent experiments.

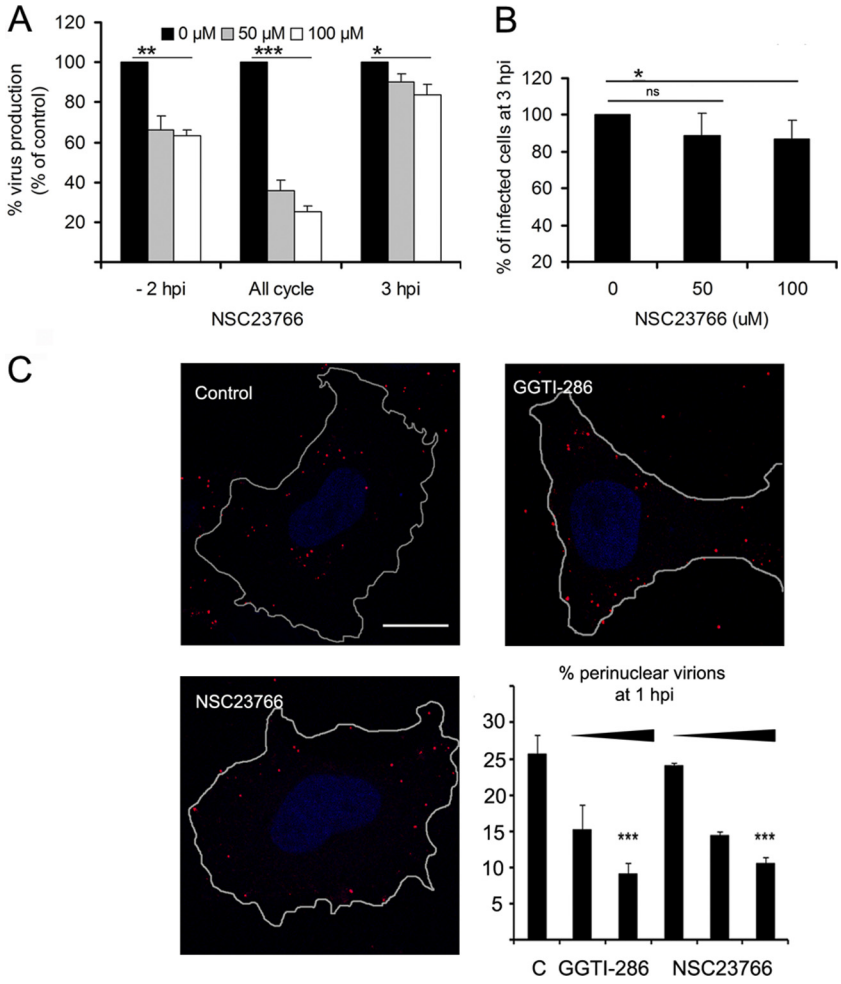

FIG 6 (A) Virus progeny at 24 hpi were determined by plaque assay from ASFV-infected cells in the presence of the specific Rac1 inhibitor NSC23766. Increasing, but nontoxic, concentrations of NSC23766 were added to cells before (−2 hpi), after (+3 hpi), or throughout infection. (B) The number of infected cells at 3 hpi in the presence of a range of concentrations of NSC23766 is shown as a percentage of control nontreated cells. (C) Virion distribution at 1 hpi in ASFV-infected Vero cells after incubation with increasing concentrations of GGTI-286 (10 and 30 μM) or NSC23766 (10, 50, and 100 μM) was examined. Representative confocal 0.1-μm sections from the z-axis are shown where virions were identified with mouse anti-p72 monoclonal antibody, followed by Alexa Fluor 594 anti-mouse IgG (red). Nuclei (blue) stained with Hoechst and cell contours are shown. Bar, 16 μm. A bar graph shows the percentage of virions exhibiting perinuclear localization. The data represent medians and SD from three independent experiments where 30 infected cells were analyzed in each case. A high MOI (>10 PFU/cell) was used. Each point represents the means ± the SD for three experiments. Values that are significantly different from each other are indicated (***, $P < 0.001$; **, $P < 0.01$; *, $P < 0.05$).

results relevant to reach perinuclear sites for an efficient virus multiplication. Also, Vero cells were transfected with plasmids encoding wild-type Rac1 (wt), dominant-negative Rac1 mutant (17N), or constitutively active Rac1 mutant (Q61L). After 24 h, the cells were mock infected or infected with a high MOI using highly purified ASFV. However, in transfected cells we were not able to find differences either in the number of internalized virus particles or in their positions with respect to the host cell nucleus at 1 hpi (data not shown).

ASFV infection induces microtubule hyperacetylation. Inhibition of Rac1 signaling negatively affected perinuclear virions localization but not entry itself, suggesting the involvement of Rac1 in following steps of infection immediately after ASFV entry. Early after ASFV entry into host cells, the microtubule network is essential for an efficient infection (3), and the acetylation/deacetylation balance of tubulin regulates microtubule dynamics (49), which is regulated by Rho GTPases. In addition, by using confocal microscopy, we detected the association of virions with acetylated microtubules during the first hour after virus inoculation in Vero cells (Fig. 7A). Since hyperacetylation is a quantitative indication of microtubules stabilization, we next analyzed tubulin acetylation levels from Vero cell extracts at a range of times postinfection by immunoblotting. Tubulin acetylation increased 2.5- to 4-fold from 15 to 30 min postinfection compared to mock-infected cells. At 45 min postinfection, tubulin acetylation levels showed a 2-fold increase, which was maintained for up 2 hpi and returned to basal levels by 3 hpi (Fig. 7B). In contrast, the levels of total α-tubulin remained unaltered. The inactivation of Rho GTPases with increasing concentrations of CdTB before infection restored tubulin acetylation levels to those obtained with mock-infected cell extracts (Fig. 7B). We specifically confirmed a reduction in tubulin acetylation levels in cells incubated with the geranylgeranylation inhibitor GGTI-286. Moreover, we observed similar re-

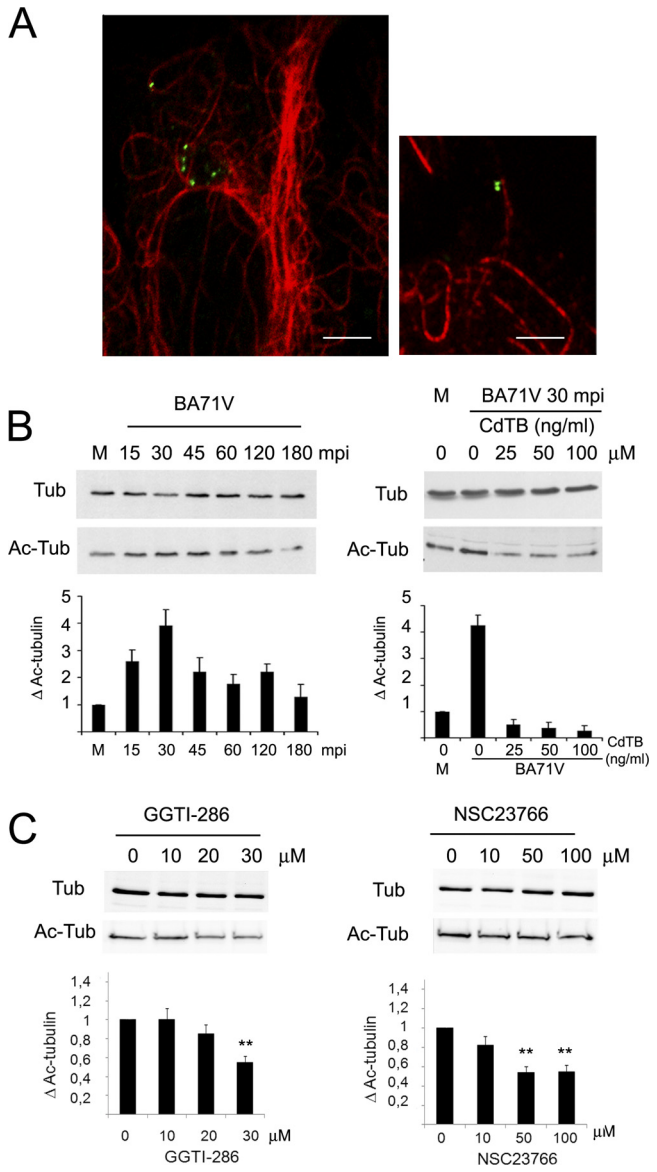

FIG 7 (A) Representative confocal microscopy image of ASFV-infected Vero cells at 30 min postinfection (mpi). ASF virions (green), detected by an antibody against viral protein pE120R, are coincident with acetylated microtubules (red). Bar, 10 μm. Total α-tubulin (Tub) and acetylated α-tubulin (Ac-Tub) levels were assessed by immunoblotting with specific antibodies from Vero cell extracts at a range of times during infection (B, left panel) and from infected Vero cells at 30 min in the presence of increasing concentrations of CdTB (B, right panel). (C) Similarly, acetylated tubulin levels were assessed from cell extracts after incubation for 2 h with increasing concentrations of GGTI-286 or NSC23766. In all cases, the band intensities were quantitated, and the acetylated tubulin in mock-infected or untreated Vero cells was considered as 1-fold for comparison with infected or inhibitor treated cells. Each bar represents the mean and SD corresponding to three independent experiments. Values that are significantly different from each other are indicated (***, $P < 0.001$; **, $P < 0.01$).

ductions in tubulin acetylation levels after inhibition of Rac1 signaling with increasing concentrations of specific Rac1 inhibitor NSC23766 (Fig. 7C). Taken together, these data suggest that Rac1 GTPase contributes to the microtubule hyperacetylation induced by ASFV during the early stages of Vero cell infection.

DISCUSSION

In this work, we have described the antiviral effects of statins on ASFV and how these are likely mediated by inhibition of prenylation of Rho GTPases. The initial results reported here demonstrate that lipid posttranslational modifications of host cell factors are important for an efficient infection and could participate in various stages of ASFV infection. We found that statins negatively affected virus production and infectivity (understood as infected cells at 3 hpi expressing ASFV early proteins), and this effect was fully reversed by the addition of immediate precursor Mev, whereas the addition of isoprenoid GGPP only restored virus infectivity. Specific inhibition of the prenyltransferases FTase-I and GGTase-I revealed that the incorporation of FPP is required during early stages of ASFV infection and that it is relevant for the subsequent development of infection. However, geranylation also participates in diverse steps of ASFV infection. The reduction of virus progeny when geranylation was inhibited after virus entry suggests that intact pools of GGPP or geranylated proteins during a later stage of ASFV infection are also crucial for correct viral replication. In this regard, ASFV encodes a *trans*-prenyltransferase (open reading frame *B318L*) that catalyzes the condensation of farnesyl diphosphate and isopentenyl diphosphate to GGPP and longer chain prenyl diphosphates (1, 2). *B318L* is an essential gene whose expression occurs late during virus infection, and its protein remains associated with precursor viral membranes derived from the endoplasmic reticulum at the viral assembly sites. These features are consistent with the hypothesis that GGPP synthesized by *B318L* serves as a substrate for the prenylation of cellular or viral proteins and that this posttranslational modification is required during virus replication and morphogenesis as described for hepatitis δ virus and murine leukemia virus (23, 34, 39, 49).

Isoprenoid intermediates are crucial for multiple cellular functions, such as the posttranslational modifications (prenylation) of a large variety of proteins, among which the small GTP-binding proteins Ras and Ras-like proteins, such as Rho, Rap, Rac, and Rab. Since prenylation of Rab GTPases is dependent on GGTase II, which is not affected by the inhibitor GGTI-286, the main focus of the present study was the Rho GTPase family. These are key regulators of the cell cytoskeleton, cell cycle, gene expression, and vesicle trafficking (19, 51) and are involved in the entry of diverse viruses into the host cell (14, 42, 48, 52) but also in viral morphogenesis (27, 61), infection spreading (12), or virus-induced cell motility (61, 66). In this regard, a general inhibition of Rho GTPase-mediated signaling could affect simultaneously diverse and relevant cellular processes that may explain the abnormal viral factory size and extensive accumulation of envelope precursors and immature virions observed when ASFV infection takes place under these conditions. It has been reported that Rho GTPases also participate in the morphogenesis of diverse viruses. For instance, RhoA is activated during late stages of respiratory syncytial virus infection and is crucial for correct filamentous virion morphology (26). During late infection, the alphaherpesviruses HSV-2 or pseudorabies virus promote actin rearrangements, presumably by viral protein US3 regulation of RhoA, Cdc42, and Rac1 activity balance (20, 47). Our observations with TEM on late stages of ASFV infection revealed a severe decrease of filopodia after CdTB treatment, which could be explained by a general Rho GTPase-mediated signaling inhibition with consequences on cor-

tical actin barrier regulation. However, and given that a high number of immature virus particles are accumulated at the cell surface after CdTB treatment, we cannot rule out the possibility that mature ASFV particles were required for stimulating filopodia formation, as reported for vaccinia virus-induced actin tails that resemble filopodia (reviewed in reference 56).

Our data with CdTB indicated that cellular signaling pathways regulated by Rho GTPases are activated during early stages of ASFV infection; however, its inactivation did not affect virus infectivity. Moreover, virus internalization was not affected by geranylgeranylation inhibition, thus demonstrating that Rho GTPases are not essential for ASFV entry itself in Vero cells.

Among the most extensively characterized members of the Rho GTPase family, we have demonstrated that Rac1 is activated during the first 30 min of ASFV infection in Vero cells. Surprisingly, Cdc42, which may act as an upstream activator of Rac1, was not induced by ASFV infection, as deduced from pull-down and also ELISA-based assays. A similar situation, Rac1 but not Cdc42 activation, was also recently described during hepatitis B virus infection (59). Rac1 regulates a wide variety of cellular functions (8) and participates in the entry of the following viruses into the host cell: vaccinia virus (44), dengue virus (65), herpes simplex virus 1 (33, 50), group B coxsackieviruses (13), and hepatitis B virus (59), among others. Most of these viruses exploit macropinocytosis in some way in order to gain access to the host cell by means of membrane ruffling or blebbing, which requires Rac1 activation (45). However, this entry strategy does not appear to be followed by ASFV, which enters the host cell by dynamin- and clathrin-dependent endocytosis (31), since specific Rac1 inhibition by NSC23766 before virus addition did not affect virus internalization, thus indicating the absence of deficiencies in ASFV endocytosis.

Thus, Rac1 may participate in further steps of early infection, such as intracellular transport to replication sites. Indeed, microtubule network integrity during the initial stages of ASFV infection is critical for successful infection (3). Our results demonstrate that ASFV infection promotes early microtubule hyperacetylation, a hallmark of the preferential stabilization of these structures. This process may be regulated by Rho GTPases, since their inhibition prevented microtubule hyperacetylation. Adenovirus and Kaposi's sarcoma-associated herpesvirus also induce microtubule hyperacetylation during early infection of human foreskin fibroblast (HFF) cells by a RhoA- and Rac1-dependent mechanism (48, 64). However, in A549 cells, microtubule hyperacetylation induced by incoming adenovirus is mediated exclusively by a Rac1-dependent mechanism (63), as we observed for ASFV. We determined that maximal Rac1 activity during early ASFV infection is coincident with hyperacetylation of microtubules (around 30 min postinfection), and tubulin acetylation levels were reduced after inhibition of Rac1 signaling with increasing concentrations of specific inhibitor.

Moreover, our results showed that specific inhibition of Rac1-mediated signaling with NSC23766 impaired virion perinuclear localization but not viral entry itself. Similar results were obtained with geranylgeranyl inhibitor which is concordant with a Rac1-mediated signaling inhibition by GGTI-286, given that Rac1 undergoes geranylgeranylation at its C terminus, and this posttranslational modification has been previously associated with an increase in Rac1 GTP binding and activation (46). However, we did not find differences in Rac1 dominant-negative mutant transfected cells affecting either the number of internalized virions or their localization to perinuclear areas. A possible explanation is that the inhibition of Rac1 in Vero cells was not complete in this case and a minimal proportion of acetylated microtubules might be sufficient to facilitate the start of ASFV infection.

Our data suggest that Rac1 modulates the intracellular transport of ASFV by inducing microtubule acetylation. In this regard, microtubules and associated molecular motors have been previously shown to be critical for ASFV trafficking from entry to replication and assembly sites (3), and these results open up the possibility that Rho GTPases could constitute an early target for statins during ASFV infection, relevant for the development of novel strategies to the eradication of African swine fever.

ACKNOWLEDGMENTS

We thank Ole Gjoerup for the plasmids encoding wild-type, dominant-negative, and constitutively active forms of Rac1 fused to GFP. The construct expressing the GST-Rac1/Cdc42 binding domain of Pak1 was a generous gift from Keith Burridge.

This study was supported by grants from Consolider Program CSD2006-00007 and by AGL2009-09209 from the Spanish Ministry of Science and Innovation.

REFERENCES

1. **Alejo A, Andres G, Vinuela E, Salas ML.** 1999. The African swine fever virus prenyltransferase is an integral membrane trans-geranylgeranyl-diphosphate synthase. J. Biol. Chem. **274**:18033–18039.
2. **Alejo A, Yanez RJ, Rodriguez JM, Vinuela E, Salas ML.** 1997. African swine fever virus *trans*-prenyltransferase. J. Biol. Chem. **272**:9417–9423.
3. **Alonso C, et al.** 2001. African swine fever virus protein p54 interacts with the microtubular motor complex through direct binding to light-chain dynein. J. Virol. **75**:9819–9827.
4. **Arakawa Y, Cordeiro JV, Way M.** 2007. F11L-mediated inhibition of RhoA-mDia signaling stimulates microtubule dynamics during vaccinia virus infection. Cell Host Microbe **1**:213–226.
5. **Bagrodia S, Taylor SJ, Jordon KA, Van Aelst L, Cerione RA.** 1998. A novel regulator of p21-activated kinases. J. Biol. Chem. **273**:23633–23636.
6. **Bernardes C, Antonio A, Pedroso de Lima MC, Valdeira ML.** 1998. Cholesterol affects African swine fever virus infection. Biochim. Biophys. Acta **1393**:19–25.
7. **Bos JL, Rehmann H, Wittinghofer A.** 2007. GEFs and GAPs: critical elements in the control of small G proteins. Cell **129**:865–877.
8. **Bosco EE, Mulloy JC, Zheng Y.** 2009. Rac1 GTPase: a "Rac" of all trades. Cell. Mol. Life Sci. **66**:370–374.
8a. **Brookes SM, Dixon LK, Parkhouse RM.** 1996. Assembly of African swine fever virus: quantitative ultrastructural analysis in vitro and in vivo.Virology **224**:84–92.
9. **Bustelo XR, Sauzeau V, Berenjeno IM.** 2007. GTP-binding proteins of the Rho/Rac family: regulation, effectors and functions in vivo. Bioessays **29**:356–370.
10. **Carrascosa AL, del Val M, Santaren JF, Vinuela E.** 1985. Purification and properties of African swine fever virus. J. Virol. **54**:337–344.
11. **Carvalho ZG, De Matos AP, Rodrigues-Pousada C.** 1988. Association of African swine fever virus with the cytoskeleton. Virus Res. **11**:175–192.
12. **Cordeiro JV, et al.** 2009. F11-mediated inhibition of RhoA signaling enhances the spread of vaccinia virus in vitro and in vivo in an intranasal mouse model of infection. PLoS One **4**:e8506.
13. **Coyne CB, Shen L, Turner JR, Bergelson JM.** 2007. Coxsackievirus entry across epithelial tight junctions requires occludin and the small GTPases Rab34 and Rab5. Cell Host Microbe **2**:181–192.
14. **del Real G, et al.** 2004. Statins inhibit HIV-1 infection by down-regulating Rho activity. J. Exp. Med. **200**:541–547.
15. **de Rooij J, Bos JL.** 1997. Minimal Ras-binding domain of Raf1 can be used as an activation-specific probe for Ras. Oncogene **14**:623–625.
16. **Diebold BA, Fowler B, Lu J, Dinauer MC, Bokoch GM.** 2004. Antagonistic cross-talk between Rac and Cdc42 GTPases regulates generation of reactive oxygen species. J. Biol. Chem. **279**:28136–28142.
17. **Dixon LK, et al.** 2005. *Asfarviridae*, p 135–143. *In*Fauquet CM, et al. (ed),

Virus taxonomy: eighth report of the International Committee on Taxonomy of Viruses. Elsevier/Academic Press, London, England.
18. **Enjuanes L, Carrascosa AL, Moreno MA, Vinuela E.** 1976. Titration of African swine fever (ASF) virus. J. Gen. Virol. **32**:471–477.
19. **Etienne-Manneville S, Hall A.** 2002. Rho GTPases in cell biology. Nature **420**:629–635.
20. **Favoreel HW, Van Minnebruggen G, Adriaensen D, Nauwynck HJ.** 2005. Cytoskeletal rearrangements and cell extensions induced by the US3 kinase of an alphaherpesvirus are associated with enhanced spread. Proc. Natl. Acad. Sci. U. S. A. **102**:8990–8995.
21. **Gao Y, Dickerson JB, Guo F, Zheng J, Zheng Y.** 2004. Rational design and characterization of a Rac GTPase-specific small molecule inhibitor. Proc. Natl. Acad. Sci. U. S. A. **101**:7618–7623.
22. **Geraldes A, Valdeira ML.** 1985. Effect of chloroquine on African swine fever virus infection. J. Gen. Virol. **66**(Pt 5):1145–1148.
23. **Glenn JS, Watson JA, Havel CM, White JM.** 1992. Identification of a prenylation site in delta virus large antigen. Science **256**:1331–1333.
24. **Goldstein JL, Brown MS.** 1990. Regulation of the mevalonate pathway. Nature **343**:425–430.
25. **Gomez-Puertas P, et al.** 1995. Improvement of African swine fever virus neutralization assay using recombinant viruses expressing chromogenic marker genes. J. Virol. Methods **55**:271–279.
26. **Gower TL, et al.** 2005. RhoA signaling is required for respiratory syncytial virus-induced syncytium formation and filamentous virion morphology. J. Virol. **79**:5326–5336.
27. **Gower TL, Peeples ME, Collins PL, Graham BS.** 2001. RhoA is activated during respiratory syncytial virus infection. Virology **283**:188–196.
28. **Guijarro C, et al.** 1998. 3-Hydroxy-3-methylglutaryl coenzyme a reductase and isoprenylation inhibitors induce apoptosis of vascular smooth muscle cells in culture. Circ. Res. **83**:490–500.
29. **Heasman SJ, Ridley AJ.** 2008. Mammalian Rho GTPases: new insights into their functions from in vivo studies. Nat. Rev. Mol. Cell. Biol. **9**:690–701.
30. **Heath CM, Windsor M, Wileman T.** 2001. Aggresomes resemble sites specialized for virus assembly. J. Cell Biol. **153**:449–455.
31. **Hernaez B, Alonso C.** 2010. Dynamin- and clathrin-dependent endocytosis in African swine fever virus entry. J. Virol. **84**:2100–2109.
32. **Hernaez B, Escribano JM, Alonso C.** 2006. Visualization of the African swine fever virus infection in living cells by incorporation into the virus particle of green fluorescent protein-p54 membrane protein chimera. Virology **350**:1–14.
33. **Hoppe S, et al.** 2006. Early herpes simplex virus type 1 infection is dependent on regulated Rac1/Cdc42 signaling in epithelial MDCKII cells. J. Gen. Virol. **87**:3483–3494.
34. **Hwang SB, Lai MM.** 1993. Isoprenylation mediates direct protein-protein interactions between hepatitis large delta antigen and hepatitis B virus surface antigen. J. Virol. **67**:7659–7662.
35. **Jaffe AB, Hall A.** 2005. Rho GTPases: biochemistry and biology. Annu. Rev. Cell Dev. Biol. **21**:247–269.
36. **Jouvenet N, Monaghan P, Way M, Wileman T.** 2004. Transport of African swine fever virus from assembly sites to the plasma membrane is dependent on microtubules and conventional kinesin. J. Virol. **78**: 7990–8001.
37. **Jouvenet N, et al.** 2006. African swine fever virus induces filopodia-like projections at the plasma membrane. Cell Microbiol. **8**:1803–1811.
38. **King DP, et al.** 2003. Development of a TaqMan PCR assay with internal amplification control for the detection of African swine fever virus. J. Virol. Methods **107**:53–61.
39. **Lee CZ, Chen PJ, Lai MM, Chen DS.** 1994. Isoprenylation of large hepatitis delta antigen is necessary but not sufficient for hepatitis delta virus assembly. Virology **199**:169–175.
40. **Li E, Stupack D, Bokoch GM, Nemerow GR.** 1998. Adenovirus endocytosis requires actin cytoskeleton reorganization mediated by Rho family GTPases. J. Virol. **72**:8806–8812.
41. **Liao JK, Laufs U.** 2005. Pleiotropic effects of statins. Annu. Rev. Pharmacol. Toxicol. **45**:89–118.
42. **Locker JK, et al.** 2000. Entry of the two infectious forms of vaccinia virus at the plasma membrane is signaling-dependent for the IMV but not the EEV. Mol. Biol. Cell **11**:2497–2511.
43. **McTaggart SJ.** 2006. Isoprenylated proteins. Cell. Mol. Life Sci. **63**: 255–267.
44. **Mercer J, Helenius A.** 2010. Apoptotic mimicry: phosphatidylserine-mediated macropinocytosis of vaccinia virus. Ann. N. Y. Acad. Sci. **1209**: 49–55.
45. **Mercer J, Helenius A.** 2009. Virus entry by macropinocytosis. Nat. Cell Biol. **11**:510–520.
46. **Michaelson D, et al.** 2001. Differential localization of Rho GTPases in live cells: regulation by hypervariable regions and RhoGDI binding. J. Cell Biol. **152**:111–126.
47. **Murata T, Goshima F, Daikoku T, Takakuwa H, Nishiyama Y.** 2000. Expression of herpes simplex virus type 2 US3 affects the Cdc42/Rac pathway and attenuates c-Jun N-terminal kinase activation. Genes Cells **5**:1017–1027.
48. **Naranatt PP, Krishnan HH, Smith MS, Chandran B.** 2005. Kaposi's sarcoma-associated herpesvirus modulates microtubule dynamics via RhoA-GTP-diaphanous 2 signaling and utilizes the dynein motors to deliver its DNA to the nucleus. J. Virol. **79**:1191–1206.
49. **Overmeyer JH, Maltese WA.** 1992. Isoprenoid requirement for intracellular transport and processing of murine leukemia virus envelope protein. J. Biol. Chem. **267**:22686–22692.
50. **Petermann P, Haase I, Knebel-Morsdorf D.** 2009. Impact of Rac1 and Cdc42 signaling during early herpes simplex virus type 1 infection of keratinocytes. J. Virol. **83**:9759–9772.
51. **Qualmann B, Mellor H.** 2003. Regulation of endocytic traffic by Rho GTPases. Biochem. J. **371**:233–241.
52. **Quinn K, et al.** 2009. Rho GTPases modulate entry of Ebola virus and vesicular stomatitis virus pseudotyped vectors. J. Virol. **83**:10176–10186.
53. **Ridley AJ.** 2001. Rho family proteins: coordinating cell responses. Trends Cell Biol. **11**:471–477.
54. **Rodriguez JM, Garcia-Escudero R, Salas ML, Andres G.** 2004. African swine fever virus structural protein p54 is essential for the recruitment of envelope precursors to assembly sites. J. Virol. **78**:4299–4313.
55. **Sander EE, et al.** 1998. Matrix-dependent Tiam1/Rac signaling in epithelial cells promotes either cell-cell adhesion or cell migration and is regulated by phosphatidylinositol 3-kinase. J. Cell Biol. **143**:1385–1398.
56. **Smith GL, Vanderplasschen A, Law M.** 2002. The formation and function of extracellular enveloped vaccinia virus. J. Gen. Virol. **83**:2915–2931.
57. **Stefanovic S, Windsor M, Nagata KI, Inagaki M, Wileman T.** 2005. Vimentin rearrangement during African swine fever virus infection involves retrograde transport along microtubules and phosphorylation of vimentin by calcium calmodulin kinase II. J. Virol. **79**:11766–11775.
58. **Subauste MC, et al.** 2000. Rho family proteins modulate rapid apoptosis induced by cytotoxic T lymphocytes and Fas. J. Biol. Chem. **275**: 9725–9733.
59. **Tan TL, et al.** 2008. Rac1 GTPase is activated by hepatitis B virus replication: involvement of HBX. Biochim. Biophys. Acta **1783**:360–374.
60. **Valdeira ML, Bernardes C, Cruz B, Geraldes A.** 1998. Entry of African swine fever virus into Vero cells and uncoating. Vet. Microbiol. **60**: 131–140.
61. **Valderrama F, Cordeiro JV, Schleich S, Frischknecht F, Way M.** 2006. Vaccinia virus-induced cell motility requires F11L-mediated inhibition of RhoA signaling. Science **311**:377–381.
62. **Van Aelst L, D'Souza-Schorey C.** 1997. Rho GTPases and signaling networks. Genes Dev. **11**:2295–2322.
63. **Warren JC, Cassimeris L.** 2007. The contributions of microtubule stability and dynamic instability to adenovirus nuclear localization efficiency. Cell Motil. Cytoskeleton **64**:675–689.
64. **Warren JC, Rutkowski A, Cassimeris L.** 2006. Infection with replication-deficient adenovirus induces changes in the dynamic instability of host cell microtubules. Mol. Biol. Cell **17**:3557–3568.
65. **Zamudio-Meza H, Castillo-Alvarez A, Gonzalez-Bonilla C, Meza I.** 2009. Cross-talk between Rac1 and Cdc42 GTPases regulates formation of filopodia required for dengue virus type 2 entry into HMEC-1 cells. J. Gen. Virol. **90**:2902–2911.
66. **Zwilling J, Sliva K, Schwantes A, Schnierle B, Sutter G.** 2010. Functional F11L and K1L genes in modified vaccinia virus Ankara restore virus-induced cell motility but not growth in human and murine cells. Virology **404**:231–239.